Australia's National
Science Agency

Topic 5 Stage 4 Restoration and Black Start

Final Report

Sorrell Grogan, Babak Badrzadeh

May 2025

Australian Research in Power System Transition

Citation

Grogan, S. and Badrzadeh B. (2025) Topic 5 Stage 4 Restoration and Black Start. CSIRO, Australia.

Copyright

Important disclaimer

Contents

Figures

Tables

1 Acknowledgments

The research presented in this report was funded by CSIRO, Australia's national science agency, and carried out as part of CSIRO's contribution to the initiatives of the Australian Power Systems Renewables transition. This research supports Australia's transition to a stable, secure and affordable power system and contributes to critical research identified by the Consortium required to accelerate the decarbonisation of our electricity grid.

The research presented in this report was supported by the Australian Energy Market Operator, a stakeholder in the AR-PST Consortium, who provided subject matter expertise towards these research findings.

The researchers wish to acknowledge the expertise and efforts provided by:

- Shakil Khan and Thomas Brinsmead at CSIRO, and Ehsan Farahani at AEMO, for their guidance and advice.
- Denis Kho and Deepak Ramasubramanian at EPRI in developing and tuning many of the models used in this research.

Executive summary

A major supply disruption (also known as “system black”) is a high-impact, low-probability event whereby a power system suffers a partial or complete collapse (i.e., zero voltage). Such a scenario requires the system to be restarted (also known as “black started”) using self-restart capable generators that can energise the nearby network, load, and other non-black start capable generators in the collapsed region. Although not a new concept, as penetration of inverter-based resources (IBRs) increases throughout the National Electricity Market (NEM) and existing synchronous coal and gas generators retire, providers of black start generators are diminishing. This project continues to investigate the role IBRs can take in system restart, under 100% IBR penetration conditions, continuing from existing research performed through 2022, 2023 and 2024. The following key topics are the focus of the 2024-25 research program on Topic 5:

- Dynamic modelling of Distributed Energy Resources (DER) control systems and distributed energy source variations for a 100% IBR restart scenario. Using an EPRI-developed DER model, the work investigates any destabilising effects of DER on a restarting system when the restart source is comprised of a GFM Battery Energy Storage System (BESS) black-starter.
- Evaluation of alterations to grid-following (GFL) IBR operational, and any high-level, operator-accessible, settings to enhance stability during 100% IBR system restoration, extending to hybrid (IBR and synchronous) plant. This determines how existing IBR plant in the NEM can best aid in the restart process using “on the day” operational strategies.
- Evaluation of IBR black start sources on network protection relay functionality. Studies consider any undesired performance of network protection relays when an IBR source is used as the black starter that may prevent the successful restoration of the network.
- Development of an analytical screening tool to estimate the timeline of required grid-forming (GFM) IBR amounts to replace the network energisation capability of the retiring synchronous generators across the NEM.

This work is both strongly aligned with the Topic 5 research roadmap, and by virtue of the development and use of Electromagnetic Transient (EMT) models to complete many of the insights, produces open, shareable and improvable EMT network models to be provided with the broader research community. The following are a selection of key insights from the hundreds of simulations and scenarios evaluated, which highlights this works relevance not only to the research roadmap, but the immediate challenges faced by the NEM in system restart:

- DER energy source variations across the length of a feeder showed no adverse impact on the restarting system, so long as the black start source has appropriately tuned active voltage and frequency control for system restart and unit import/export limits were not violated.
- DER penetration levels beyond 80% of the nameplate rating of the GFM BESS black starter saw DER phase-locked loop (PLL) tracking instabilities begin to manifest even in the absence of any disturbance. However, such behaviour was not observed when a synchronous machine black start source was used.

- The most common cause of instability seen in a restarting system with large amounts of GFL IBR was an ill-conditioned park power controller (PPCs) on GFL plant, rather than inner control loop instability typically attributable to low system strength. Such instability can be avoided by selecting a direct power control mode of the PPC.
- Major disturbances or transformer energisations next to AC or DC-coupled hybrid plant with high internal power transfer may result in very large MW injections or absorptions to or from its point of connection, destabilising and collapsing the restarting system.
- Transformer differential protection harmonic blocking thresholds may need to be reduced to lower levels to allow successful energisation of transformers from all black start sources, but GFM BESS black start scenarios require smaller threshold reductions.
- GFM IBR devices generally appeared to be able to energise larger sizes of transformers without tripping transformer differential relay protection upon energisation. It is hypothesised that the current-limited nature of IBR devices may be advantageous in this regard, and this should be an area of immediate future research.
- To maintain the same network restoration capability as today, for every large synchronous machine retiring in the NEM soon, approximately 35-40% of its nameplate rating will be required in the form of GFM IBR. Approximately 2 GVA of such GFM IBR will be required by 2028.

The work in this stage has both further highlighted the usefulness of GFM technology (particularly GFM BESS) to play a leading role in system restart within the Australian context and uncovered many further avenues of enquiry for future research rounds to better exploit the inherent advantages of GFM IBR technology (and identify problematic scenarios to avoid). Future work recommendations include more detailed investigations into the use of REZs to provide system restart, exploration of how other consumer end-devices could play a role during restart, evaluations on the current-limited nature of IBRs being useful to avoid protection relay maloperation, and improvements to generic GFM IBR models to better reflect limitations real OEMs include in their equipment.

2 Introduction

The Topic 5 remit considers the low probability but high impact scenario of a power system that has electrically collapsed and needs to be independently restarted and returned to a normal operating state. This is a challenging scenario to manage at the best of times with known technology but is becoming even more complex and uncertain as the generation mix shifts to becoming dominated by inverter-based resources (IBR) and load continues to increase its share of distributed energy resources (DER) [1].

2.1 Significance

The work being completed in this Stage and Topic is directly related to the evolution of the Australian power system to an inverter-dominated paradigm and is now more important than ever. Notably, a recent Issues Paper published by the AEMC [2] points out that, amongst other concerns:

- Procurement options for system restart sources are dwindling and resulting in some periods where the system restart standard [3] cannot be met with traditional synchronous plant.
- Alternative options for primary restart and restart support services, such as the potential use of new and existing IBR, are urgently needed and the technical feasibility of such options must be evaluated as a matter of priority.
- There is concern that large amounts of DER and the dynamic performance of the distribution system will undermine the ability of the system to be restarted during daylight hours, and that such concerns should be investigated and if needed, solutions found.
- The operation of protection mechanisms may be affected by the changing properties of electricity which IBR plant deliver to the system. This should be tested and if found to be material, a solution found.

Given that much of the work being considered in Stage 4 directly investigates these live concerns of the AEMC and the Reliability Panel [4], the work is pertinent to very real, very urgent issues in the Australian context. Specifically, the scenarios being considered are related to the above as follows:

- The investigation of high levels of distributed energy resources (e.g. solar PV) during 100% IBR restart.
  - This is a pressing issue currently in the NEM whereby there have been discussions about the potential for delaying system restart to non-daylight hours as to avoid the need to deal with the uncontrolled output of DER on the system. The work in

Milestone 1 has been considering a 100% IBR dominated system to investigate what steps, if any, should be taken to accommodate this specific situation.

- How to best accommodate the considerable existing fleet of IBRs in the NEM without the need to re-open technical negotiations with plant owners, maximising the chances of a successful system restart.
  - Australia already has a substantial fleet of IBR, that due to its connection locations and long remaining lifespan, will almost certainly need to contribute to restart paths as more of Australia's restart-capable synchronous machines retire. However, the controller settings of these existing IBR devices have not been specifically tuned to cope with a system restart scenario, and re-opening negotiations to tune these devices for a low-probability, high-impact scenario may be a very unappealing prospect for plant owners. Hence, the work in Milestone 2 has investigated how such existing IBR can be accommodated within a restart process on a no-regrets, best-effort basis, without the need to re-open negotiations, by determining which (relatively less burdensome) *operational* changes can maximise plant stability during restart. However, it is important to note that as this approach may ultimately have limited success. Such work is not a replacement for investigating more comprehensive Australian restart scenarios with specific inverter installed designs and settings.
- Addressing the concerns of Australian network operators that presently installed protection relays may no longer be fit for purpose once substantial numbers of synchronous machines retire from the system.
  - Given the current limitations of existing IBR technology, fault current magnitudes and quality are presently believed to be strongly reliant upon the presence of online synchronous machines, which are a dwindling resource in Australia. As the dependable operation of certain protection relays in the network relies on several system characteristics (e.g., high fault current magnitude, unbalanced current provision) always remaining present in the power system, this may no longer be valid as the Australian generation fleet shifts from synchronous-dominant to IBR-dominant. Milestone 3 work will investigate how such protection relays may operate with such a different, IBR-dominant, set of generators comprising a restarting system in the Australian context.
- Understanding approximately when, over the evolution of the power system, the procurement of IBR-based system restart sources will become a necessity.
  - The retirement of restart-capable thermal plant across the NEM is occurring rapidly, hence the need to procure IBR restart sources will become a necessity. Milestone 4 work will look to establish a high-level methodology, and calculation tool, to estimate when and what quantity of IBR restart sources will need to be procured as the NEM evolves.

The models being developed to investigate these issues have similar topologies to those expected to be present in the NEM during restart. A limited-area, detailed model has been

developed for Stage 4 with realistic, though not real, topologies, using configurations and network asset types that are typical of, and often used in, some NEM jurisdictions. This has largely been based on the practical experience of the researchers, who have worked on developing operational system restart scenarios in the NEM.

2.2 Previous stages

Previous work completed by researchers undertaking Stage 3 developed an important baseline which this work builds upon. Most importantly for the Stage 4 focus areas currently underway, the previous researchers determined that:

- Grid-forming (GFM) technology, such as a battery energy storage system (BESS) is capable of hosting up to 10-times its MVA rating in grid-following technology (provided network impedance is sufficiently small such that it is has a negligible impact on system strength provision).
- The Dynamic performance and stability of a GFM BESS black starter is superior to that of a combination of synchronous condenser plus a grid-following (GFL) BESS for scenarios early on in a restoration sequence (and potentially better than a synchronous generator), noting that fault-current limitations and sustaining sufficient energy reserve may still be problematic for GFM BESS technology.
- Voltage and frequency protection settings of plant that are appropriate during system normal, are likely to still be acceptable during system restart scenarios. However, it is noted that changes to frequency control settings during restart may be of benefit by improving general system stability.

2.3 Stage 4 focus areas

Using the above findings as a basis for this work, Stage 4 studies considered restarting a power system that comprises 100% IBR resources. Three major areas of investigation are based on offline EMT modelling and correspond to the first three milestones in the project plan. The project plan also includes one further area focusing on timeline and procurement needs of the NEM as it evolves to become IBR dominated, resulting in a fourth and final milestone. These research target areas and milestones are as follows:

- Milestone 1: Dynamic modelling of DER control systems and distributed energy source variations for a 100% IBR restart scenario.
  - A DER model developed by EPRI with dynamic representation of inner and outer inverter control loops is used. The work investigates any destabilising effects of DER (i.e., rooftop PV) on a restarting system when the restart source is comprised of a GFM BESS black-starter. Additionally, studies determine whether the black-start source type (i.e., IBR vs. synchronous) has a material impact on the stability and performance of the DER itself, and what its tripping and other susceptibility mechanisms are likely to be.

  - Target areas: Understanding the impact of distributed energy resources behaviour during system restart.
- Milestone 2: Evaluation of alterations to GFL IBR operational, and any high-level, operator-accessible, settings to enhance stability during 100% IBR system restoration, extending to hybrid (IBR and synchronous) plant.
  - This considers the problem of how existing IBR plant in the NEM can aid in the restart process without modification to deep controller settings affecting stability (e.g., PI controller gains), despite such plant not being specifically designed to operate in a restart scenario. It considers “on the day” operational strategies that could be employed by system operators to maximise success.
  - Target areas: Maximising the contribution of grid following inverters during system restoration through modifications to GFL-plant only.
- Milestone 3: Evaluation of IBR black start sources on network protection relay functionality.
  - Studies to be completed are to consider if there is any undesired performance of network protection relays when the system restart source is provided by an IBR resource, as opposed to a traditional synchronous machine source. Maloperation of network relays could have a variety of consequences for a fragile restarting system, hence their failure mechanisms should be understood.
  - Target areas: Understanding the impact of network control and protection settings on IBR system restart; Integrating protective relay response into power system restart modelling and simulation tools.
- Milestone 4: Development of an analytical screening tool to estimate the amount of GFM IBR restart sources required in a rapidly decarbonising system. Based on the published retirement dates of key restart-capable thermal generators across the NEM, previous research insights into GFM BESS restart capability, and previous system restart analysis experience, a tool is to be developed to estimate the quantity of IBR-based SRAS required to be procured as a replacement as the system evolves.
  - Target areas: Estimation of time frame over which retirements of conventional plant are likely to make IBR system restart necessary and/or comparable in cost to convention restart options.

The above work is both aligned with the original System Restoration roadmap and the target areas called upon for the 2024-25 year.

3 Methodology

3.1 Modelling

All plant in all scenarios considered are inverter-based, with no spinning machines in the system, unless a specific comparison to a synchronous machine black-starter is required.

3.1.1 Modelling software

To create and run these EMT models, PSCAD™ v5.0.3 was used, with Intel® Fortran Compiler Classic 2021.12.0 (64-bit), part of the Intel® OneAPI suite.

3.1.2 Topology

The topology of the limited area network used for restart modelling was arranged to be like a real location in the NEM that participates in system restart, but not identical as to preserve the anonymity of the location. It consists of:

- Multiple voltage levels that would be typical for a restart scenario.
- Line distances like those that exist in the real system within the area.
- Transformer sizing and impedances are like those commonly used in the network for the given voltage levels.

Additional fictitious lines and renewable energy zones were included to allow for analysis of the target phenomena called for in this work.

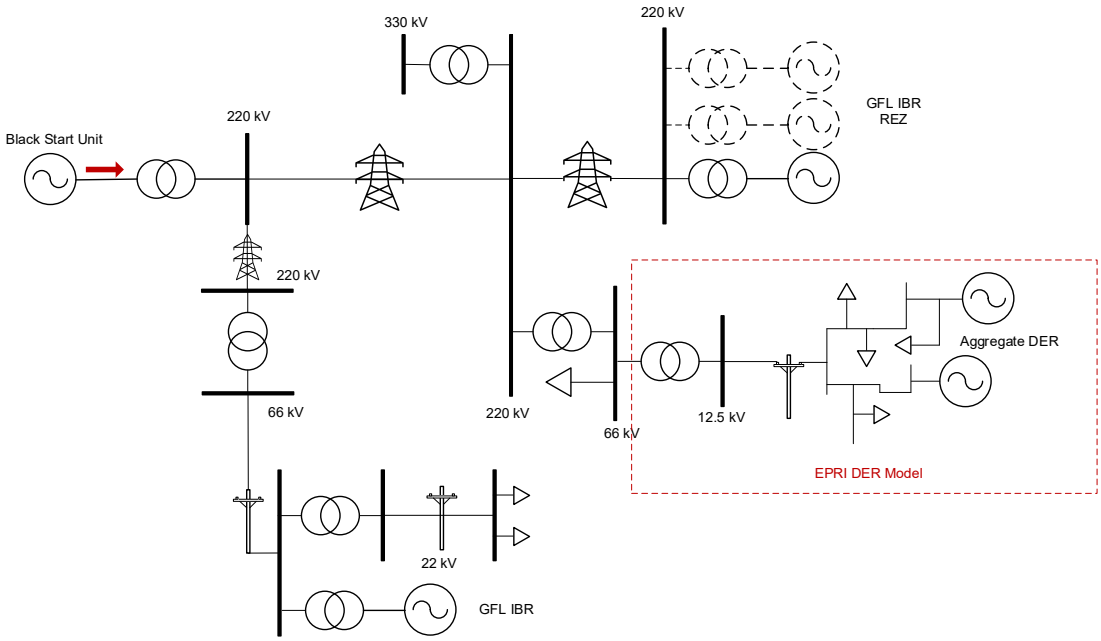

Figure 1 Limited area network model topology

3.1.3 Transmission Lines

Transmission lines (200 kV+) are built in geometric form, using common representations of tower layout, and bundling and geometry used in the Victorian region. Line data is taken from the Nexans overhead line catalogue[1] for conductors typically used for transmission in the Victorian region (ACSR Pawpaw and Mango being common for conductors). Transposition was considered to be ideal for each circuit.

An example layout is shown in Figure 2.

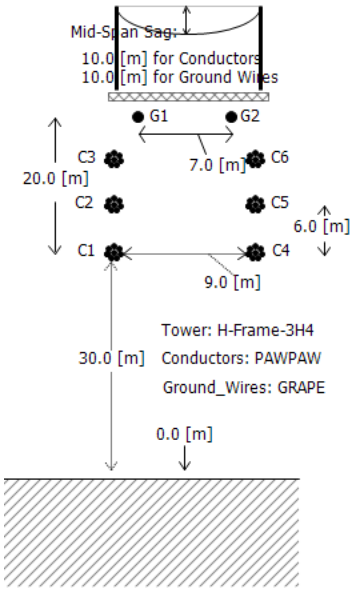

Figure 2 A common 220 kV tower approximate geometric layout

3.1.4 Sub-transmission lines

Sub-transmission lines (<150kV) were modelled on the typical 66 kV network used in the Victorian region, which is a considerably more compact distribution pole-top arrangement (given the non-linear relationship[2] between breakdown voltages and distance). Conductors were again based on those commonly used in the region and the parameters provided in the Nexans catalogue.

3.1.5 Transformers

Transmission network transformer models were represented as standard 3-winding transformers at an appropriate voltage level and MVA rating used within the Victorian region. Leakage reactance and copper loss impedances are based on typical values seen for

[1] https://www.nexans.com.au/.rest/catalog/v1/family/pdf/26818/Type-ACSR-GZ

[2] http://www.kronjaeger.com/hv/hv/msr/spk/

these transformers (10-15% and <0.5% respectively). Magnetizing current was set to 0.5% of rating, which is a conservatively large estimate for transformers of transmission network-size. For studies that looked at energisation of a transformer, saturation (Jiles-Atherton) and hysteresis were enabled in simulation, air core reactance was set to twice the leakage reactance amount [5]. Flux remanence was enabled with the profile of 0.8/-0.8/0, which corresponds to the "worst" energisation point to be on the A phase crossing from negative to positive voltage (see section 4.3.2 for more information).

3.1.6 3-winding versus Autotransformer

Limited studies were done to test whether there is a material difference in inrush currents between 3-winding and autotransformer arrangements in a realistic scenario where there is appreciable impedance between the energisation source and the transformer to be energized. While not exhaustively true and not applicable to every black-start situation, it was evident that the difference in inrush current is small enough that 3-winding transformers are sufficient for these generalized studies[3]. This was preferable to also using the PSCAD™-provided intermediate model of a 3-winding, 3-limb transformer in autotransformer configuration, which had problematic numerical instability issues causing repeated crashing of the simulation.

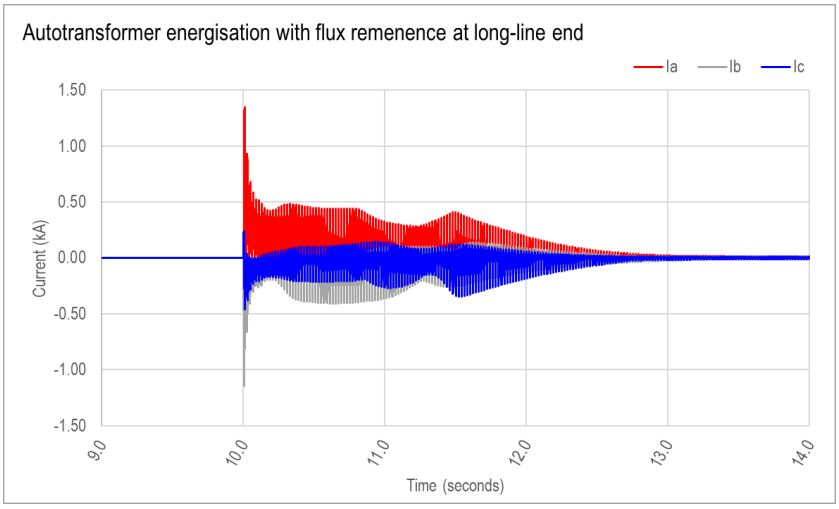

Figure 3 Autotransformer inrush profile from EMT studies

[3] In studies for system restart in a real system, inrush profiles are heavily influenced by both the unique parameters of each transformer and their structural arrangement. Such a simplification should not be extended to such studies.

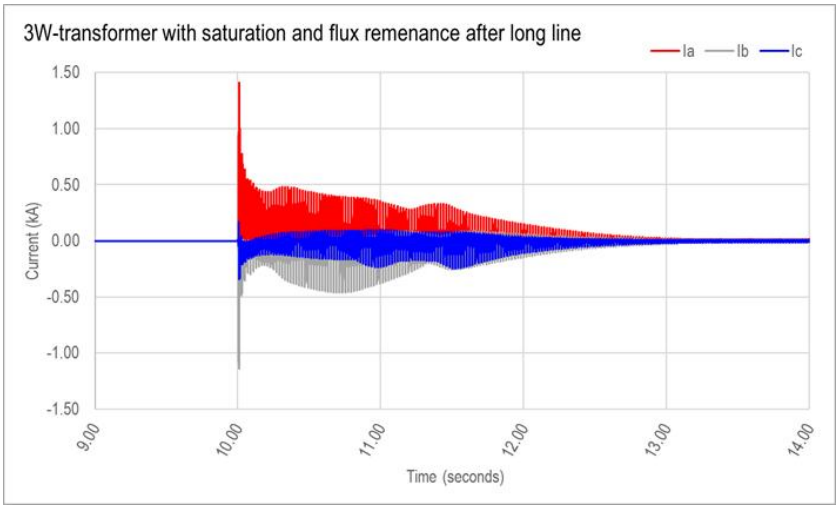

Figure 4 3-winding transformer inrush profile from EMT studies

3.1.7 Surge Arresters

Surge arrester profiles were based on ABB EXLIM devices, using publicly available data [6]. Notably the following profiles were chosen for the given voltage of the system.

- 220kV system: Model variant 192/152 kV
- 330kV system: Model variant 276/220 kV

Note that the profile given in the ABB datasheet causes an incongruity which PSCAD (rightly) reports on as a warning. This can be fixed by setting the 6th current point to be 9.5 kA (as opposed to 10 kA).

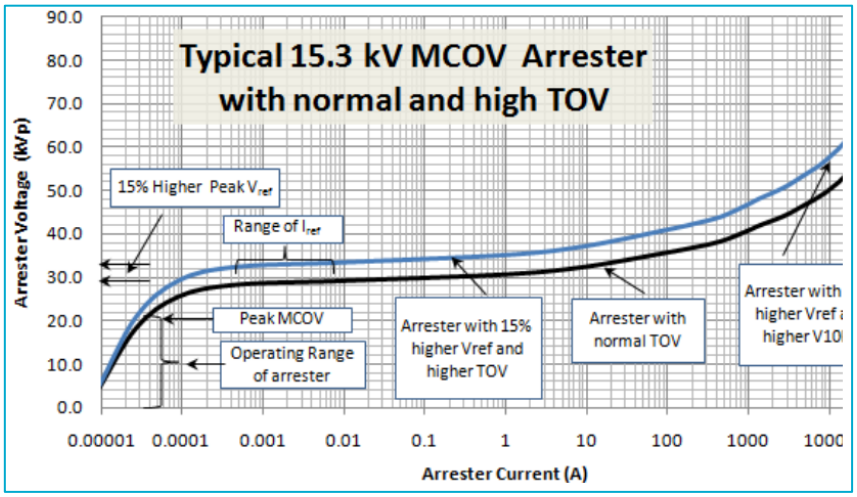

Figure 5 Example surge arrester profile [7]

3.1.8 Black starting GFM BESS model

The GFM BESS “black starter” model was adapted from an EPRI model publicly via the PSCAD website [8]. Several modifications were made to convert this device to operate as a

BESS, most notably changes to controller operational limits and functions to allow four-quadrant operation, as well as bypassing of both the in-built PV MPPT and boost controllers provided in the model. Battery representation was in-line with the typical approach used by BESS OEMs when representing their equipment for PSCAD studies, via use of a current-limited DC voltage source.

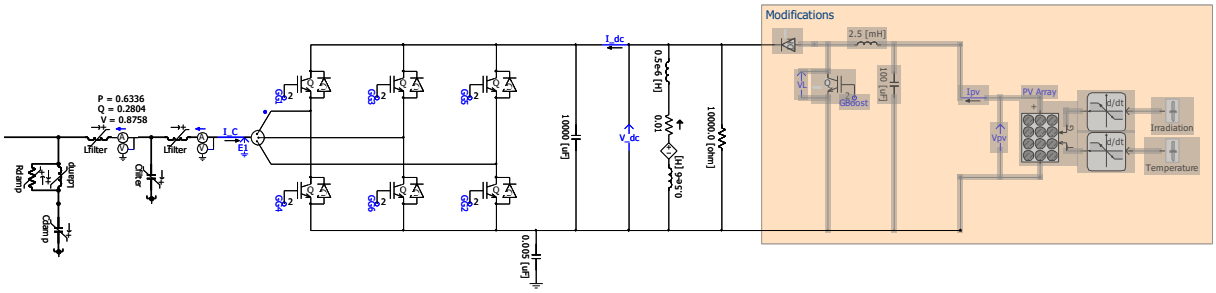

Figure 6 Key hardware modifications to allow functionality as a BESS

Various operating modes and settings were explored throughout the work, however the most crucial modes and settings to note are as shown in Table 1.

Table 1 Black start GFM BESS unit key settings

Setting	Value
Unit size	100 MVA (400x 0.25MVA)
Maximum active power input/output	± 90 MW
Maximum reactive power input/output	± 39.5 MVAr
Voltage Droop	4% (Gain = 25)
Frequency Droop	3% (Gain = 33.33)
Synchronisation Mode	Droop or VSM
Inertia Constant (VSM mode only)	Variable

Note that the within the model, the VSM mechanical time constant (MTC) is not identical to the inertia constant often used. There is an extra step required to convert from an inertia constant H (in energy units, joules) to the VSM mechanical time constant (in seconds):

$$MTC_{VSM} = 2 \cdot H \cdot F_{droop\_gain}$$

Where F_{droop_gain} is the reciprocal of the frequency droop amount. For example, to set the model for a desired inertia constat of 7s with a frequency droop of 3%:

$$MTC_{VSM} = 2 \cdot 7 \cdot \frac{1}{0.03} = 466.7$$

All the other settings in the model relating to control system stability were left as provided by EPRI, as it was found there was no need to alter these settings to achieve robust and stable performance from the model for a variety of scenarios investigated.

3.1.9 Other IBR models

Other models used in this study were provided by two confidential OEMs, and consisted of:

- GFL and GFM Solar farms

- GFL and GFM BESS
- GFL and GFM hybrid installations

These six model variants are strictly confidential and will not be released as part of the models developed for this work.

3.1.10 Synchronous machine

The synchronous machine model used in these studies is based on anonymised open-cycle gas turbine plant that has had its parameters further obfuscated as to retain similar performance but without sharing the same values as a real device. It has been sized to be the same as the GFM BESS model MVA rating. Machine saturation data is included.

The automatic voltage regulator (AVR) and exciter model in use is an (PSCAD) AC1C model, available in the default PSCAD™ library. Again, it has been parameterized with slightly modified real AVR parameters for the mating rotating machine. Limiters were not included for this work; however care was taken to monitor the field current and the apparent power of the machine to ensure it is not operating beyond normal bounds for an extended period of time.

The governor model used is a Woodward Gas Turbine-Governor model (GASTWD). It is once again parameterized with a slightly modified set of parameters that are appropriate for the specific machine model being developed. The E-TRAN library version of the controller structure is used as this has been well tested and provides fast initialization.

3.1.11 Breakers

As is required in black start studies, a breaker-node approach was used. This can be readily achieved using the default breaker models included with PSCAD™, however a crucial adjustment is made to allow them to be appropriately used in system restart analysis.

By default, the PSCAD™ breaker model has an open impedance of 1e6 ohms, which may appear large, but when working with voltages of several hundred kilovolts, is insufficient. Using the default breaker parameters when attempting to energise a transformer with flux remanence and saturation will result in sufficient leakage current through the “open” breaker to re-establish a flux in the transformer core, such that once the breaker is closed, there is very little if any additional inrush current required by the transformer. This consistently leads to over-optimistic results when it comes to transformer energisation in black start studies.

The correction for this is straightforward: Set the breaker open impedance to at least 1e9 ohms, and ensure “open at any current” is set to No.

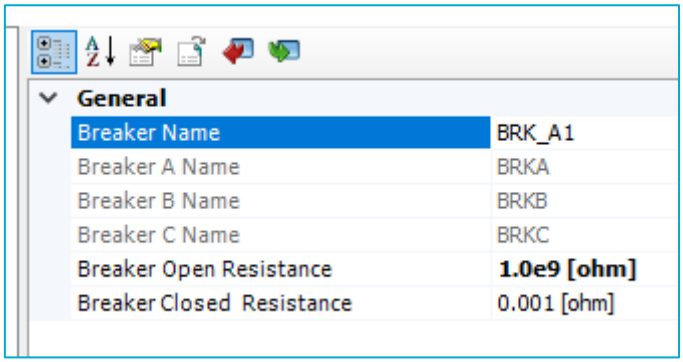

Figure 7 Crucial change to breaker settings for system restart work

3.1.12 Distribution and DER model

The distribution system, composite load and DER models for this work were developed by EPRI. Full details of the model are available through the EPRI website [9], with a brief overview provided here. Importantly, DER in this work refers only to rooftop photovoltaic solar generation. Other forms or interpretations of the term DER were not used in this work.

The topology of the feeder, load and DER model is shown in Figure 8 below. It consists of MV feeder representations, induction motor loads, configurable static loads, and both single- and three-phase inverter generation embedded at both the MV and LV levels (including proteciton mechanisms).

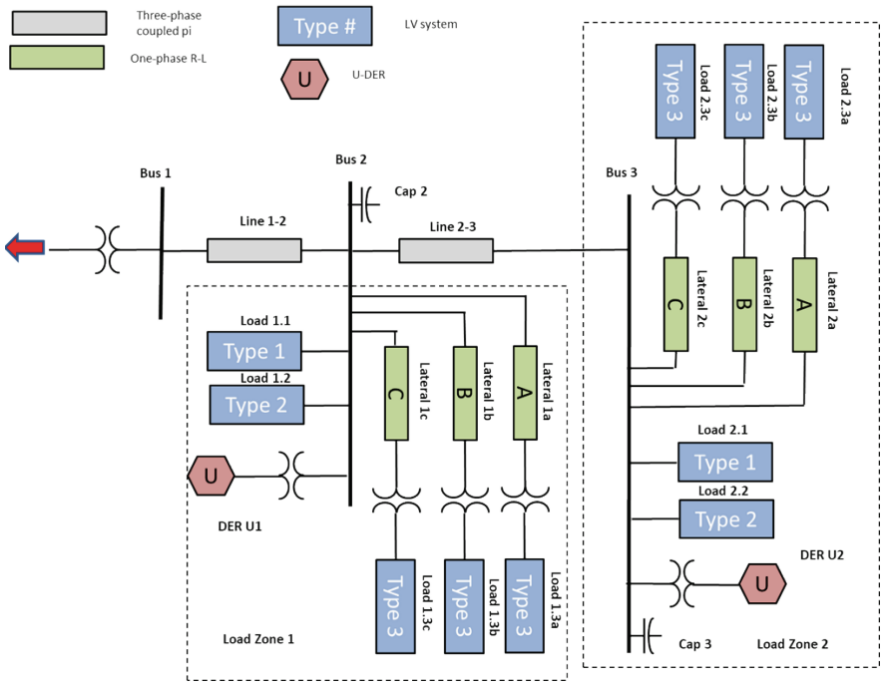

Figure 8 DER Feeder topology

For the work carried out, this feeder representation was configured based on expected proportions of load types and DER commonly seen in an Australian context. Importantly, DER can be seen at extremely high levels which can push the feeder well into reverse flow,

and the proportion of induction motor load is not as high as proportions commonly seen in a North American context. Details of a typical configuration used in this work is available in Appendix B

The larger 3-phase DER module consists of a controlled voltage source behind an impedance, which uses:

- A generic phase-locked loop (PLL) to synchronise at the point of connection.
- Real power and voltage control based on the WECC REEC_B model [10]
- An ability to respond to frequency and voltage deviations in line with requirements that may be applied to larger DER devices.

Smaller single-phase DER modules consist predominantly of a simple PLL-synchronisation mechanism looking to maximise active power export only (i.e., no voltage or frequency control). This is consistent with some much of the DER technology currently in service in the NEM today, although newer installations notably have obligations to respond to voltage and frequency deviations[4].

Both DER types have protection mechanisms applied consistent with maximum disconnection times of Australian Standards AS4777:2020 (Australia A).

- Underfrequency trip settings are set to 47 Hz for 2.0 seconds (passive anti-islanding).
- Overfrequency trip settings are set to 52 Hz for 0.2 seconds (passive anti-islanding).

Voltage trip settings are as per the profile shown in Figure 9.

[4] Whether this occurs in reality or not is an ongoing investigation, and readers are referred to GPST Topic 9.

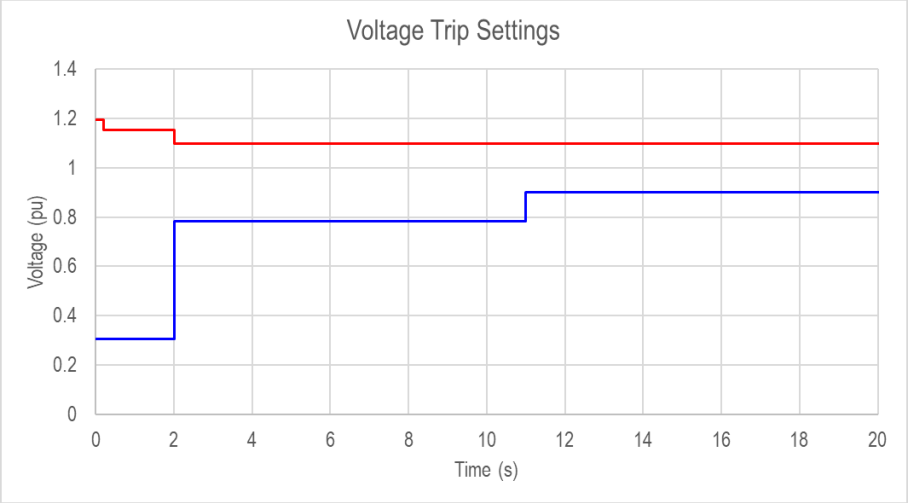

Figure 9 Voltage Trip Settings (right-hand side extends to infinity)

3.1.13 Network protection relays

Network protection relays used in these studies are based upon the soon to be released protection relay libraries developed by Manitoba Hydro International. These have been under development for almost 10 years and are at the final stages of development before final release to the broader public. Components of this library are shown in Figure 10.

The relays of most importance for these studies are the transformer differential relays (with harmonic blocking) and line distance protection, as these have the largest potential for maloperation during system restart due to transformer inrush currents appearing as an internal fault and insufficient total and negative sequence current provision (respectively).

The protection relays used were expertly parameterised for each corresponding network element by EPRI personnel with extensive experience in this area.

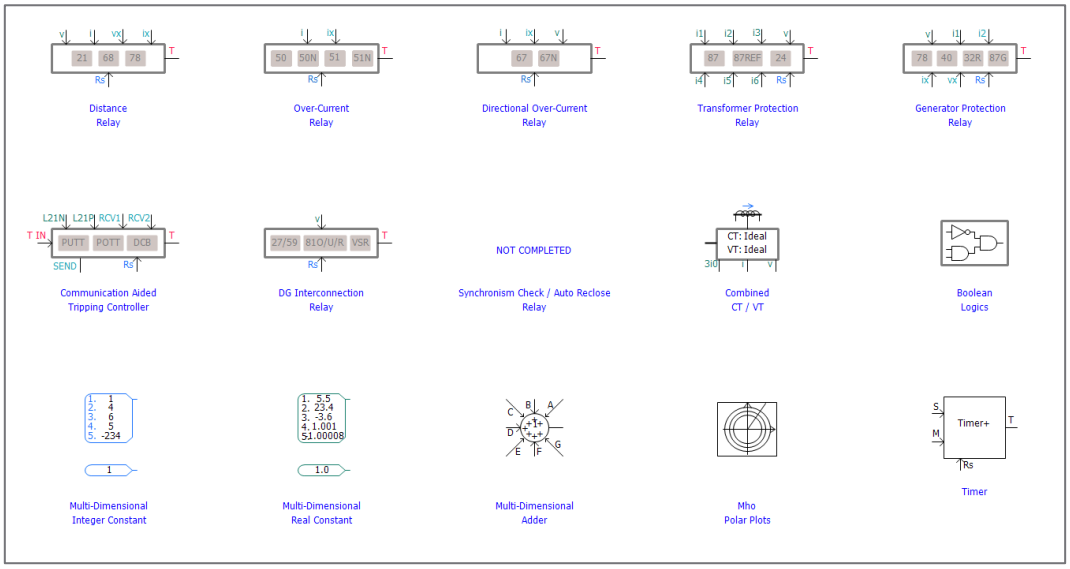

Figure 10 The PSCAD protection library suite under development

3.2 Analysis

The following outlines both the techniques and reasoning used to establish the cases used for the Stage 4 work, and the methods for analysing the output to determine whether a case is robust and stable, or what specific conditions had led to the failure.

3.2.1 Metrics

Evaluation of the performance of the system under test was completed using both qualitative and quantitative metrics, along with drawing on the experience of the researchers in evaluating real system restart performance studies.

The following metrics were evaluated within the studies:

- Plant protection relay operation (or pickup), indicating failure to ride-through a given disturbance or self-protection operation due to excessive unstable behaviour or voltage and frequency beyond acceptable bounds.
- Stability of each plant output, ensuring that the active and reactive power of each plant rapidly returns to an equilibrium, within its capability profile, without excessive or unbounded oscillations.
- Transmission system voltage response, ensuring that disturbances does not result in excessive overvoltages which could be likely to activate protection mechanisms, and that undervoltages are consistent with the disturbance applied and not instead due to the inability of online plant to meet system voltage support needs.
- System frequency response, ensuring that the system's response to disturbances does not result in excessive frequency variations likely to have operated plant or network protection relays, and ideally, that frequency remains within the operational frequency tolerance band (49.0 to 51.0 Hz) or at least within the extreme frequency excursion tolerance limit (47.0 to 52.0 Hz).

- Surge arrester (absorbed) energy, where sudden, large increases is indicative of conduction and hence an unacceptably high system peak voltage, indicating potential damage to primary equipment. An example is shown in Figure 11 below, where the sudden increase at t=5.0 s is indicative of surge arrester conduction.

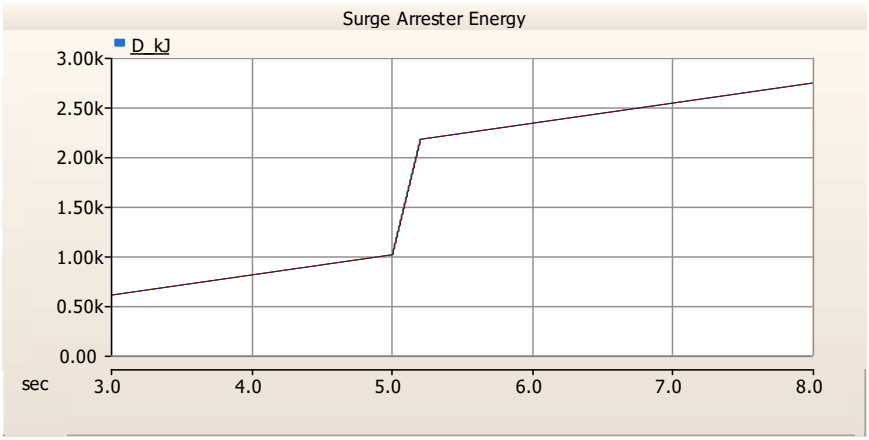

Figure 11 Surge arrester energy during simulated line energisation

- (Renewable generation) Park controller command setpoints, assessing these for reasonable responses to changes of the system state, and confirmation that slower instabilities are born from outer controllers in a system rather than from 'traditional' fast controller system strength issues.
- Controller references (direct current: Id_{ref}, quadrature current: Iq_{ref}, PLL frequency) internal to the inverters when major, fast instabilities are observed in resultant quantities (described above in this list of dot points). These quantities are strong indicators of inner-controller instability issues within inverters (as opposed to outer, slow controllers of the PPCs) and are strongly correlated with low system strength conditions.
- DER PLL frequency tracking behaviour (where relevant). For DER studies, the PLL frequency is a key indicator of internal controller stability, and loss of tracking is strongly correlated with low system strength conditions.
- DER protection relay operation (where relevant). Operation of these protection mechanisms indicate an unambiguous exceedance of acceptable system state (voltage and frequency) and an inability of DER to withstand the disturbance.
- Network protection relay operation and internal measurement quantities. These can be categorised as follows:
  - Operation of a network protection is an indicator of either:

    : a true positive, that the system state is beyond what is allowable for the assets in operation (e.g., voltage and/or frequency beyond bounds, asset current beyond acceptable levels), or

    : a false positive, that the quantities on which the protection relays operate upon are insufficient / have been corrupted enough to falsely trigger the

relay (e.g., excessive voltage or current harmonics results in a miscalculation of system state, resulting in a false trip of the relay).

  - A false negative, A disturbance that should result in operation of protection relays fails to so, resulting in possible damage to primary equipment (e.g., fault current is insufficient to trigger overcurrent-based relays).

- Voltage along a distribution feeder, as connection and disconnection of reactive power-insensitive DER may result in large over- and undervoltage events, and sustained undervoltage events may result in induction motor stalling. Similarly, DER feeder active and reactive current draw is monitored, to identify excessive draw that indicates motor stalling.
- For transformer energisation studies, current waveforms into the transformer and their harmonic components are monitored, to identify whether an energisation has completed successfully or if insufficient overcurrent availability from the system has resulted in a "stalled" energisation that causes extended undervoltages and an inability to establish a stable and equal flux in the transformer core.
- System voltage harmonics, measured at key buses (most notably at the high-voltage point of connection of the black-start unit) online and continuously throughout the simulation. Sustained voltage harmonics can be an indicator of:
  - A system that has failed to return to equilibrium.
  - A network or controller instability that has been excited.
  - The system lacking a characteristic (e.g., overcurrent) to allow energisation of assets with minimal sustained distortion.

  While some level of harmonics are ever-present in a real system (especially during disturbances), the decay of voltage harmonics following a state change gives insight into the ability of the system to recover quickly, and hence of its robustness.

3.2.2 Case establishment

When choosing and developing cases, the following was considered.

DER cases (milestone 1)

DER investigations were conducted from two different perspectives:

- The impact of DER on a 100% IBR system, from the perspective of whether high levels of DER (relative to the restart source) influence the ability of the upstream system to maintain stability.
- The impact of the type of the restart source (GFM BESS or synchronous machine) on the ability of DER to maintain its own stability in the face of common disturbances during a system restart scenario.

Generation types (synchronous versus converter based) and their ratios were chosen to investigate how various combinations can affect restart performance from the above two

perspectives, including the addition of GFL devices in the system to consider how this may alter the performance of the DER under test.

Additionally, sensitivity analysis was conducted to determine whether DER performance during disturbances was materially altered depending on the feeder loading (see Section 4.1.3). This analysis showed that the DER portion of the feeder model had no appreciable change in behaviour depending on overall feeder loading. Hence, in order to induce the worst-case scenario in all studies considered, it was decided to focus on the scenario that could cause the greatest change in state in the overall system, being the 150% DER penetration ratio (to underlying load, i.e., 45 MW DER export on a feeder with 30 MW underlying load).

Operational changes cases (milestone 2)

The following variables were considered when establishing cases that sought to determine what operational changes could improve system stability:

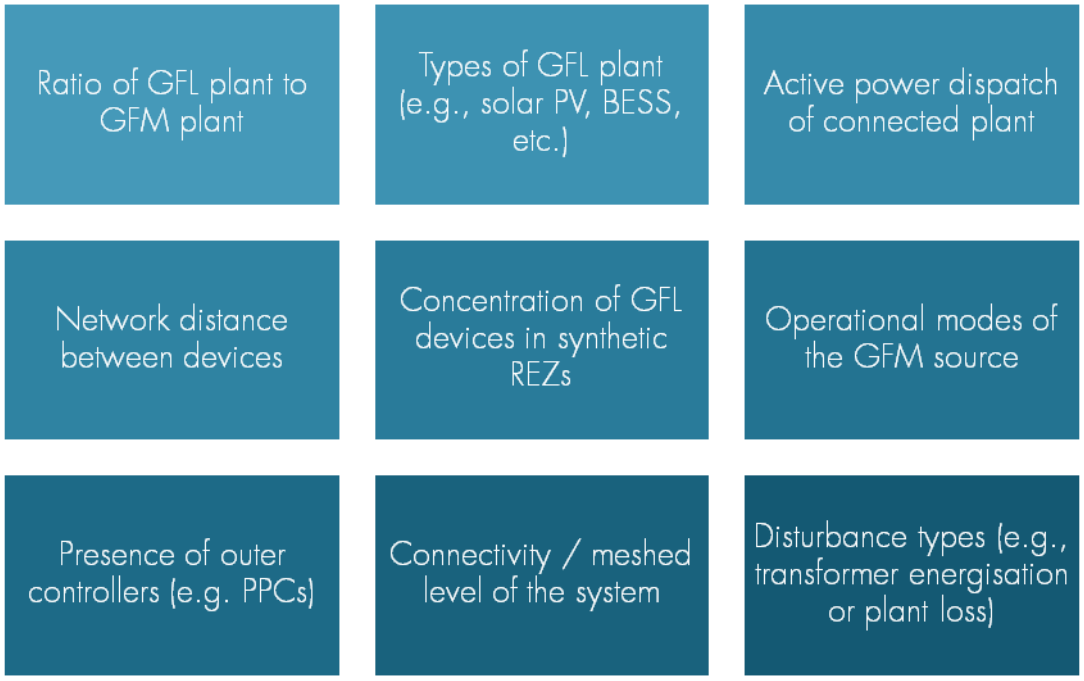

Figure 12 Variables considered for operational changes cases

With many degrees of freedom, it was not feasible to investigate all permutations of the above in the time available. Instead, engineering judgement was used to focus on items that showed the highest level of insight and practicality to be implemented in a real system. Where particular combinations were identified to be of interest but could not be investigated, these were flagged for future research. The cases selected for investigation are described later in this report in Section 4.2.4 to 4.2.12.

Network protection relay cases (milestone 3)

The network protection relay scenarios sought to evaluate the difference in performance of a system being restarted by a synchronous machine versus a GFM BESS restarting device.

Specifically, scenarios were evaluated that had not been considered in previous research stages [11] [12], including:

- Consecutive energisation of multiple transformers in series configuration and whether the differential relays for each transformer correctly block for subsequent energisation conditions.
- How reduced inrush currents (including reduced negative sequence components) supplied from GFM BESS affect the ability of the protection relays to correctly discriminate fault conditions.

The cases developed were based on the aforementioned limited area network model, specifically looking at multiple transformer energisation at the end of long lengths of transmission line; a known challenge for system restart. An example of the case setup used is shown in Figure 13.

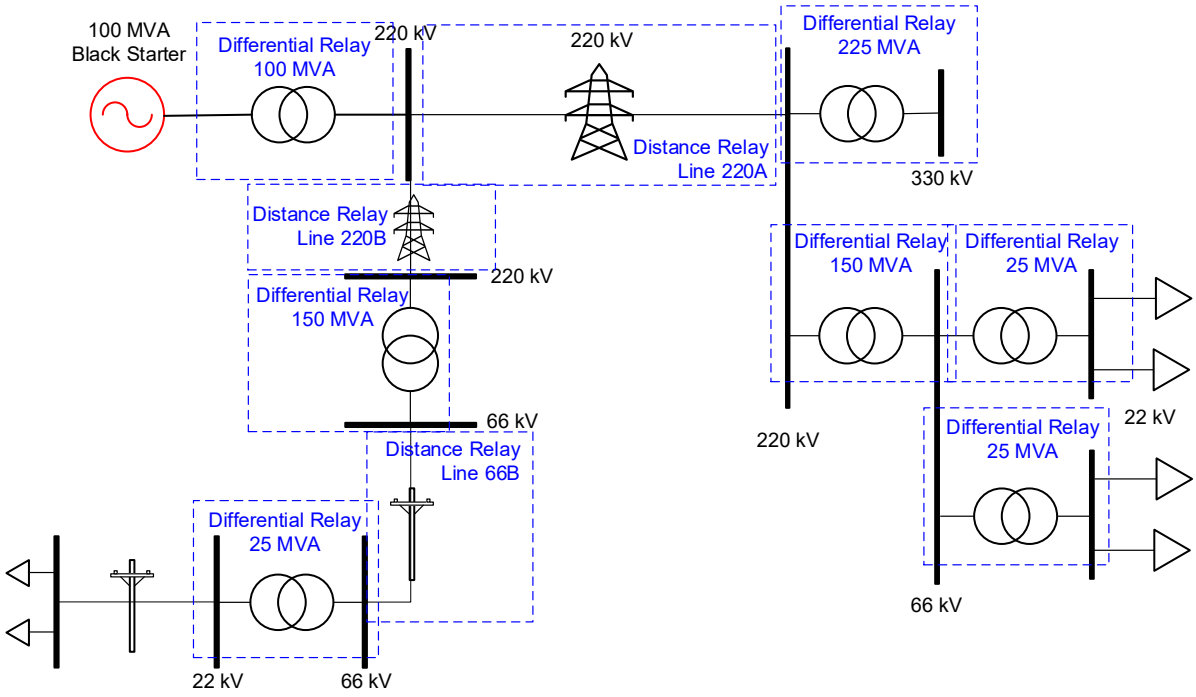

Figure 13 Typical topology used for protection studies

The performance of a scenarios under analysis in the network protection space was evaluated based on whether a relay:

- Tripped correctly for a valid fault condition.
- Tripped incorrectly for a non-fault condition.
- Failed to trip for a valid fault condition.

Additional considerations were also given to assessing the level of harmonic distortion in both current and voltage during both network element energisation and several seconds post-energisation. This allowed extra insight into which components are most dominant in

generating harmonics in these scenarios, and how any harmonic blocking elements could be adjusted to maximise the likelihood of correct relay operation.

Procurement timeline (milestone 4)

During the development of scenarios to estimate the time frames along which it will become desirable to procure system restart services from IBR, it was determined that attempting any more than a high-level approximation of the level of IBR technology required to replace retiring synchronous machines would not be prudent, as during system restart, it is often the very specific nature of the surrounding network and the specific generator being used that will determine the success of the restart.

Instead, it was agreed with stakeholders that the following approach could be used:

- Benchmark the capabilities of a synchronous generator against a GFM BESS to be able to energise a long transmission line and a large transformer located at the end of that transmission line.
- Hence, determine the ratio of GFM BESS required to approximately match the capability of a synchronous machine.
- Plot the expected decline in synchronous sources in the NEM over the next 10 years.
- From the above, estimate the amount of GFM BESS required to replace each of the synchronous machine closures to provide a high-level estimate of how much GFM BESS restart sources could be required over the next 10 years.

While the initial benchmarking is completed in PSCAD, this milestone is predominantly a desktop exercise to be completed in spreadsheets to give indicative figures to determine the urgency of IBR restart rollout in the NEM.

4 Results

4.1 Milestone 1 – DER in System Restart

The focus of this work is to better understand how varying penetration levels of DER can affect the restart viability of both a 100% IBR and synchronous system restart, and evaluate how common disturbances that could be experienced during system restart affect the performance of a DER-rich system.

A summary of the case variants investigated in this work is provided in Table 2. These are used throughout the analysis to determine the conclusions summarised in the next section.

Table 2 DER investigation case variants

Black Start Source	Variation	Disturbance
Grid Forming BESS	0%, 50%, 100%, 150% DER penetration	Transformer energisation
	Additional nearby grid-scale GFL IBR	DER & load pickup
	-	Phase angle jumps
	-	DER mass re-connection
	-	DER energy source changes
Synchronous Machine	0%, 50%, 100%, 150% DER penetration	Transformer energisation
	Additional nearby grid-scale GFL IBR	DER & load pickup
	-	Phase angle jumps
	-	DER mass re-connection
	-	DER energy source changes

4.1.1 Key findings summary

- The black-start source influences the likelihood of DER protection operating during restart when transformers are hard-energised[5] in the system. Through the studies completed it was seen that:
  - GFM BESS restart technology will result in shallower voltage dips than synchronous sources, but recovery to nominal voltage envelopes can take seconds to tens of seconds, leading to DER trips.

[5] System voltage is at 100%/nominal values when the circuit breaker is closed to energise the asset, as opposed to soft-energised where the system voltage is at 0%, the circuit breaker is closed, and then the system voltage is ramped to 100% over several tens of seconds.

  - Synchronous restart technology will result in slightly deeper voltage dips but recovery to nominal voltage envelopes occurs more quickly - within a few seconds, reducing subsequent DER trips.
- Analysis of voltage waveform harmonic components during disturbances showed major differences (between synchronous and GFM BESS based restart options) in the presence of certain lower-order harmonics. Furthermore, it was noted that throughout the studies that both frequency measurement tools and fast controllers such as PLLs showed greater stability during disturbances when a synchronous source was used, possibly indicating a link between synchronisation ability and the presence of certain system harmonics. This is a recommended area of further study.
- Extended voltage dips during transformer energisations were observed to be the primary cause for DER to trip offline for the scenarios considered. Depending on the restart technology, this may be both a problem and an opportunity during the restart process.
- For DER to restarter MVA ratios up to 45:100 (the maximum studied in this scenario), DER mass-reconnection following feeder pickup did not destabilise the restarting system (both for GFM BESS and synchronous restart options), provided that the minimum active power export requirement of the synchronous machine was met. However, transient overvoltages were observed, which may have adverse local effects, including tripping of plant and protection relays.
  - When additional GFL plant was connected to the extent of the (marginal) limit of stability during restart for the given case, such DER reconnection disturbance events still did not destabilise the system.
- DER energy source variations across the length of a feeder[6] showed no adverse impact on the restarting system, as both synchronous and GFM BESS technology were easily able to compensate for what were ultimately slow changes in system voltage and frequency.
- For the distribution network and DER model studied, the DER's response to a system phase angle jump behaviour does not appear to be materially affected by the restart source. Both GFM BESS and synchronous black start sources saw the DER ride through major phase angle changes without issues.
  - Synchronous-based restart saw voltage variations of greater magnitude and slower recovery time than GFM BESS scenarios.
  - GFM BESS-based restart saw slightly poorer (more delayed) PLL synchronisation ability than synchronous scenarios.
- DER penetration levels beyond 80% of the nameplate rating of the GFM BESS used during black start saw DER PLL tracking instabilities begin to manifest even in absence of any

[6] DER sources were spatially distributed across the feeder, but were all of the photovoltaic type

disturbance. However, such behaviour was not observed when a synchronous machine black start source was used.

- Initial studies into whether the presence of DER degrades the available system strength for the rest of the system were inconclusive, tending towards there being no strong link. This is a recommended area of further study.

4.1.2 Milestone objectives

The objectives of this milestone included investigating:

- The effect of MW ratio of DER energised to the black-start unit.
- The effect of the type of black-start unit (i.e., synchronous or IBR) on the performance of the DER
- DER's response to common disturbances typically experienced in a restarting system.
- The impact of DER energy source variations on system state (primarily frequency and voltage, but also including power flows).
- Any practical mitigation strategies to any instabilities discovered.

Importantly, the analysis considered two interaction directions, in that there was analysis both on the black-starter's performance in the presence of alternative configurations of DER, and DER's performance with alternative black-start technology.

4.1.3 The impact of grid-scale generation on DER performance

Studies using the EPRI-developed DER model in this work show that for modest levels of DER in a restoring system (i.e., DER MW rating < 50% black start unit MVA rating) the impact of grid-scale generation on DER behaviour is largely a endogenous problem in which the pre-defined internal DER protection settings are likely to be the determining factor. For modest penetration levels, DER is likely to trip for sustained undervoltages, sustained frequency deviations and other disturbances with which a corresponding protection mechanism is associated, more-so than exhibit instability. However, as will be shown in Section 4.1.5, for a 100% IBR restart scenario, when the DER MW amount exceeds more than approximately 80% of the GFM BESS black start unit MVA rating, ongoing PLL instability of DER is observed which is indicative of a system problem – a trend that was not seen when a synchronous machine was used as the black start unit.

Of further note are the differences in DER voltage and frequency recovery profiles that the bulk generation restart source may deliver in response to a typical disturbance during restart – most critically during transformer energisation. Figure 14 compares the voltage and frequency recovery trajectories (as measured at the DER-rich feeder head) following a large transformer energisation, with two different (but equally sized and located) black start sources.

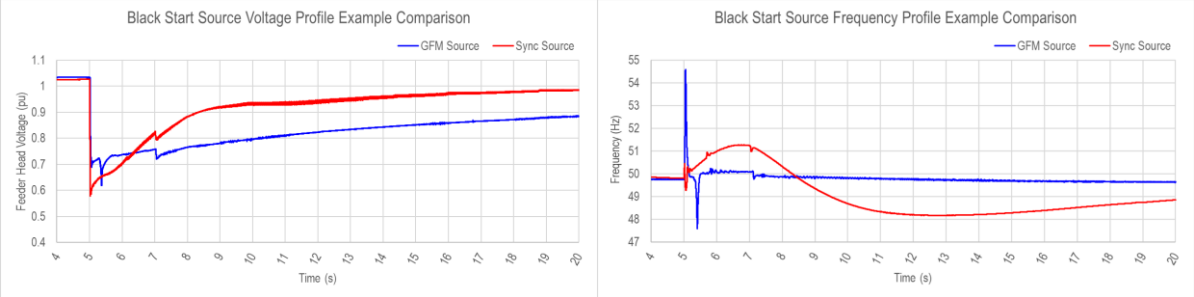

Figure 14 System voltage and frequency profiles for different black-starters subject to a transformer energisation

In the above, there are non-ideal aspects regardless of the option chosen:

- The synchronous machine black-starter imposes an initially deeper (than the GFM BESS) voltage dip (which may increase the risk of motor stalls and disconnection of load), but the profile recovers faster than a GFM BESS black start solution, reducing the chance of DER trips due to sustained undervoltage[7].
- The GFM BESS black-start source does not exhibit such a deep voltage dip as the synchronous machine, but has a more linear (constant rate of change) recovery to nominal voltages that is also far slower, which can potentially trigger extended undervoltage protection mechanisms.
- The GFM BESS has a generally flat frequency response to the disturbance[8].
- The synchronous machine, by virtue of its inherent dynamics, has a large and (relatively) slow frequency variation following the transformer energisation which may have greater potential to trigger disconnection of other plant or disconnection mechanisms.

The above differences in system performance between a GFM BESS and a synchronous machine hence forms a comparative baseline used in the rest of these studies on the effect of the black-starter on DER performance.

Transformer energisation

As may well be expected, the sustained undervoltage following transformer energisation is a common and major recurring challenge during system restart. It affects the ability of both grid scale generators and DER to remain connected to the system, with wide-spread extended undervoltages across the system common for situations where the transformer is energised in direct opposition to its flux remanence. The situation is exacerbated when the

[7] It is recognized that the presence of DER is a known challenge for synchronous restart due to the erosion of load required to maintain stability of synchronous machines due to minimum active power export requirements, however the instantaneous trip of a DER device may induce a transient on the system which itself may problematic for the fragile system to withstand.

[8] The frequency spikes seen in the above image are a function of the measurement method chosen to produce this image (filtered zero-crossing of voltage), but this itself is worth further exploration as it is not present for a synchronous black-start source. Further discussion is provided in Harmonic components of voltage waveforms.

available overcurrent of generators is insufficient to meet the inrush requirement of the transformer being energised, potentially extending the flux re-establishment time to tens of seconds to minutes, all the while with the system experiencing low voltages with high harmonic distortion. This is of particular concern in a system being restarted by an inverter-based source, which typically does not have the same inherent overcurrent capability that a synchronous machine provides.

Such events can exceed the limits set for the undervoltage timers in both network and generator protection relays, or cause maloperation of protection relays due to the high harmonic content of waveforms (as will be explored for Milestone 3, in Section 5.3). Additionally, the supressed voltages can cause motor stalling (both in the distribution network and in the auxiliaries of other non-black start utility-scale generators), or the tripping of DER.

Figure 15 below shows a common response seen throughout this work, of each of the DER and transmission connected GFL IBR, in response to a transformer being energised in a GFM BESS-based system restart.

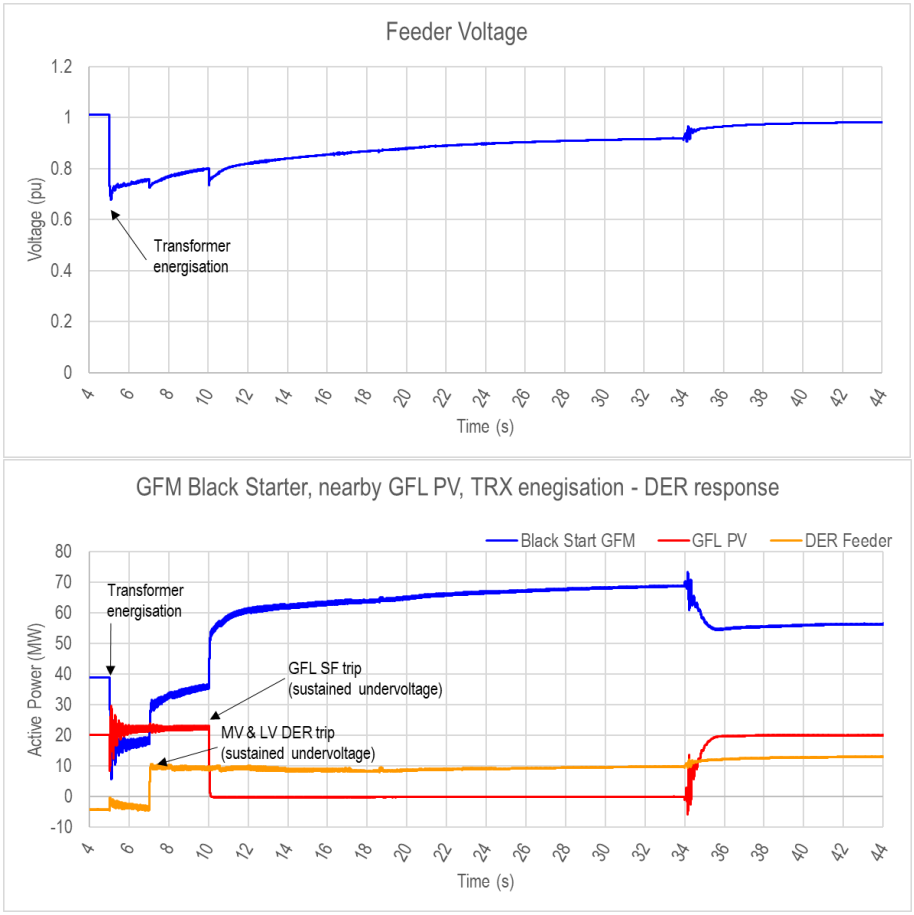

Figure 15 Voltage and active power response of a GFM BESS-restarted system with a transformer energisation

Notably, the extended voltage recovery profile results in undervoltage protection tripping of both DER and grid-scale GFL IBR connected at the transmission level.

Importantly, such behaviour was seen to be inherent to the black-start source, and was not significantly affected by the ratio of DER in a system, either for better or worse.

In particular, the following (Figure 16) shows a sensitivity study of how a feeder with 0%, 50%, 100% and 150% DER penetration responds when an upstream transformer energisation occurs in a GFM BESS based system restart. Regardless of the penetration level, the voltage response is effectively identical and the frequency response very similar– and the extended voltage depression experienced by the system triggers undervoltage protection of DER after two seconds, along with tripping of some distribution load (mostly motor load).

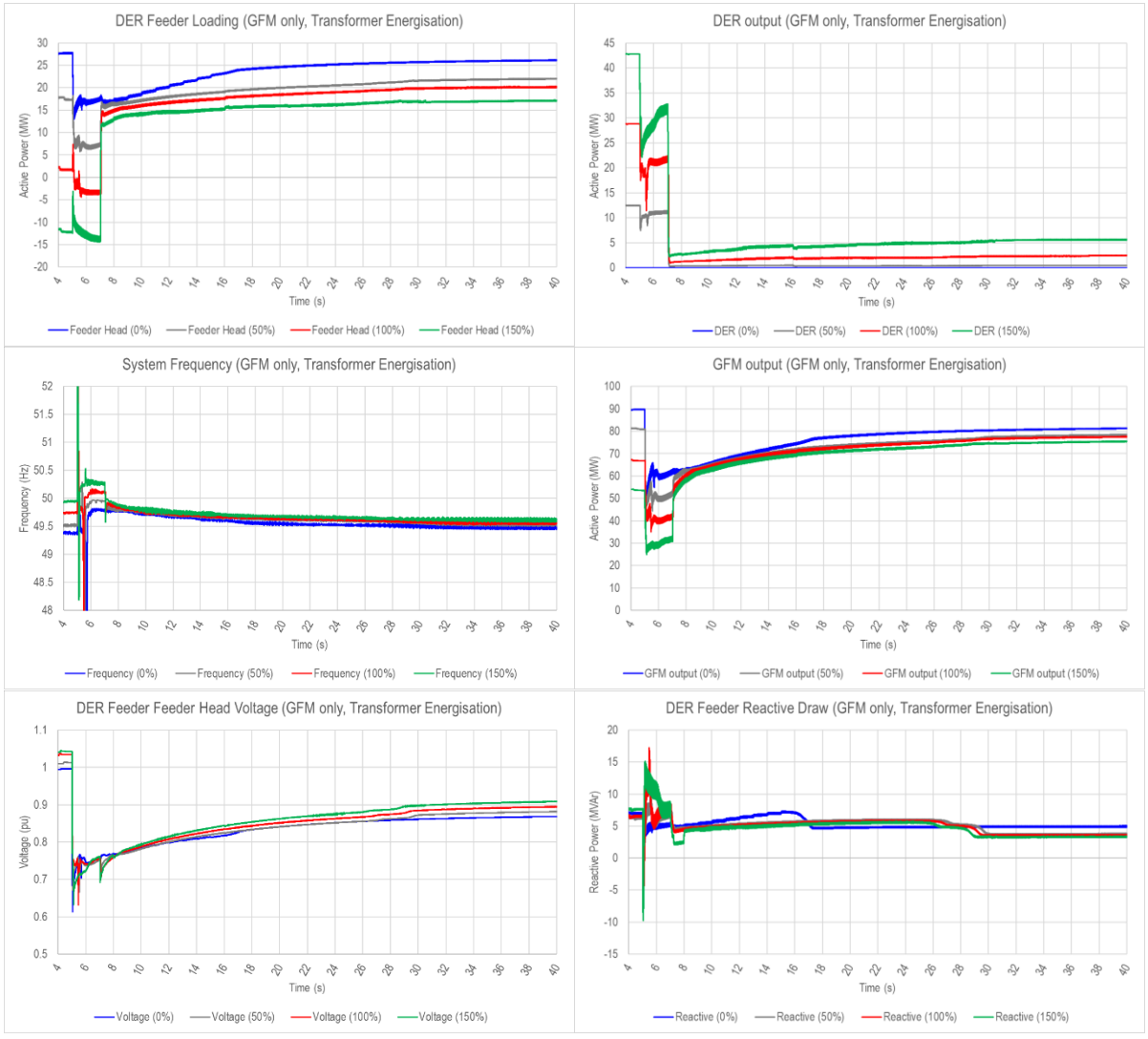

Figure 16 System performance for varying DER ratios

The conclusion is that transformer energisation in a GFM BESS restarted system is likely to result in increased DER disconnection on undervoltage, comparatively to that of a synchronous machine-based restart.

Phase angle jump

A test disturbance representing a phase angle jump was implemented through an idealised MV feeder transfer event – a feeder was transferred to another bus with a phase difference. The phase angle difference between buses was intentionally set to a high value (60 degrees) to induce any potential phase-angle jump instability from the devices.

The scenario was repeated for a grid-forming BESS black-starting device, and a synchronous machine black starting device to investigate whether the restart source has any effect on the ability of the DER to maintain stability during the disturbance.

The topology of the arrangement is shown below.

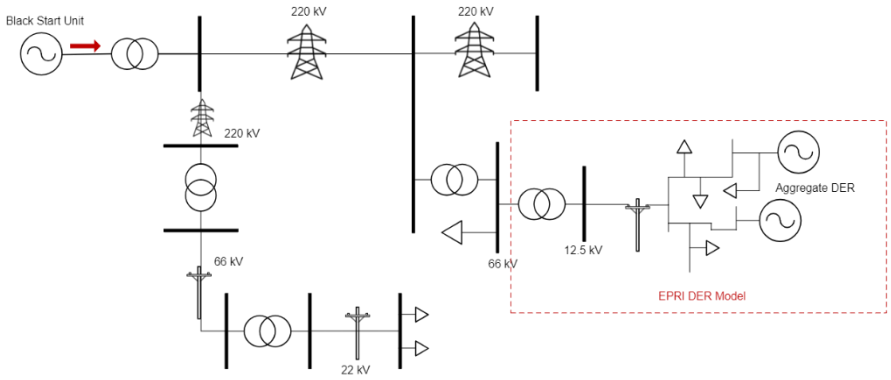

Figure 17 Phase angle jump topology arrangement

Grid-forming black start source

The DER response to a large phase angle shift for this scenario produces the following behaviour:

- A transient dip in DER active power export which is readily compensated by the GFM BESS black starter.
- At the transmission level, a voltage dip with a peak drop of 5.5%, that rapidly recovers to a stable value close to pre-disturbance value.
- At the distribution level a relatively large voltage swing (~9% peak-peak), but which rapidly settles back to a pre-disturbance value.
- DER PLLs retain tracking reasonably well, although it is noted that the variance is higher than that for the synchronous machine-based case.

The case shows no sign of instability, nor was any DER protection operation observed. It appears that for a black-start scenario driven by a GFM BESS device that a modest amount of DER (~45% of black-starter unit rating) can tolerate large phase angle jumps, given the DER representation used in this model.

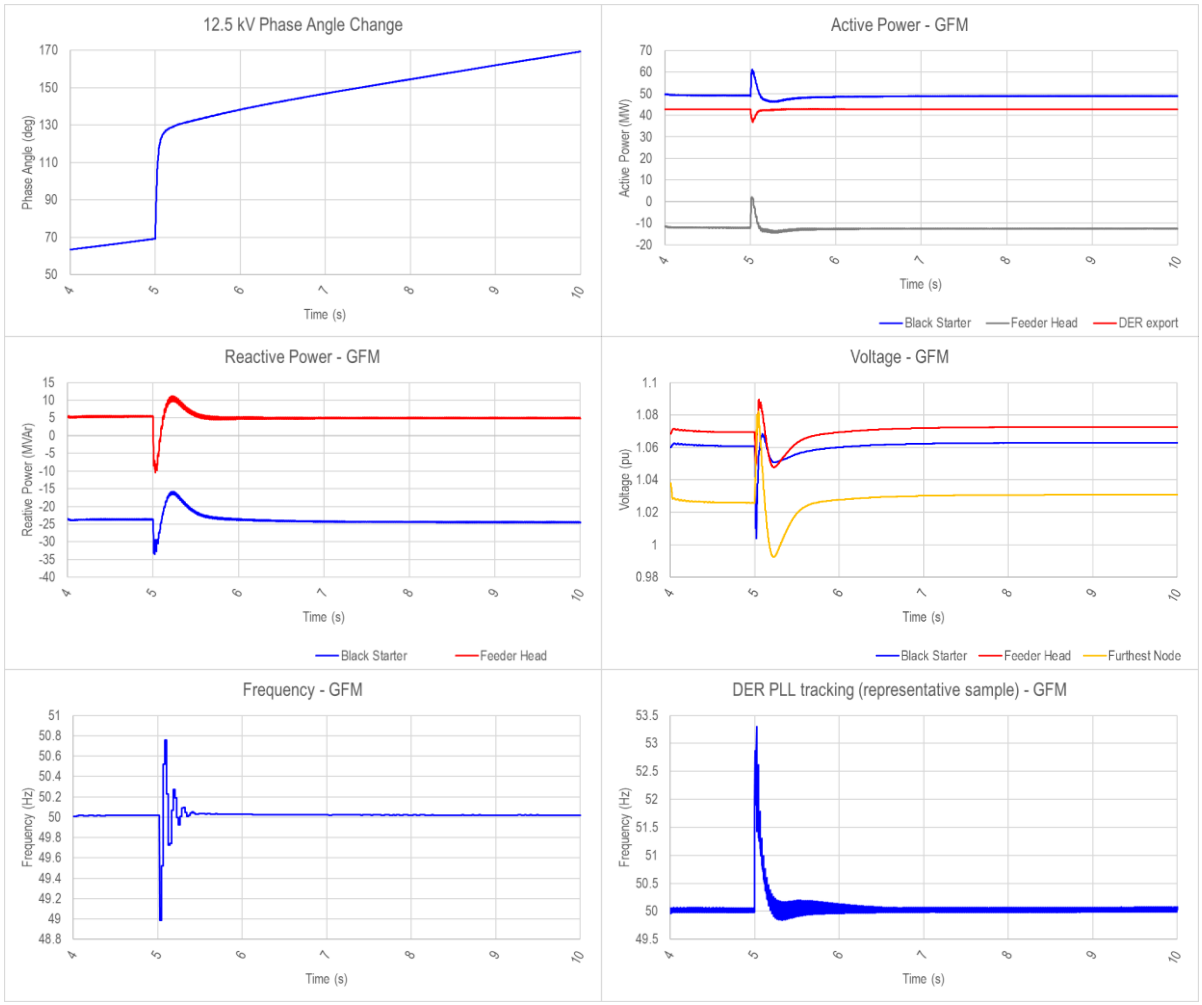

Figure 18 DER response to phase angle shift with GFM BESS black starter

Synchronous black start source

The DER response to a large phase angle shift for the similar scenario with a synchronous machine restart source produces the following behaviour:

- A transient dip in DER active power export which is readily compensated by the synchronous black starter.
- At the transmission level, a 3% peak-peak voltage swing, that rapidly recovers to its pre-disturbance level.
- At the distribution level a comparatively larger voltage swing (~12% peak-peak), but which rapidly settles back to a pre-disturbance value.
- DER PLLs retain tracking well, with less variance than that observed in the GFM case, indicating a stronger synchronisation occurring between the DER and the black starter units.

The case shows no sign of instability, nor was any DER protection operation observed. It appears that for a black-start scenario driven by a synchronous device that a modest

amount of DER (~45% of black-starter unit rating) can tolerate large phase angle jumps, given the DER representation used in this model.

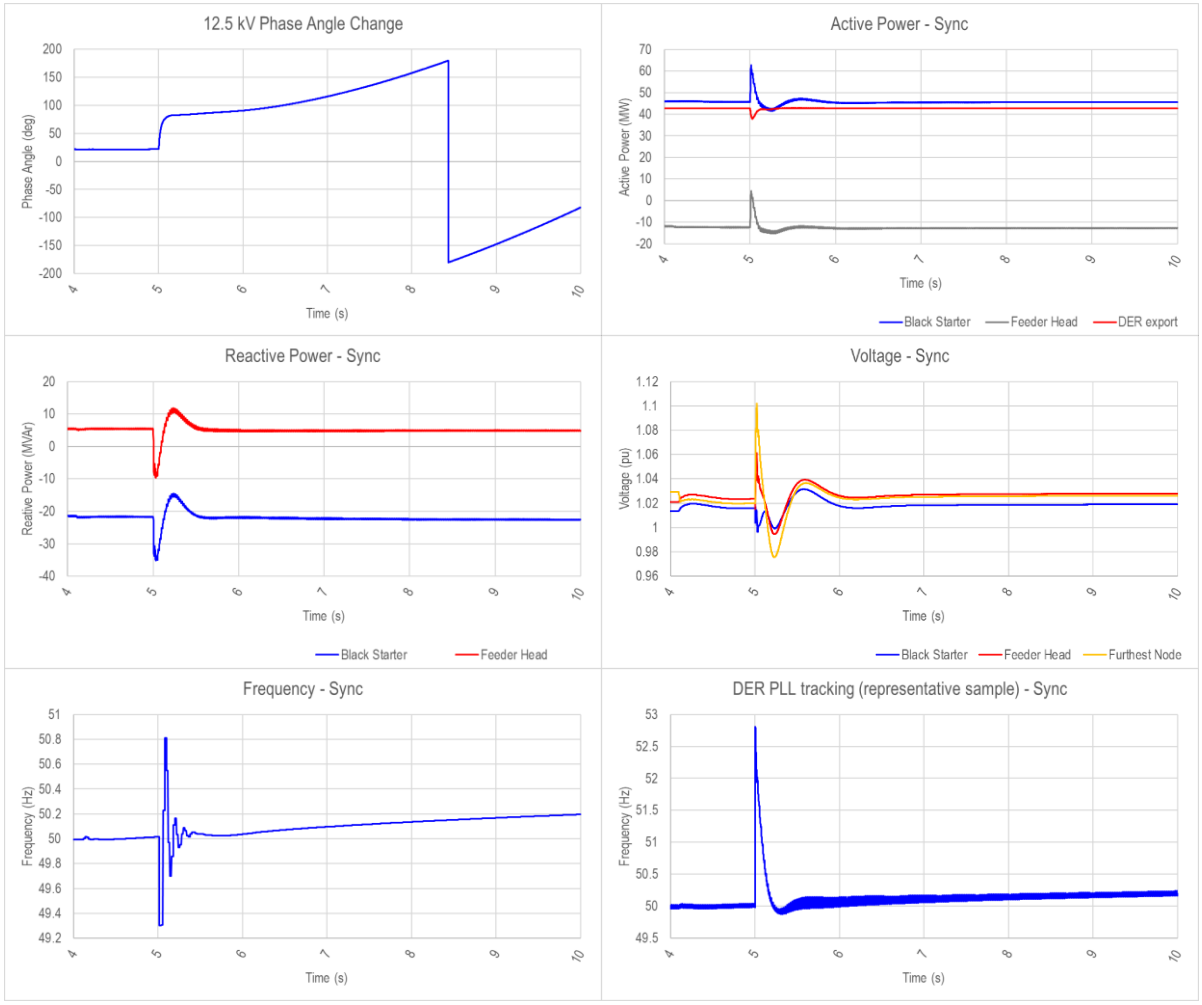

Figure 19 DER response to phase angle shift with synchronous black starter

High penetration of transmission-scale GFL devices

Initial studies were performed to determine whether DER could have an impact on the resilience of the power system from a system strength perspective; that is, determining whether DER "consumes" system strength like a grid-scale GFL IBR plant [13] [14]. These studies were exploratory only based on stakeholder feedback and were not comprehensively evaluated. This is an area for further work.

To test this, a marginally stable case was developed, whereby a 100 MVA GFM BESS black starting unit and an 800 MVA grid following solar farm (230km away on a 220 kV network) are energised at low MW export levels (This recognises that system strength stability issues are a function of MVA rather than MW, although MW export can have an additional effect on system stability). Through empirical testing in Milestone 1, this arrangement is known to be on the very edge of GFL inverter capacity limits for [frequency?] stability and even relatively minor disturbances could result in the GFL device losing stability and subsequent system collapse.

A small 25 MVA sub-transmission-to-distribution transformer is then hard energised (circuit breaker is closed with the system voltage at nominal) at “the worst possible moment” where the instantaneous system 3-phase voltage requires an instantaneous flux establishment in exact opposition to the transformer’s existing static flux remanence, causing large inrush current draw. The resultant disturbance results in a barely stable system that only just returns to equilibrium. This was repeated for DER being enabled and disabled, with efforts to recreate similar voltages and active and reactive power export amounts for the black start unit and GFL device. The topology of this arrangement is shown in Figure 20.

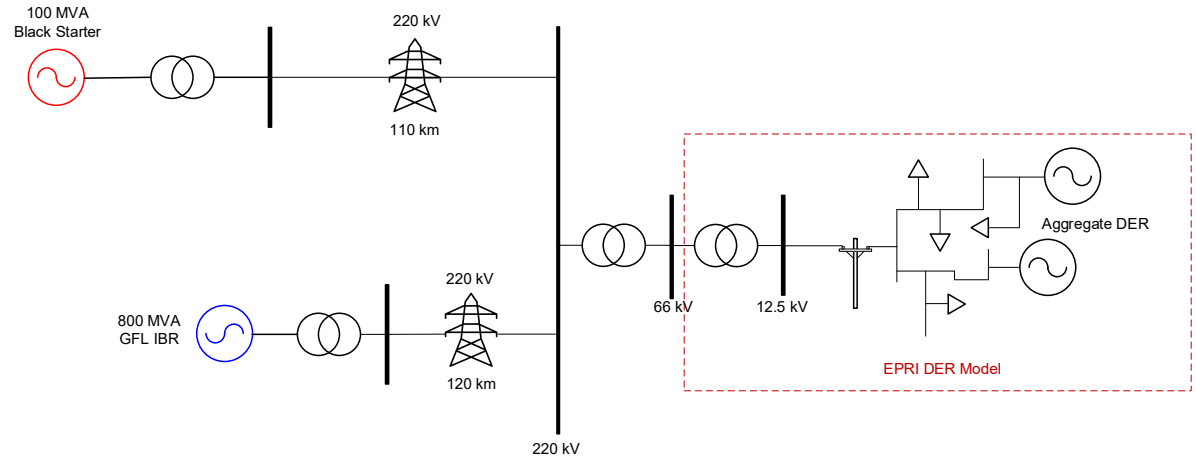

Figure 20 Topology for analysis

From these studies alone, it is not conclusive whether DER has a destabilising effect due to a “consumption” of system strength. Figure 21 and Figure 22 show the results of DER being enable and disabled in the system respectively. Clearly there is an effect of DER being present in the system, and the DER itself uses PLLs to remain synchronised with the broader system which is subject to instability. However, there are also very large impedances and multiple transformation levels between utility-scale GFL devices dependent on system strength and DER, meaning higher-frequency transient responses (a primary factor when it comes to system strength) are unlikely to interact between the transmission and distribution systems. Instead, it may be that bulk energy movements from DER (e.g., tripping, reconnection) at inopportune moments could push a marginally stable system beyond its stable envelope, but such events would be equivalent to those due to DER for other technologies as well. This area is recommended for further research.

DER enabled case

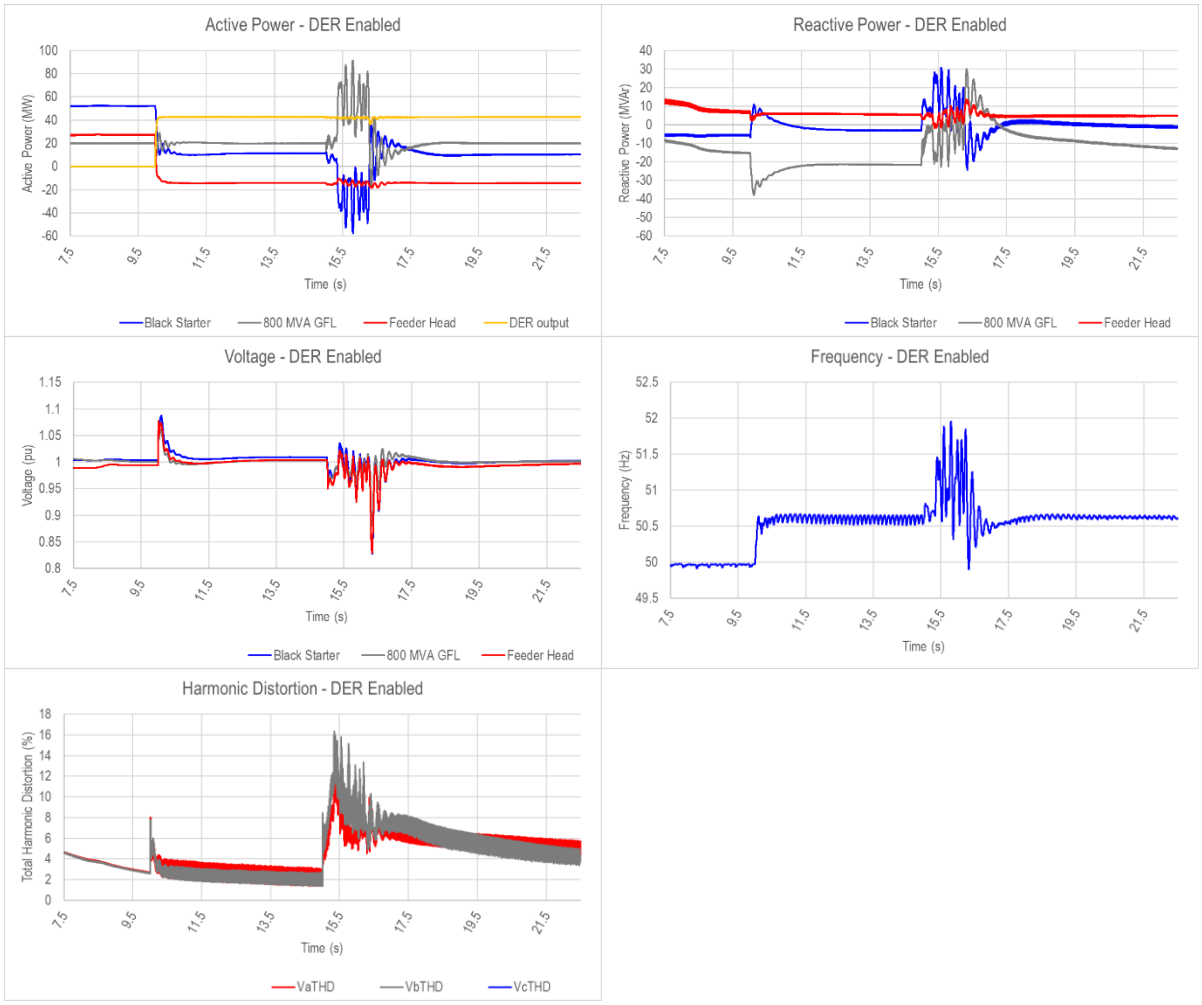

Figure 21 Marginally stable case with DER enabled responding to a disturbance

DER disabled case

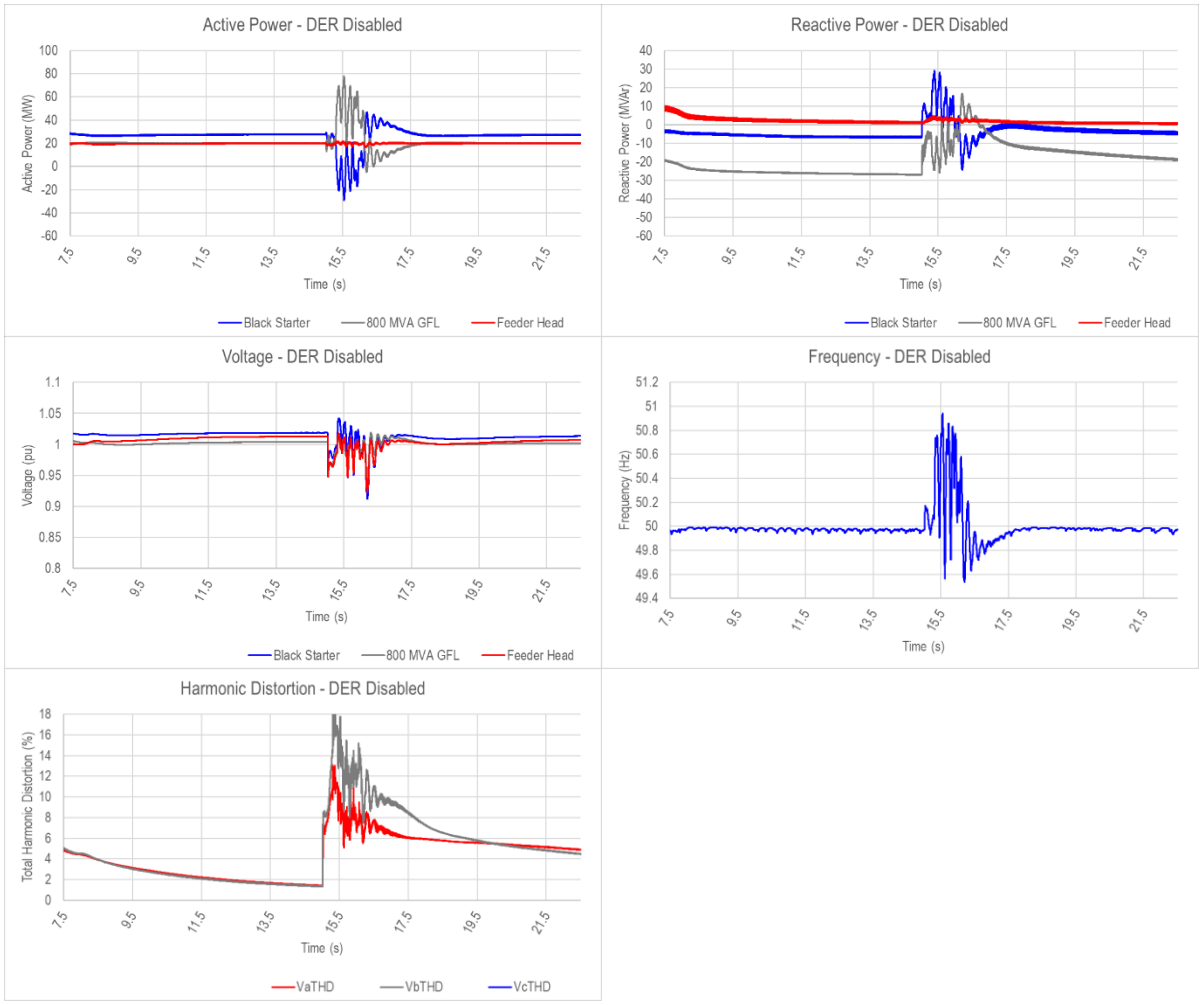

Figure 22 Marginally stable case with DER disabled responding to a disturbance

4.1.4 The impact of DER on the restarting system

Effect of DER bulk-reconnection

A major concern regarding energising distribution feeders with DER during system restart is the effect that the uncontrolled reconnection of DER will have on the fragile restarting system. That is, a sudden reconnection of potentially unstable DER could result in voltage and frequency variations that ultimately collapse the restarting system.

To test the validity of this concern, a case was established where a 100 MVA black starting unit energises a feeder containing approximately 45 MW of DER, offsetting the 30 MW load on the feeder (so -15 MW net flow). This represents a DER to black-starter MW ratio of 45% and assumes that the feeder in question has DER at 150% of maximum load capacity. These are very high ratios, and during an actual black start, efforts will always be made to avoid high-DER penetration feeders such as this. However, it serves as a good starting point for a proof of concept – if the fragile system can tolerate this, lower ratios can almost certainly be accommodated.

The 30 MW underlying load is hard-energised, and the DER comes online 7 seconds later. The DER component of the distribution load was enabled in such a way to represent a theoretical worst-case scenario where all DER reconnects at full export power simultaneously. This is unlikely to occur in reality. However, again, if the fragile restarting system can withstand this case, it follows that a more gradual return of DER export is a less challenging.

This scenario was repeated for both a GFM BESS black starter and a synchronous machine black starter in a limited area network. The general case topology is shown in Figure 23.

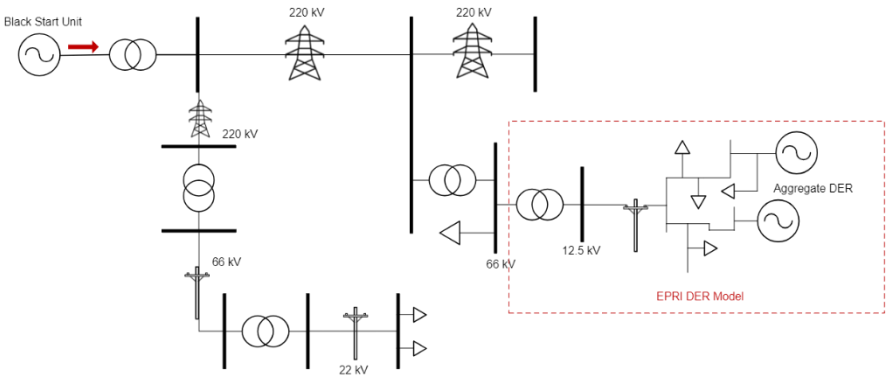

Figure 23 Case topology

Note that it is typically several minutes between energisation of a feeder and DER reconnection to the grid, however inclusion of such a delay is not practical for EMT simulation timeframes, hence the DER reconnection timeframe is shortened, and occurs soon after the system returns to equilibrium following load energisation.

The results presented below suggest that so long as the DER export does not breach the minimum active power export limit of the black-starting source, the sudden change in net

load is readily absorbable by even a weak system comprising only a single black start device over 100km away.

GFM BESS-based system restart

Upon DER reconnection at t=10s, a transient overvoltage is observed. However, it is rapidly accommodated by the GFM BESS, returning to a nominal steady state value within a second. There is a corresponding sharp frequency increase, but the RoCoF appears to be of no concern to the GFM BESS, and the high resulting steady state frequency in principle could be corrected through setpoint manipulation to bring the system back into more acceptable ranges. Harmonic distortion of the voltage waveform remains at acceptably low values.

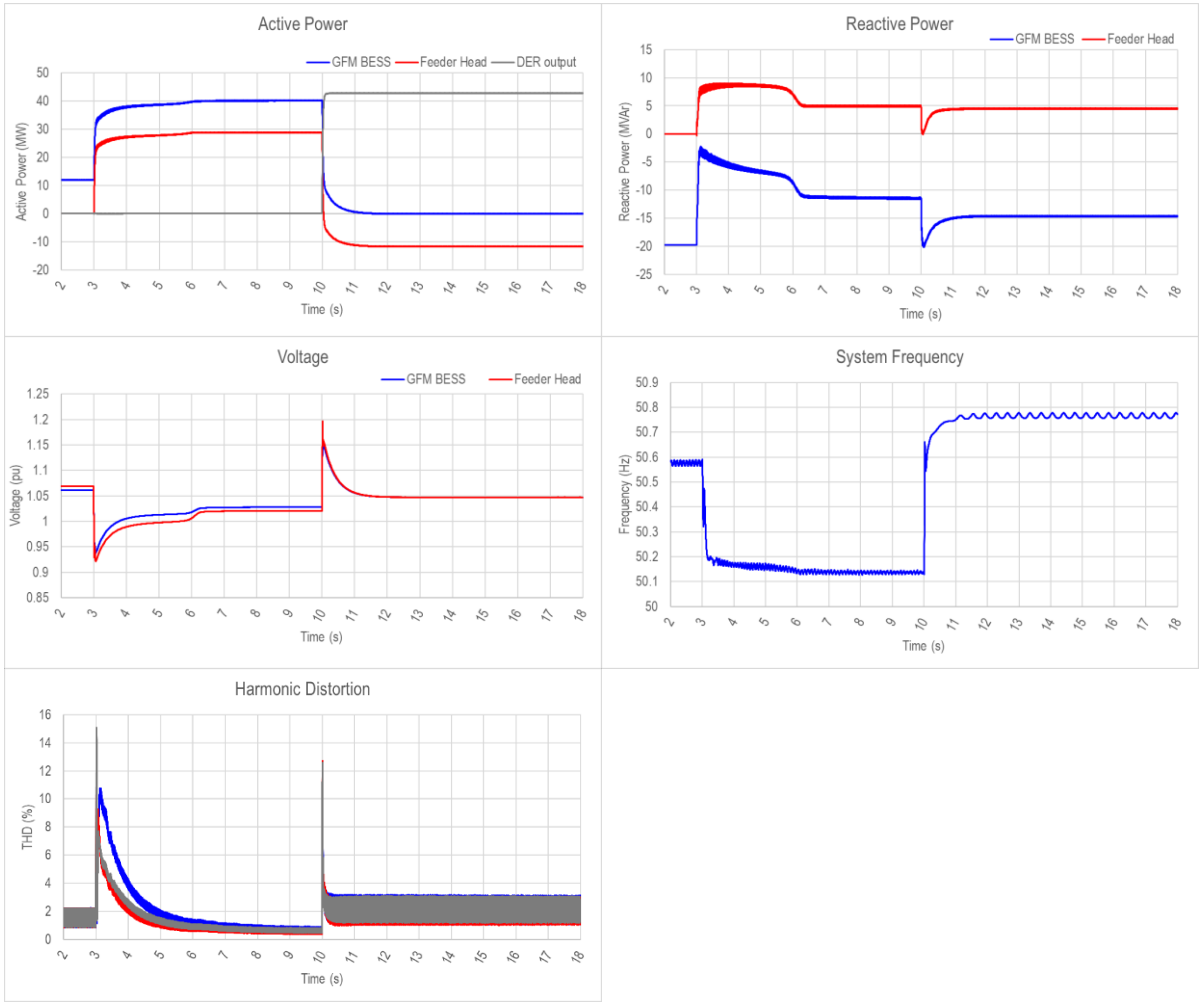

Figure 24 A GFM BESS-based restarting system response to load pickup and sudden DER energisation

Synchronous machine-based system restart

Upon DER reconnection at t=10s, a substantially longer transient overvoltage is observed (for the synchronous restart source compared with the GFM BESS case), which ultimately returns to a nominal steady state value within three seconds. Frequency variations are far slower to stabilise, consistent with synchronous machine and governor behaviour, but also has peaks and nadirs far in excess of those seen for the GFM BESS – this may be problematic

for some network protection relays. Total harmonic distortion of the voltage waveform is notably higher and more variable than that for the GFM BESS case.

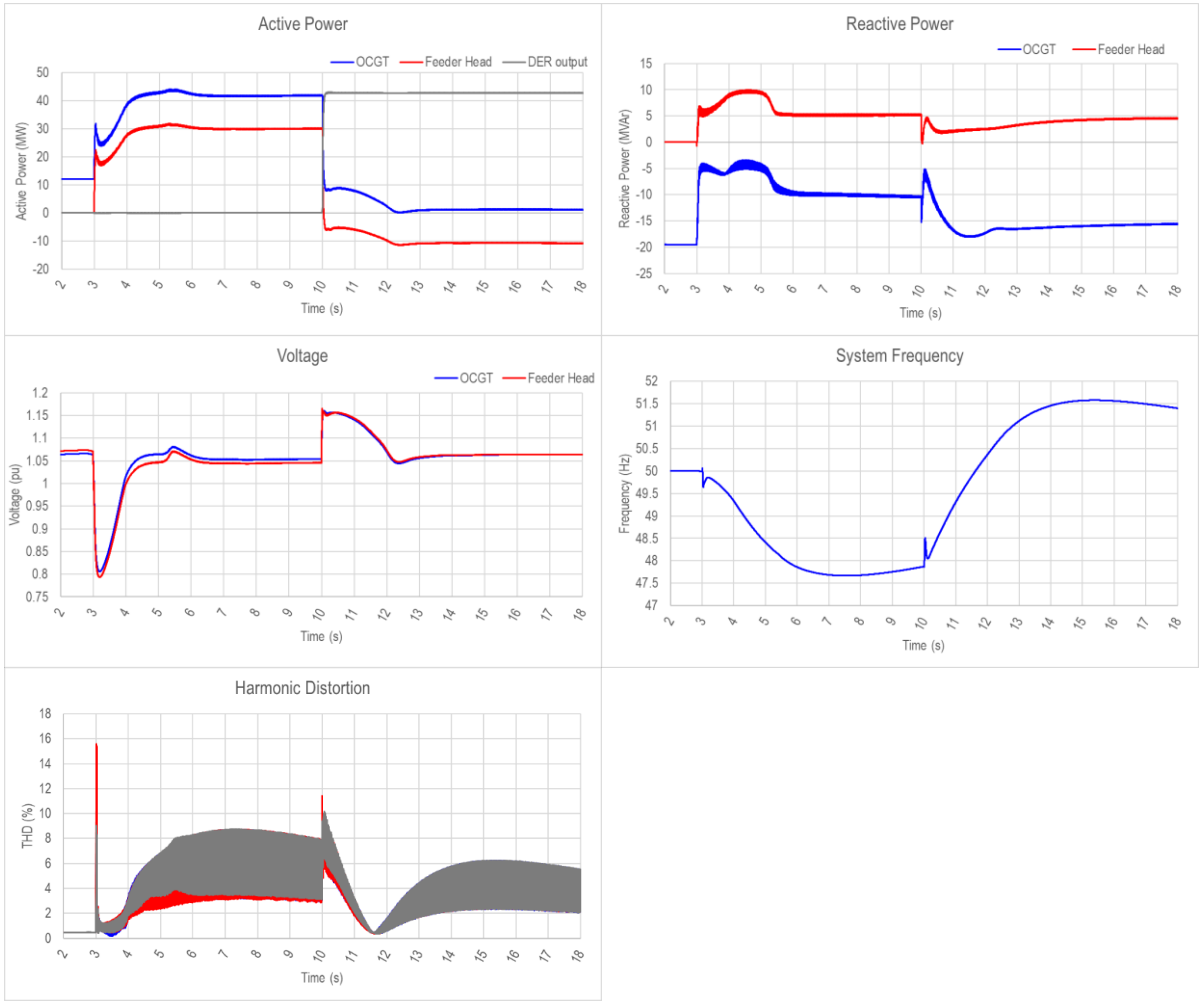

Figure 25 A Synchronous Machine-based restarting system response to load pickup and sudden DER energisation

Aside from the poorer transient performance, the crucial limitation of the synchronous machine response is the need to meet a minimum active power export level. This is inherent to the technology. Provided that the export headroom and state of charge allow it, the GFM BESS restart option will have therefore greater ability than the synchronous machine option to accommodate DER export, and potentially to have better transient responses to the disturbances DER reconnection incurs.

GFM BESS-based system restart with additional GFL plant

The same GFM BESS case previously mentioned was used with an additional 200 MVA GFL solar farm online (at low MW output) at a location 120 km away from the DER (230 km away from the GFM BESS). While the aim was originally to determine if the sudden DER reconnection could potentially destabilise the GFL inverters at the end of a *very* long circuit, it was seen that the additional presence of this GFL plant did not result in a destabilised

system, but rather aided in minimising under- and over-voltages from the pickup of load and DER, respectively. Frequency variations remained similar to that of the GFM-only scenario.

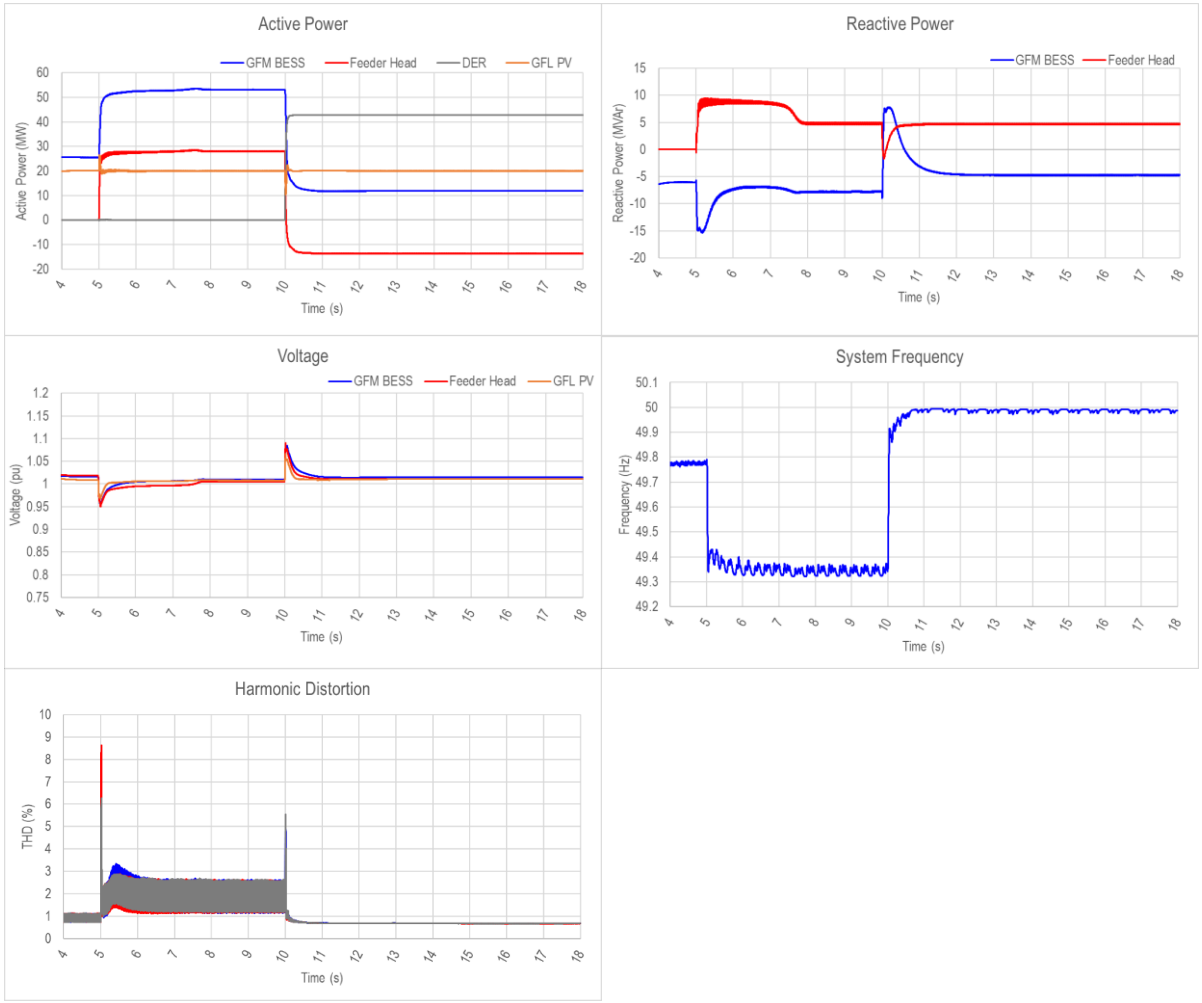

Figure 26 A GFM BESS-based restarting system response to load pickup and sudden DER energisation with additional 200 MVA GFL plant

This is not to say that this particular system is dynamically stable for most typical disturbance types, but rather that the disturbance event that the DER reconnection represented did not destabilize such a system. For the same level of DER sudden reconnection (45 MW), stable results were also observed when the GFL plant size was increased to 800 MVA. This is shown in Figure 27.

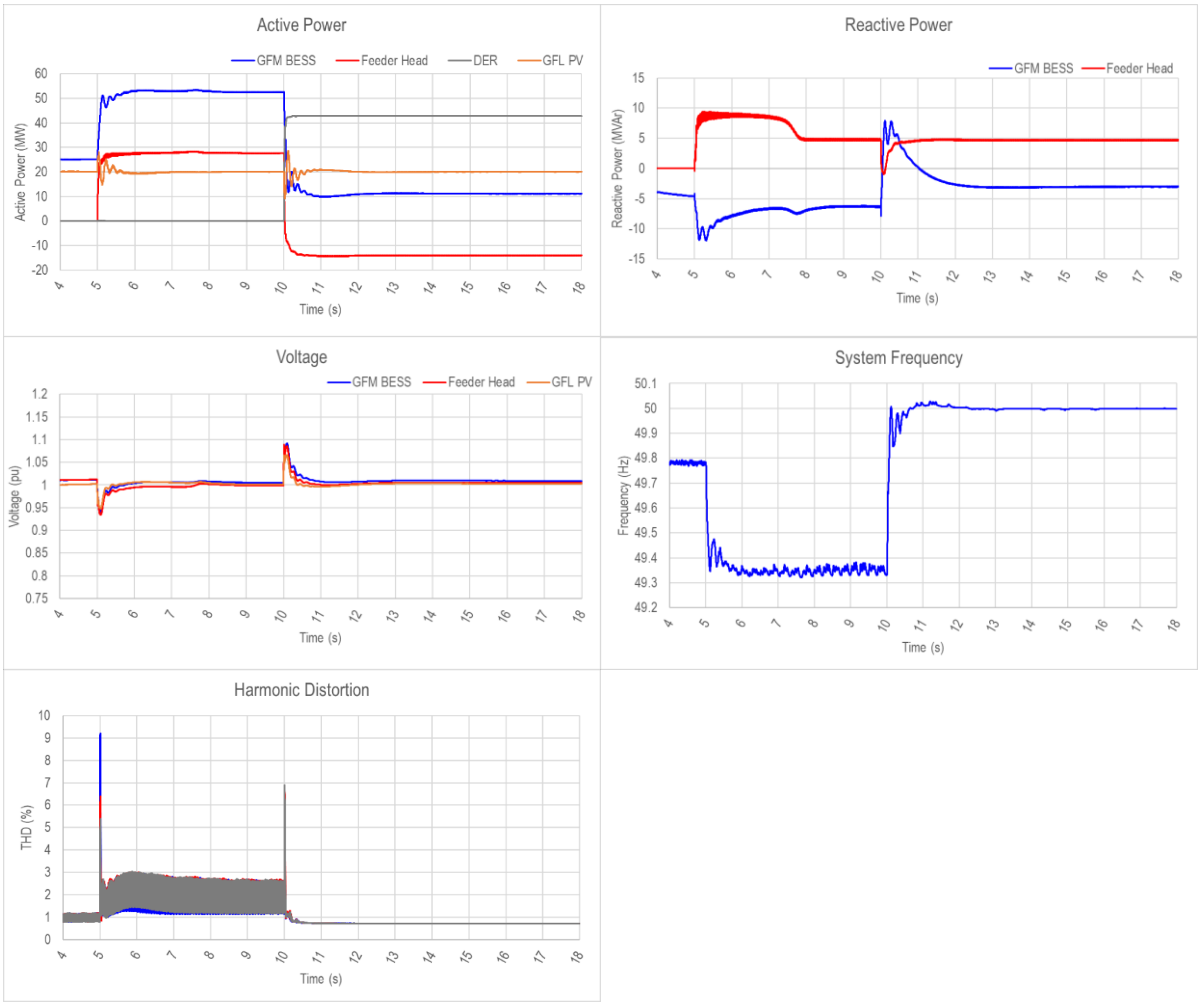

Figure 27 A GFM BESS-based restarting system response to load pickup and sudden DER energisation with additional 800 MVA GFL plant

As can be seen above, there is a slightly more oscillatory response on both the load energisation and DER reconnection (Compare Figure 24, with less/ without the additional GFL generation), but there is still a reasonably well damped and stable response overall. However, such a configuration is known to be at the borderline of system stability and, regardless of this satisfactory response to DER reconnection, would likely become unstable the next time a transformer is energised. This simulation study is only able to show that a 45 MW load reduction is insufficient to destabilise the configuration.

Effect of DER energy source variations

A key area of investigation was to evaluate the effect of DER energy source variations on the performance of a restarting system. In particular, this is where uncontrolled variations in solar irradiance result in changes to DER output, which may be sufficient to disrupt the upstream network equilibrium. Such changes could result in frequency variations or localised voltage changes with the potential to push the system well outside its normal operating envelope. Hence it is important to understand if these could destabilise a fragile restarting system.

In simulation, energy source variations to the DER are ideally achieved by altering the availability of the irradiance of the DER devices. However, this functionality was not available in the DER model and instead active power setpoints were set to follow a commanded reduction trajectory over the simulation time period. The applied profiles for various locations are shown in Figure 28 below.

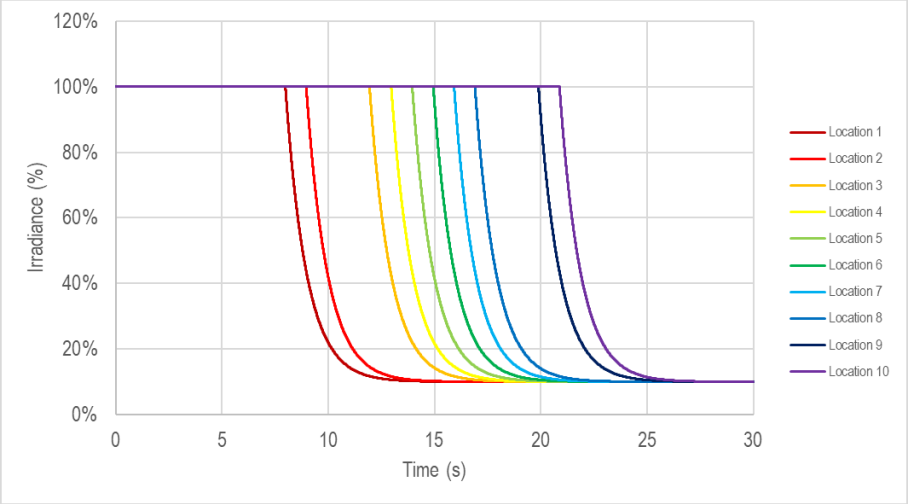

Figure 28 Irradiance change over time

Note that rather than a simultaneous global reduction of all DER device outputs along the feeder , power reductions were applied based on the location of the feeder over time, to reflect a situation where a cloud-front is moving across a region. The feeder was broken into four geographical areas and stepped from full output power to near-zero with a time-stagger between regions. These steps were passed through a slow first-order filter to better reflect the smoother aggregate response of DER being affected from cloud cover.

However, in reality the energy source variation across a feeder is likely to occur even less rapidly than this smoothed profile, with fast cloud cover still likely to take minutes to reduce irradiance across a typical Australian suburban feeder, rather than seconds as in this simulation. Regardless, such a profile was required as running EMT simulations for minutes' worth of simulation time is impractical (potentially requiring hours of real-time per run), and condensing such variations will allow a "worst-case" scenario to be evaluated, as the rapid variation is likely to exacerbate any negative effects that such rapid variations could impress upon the system.

Scenarios were developed and the system performance evaluated for a restarting system comprising alternative restart technologies.

Case setup

As the maximum effect of loss of DER generation will be seen with feeders with a high proportion of DER, it was decided to focus primarily on a feeder under reverse flow. Specifically, the 150% DER feeder previously described was used, with the following parameters.

- Feeder head: -13 MW
- Underlying demand: 29 MW (see load parameter sheet in appendix)
- DER output: 42 MW (mixture of 3-phase and single-phase inverters)

The remainder of the case was set up with:

- A 100 MVA GFM BESS black start unit (GFM studies)
- A 100 MVA OCGT black start unit (Sync studies)
- Approximately 60 MW of distribution load energized (without DER) across the remainder of the system
- 235 km of 220kV transmission network circuits
- 15 km of 66 kV sub transmission circuits.
- Various transformers of appropriate size.

For all cases, it was assumed that the black-start sources had been able to hard-energise all these components successfully, in line with previous research and other Milestone conclusions in this work. The system was hence initialized at time zero with all components excluding the DER already energized.

Scenario 1 – with additional utility-scale GFL

Note the topology of this case. There is an additional 200 MVA grid-following solar farm that has been connected to the system.

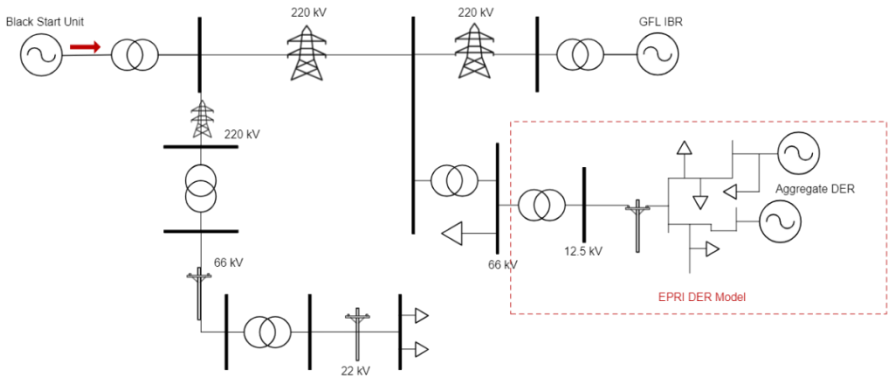

Figure 29 Case topology

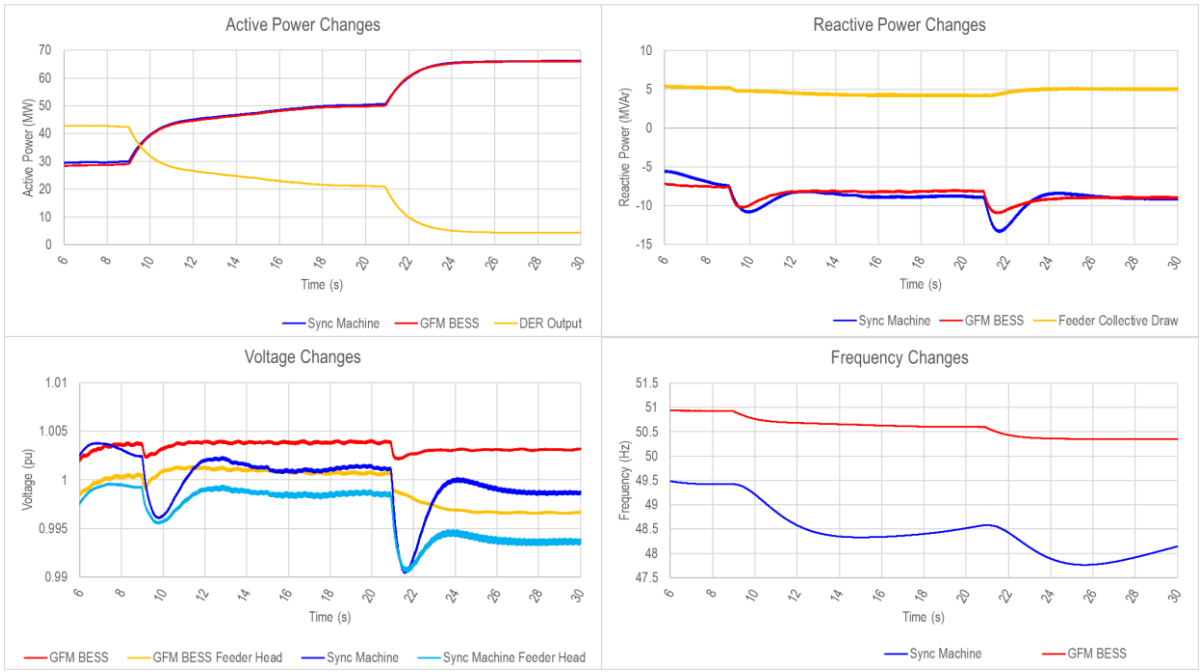

Figure 30 System response to cloud cover - with additional GFL

Voltages at the furthest bus within the combined distribution and DER model were 4% lower than the feeder head when DER was at full output, and 8% lower than the feeder head when the DER was near zero output.

Scenario 2 – without additional utility-scale GFL

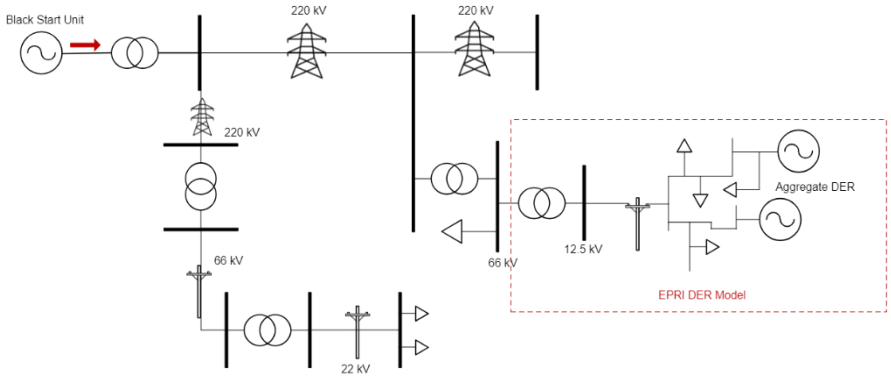

Figure 31 Case topology

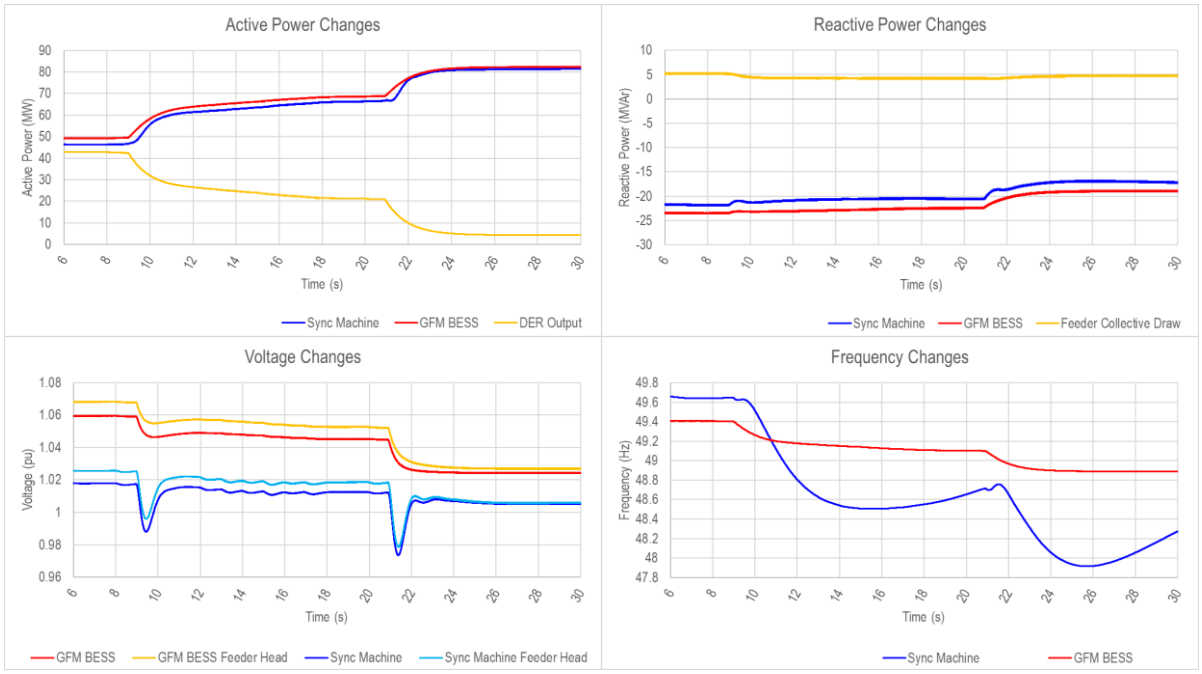

Figure 32 System response to cloud cover - without additional GFL

For the second scenario without the additional 200MVA of GFL, voltages at the furthest bus within the combined distribution and DER model were 4% lower than the feeder head when DER was at full output, and 8% lower than the feeder head when the DER was near zero output. These voltage results are essentially identical to the first scenario with GFL.

4.1.5 Additional insights

Harmonic components of voltage waveforms

A comparison is shown in Figure 33 of system voltage waveforms at the moment of transformer energisation, between a GFM BESS and a Synchronous Machine as a black starter.

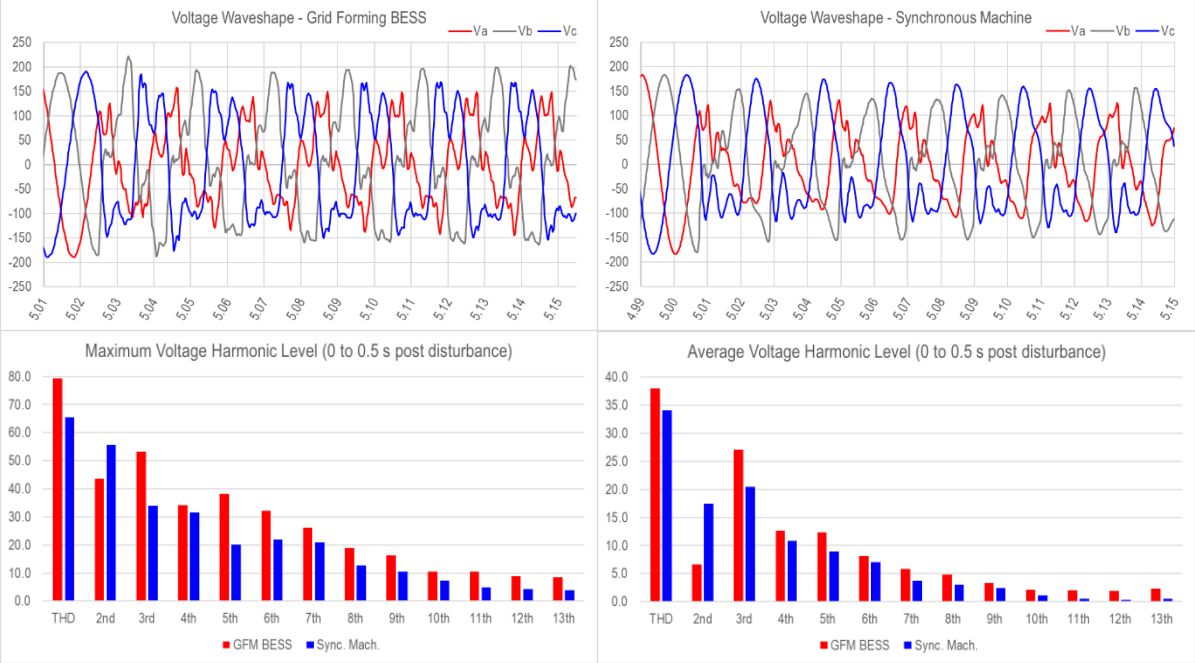

Figure 33 Comparison of system voltage waveshape and harmonics between GFM BESS and synchronous machine black starters

Note the following aspects:

- The IBR device results in an overall greater voltage distortion compared to the synchronous machine, which both instantaneous maximum and on average is greater for the synchronous machine, for each harmonic **except for the second**.
- Many 'typical' forms of frequency measurement (PLL, FFT and filtered zero-crossing detection) have a greater variance from the true value of the system frequency during transformer energisation, indicating a greater propensity for control systems reliant on fast frequency measurements to misread true system frequency during high voltage harmonic disturbances with an inverter-based grid firming source. Figure 34 shows an example of the difference in frequency measurements between when an IBR and synchronous source is used, where there is considerably higher frequency measurement variation when an IBR source is used.
  - Although it is unclear whether such approaches are used in all equipment in the field, the researchers noted that many OEMs do indeed use one of these variants (i.e., FFT, filtered zero-crossing, or inbuilt PSCAD library PLLs) in their PSCAD models for controller-input frequency measurement purposes.

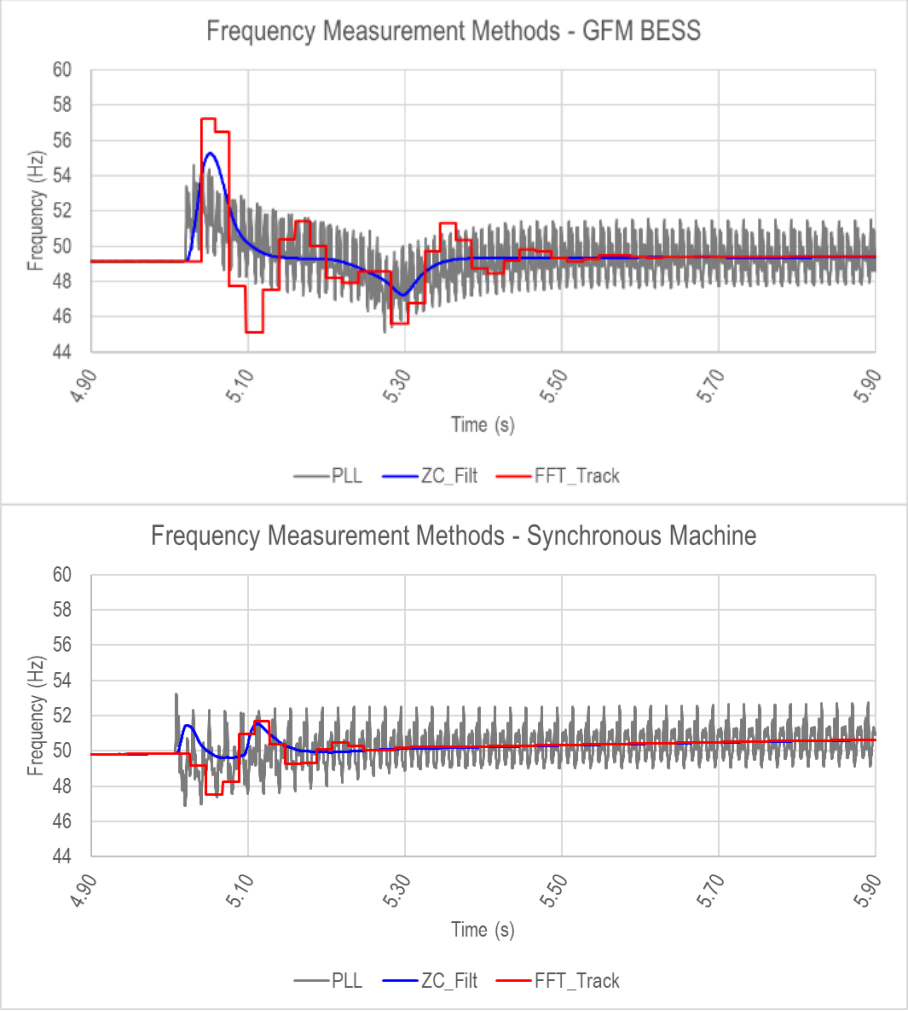

Figure 34 Difference in frequency between using IBR and synchronous restart sources for various common frequency techniques

A line of further enquiry may be: Is it simply the increased distortion at higher harmonic orders that is challenging for grid-following IBR devices to withstand, or does the second harmonic component which may be reduced in IBR-dominant grids provide a fundamental synchronising function to the broader system that is not yet well understood?

Stability sensitivity studies for DER inner control loops

Given the relatively unshakeable nature of the fast inner controllers witnessed within the DER models, tests were completed to determine what circumstances would be required such that inner controller instability begins to manifest within a system comprising high levels of DER.

It is important to note that the PLLs within the DER models used are not of a particularly advanced design; they use the synchronous reference frame (SRF) approach, which is an extremely common and simple method used to determine the system frequency to feed into other fast inner current controllers. An example of the topology used is shown in Figure 35.

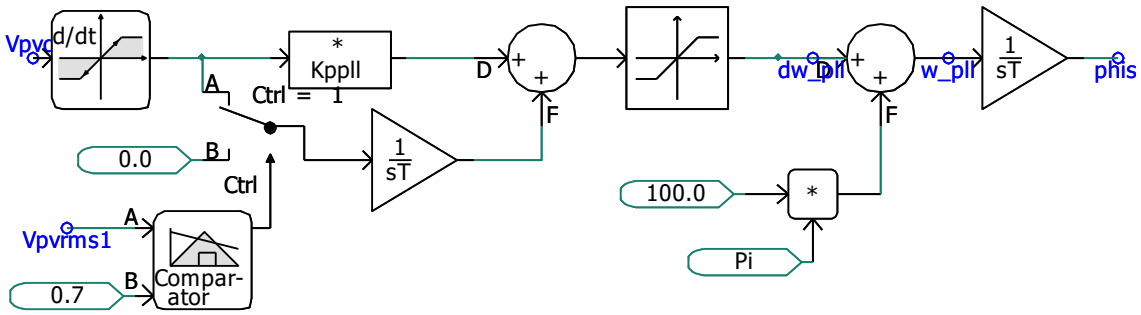

Figure 35 SRF PLL used within the DER models

As such a common and simple method is used to calculate frequency and phase angle for use in the remaining inner current controllers of the DER models, this serves as an ideal base to determine how system conditions must vary for instability to begin manifesting, without being clouded by advanced PLL methodologies[9] which may show uncommonly superior performance in weak grid scenarios.

The scenarios for the DER inner controller instability trend were developed as follows:

- A fixed size (100 MVA) GFM BESS black starter was used.
- The amount of DER in the system (relative to the size of the black starter) was increased in 40% increments until instability was observed during the simulation.
- A comparison was made between the same DER penetration scenario when a synchronous machine was used.

The topology shown in Figure 36 was used to perform these tests. The test sequence is as follows:

1. DER is brought online from t=0 s and ramped to its target output.
2. A disturbance is applied at t=10.0 s in the form of the energisation of the 225 MVA transformer (shown in orange in Figure 36) to induce a dynamic response from all elements in the system.
3. The response from the DER is then observed.

In particular, determining if instability has manifested can quickly and effectively be identified by monitoring both the PLL frequency variations of the DER, and the overall voltage harmonic distortion of the system, where high variance of either indicates off-nominal current injections are likely occurring as the DER inner controllers struggle to maintain phase angle tracking and hence stability.

[9] Note that it is likely that modern PV inverter OEMs are likely to use more advanced approaches that SRF, however this cannot be comprehensively confirmed.

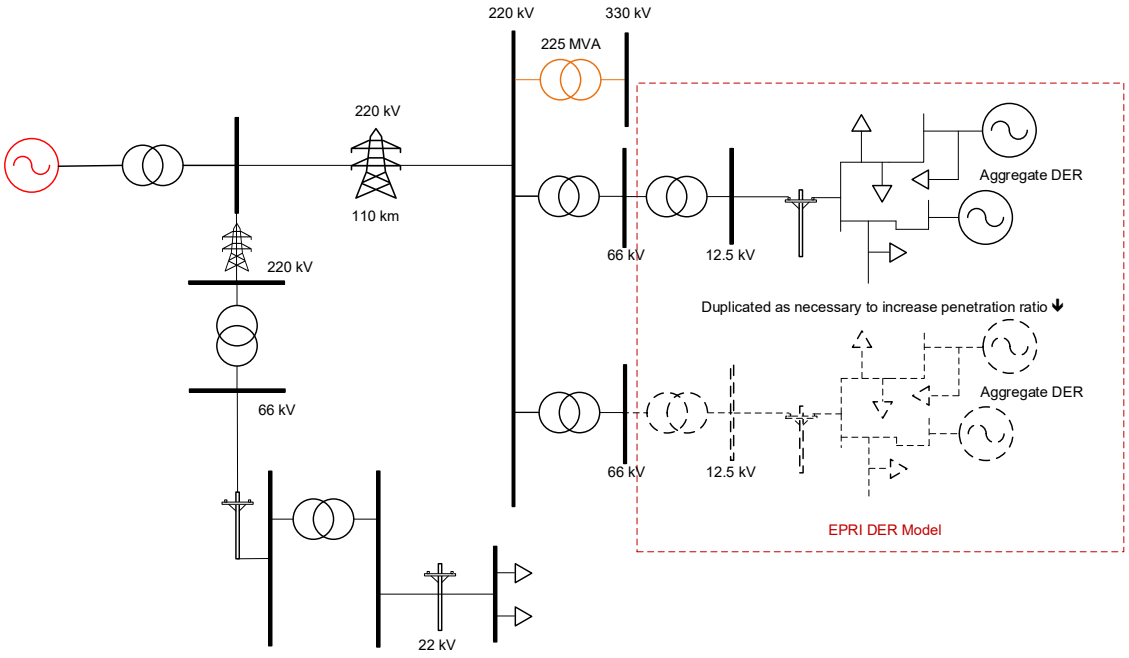

Figure 36 Topology arrangement for DER controller instability investigation

Note that for the purposes of this investigation, the DER protection mechanisms (voltage and frequency protection) were disabled such that the DER devices remained online following the disturbance and DER controller stability could be observed.

40% DER Penetration

This scenario considered 100 MVA black starter with 40 MW of DER connected and a transformer energisation at t = 10.0 s.

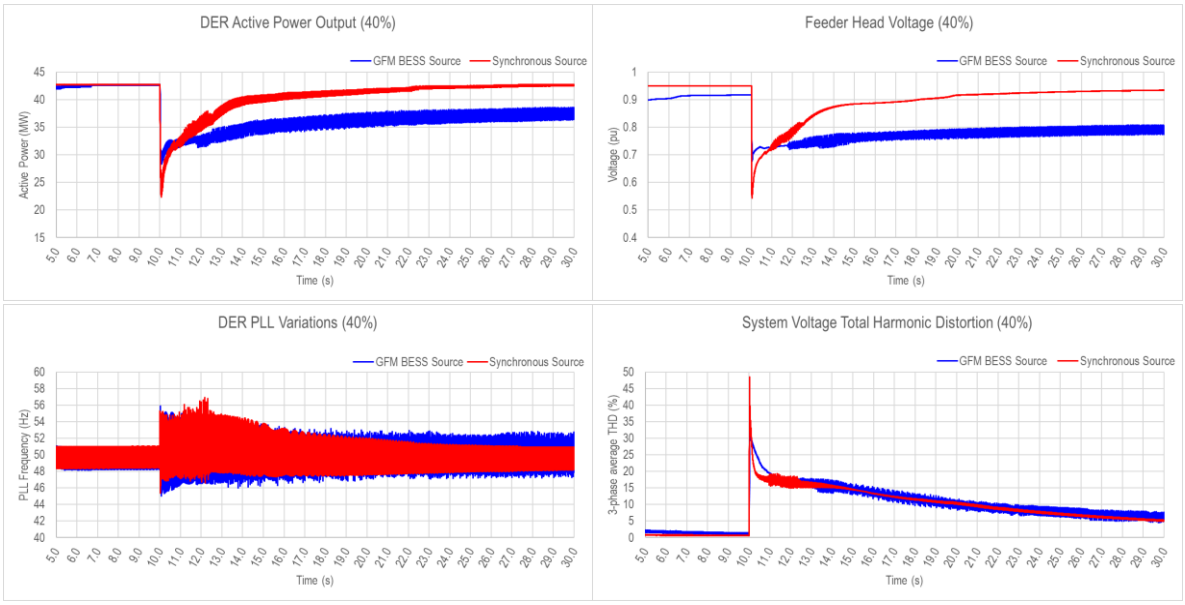

Figure 37 Comparison of key performance indicators for a system with 40% DER penetration

Prior to the disturbance, the key performance indicators as shown above were similar in their value and (low) variance, indicating a system that is stable. Following the disturbance

however, material differences appear in their value and variance. In particular, while DER PLL variance begins to decay to pre-disturbance levels for the synchronous machine scenario, it remains high for the GFM BESS scenario. This improper PLL tracking leads to increased error in converter output, leading to non-fundamental components being injected into the system, and hence, increased harmonic distortion and variance (or more correctly, error) in RMS calculated quantities.

80% DER Penetration

This scenario considered 100 MVA black starter with 80 MW of DER connected and a transformer energisation at t = 10.0 s.

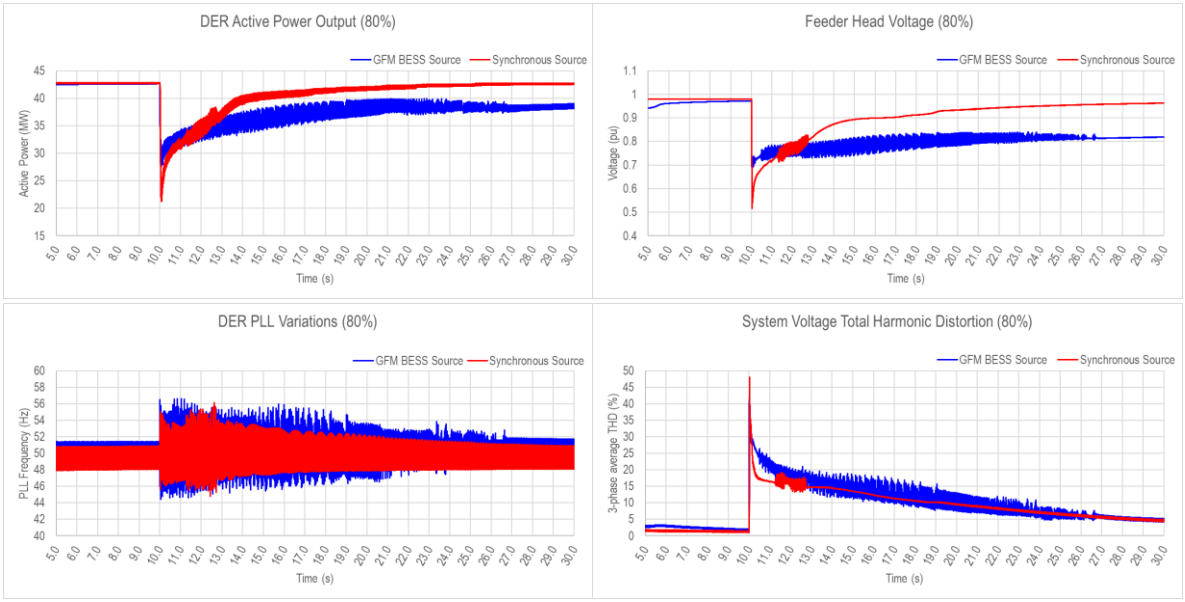

Figure 38 Comparison of key performance indicators for a system with 80% DER penetration

A repeat of the 40% DER scenario occurs here, with even higher PLL variance in the GFM BESS black start source case, leading to even higher harmonic distortion and larger error in the RMS quantities. Prior to the disturbance however, the low error in RMS quantities is indicative of a stable system. Note that post-disturbance values for the synchronous machine-based case do not show the same sustained increase that the GFM BESS values do.

120 % DER Penetration

100 MW black starter with 120 MW of DER connected and a transformer energisation at t = 10.0 s. **N.B.** Additional static load brought online to prevent synchronous machine entering reverse active power.

With DER penetration now exceeding 100% of the nameplate capacity of the GFM BESS black starter, even prior to the disturbance there is an excessive variance in the PLL variation and harmonic distortion resulting in increased distortion throughout the system. This is indicative that a sustained instability threshold in the system has been reached.

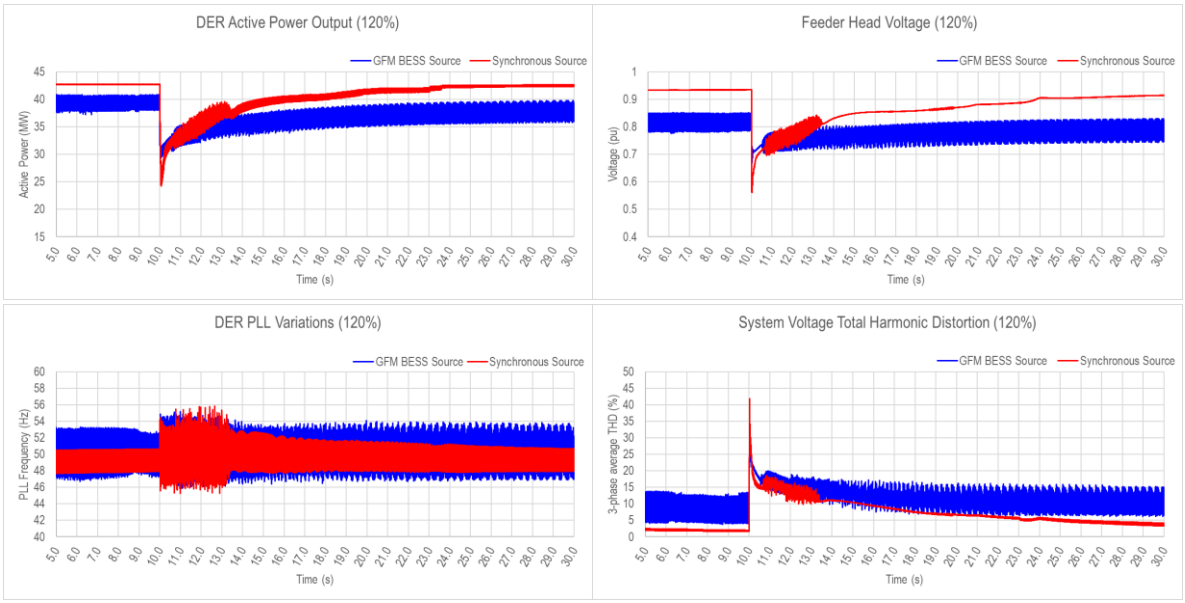

Figure 39 Comparison of key performance indicators for a system with 120% DER penetration

It can therefore be concluded that for GFM BESS technology black start, a key steady-state stability breakpoint exists between the 80% to 120% DER penetration level.

A more specific threshold can be determined; however it is important to recognise that there is likely to be a high degree of stability dependency on the specific GFM BESS black starter algorithms and the DER frequency tracking algorithms used in the real system, hence there may be limited value to attempt to find more than a coarse range of an instability threshold using the generic models used in this analysis.

Comparison of key performance indicators across DER penetration levels

Overlaying the above three increasing DER penetration scenarios for the black-start unit shows the increasing level of pre- and post-disturbance variance on PLL frequency tracking and voltage harmonic distortion.

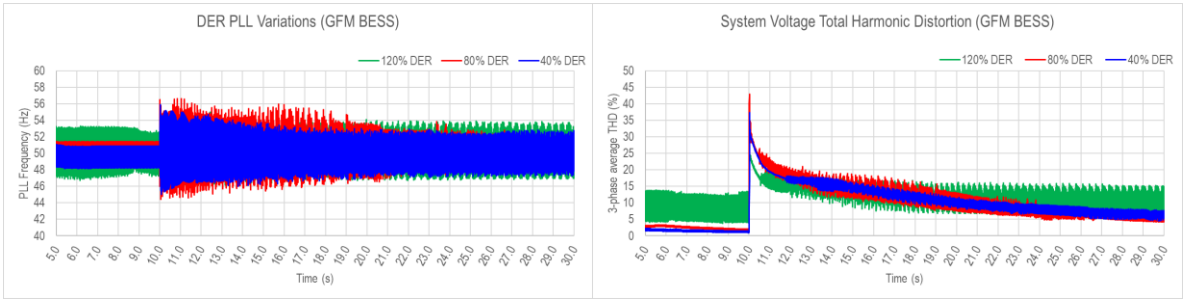

Figure 40 Comparison of PLL variations and system distortion for varying DER levels in a GFM BESS restoration

Repeating the same comparison for the synchronous machine option, however, shows less far pronounced differences, and for the most part, very similar stability performance despite DER penetration exceeding the synchronous machine nameplate.

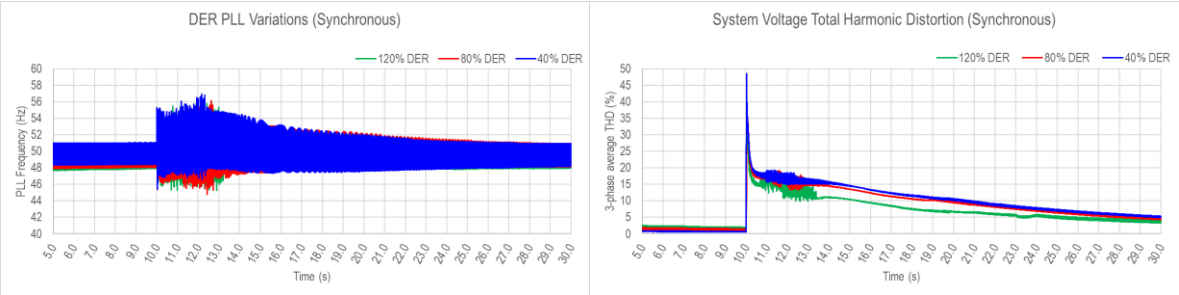

Figure 41 Comparison of PLL variations and system distortion for varying DER levels in a Synchronous machine restoration

4.2 Milestone 2 – Operational Changes to IBR Restart

The focus of this Milestone is to determine what operational changes could be made on the day of restart (rather than considering more intricate control system changes that would need to be studied, designed, and implemented ahead of time) that would allow a 100% IBR system to better accommodate the existing GFL fleet, which may not be explicitly designed or tuned to operate during black start scenarios.

4.2.1 Key findings summary

The following are a summary of the problems and solutions found for the studies conducted as part of this work.

- The most common cause of instabilities seen in the studies was an ill-conditioned PPCs on GFL plant.
  - The most reliable way to improve stability in a high-IBR system without reducing the MVA of online GFL IBR generators was found to be disabling the PPC and issue open-loop commands (i.e., P and Q setpoints at an inverter level) to the GFL devices.
  - This was particularly prominent when dealing with hybrid plant, where OEMs that used multi-layer PPC structures (i.e., a PPC for each technology plus an overarching PPC) saw the multiple PPC devices fight with one another as control loops cascaded, and delay instability mounted.
- Major disturbances or transformer energisations next to hybrid plant result in very large MW injections or absorptions from and to the hybrid plant, destabilising and collapsing the system.
  - During disturbances, it may be possible that a portion of the hybrid plant remains relatively unchanged in its output, while the remaining portion disconnects or otherwise reduces its output, resulting in an undesired net output.
  - Switching the PPC to open loop will not mitigate this issue, as it's a result of the individual inverters entering into fault ride-through (FRT).
  - **The power exchange within a hybrid plant matters greatly**. Where possible, only use one component of the plant (e.g., only the BESS portion, or only the solar portion) to interface with the broader system, or if this is not possible, limit the power exchange between different components within the hybrid plant to as little as possible.
    - As will be discussed in later sections, this is because even if the power exchange with the broader power system is low, during a system disturbance, it is possible that the hybrid plant's internal power exchange amount may suddenly appear at the point of connection if one hybrid plant component suddenly ceases power transfer and the other does not.
- Some GFL equipment may have relatively tight cut-in voltage and frequency requirements that must be satisfied before the device connects to the system. Such readings may be

affected by a “noisy” system or protracted low voltages following extended or incomplete transformer energisation, preventing the devices from connecting to the system.
  - Restoration paths involving transformer energisations must have been studied in detail and flux remanence issues can be pre-identified and avoided.
  - Ample time (potentially minutes) should be left for voltage and current distortion levels to settle before attempting the energisation of GFL plant with such sensitivities.
- Transformer energisations next to a GFL plant that is already online can destabilise the already energised GFL plant.
  - Energisation of a large transformer is equivalent to a fault on the system with an extended clearance time.
  - While it can be useful to have other GFL devices online prior to energising a transformer (as their inverters will respond in their FRT profile to inject current to support the system), and that overall system robustness *may* be improved by setting PPCs into an open-loop control mode, it is important to realise that these inverters **will** go into FRT mode and potentially cease the supply or absorption of MW while doing so.
  - In this way, it is important to ensure that while transformers are being energised, neighbouring GFL devices should be brought online first, but should not be exchanging energy with the balance of the power system to a level beyond what the system could safely stand to lose during a fault.
- Wider frequency droop from the GFM IBR means they are more likely to be off nominal frequency more often, meaning GFL IBR devices may not even attempt to connect. Once connected however, the GFL IBR frequency capability is normal.
  - Consider energising and reconnecting GFL plant first where possible and provide them with an active power setpoint near 0MW, before connecting any load that may result in a system frequency transient that would push frequency out of (GFL) reconnection tolerance bounds.
  - Introduce an active power setpoint bias to IBR as needed to bring frequency into line with targets, in addition to having droop control enabled.
  - Change GFL IBR cut-in frequency on those particular units to be energised (this is less desirable as this setting change is often required on per-inverter basis).
- Tight frequency droop in GFM IBR devices is akin to high controller gains in GFL devices. Instability is likely to be seen in a restarting system if the droop settings in GFM IBR are too tight.
  - It is thus recommended to relax GFM frequency droop in order to reduce the chance of frequency induced oscillations owing to a GFM attempting to control things too tightly. Studies showed a droop greater than 3% saw reasonable stability.

- GFM technology that relies solely on droop mode will have an inherent frequency droop profile, i.e., a true “isochronous mode” maintaining a constant system frequency at 50 Hz may not be achievable.
  - It is recommended to use active power setpoint biases to manually correct frequency when required.
- With PPC frequency controllers enabled, faults may cause the operating point of all generators in the system to shift, potentially leading to system instability or collapse.
  - During a fault, the active power operating points of the system may shift. This could be by several means, but generally a local voltage depression will cause a reduction in active power demand from total load, causing a shift in frequency and a corresponding shift in the active power output of devices operating under frequency droop.
  - This may mean that a device operating near a limit prior to a disturbance may hit its limit following the disturbance, leaving no room for further frequency regulation.
  - When planning a restart route, it is therefore recommended to ensure that generators to be energised have sufficient headroom in both directions to maintain frequency control for most conceivable disturbances.
- Steady-state instability was occasionally observed after energising a large plant with its PPC disabled, long after transformer inrush phenomena has settled, and in the absence of a grid disturbance.
  - If such instability has been observed with plant-level outer control loops (e.g. PPC) disabled and in the absence of a system disturbance, this is highly likely to be a genuine system strength problem – inner control loops of the individual inverters are struggling to maintain stability due to the very weak nature of the voltage waveform in the system.
  - Realistically, the only on-the-day operational solution available is to **reduce the number of online units in the plant (i.e., MVA reduction as opposed to MW reduction)**. From the experiments performed, alteration of the MW output has minimal effect on the stability of the already marginally stable system.
- Where individual inverters within a large park have not (re-)connected despite having been energised for a while and where this is due to their own individual control system detecting unsuitable conditions for reconnection (such as frequency cut-in bands not being met), their coordinating PPC may have wound-up in the interim and the setpoints that it sends to individual (coordinated) inverters may be at maximum. When inverters do eventually (re-)connect, it may result in a large step-change to the system.
  - It is therefore recommended to hold all target setpoints (such as active power, or Q setpoint if in Q-control mode) at zero until it is confirmed that all inverters have successfully connected.
- Re-energising GFL devices may suddenly inject active power into the system at a rate that destabilises the stability of the island.

  - For larger plant of comparable or greater size to the GFM black-starter, and where on-the-day settings allow such a change, it is recommended to reduce the ramp-rate of GFL PPC for active power, such that it reaches its target setpoint slowly, to allow other plant to respond. Alternatively, where setpoint ramp rates cannot be dynamically reduced on the day, it is instead recommended to manually slowly increase the active power setpoints of individual inverters.
- Sympathetic inrush from large connection point transformers in a REZ: i.e. Large transformers sequentially energised nearby to one another, as would occur in a REZ restart scenario, can cause an undesirable transformer re-energisation phenomenon to occur, whereby previously energised and stabilised transformers become unbalanced in flux and draw highly unbalanced, distorted phase currents from the system.
  - It may be exceedingly challenging to ameliorate the effects of sympathetic inrush without modification of the primary equipment. However, it was observed that, provided there were no poor IBR controller interactions, having plant downstream from the transformers online (even at low output values) would allow energised transformers to retain some form of relatively balanced current draw. Nevertheless, this was still not ideal.
  - Following from above, a recommended sequence to re-energise a REZ is to pick up GFL IBR plant one site at a time. One site entirely should be brought online and capable of contributing output before attempting to energise the next site (including energising the corresponding connection point transformer)
- Slow (<5Hz), poorly damped instability was observed manifesting across all quantities in a system with multiple GFM devices separated by a considerable amount of network impedance in an “early” stage of a system rebuild (i.e., with minimal interconnections established).
  - This is likely due to the inertia constants of the controller settings in VSM GFM devices being set inappropriately for a very weak system. Larger inertia constants are not necessarily better in a restart scenario, though they can be helpful for stability during system normal conditions.
  - Generally, GFM devices that employed a frequency Droop controller rather than VSM appeared to be more stable for the restart scenarios studied. However, this may be OEM-specific, and a firm conclusion cannot be drawn at this stage.
- Disturbances that induce large phase-angle shifts (e.g., fault and loss of load, an intraconnecting line or a section of the system) may result in some GFL IBR losing stability.
  - It is recommended to establish zones that are closed to supply-demand balanced wherever possible; have generation supply load as close as possible to the electrical location of the load. In this way, should there be a loss of an interconnecting element, the resultant phase-angle shift experienced by the system would be minimised.

  - N.B. This is not to say that should the loss of an intraconnecting circuit happen, that a GFL generator should or would be able to remain as an island.

Failed lines of enquiry

The following items were investigated to determine if they could aid in maintaining stability in a 100% IBR restarting system. However, they did not yield positive results.

- Does altering the VSM GFM frequency droop gain reduce the instability seen in a marginally stable case? (genuine system strength instability)
  - No, the instability remains, but the periodic nature of the instability changes – lower frequency oscillations with reduced droop gain, higher frequency oscillations with increased droop gain.
- During steady state, does the internal power interchange between a hybrid plant have any bearing on the stability of a GFL plant?
  - For steady-state conditions, no, rather it appears that instability is more dependent on the *number* of the units online, not the MW generation setting, even within a hybrid plant connection point. However, for fault conditions, there is a strong link to between internal power interchange and system instability, as the internal units come out of fault ride-through mode and attempt to re-establish an internal equilibrium, even with manual setpoints (PPC disabled).
- Does adding an additional individual GFL plant that has a better controller (better tuned / more stable) help with stability in a REZ?
  - No, it appears that it doesn't. It didn't necessarily make it worse, but it does change the instability profile.
- When you have two VSM GFMs oscillating against one another, does making the system more meshed alleviate the oscillation?
  - No, and potentially quite the opposite, it can make it far worse and unbounded.
- Does switching in large amounts of resistive load behind a transformer help damp the oscillations seen due to transformer energisation with flux remanence?
  - No, from the studies performed, very little behind the secondary appears to affect the decay time of transformer inrush current.

General observations

- Frequency is no longer a relatively uncoupled component. It is tightly linked to voltage in such weak systems, especially where the GFM BESS works on a frequency droop basis. Faults, general depressions and even voltage setpoints of other plant can have a material impact on the energy balance of the system (e.g., lower voltage results in reduced power consumption, results in an increased frequency)
- PPCs that have been tuned assuming a decoupled nature of voltage and frequency elements may be a liability when attempting to rebuild a system, especially when early in the restart process. It was repeatedly found that most instabilities were not due to the fast (inner) control loops of the GFL devices losing stability, but that the outer voltage and

frequency control loops of the PPCs were not performing stably in the weak system. As such, stability may be best achieved by disabling the PPC and thereby putting into open-loop control mode the P and Q setpoints of the IBR otherwise subject to an additional outer control loop arising from the PPC.

- Two GFM BESS in a REZ that have been energised by a remote black-starter tends to operate quite stably, so long as their respective inertia constants are low and they operate to the same droop profile.
- The work here reaffirms the conclusion from previous researchers [12] that ratios up to approximately 10:1 of GFL to GFM IBR devices can be accommodated before instability will be observed. This is an approximate figure only, as network topology and impedance can alter the destabilising factors.

4.2.2 Milestone objectives

The objective of Milestone 2 (Operational Changes to IBR Restart) is as follows:

- To investigate strategies that can be employed in an operational timeframe to aid in restoring, from a grid-forming IBR source a system that hosts a large proportion of grid-following technology, in a stable and robust manner, with a focus on hybrid (solar/BESS) installations.
- Identify circumstances that would warrant additional attention when performing system-specific black start studies when considering a 100% IBR scenario that may not be immediately obvious.
- To develop a "realistic, but not real" releasable model to be shared more broadly with the research community, that can be adapted and grown for a variety of system-restart studies, without infringing on confidential data.

Importantly, the above term *operational timeframe* refers to changes that can be made "on the day". That is, changes to sequences or strategies during restoration, or relatively simple changes to plant control modes on the restart path. Detailed changes such as control system tuning are not considered, as this would require substantial prior planning, prior analysis and alterations to an already commissioned plant[10]. Having said that, where an issue could likely only be resolved through a control system change, this was noted and initial investigations into possible solution options made.

The investigations were intentionally designed to be "wide" rather than "deep" in terms of issue identification and rectification. This is because although new instability mechanisms may exist for a 100% IBR scenario, the specific cause and solutions may not be general

[10] In the Australian context, any additional control system adjustments and tuning after commissioning would require revisiting the agreed generator performance standards and re-opening negotiation for the plant performance. This is generally deeply unpopular for plant owners due to the associated cost and uncertainty to demonstrate compliance following any change.

enough to be of value to the broader research community (e.g., the instability may have been triggered by a particular manufacturer's implementation of a control loop, which may only hold in the highly specific scenario used in this study).

In short, the work aimed to find problems and challenging situations during restart, and to develop strategies that a control-room operator could employ to enhance the stability of a grid being restored, for grids comprised entirely of existing IBR technology which may or may not be purposefully tuned to provide assistance during system restart.

4.2.3 Previous Research

This work builds on previous work by G-PST researchers [11] [12] who identified that restarting an IBR-dominated system can be achieved using a grid-forming battery. Importantly, these previous conclusions formed the launching-point of this work:

- A GFM BESS can support up to approximately 10x its MVA rating of GFL devices.
  - It is important to recognise that this finding has not considered a wide range of network impedances between the GFM and GFL devices.
- A GFM BESS is typically a superior restart source option (across some performance criteria) compared to the use of a synchronous condenser plus a GFL BESS.

Using these assumptions, more focused studies can be performed on the milestone topics, rather than focusing on general instability issues.

4.2.4 General PPC instability

A repeated issue seen throughout many of the studies was instability manifesting from PPC controllers operating upon GFL plant. Such instability is characterized by slower oscillations in the sub-3Hz range, and this attribution can be readily confirmed both by observing the output commands from the PPCs, and then by bypassing the PPC by feeding constant power setpoint references to the individual inverters within the park fleet to confirm a return to stable operation.

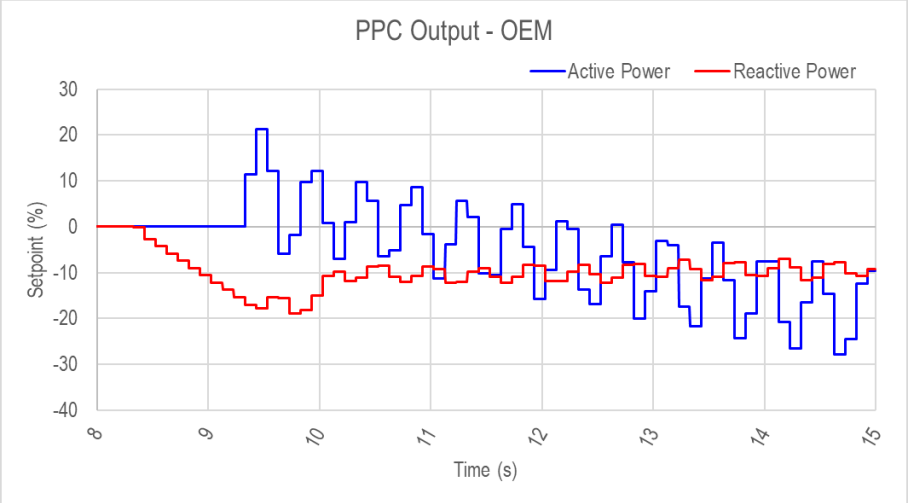

Figure 42 Example of a PPC instability in active power command

Such instability was observed for one OEM-model (inverter and PPC) and in a generic model of a solar farm, with another OEM-model showing no such signs of instability. Furthermore, instability was seen in both the active power and reactive power outputs of the PPC, indicating there are likely multiple induction pathways for instability.

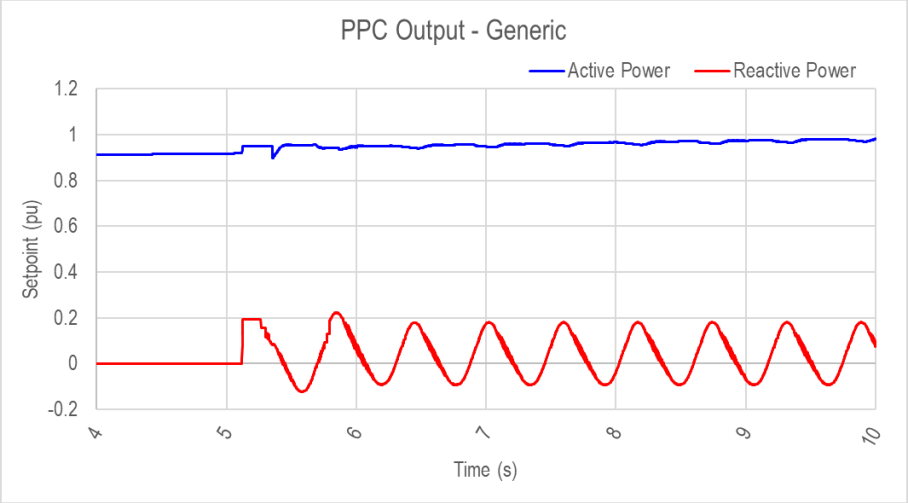

Figure 43 Example of a PPC instability in a reactive power command

Situations which induced such instability needed the following characteristics:

- MVA amount of GFL plant online far exceeds the MVA amount of GFM plant (usually ratios exceeding 8:1).
- There is an appreciable (>0.1 pu) network impedance between the GFM and GFL sites.
- The PPC has been set to control either voltage or frequency, or both.

Deeper heuristic investigations (in models that allowed changing of PPC settings) showed that three aspects were at play:

- PI controller gains internal to the PPC not appropriate for the system strength scenario at hand.

- Fast ramp rates commanded by the PPC could not be accommodated by the weak system.
- The time delay introduced by the PPC (particularly for cascaded PPCs) resulted in instability (see next section).

These are all considered to be classical stability issues that could be readily mitigated, either by re-tuning of the controllers or by altering the structure of the cascaded controller system such that controller transport and communication delays are minimised. However, as the aim of this investigation is to determine what steps could be taken *on the day* to resolve such instability, the conclusion remains that simply bypassing PPCs that exhibit such poor performance may result in the return of system stability. The cost of such a change, however, is that voltage and frequency control of the plant will be lost. Consequently, the plant must be continually trimmed moment by moment while online (in active and reactive power set points) to match the needs of the remaining system. Although this is far from an ideal scenario and assumes either personnel on site or a robust communications link, it is still preferable to an inherently unstable system with the PPC online.

PPC delays

Of note is the instability effect that even modest delays in the PPC can introduce to the system when the network impedance is relatively high. Figure 44 shows an example of a plant's performance with and without the default 250 ms processing delay enabled in the device simulation. The PPC is set to control voltage with a 4% droop, when a shallow fault results in a residual voltage of 0.92 pu at its point of connection.

As can be seen, for these two alternative scenarios, such a modest disturbance (when the PPC control is not bypassed) can result in a significantly different response. Inclusion of the processing delay resulted in a reactive power swing nearby double that when the processing delay is neglected.

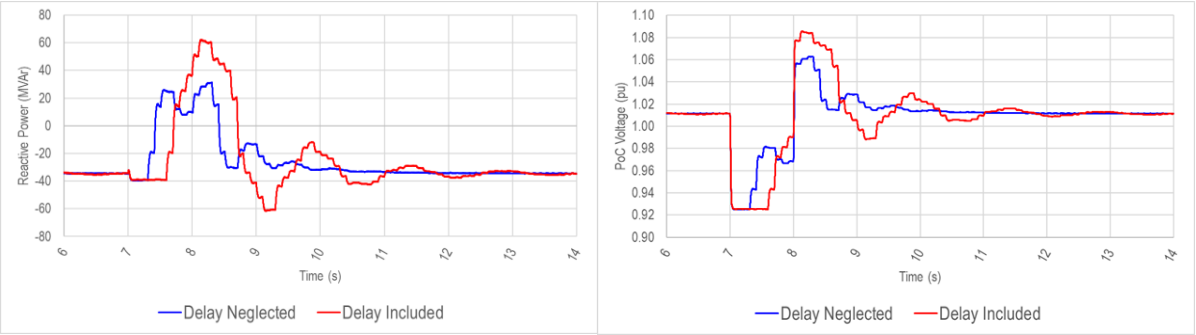

Figure 44 Effect of PPC processing delay on plant response in weak grids

Unfortunately, such delays are common in the (non-simulated) physical system and are representative of processing and communication delays through the aggregate controller. They are not necessarily able to be "tuned-out" and often have a strong linkage to the numerousness of devices within the physical plant (e.g., a string-inverter based plant is likely to have higher communication processing requirements than centralised inverters). Hence it is critical to ensure, in all studies being completed for system restart work, that an

appropriate PPC processing delay has been included in the model (i.e., representative of the system configuration), and not simply set to the default value that came with the model.

4.2.5 Impact of PPC on hybrid plant stability

It was observed that in cases where large amount (MVA) of GFL IBR is present and a network still remains weak, there may be a propensity for multi-level hybrid plant controllers to have stability issues while attempting to simply bring the plant online and ramp to a target setpoint following restoration of supply at its connection point. Such behaviour is not present in stronger (i.e., system normal) network.

The below images show in grey the active power output of a 200 MVA OEM solar-BESS hybrid plant with a -50 MW target, several seconds post energisation of its point of connection, reticulation and inverters. Two scenarios are presented, one with the PPC enabled (Figure 45 and Figure 46), and the other with PPC in open-loop mode (Figure 47) effectively bypassing the PPC.

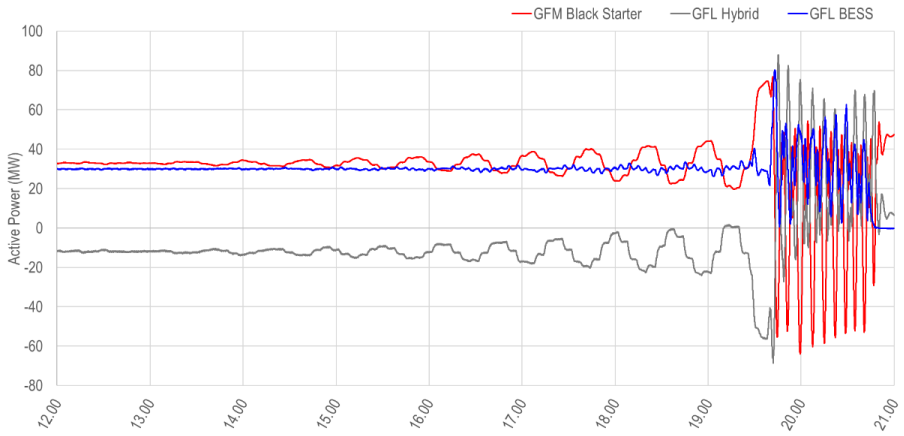

Figure 45 PPC enabled in default closed-loop control mode

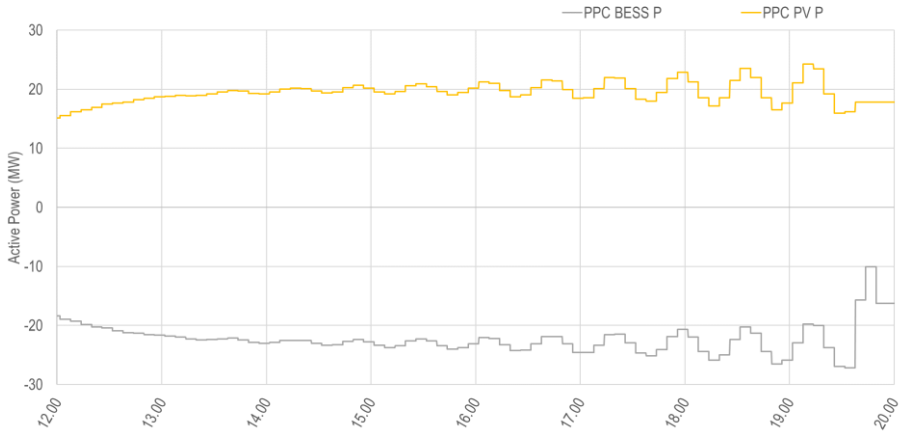

Figure 46 Commands sent from Hybrid PPC to inverters

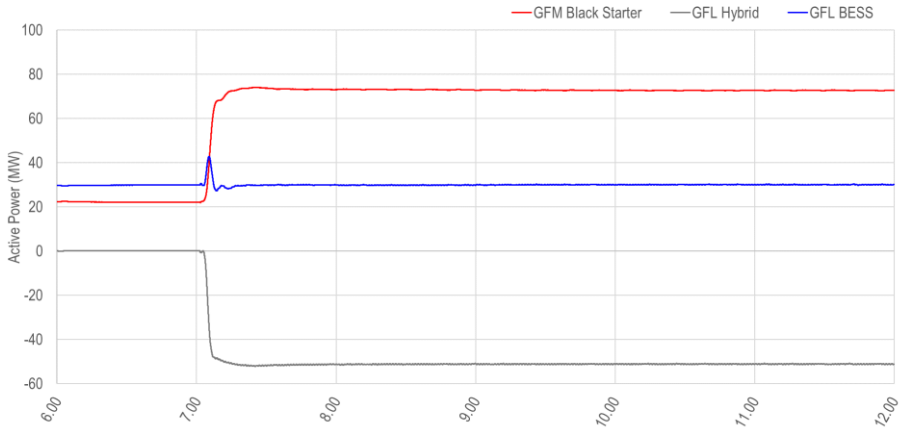

Figure 47 PPC set to open-loop control mode (direct inverter P/Q target control)

Note that in this example, the case with the PPC directly passing through an externally specified P & Q setpoint command (i.e., open-loop control) results in a sudden 50 MW absorption of active power. Despite this relatively major disturbance, all devices in the system remain stable and well damped, even though the plant is operating on the lower extreme of nominal voltage bounds (due to no Q compensation as the PPC is open loop). Additionally, although in both examples above the hybrid plant is energized at the same time, the direct-control method reaches the power setpoint target far faster than the case with the PPC enabled.

Note that in the example above, a negative setpoint (absorbing power) was chosen as the hybrid plant was to be used as a stabilizing load[11] in the original scenario being investigated. However similar behaviour is seen for MW injection scenarios, as shown in the figure below, where a +50 MW setpoint is commanded from the hybrid plant.

[11] With high penetration of DER in the distribution system, sourcing stable load during system restart to balance the system is often a major concern.

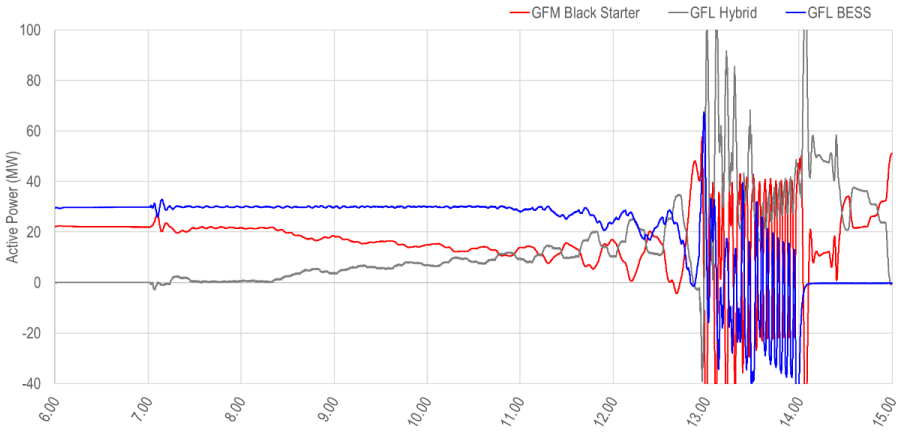

Figure 48 Repeated scenario for energy export

Hypothesis for instability

Noting that the aim of this milestone is to determine simple operational changes that can be made to restore stability to an IBR-based restarting system, rather to undertake detailed controller investigation, it was hypothesized that this PPC instability could be due to one of the more the following factors:

- PPC active and reactive power gains set to levels too high to maintain stability in a high impedance system.
- The use of multi-level PPCs in AC-coupled equipment with competing controllers (that is, a PPC for the battery, a PPC for the PV, and a PPC interfacing with the BESS and PV PPCs) and additional processing delays that each PPC introduces.
- The interaction of i) the PPC primary controllers for P & Q targets with ii) frequency correction algorithms within the PPC, especially where devices are set to begin regulating frequency to new ±0.015% standards.

In principle the PPC could be re-tuned to perform in a far more stable manner during a weak grid scenario. However, in operational timeframes there instead may be value in putting hybrid plant in open-loop control mode and therefore directly commanding P and Q setpoints, to maintain dynamic stability. This holds provided that appropriate manual reactive power compensation is taking place to maintain grid voltage stability. Note that this solution may also apply to non-hybrid installations that suffer from PPC instability.

DC Hybrid plant instability

The above scenario was revisited for a DC-hybrid plant with a single-level PPC. Instability was once again seen, but in a different and less catastrophic form compared to the AC hybrid plant. The instability also appears to be bounded for the scenario investigated.

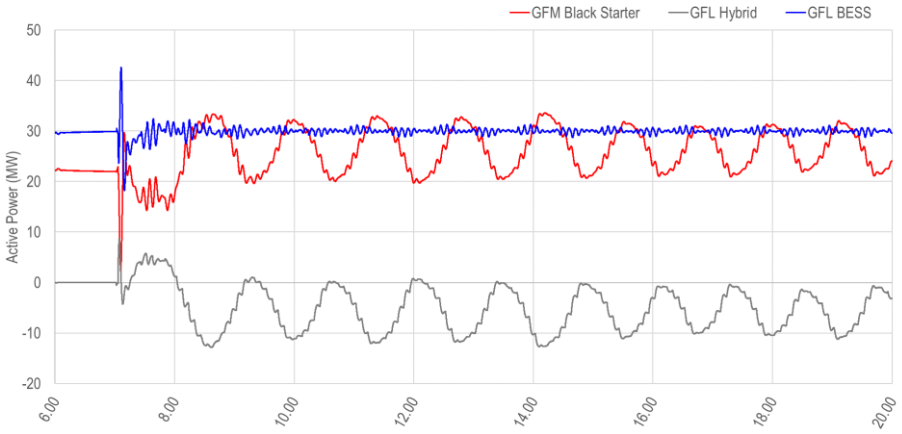

Figure 49 DC hybrid instability

Again, the instability appears to be originating within the controllers of the PPC, a conclusion drawn because direct P & Q command of the inverters results in stable plant operation at the target setpoints. However, in this case the P and Q setpoints had to be slowly ramped to their ultimate target, as the sudden application of a setpoint (i.e., a step) resulted in a system frequency collapse, apparently due to the DC plant having a more rapid injection capability than the AC system.

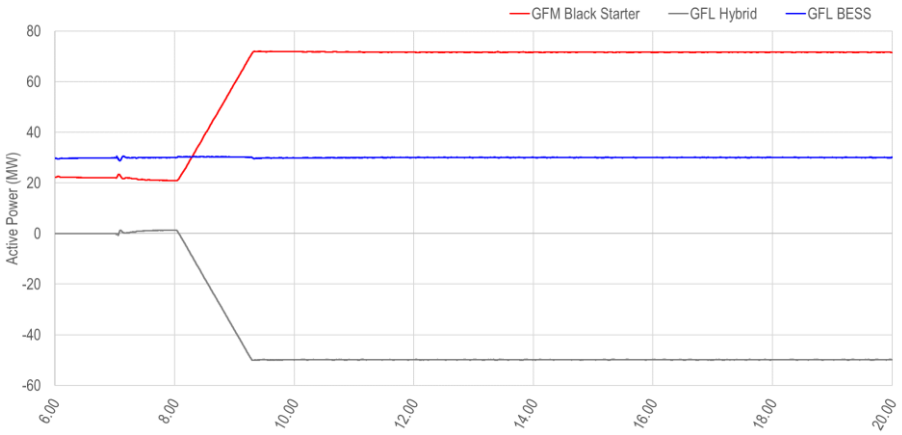

Figure 50 DC hybrid open-loop control

Given that this particular DC-hybrid configuration uses a single PPC for all outer loop control functions (voltage control, frequency control, setpoint control, etc.), competing PPC controllers and inter-PPC delays are not to be the reasons for the oscillation, and it is more likely to be interactions between the primary PPC P and Q controllers and any PPC limiters.

The conclusion that plant controller instability is best mitigated “on the day” by simply bypassing the PPC remains for this DC-coupled case.

4.2.6 Off-nominal frequency and voltage prevents device connection

OEM devices typically have target frequency and voltage bands that must be detected at the inverter terminals before the devices will attempt to connect to the network. From the OEM devices studied in this work, these “wait-to-connect” target frequency and voltage bands

were distinct from, of considerably tighter tolerance than, those that the inverters could ride-through and support after they had connected to the system.

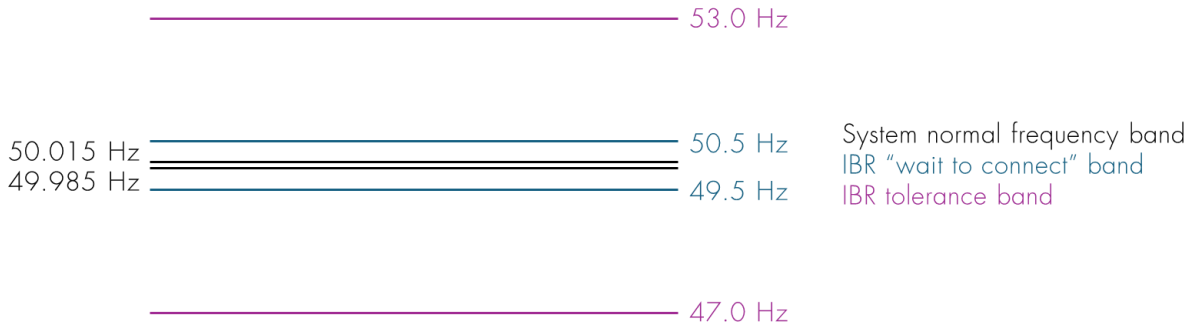

Figure 51 IBR devices "wait to connect" frequency bands are commonly much tighter than the maximum frequency variation they can tolerate, yet are comparatively generous compared to system normal frequency operating bands

Depending on the OEM, this may be an adjustable setting (as was the case for one OEM in this study), however it is undoubtedly a control system detail change that would typically require specialized resources on the ground to make the alteration (and likely also an externally energized plant).

Hence, the operational recommendation is, that when restoring a system from a GFM device with frequency droop:

- All else being equal, first energize those GFL devices that will be used in later support stages, before energizing load that may pull frequency substantially off nominal and outside wait-to-connect bounds (note the need for wider frequency droops mentioned in previous sections)
- To manually manipulate the frequency at which the system is operating, while still allowing for frequency control, apply an active power bias to the GFM device operating with droop control.
- Prioritise the restoration of GFL devices that will aid in frequency control but also will not have an overly aggressive (low value) frequency droop (high gain) as this could result in instability.

Frequency measurement corruption due to voltage harmonics

It is possible that, depending on the frequency measurement method used by the OEM, excessive voltage harmonics may result in a false frequency reading that is outside the wait-to-connect band, further delaying inverter synchronization. This issue is related to the insights discussed in Section 4.1.5

4.2.7 Internal power exchange of hybrid plant

A key variable, that was directly altered during the testing of hybrid plant responses to grid disturbances, was the internal power transfer between PV and BESS plant. This took the form of the PV device generating while the BESS was charging, with a net power injection

into the combined PV/BESS system fixed at 50 MW. The aim was to determine if internal (hybrid) plant setpoints have a bearing on individual plant stability and global system stability.

While there was not any instability observed for steady-state conditions, it was apparent that internal plant transfer had a material impact on stability in the presence of disturbances external to the hybrid plant, such as transformer energisations.

Below are two such examples. In both cases, an OEM-based 800 MVA hybrid plant is used, consisting of a 400 MVA PV component and 400 MVA BESS component, and the net transfer to the hybrid plant is +50 MW.

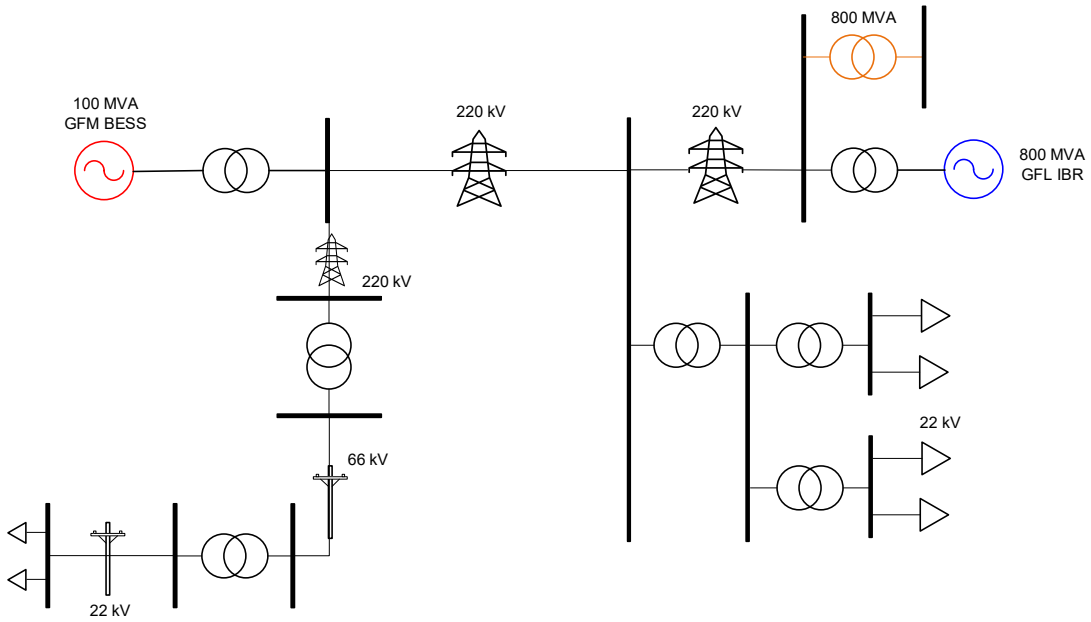

Figure 52 Case topology

In the first example this +50 MW consists of PV injecting 100 MW (red coloured generator, upper left) and the BESS (implicit in the blue IBR system, upper right) absorbing 50 MW for a net exchange at the PoC of +50 MW. The PPC is online and in default control modes (voltage droop control and frequency droop control). The disturbance is in the form of a nearby 800 MVA transformer (orange, upper right) being energized (with flux remanence behaviour).

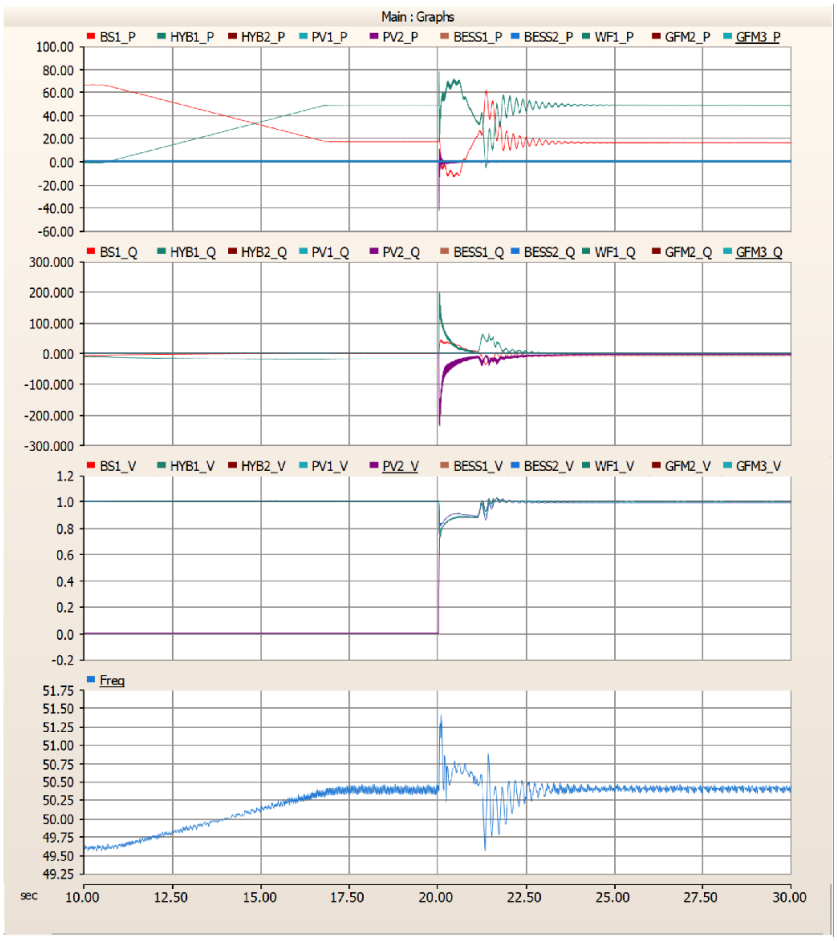

Figure 53 Hybrid plant energising a large transformer within minimal internal power exchange

Some minor oscillations in active power are observed (Figure 45, top subplot, red trace subplot) following the successful energisation of the nearby transformer, however it would be generally considered a case that has returned to stability as all voltages, frequency and plant internal commands eventually landed in a stable state.

In the second example, the plant, disturbance and net power interchange with the grid remains identical, only the internal power exchange is increased to 400 MW from the PV and -350 MW from the BESS. The PPC remains online.

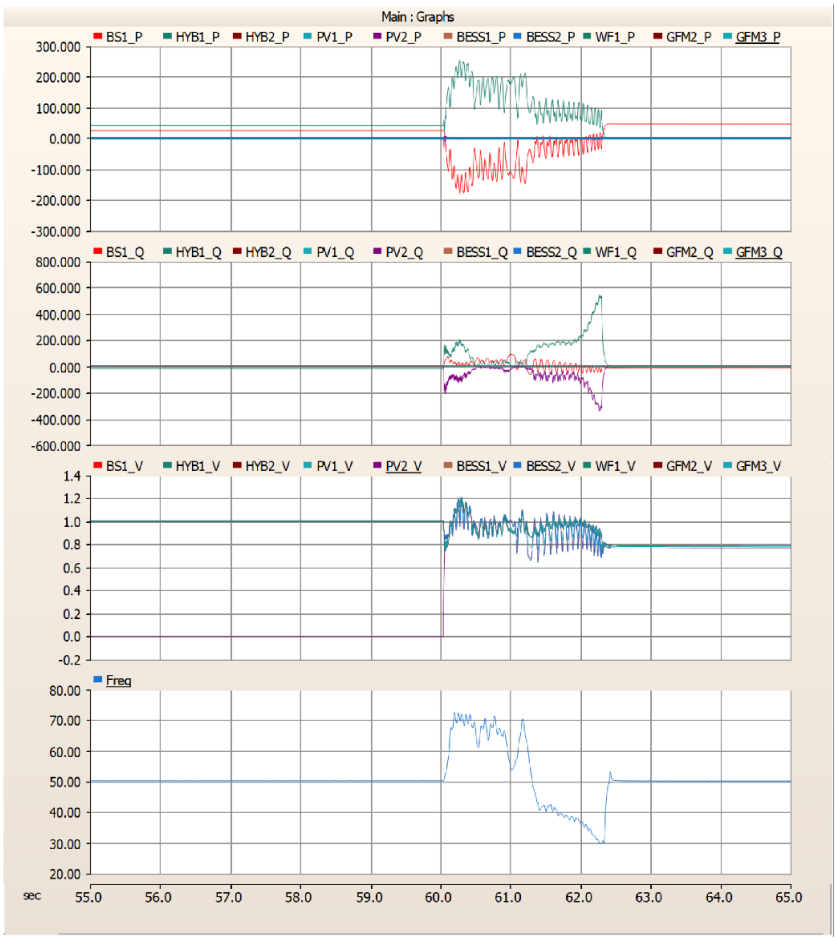

Figure 54 Hybrid plant energising a large transformer within large internal power exchange

In this case there is an immediate loss of system viability with a catastrophic MW mismatch resulting in system frequency (Figure 46, fourth subplot, blue trace) well outside operable bounds. A variety of protection relays would have operated, likely resulting in a system collapse. Any continued simulation beyond this point has limited value.

Given the previous identification of potential PPC instabilities, the above was repeated without the PPC in service (i.e., direct-control mode of P & Q) to determine whether the PPC contributed to precipitating the instability. Power transfer internal to the plant remains high (+400/-350) for this case/scenario, as does the disturbance. As can be seen in the Figure 47 below, the result is much the same, in that an excessive MW mismatch occurs resulting in what would be in reality a complete system collapse.

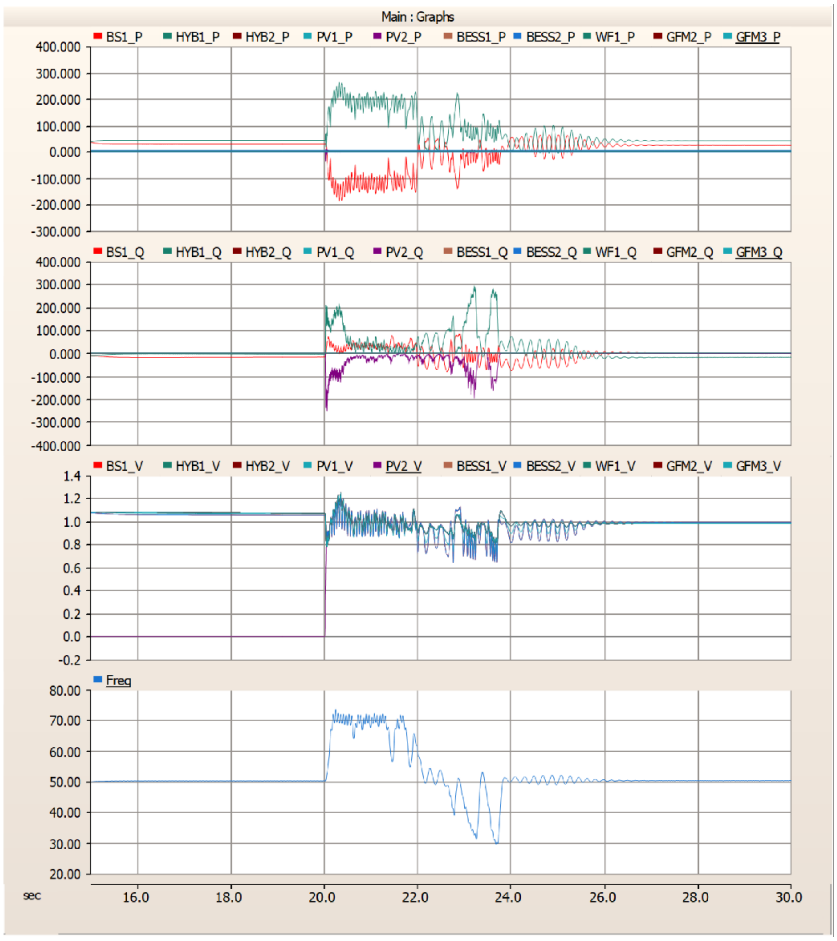

Figure 55 Hybrid plant energising a large transformer within large internal power exchange and PPC disabled

Investigating this response in more detail reveals that the discrepancy of MW balancing during a disturbance comes from a combination of the reticulation impedances and fault ride-through strategies of the PV and BESS aggregate inverters, which are different for each. The more distributed nature of the PV inverters saw a minimal cessation of active power during the fault, while the BESS inverters, located near the point of connection, entered deep into fault ride-through mode and consequently ceased active current injection.

The recommendations from this study have two aspects:

- For on-the day operation, hybrid plant should limit its internal active power transfer to quantities that the external system could tolerate to instantaneously absorb and still maintain equilibrium (i.e., minimize internal transfer as much as possible).
- For longer-term planning, hybrid FRT settings should be coordinated in such a way that consistent (similar) behaviour is displayed by constituent plant, so that the grid is not exposed to intolerable injections of active power (this may be challenging given the myriad of disturbances possible and the range of differences in reticulation).

4.2.8 Windup of PPC controllers in the absence of connected inverters

It was observed in several studies with one OEM inverter model, that where a plant had been energized for an extended period of time, but the inverters had not synchronized to

the balance of system (e.g., owing to terminal voltage or frequency being beyond the wait-to-connect thresholds), the PPC command to the inverters nevertheless continued to ramp to target. As a result, when the inverters did eventually synchronize to the system, they immediately jumped to their ramped target output quantities, causing a major voltage and frequency disturbance to a fragile system, that in reality would have collapsed the restoring system.

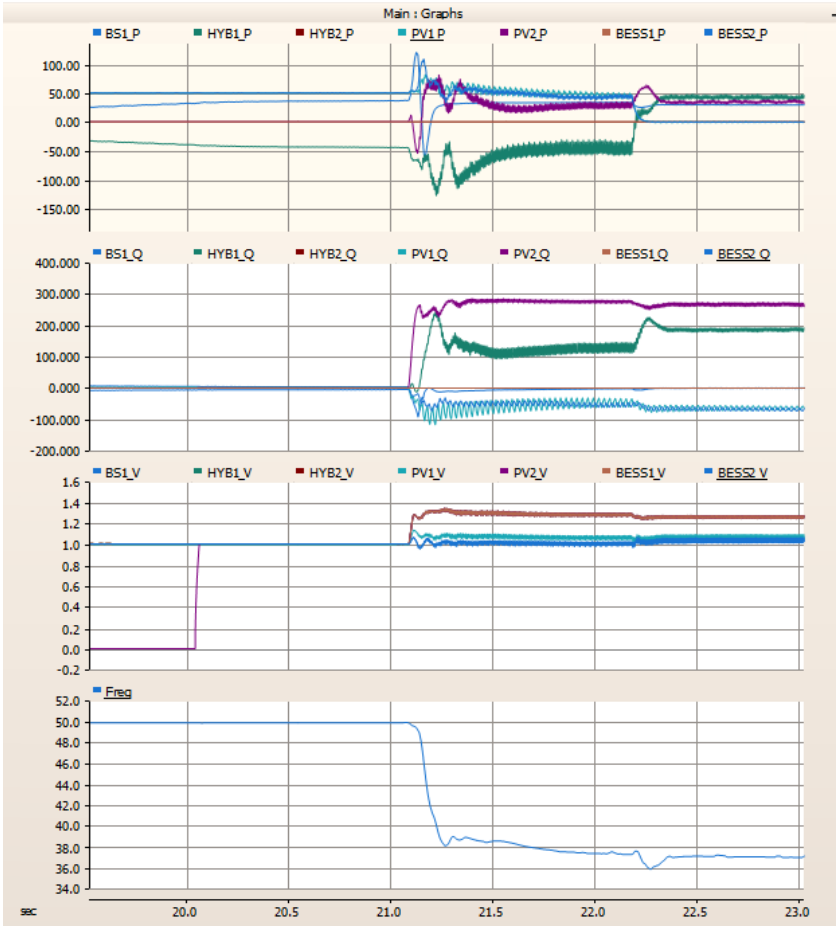

Figure 56 Pre-connection controller windup leading to instability on connection

It is unclear whether such behaviour would be reflective of the actual plant in the field, or if it is simply a modelling artefact. However, observing such behaviour even once from an OEM model leads to the recommendations to:

- Confirm with plant owners / technology providers that the PPC considers the online status of the units it controls before attempting to send or update a setpoint command (i.e., there is a form of feedback active)
- On the day, hold all target power setpoints at zero and place the voltage controller in open-loop mode while the plant is energizing and initializing, before attempting to ramp the plant to a target power.

Shallow fault behaviour of GFL devices

Throughout the runs attempted, it was seen that there was a greater likelihood for instability where a disturbance on the system imposed a long (i.e. multi-second), shallow

voltage depression, such as may occur for a large transformer energisation on the system. In contrast, deep faults which saw devices clearly enter into a fault ride-through mode appeared to be less onerous. It was unclear whether such instability is a result of PPC frequency controllers remaining active during the disturbance (the minimal voltage drop is insufficient to trigger temporary disablement), whether the instability manifested from a deeper, faster control loop within the GFL device, and whether the issue is manufacturer-specific. Also noteworthy is that the instability occurs upon fault clearance, rather than during the fault. Despite the precise mechanism of the instability not being identified, there is a strong recommendation, when developing system restart plans, to test specifically for scenarios where a sustained low voltage is imposed on the network. This is to confirm the ability of controllers present to maintain stability under these apparently milder conditions, rather than only considering the typical “deep” fault scenario (which are typically considered to be the most arduous for system normal studies). Figure 57 shows an example of this behaviour, where a deep, short fault is applied at t=15.0 s, while a one second shallow voltage depression is applied at t=20.0 s.

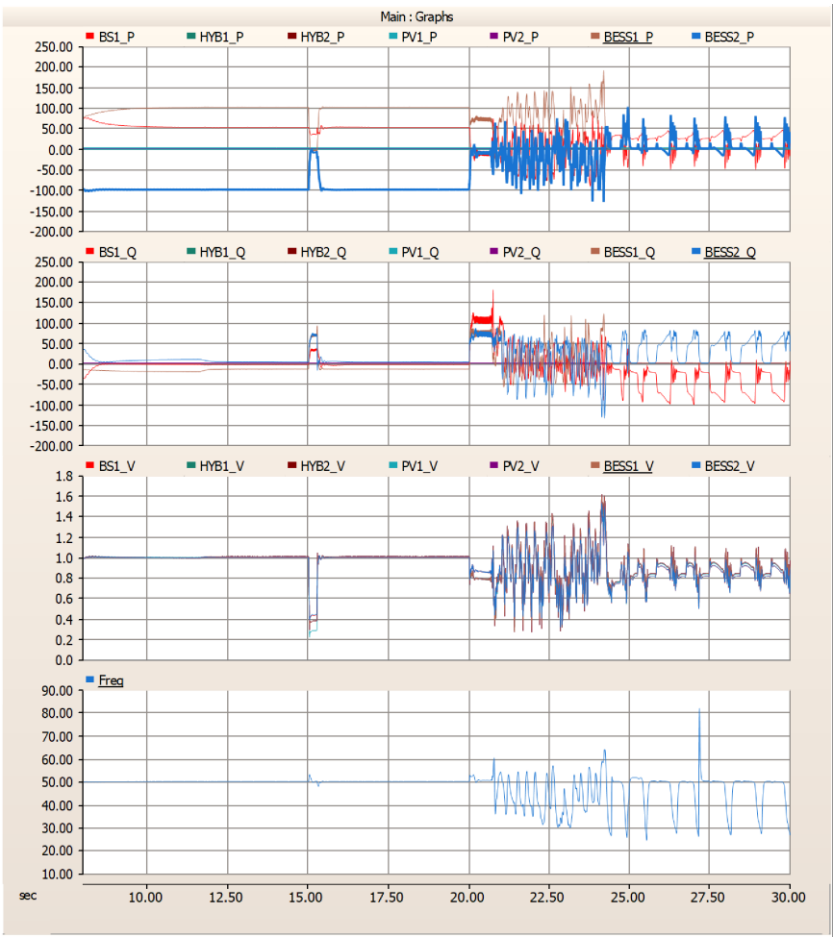

Figure 57 Deep and shallow fault application during restart

Shifting of system balance points

In addition to the potential for shallow faults to precipitate an instability of the system under study, it was observed that where multiple IBR devices with PPCs are online in a weak

system, long, shallow faults could result in the active power operating point of the devices comprising the system to shift to a new equilibrium upon fault clearance. The mechanism for this is by some IBR plant entering fault ride-through mode, while others do not. This resulted in some frequency controllers being active, and others not as they shifted to reactive power priority injection during the fault. Depending on which site was providing frequency control prior to the fault, alternative shifts in system equilibrium could be observed post-fault. An example of this is shown in Figure 58.

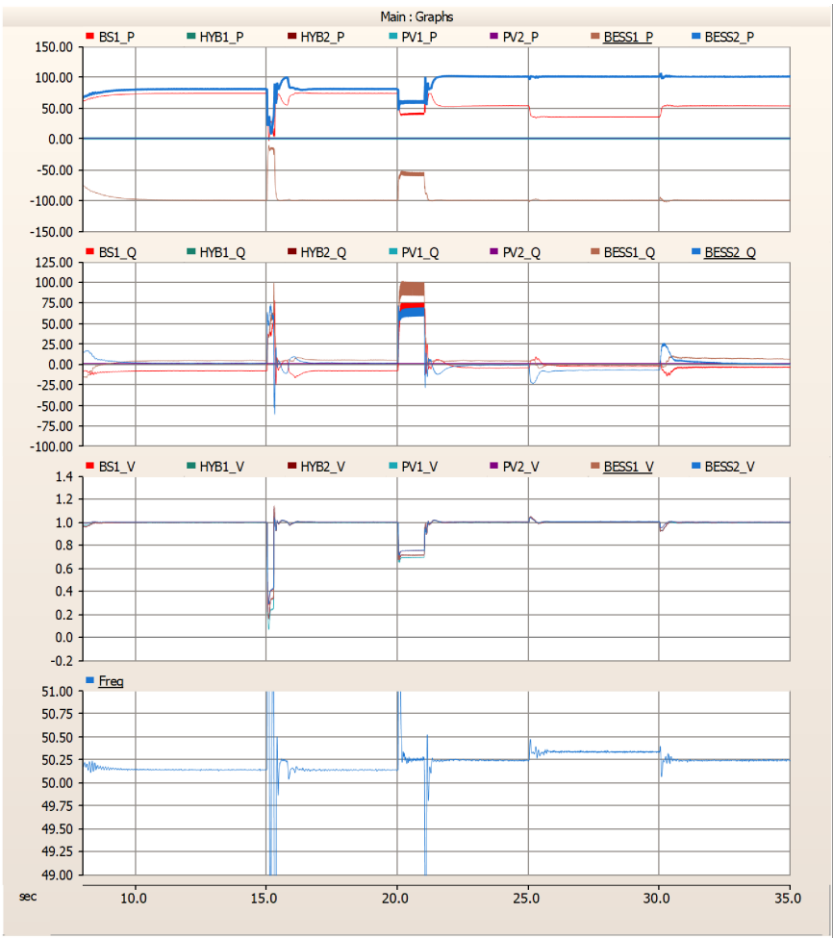

Figure 58 Post-fault equilibrium shifts during restart

The recommendation following from this observation is that IBR plant being re-energised in an early system restart should always maintain headroom to account for a possible shift in system setpoint equilibrium following a shallow, long disturbance that has the possibility to shift the setpoint of individual IBR frequency controllers. If insufficient headroom from frequency-sensitive plant is available, there may be increased chances for post-fault oscillations and heightened risk of system frequency collapse.

4.2.9 MW ratios to reduce steady-state instability

It was observed that minor steady-state instabilities developed in the restarting system for a particular OEM of GFL plant when the GFL to GFM ratio approached 8:1. This occurred with the PPC out of service, which immediately precludes the PPC instability issues discussed

previously. The instability occurred in the absence of any major disturbances, and in the example here, was most prominent in reactive power output.

Given that the PPC was not enabled and that inverters were being commanded in open-loop (target P and Q export only), the oscillations are likely to have manifested due to fast inner controller instability issues. This was seen as an opportunity to test whether a commonly used approach to attempt to reduce oscillations, namely constraining the active power output of a GFL device (only), can help reduce oscillations in a (very) weak grid scenario.

The following image shows a series of steps taken to attempt to reduce the minor steady-state oscillations within a single simulation run. During the run, the following key events occur:

1. The GFL inverters connect
2. The GFL inverters are ramped to their target aggregate output of 60 MW. This 60 MW export is shared across 800 MVA rated capacity of devices (output ~250 kW/device)
    a. N.B. the increased grid voltage due to the power export by the inverters resulted in a higher MW output than the target, as the GFL inverter is operating effectively as a current source rather than with controlled *active power*.
3. Q output is manually adjusted to bring local voltage back to target
4. The number of online GFL devices is halved without changing the active power setpoint of individual devices (400 MVA online).
5. The number of online GFL devices is halved again without changing the e active power setpoint of individual devices (200 MVA online).
6. The remaining 200 MVA of online GFL devices are redispatched by the PPC such that the original aggregate ~60 MW target is achieved.

The comparison between the initial GFL export and final GFL export states is most important. Both states have a net ~60 MW target, but only the latter stages show no signs of unstable behaviour. This serves to reiterate the conclusion that inner control loop instability phenomena is not necessarily primarily a function of MW export from the plant but is more tightly related to the total MVA of connected plant.

Hence the operational conclusion here is that, where a GFL plant is providing a contribution to the restarting system, and there is reason to believe that system strength instabilities may manifest (e.g., an older GFL plant is energized that was designed for a much higher nominal system strength), it is recommended to maximise the MW to inverter ratio (active power output per device, subject to headroom considerations) to avoid the potential for GFL instability to manifest by having too many individual inverters online.

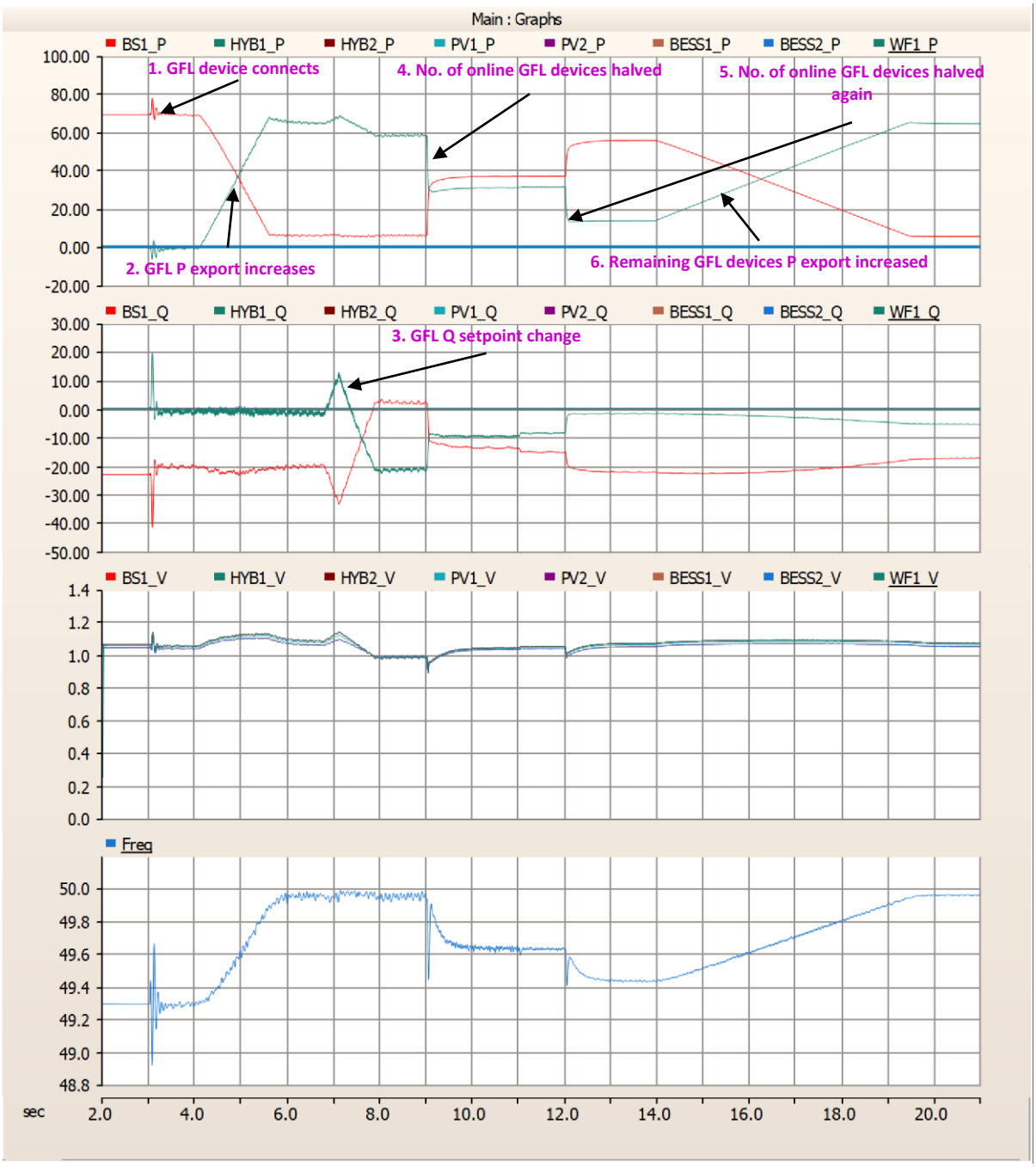

Figure 59 Sequence investigating restoring stability through MW and MVA adjustments (15a)

4.2.10 Energisation of large transformers nearby to GFL plant

As requested by an AR-PST partner, a brief investigation was conducted into the challenge of energizing large transformers that are electrically close to a GFL device that is providing energy into a restarting system (parallel connected). The aim was again to find an operational strategy that could be adopted on the day to avoid larger impacts to the system.

Such a scenario may occur in a REZ, where the first GFL device has been energized and is supporting the network, and a point of connection transformer is energized in an attempt to bring another REZ plant online.

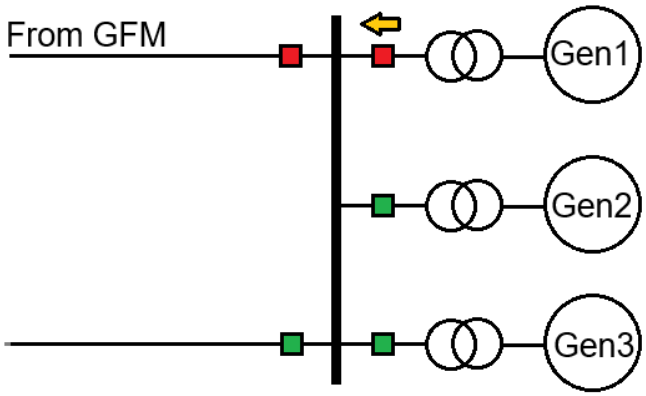

Figure 60 Energising transformer of Gen2 or Gen3 after GFL Gen1 is online and exporting

Energisation of large transformers in a restarting system is a well-known challenge due to the possibility for the transformer to have remnant flux and to be energised at a point on the voltage waveform that would lead to an induction of core flux that is opposed to the remnant flux. This would cause a particularly large transient due to the excessive current draw required to instantaneously reestablish the new flux (see Section 4.3.2). For all intents and purposes, such a transformer energisation is similar to applying a large non-linear fault to the system.

The results of the limited studies to date in Stage 4 showed that there is no obvious operational strategy to consistently mitigate the issue of a large disturbance being imposed on the system due to transformer inrush, if there are no existing pre-insertion resistors or point-on-wave breakers already installed (which themselves may have limited success in mitigating inrush). In most cases investigated, the transformer energisation triggered fault ride-through behaviour of electrically close plant due to the voltage depression during inrush. Matters were further complicated for IBR installations with internally circulating power flows (e.g. solar-BESS hybrid plant) in cases where only some devices enter FRT and others don't. In such circumstances, the disturbance may cause a fast power unbalance of the system leading to frequency collapse, as was discussed in Section 4.2.7.

Efforts were made to investigate, whether the overall system impact during energisation could be minimised by avoiding nearby LVRT activation. This was attempted by increasing the initial setting of the controlled voltage (e.g., 1.1 pu) of the point of connection of the GFL plant that is already active and nearby to the transformer to be energised, with the aim of avoiding any power imbalances. However, this operational arrangement was unsuccessful with generally worse performance than a simple FRT activation for a normal PoC voltage of around 1.0 pu, and resulting in severe energy swings and local LVRT activation voltage thresholds (0.8 pu) still breached. Figure 61 below shows a scenario where the Hybrid GFL device near the transformer being energised is commanded to set a PoC voltage of 1.12 per unit.

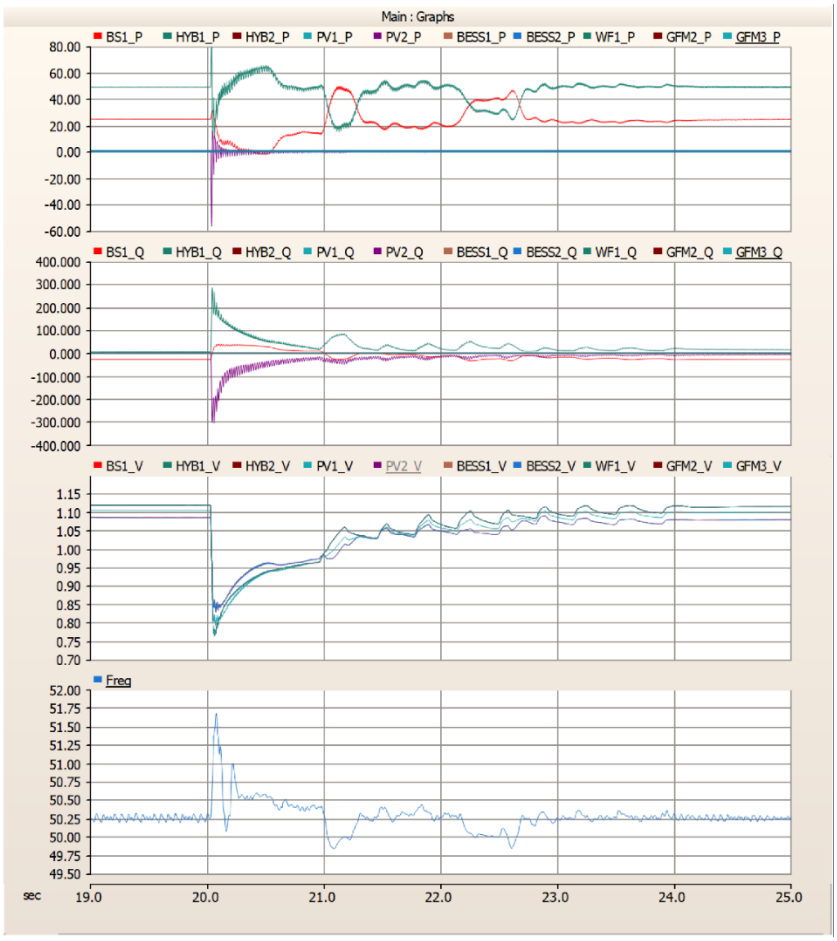

Figure 61 System response to transformer energisation with higher initial voltage

This approach was discontinued owing to the following deficiencies:

- The risk of unintendedly activating HVRT mechanisms during the transient, as GFL IBR plant in a weak system may oscillate between themselves.
- The increased current draw from the transformer for higher initial energisation voltages which, depending on the network and protection relay settings, may be even more detrimental (see image below) or may still trigger LVRT thresholds (see image below).
- The general impracticality of finding, in a single attempt on the day, an optimised target voltage setpoint that keeps all nearby plant terminal voltages in a “Goldilocks zone” of FRT avoidance and also retains system power balance – and uncertainty about whether avoiding FRT mode is generally advisable.

This is a genuine practical problem that is worthy of more detailed investigation in future Topic 5 research stages.

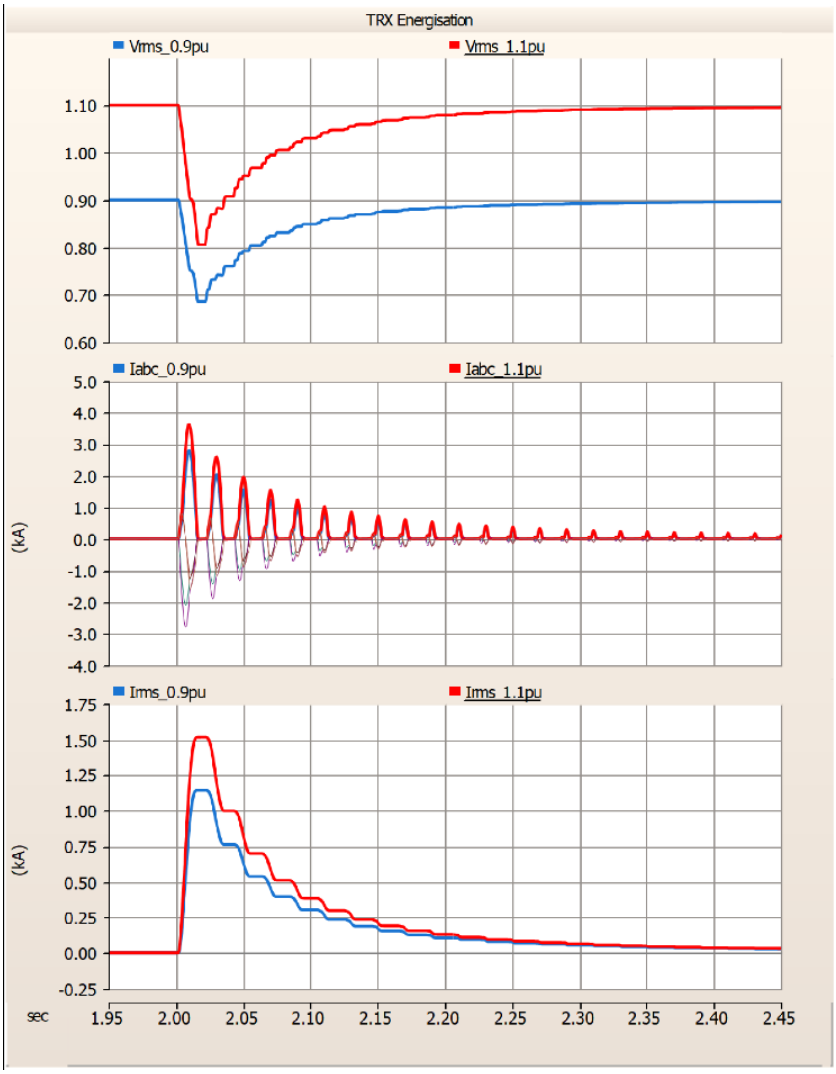

Figure 62 Simulation showing increased peak transformer inrush current and greater voltage dip magnitudes for increased initial terminal voltages

4.2.11 Operational mode of the black start unit

As the name suggests, an IBR in virtual synchronous machine mode emulates a synchronous machine, including possible oscillatory behaviour following a power balance disturbance. While changing the inertia time constant within a VSM-based GFM is not necessarily an immediate operational change that can be made "on the day" of a restart event, doing so may adversely affect system stability, which is already compromised in a weak, restarting system by the coupled nature of voltage and frequency events.

An inertia time constant that is too small (e.g., below 1 second) can make frequency control extremely challenging, because small mismatches in the active power balance (such as that due to reduction in demand caused by a voltage dip from transformer energisation) result in extreme changes in network frequency.

For the VSM models used in this work, an inertia time constant that is too large was also seen to be problematic, particularly where multiple VSM devices are simultaneously energised. Figure 63 below shows, following a fault and clearance, slow, growing oscillations in the active power output of two devices. This is the result of the devices exchanging active power with one another across the network and a subsequent inability to return to a steady state.

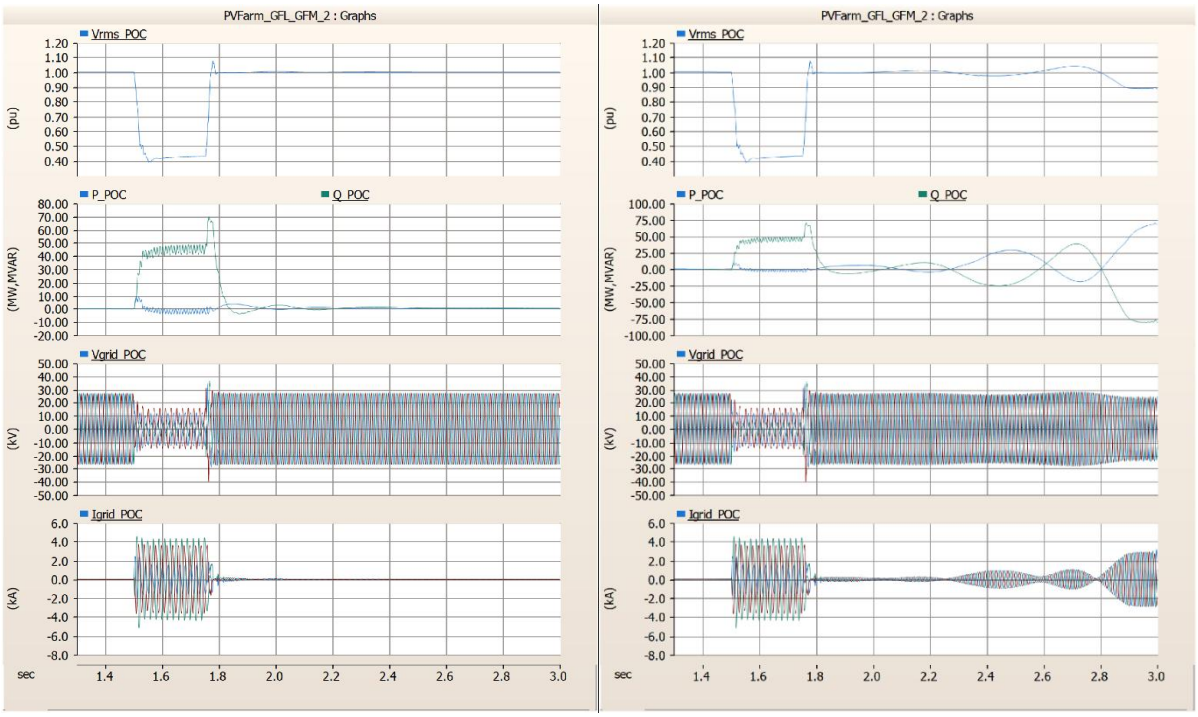

VSM GFM vs. VSM GFM (100 MVA:1000 MVA, inertia 1s:1s)

VSM GFM vs VSM GFM (100 MVA:1000 MVA, inertia 7s:7s)

Figure 63 Example of growing oscillations of multiple VSMs in a system with higher inertia constants

It is important to recognise that this behaviour may be specific to the models used here and may not appear with alternative manufacturer models that use alternative implementation algorithms. The VSM-based GFM model used was generic and was not compared against any OEM VSM model. This is because all the OEM models available for this study used only

droop-based GFM approaches. Nevertheless, the observation of one instance of undesirable interactions between VSM devices during restart is sufficient to demonstrate its credible possibility.

Note that it was seen that VSM GFMs with large inertia time constants returned to stability if another nearby GFM plant was a droop-based GFM plant, as shown in Figure 64.

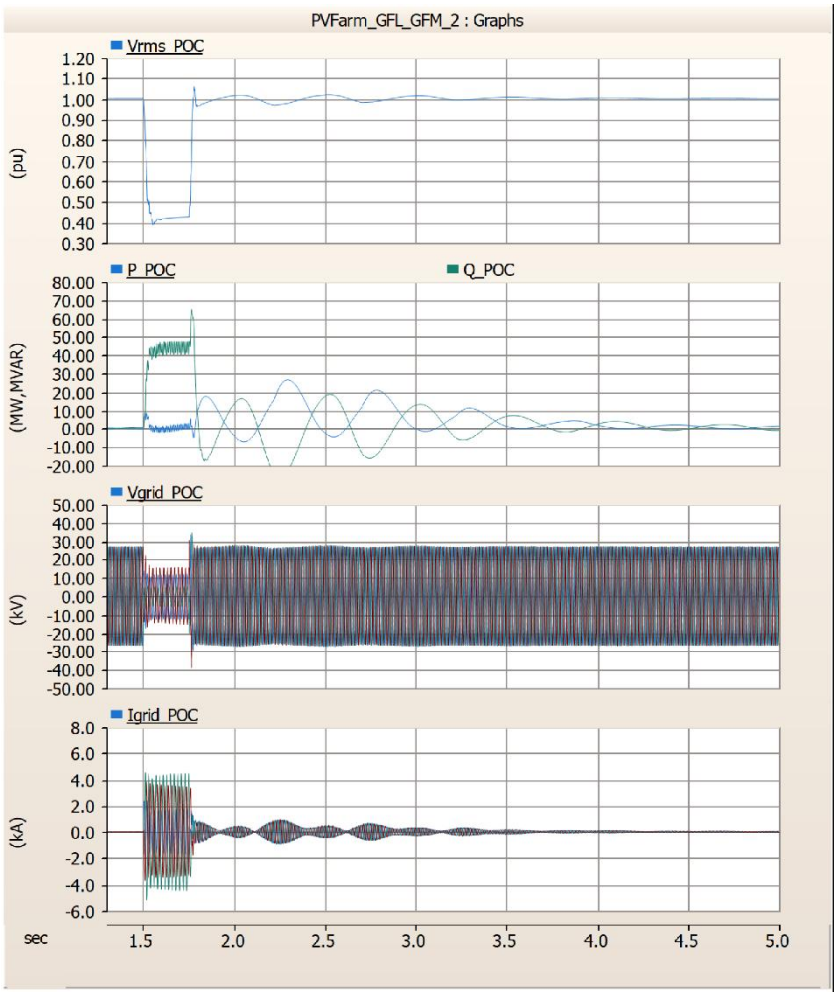

Figure 64 A 100 MVA, H=7s VSM GFM and 100 MVA Droop-based GFM returning to stability post fault

Droop GFM IBRs

The behaviour of GFM IBRs operating in droop mode was not observed to be similarly sensitive to either the selection of internal control constants, nor the presence of multiple droop-based GFM IBR. These observations held with the frequency droop of the GFM devices limited to 1% or greater, with 3% being chosen for the majority of the droop-based studies.

An example is shown in Figure 65 below of two droop-based GFM devices (one 100 MVA, one 1000 MVA) subjected to the same fault as the VSMs previously. The devices returned to stability rapidly and showed no signs of adverse interactions.

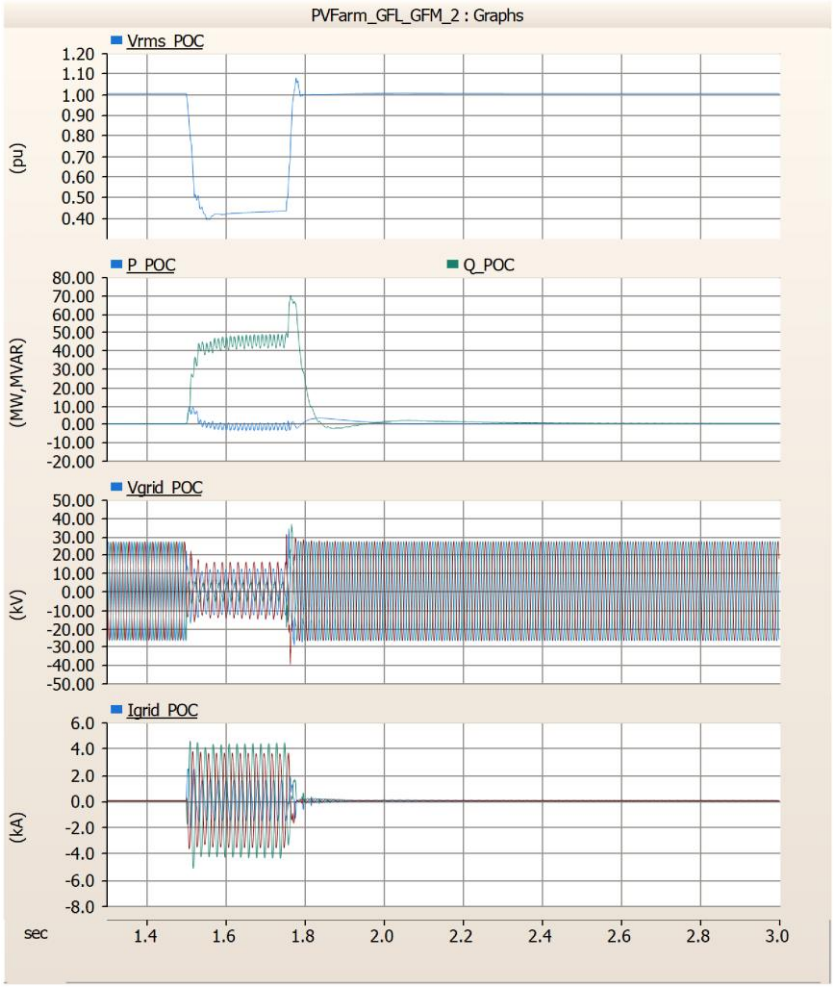

Figure 65 Two droop-based GFM BESS devices remaining stable post-fault

Hence, a preliminary recommendation, though recognising the lack of a variety of OEM VSM-based GFM devices and VSM algorithms considered, is that where multiple GFM devices are to be energised in a weak system, it may be possible to reduce the likelihood of adverse interactions by energising droop-based GFM devices first. However, this preliminary recommendation should be validated using OEM-specific plant models and the specific network topology. It was also noted that, of the two OEM-specific GFM inverters available for this research, both had a droop-based strategy (only) in their equipment.

4.2.12 Destabilisation of droop-based GFM

It was found to be particularly challenging to destabilise droop-based GFM devices, even for cases with extremely large short-circuit ratios evaluated at the plant point of connection. At first glance this contradicts most literature on GFM instability which indicates instability manifesting in strong grids [15]. However, on further investigation, it was found to be entirely consistent; the key differentiator in the models in our studies is the presence of impedances between the GFM control point and the remainder of the network, impedances which are often neglected in research examples. By neglecting these additional intervening impedances, increasing grid strength effectively results in two voltage sources being represented as directly connected to one another.

This was demonstrated using the open GFM model (droop mode) provided by EPRI, where the voltage control node of the device is at the capacitor of the L-C-L filter. Instability was observed when bypassing all upstream impedances and connecting a strong voltage source at the control node. However, this situation is unrealistic as there will always be some inductance between the capacitor node and the remainder of the grid.

Figure 66 shows the common GFM coupling arrangement considered in some research papers (top topology) [16] [17] and the more realistic arrangement that would occur in the field (bottom topology). Specifically, as in the bottom topology, there will always exist an inductance L2 in a grid connected inverter between the control node and the grid, be it in the form of the filter inductance to meet harmonic emission limit requirements, unit transformer reactance, reticulation impedance, or step-up transformer reactance.

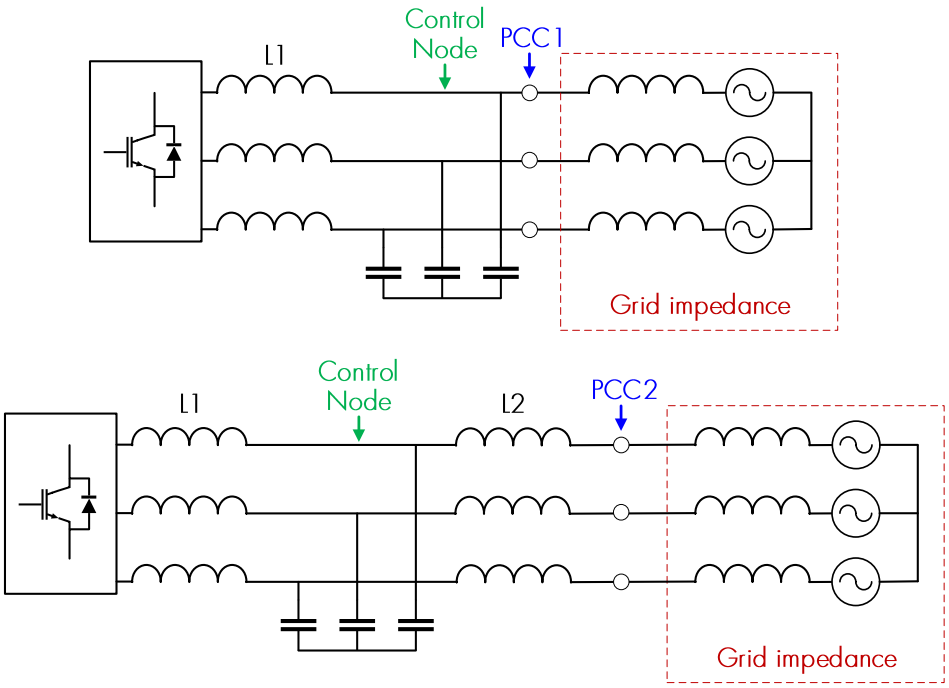

Figure 66 Commonly considered coupling arrangement (top), realistic coupling arrangement (bottom)

A series of tests were conducted to subject droop-based GFMs to a variety of destabilising scenarios in a SMIB or MMIB model.

In these scenarios, the SCR is altered in discrete steps throughout the run, and once the system has settled a fault is applied to determine whether the device will return to a stable state. An example of the case arrangement is shown in Figure 67, where the SCR is altered by adjusting the impedance near the infinite source. A typical result seen is shown in Figure 68.

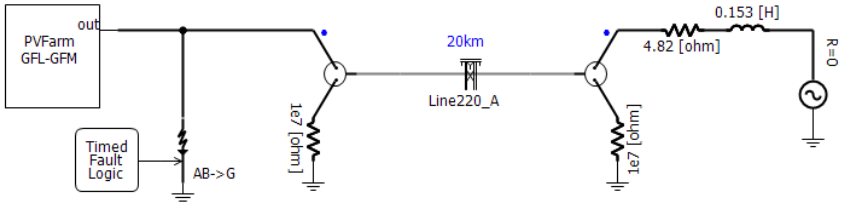

Figure 67 SMIB case setup

No instability was observed for cases where the GFM IBR was required to inject or absorb only up to 1pu energy at SCRs below 1.0 (which is to be expected). A selection of results is available in Appendix C .

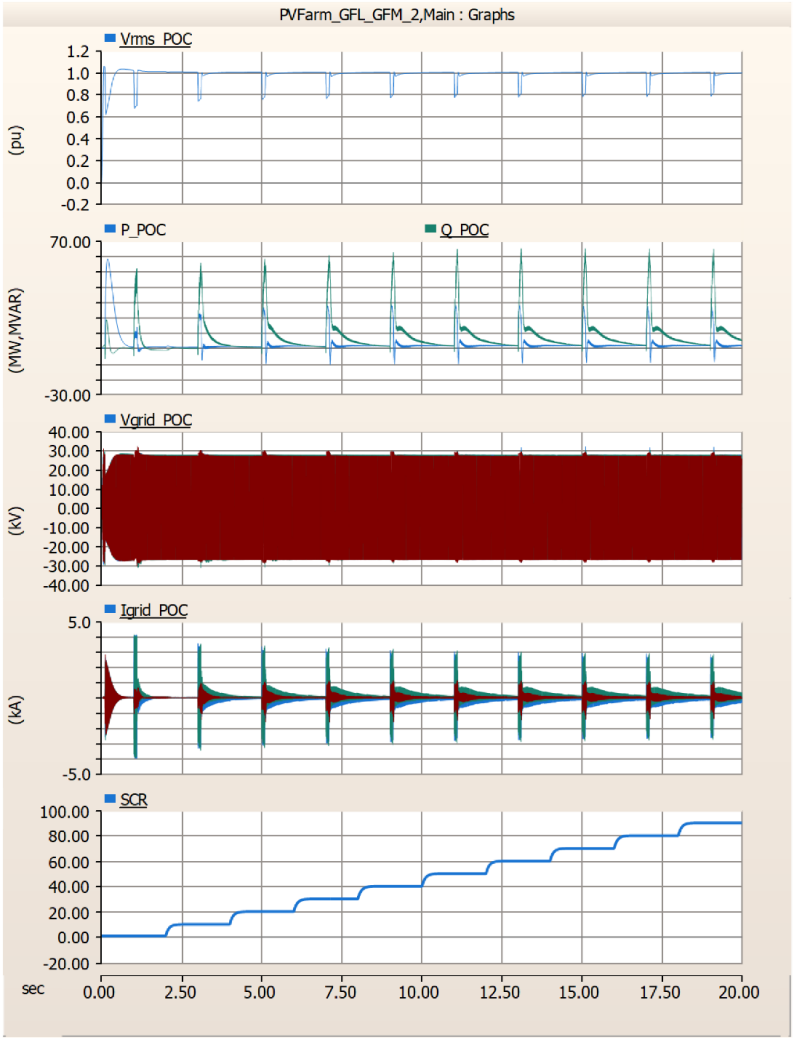

Figure 68 EPRI generic droop GFM. 3% frequency droop mode. Variation of grid strength (SCR) from 1.0 to 9.0, X/R held at 10

4.3 Milestone 3 – Protection operation during 100% IBR restart

Milestone 3 sought to identify whether the behaviour of protection relays is sensitive to the devices used for system restart, particularly for the scenario where multiple cascaded transformers, energised discretely in series, may experience false tripping of differential and distance protection relays.

4.3.1 Key findings summary

The following table summarises the cases investigated in this work and their conclusions.

Table 3 Milestone 3 case conclusions

Case	Protection Type	Black starter	Trip on energisation	Trip on fault	Notes	Result
01	Line Distance – 110km 220kV line	OCGT	No	Yes	-	Pass
02	Line Distance – 110km 220kV line	GFM BESS	No	Yes	-	Pass
03	Transformer Differential – 225 MVA at line end	OCGT	No	Yes	Flux remanence disabled	Pass
03a	Transformer Differential – 225 MVA at line end	OCGT	Yes	N/A	Flux remanence enabled	Fail
04	Transformer Differential – 225 MVA at line end	GFM BESS	No	Yes	Flux remanence enabled	Pass
04a	Transformer Differential – 225 MVA at line end	GFM BESS (OEM)	Yes	N/A	Flux remanence enabled	Fail
04b	Transformer Differential – 225 MVA at line end	GFM BESS (OEM)	No	Yes	Flux remanence disabled	Pass
04c	Transformer Differential – 150 MVA at line end	GFM BESS (OEM)	No	Yes	Flux remanence enabled Harmonic blocking thresholds reduced	Pass
05	Multiple Transformer Differential – 150 + 25 + 25 at line end	OCGT	No	Yes	Flux remanence enabled Harmonic blocking = 15%	Pass
06	Multiple Transformer Differential – 150 + 25 + 25 at line end	GFM BESS (OEM)	Yes (1st transformer on 2nd transformer energisation)	N/A	Flux remanence enabled Harmonic blocking = 15%	Fail
06a	Multiple Transformer Differential – 150 + 25 + 25 at line end	GFM BESS (OEM)	Yes (2nd transformer on 2nd transformer energisation)	N/A	Flux remanence enabled Harmonic blocking = 15%	Partial pass
07	Multiple line distance – 110 km 220 kV + 5 km 220 kV + 70 km 66 kV line	OCGT	No	Yes	220A line tripped for out-of-zone fault	Partial pass
08	Multiple line distance – 110 km 220 kV + 5 km 220 kV + 70 km 66 kV line	GFM BESS (OEM)	No	Yes	-	Pass

Furthermore, the following general findings were concluded.

- For transformer differential protection relays, the harmonic blocking thresholds (Ih_x/Iop) may need to be reduced to allow successful energisation of transformers from all black start sources. In this work, setting such thresholds to 10-20% of fundamental RMS current

saw successful energisation from (all/both) OEM-specific IBR sources without compromising the fault detection ability of the differential protection relays.

- The generic models investigated showed a greater ability than the OEM models to allow transformer energisation without tripping differential protection. Further investigation is required to determine whether this is because the generic models employ better algorithms for energy delivery, and/or because the OEM versions more accurately reflect actual plant limitations. This is a key recommendation for further research.
- Multiple energisations of transformers may increase differential relay tripping when an IBR source is used. However, such maloperations can be minimised (N.B. not entirely prevented) if sufficient time between energisations allows current distortion to decay, in particular, when negative sequence current supplied from the black starter has decayed to pre-disturbance values (or zero).
- Multiple energisations of transformers in series may cause false tripping of differential protection relays, which both GFM BESS and OCGT restart technologies. No simple remedy was found outside of changing protection relay settings.
- There is evidence of 4th harmonic reprise on GFM BESS transformer energisations.

4.3.2 Methodology

These scenarios were tested with the limited-area model previously developed (see Section 3.1), with some modifications to include protection relays and additional fault elements. Transmission line distance, and transformer differential, protection relays were applied to most of the network elements, as shown in Figure 69.

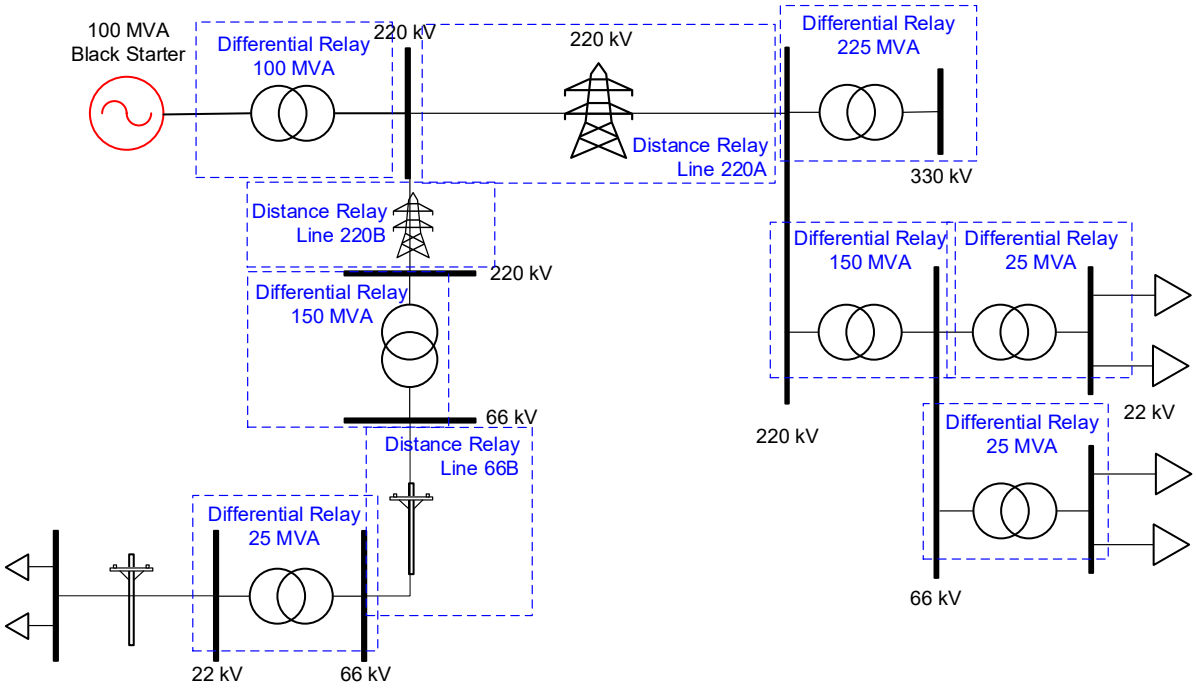

Figure 69 Location and type of protection relays in the limited area case

The following scenarios were then investigated to determine whether the protection relays tripped correctly for a valid fault condition, tripped incorrectly for a non-fault condition, or failed to trip for a valid fault condition.

Table 4 Scenarios considered for milestone 3

Scenario #	Area of analysis	Black-start source
1	Line differential protection relay behaviour for line energisation and fault application	Gas Turbine
2		Grid forming BESS
3	Large (225 MVA) transformer differential protection relay behaviour for line-end transformer energisation and internal fault application	Gas Turbine
4		Grid forming BESS
4a, b, c		Grid forming BESS (OEM model)
5	Multiple transformer differential protection relay behaviour for multiple line-end series transformer energisations and internal fault applications	Gas Turbine
6		Grid forming BESS
7	Multiple line distance protection relay behaviour for multiple series line energisations and fault applications	Gas Turbine
8		Grid forming BESS
9	Large (225 MVA) transformer differential protection relay behaviour for line-end transformer energisation and fault application using pre-insertion resistors	Gas Turbine
9a		Grid forming BESS

Throughout these investigations, and as data suggested it would be worthwhile considering, additional cases were examined. These were predominantly on:

- Adjustments to harmonic blocking thresholds of transformer differential protection relays.
- Quantification of harmonic components of voltage and current during transformer energisation.

- Sizing of pre-insertion resistors to avoid transformer tripping.
- Confirmation of worst-case scenarios for energising transformers with flux remanence enabled.

Transformer flux remanence

Crucially to the investigation of all scenarios, the flux remanence of the transformer(s) was set to 0.8/-0.8/0. This setting establishes a fixed stationary flux in the core of +80% of nominal in the first limb (A), -80% of nominal in the second limb (B), and 0% in the third limb (C), as shown in Figure 70.

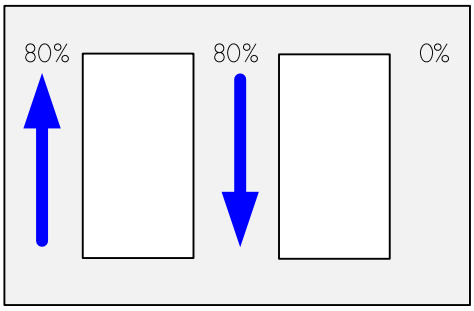

Figure 70 Flux remanence in the transformer core

By doing this, we reflect a scenario whereby a transformer has been recently de-energised in a worst-case known state, leaving the core flux 'frozen' in a moment of time. This will allow us to evaluate transformer re-energisation at the worst possible moment in the voltage cycle of the re-energising source, whereby the transformer is required, near instantaneously, to re-establish its core flux in the opposite direction to the remnant flux, drawing large amounts of current.

For this arrangement of 0.8/-0.8/0, the worst possible moment to re-energise this transformer is when the A-phase voltage is crossing from negative to positive through zero. This can be confirmed by performing statistical analysis to measure inrush current peak magnitude, as shown in Figure 71.

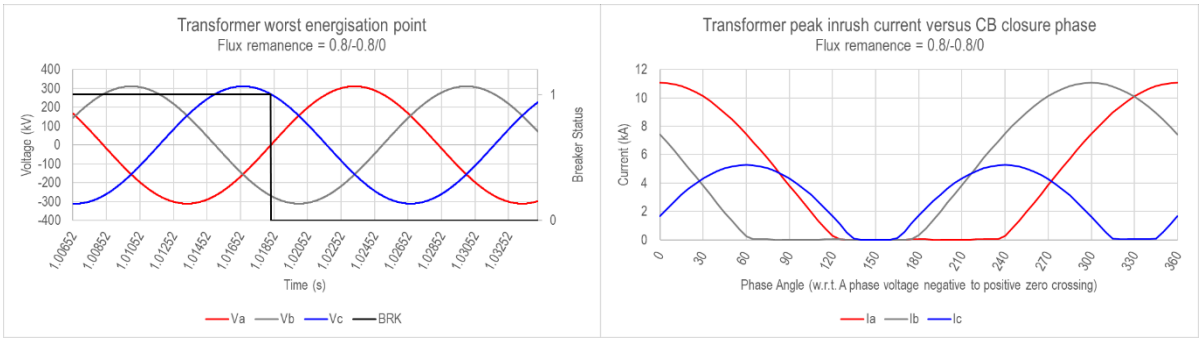

Figure 71 Identifying the worst moment to close the transformer breaker

Although there are potentially multiple circuit breaker closure points which will induce the worst inrush current on different phases, the use of the phase A negative to zero crossing point allows the use of a convenient sequencing block in PSCAD (shown below) to reliably induce the maximum possible inrush current each time a test is performed.

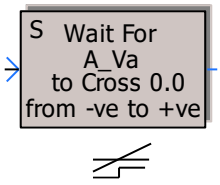

Figure 72 PSCAD zero-crossing detector sequencer

Hence in these studies, all transformers were energised on the negative to positive A-phase voltage zero-crossing.

Transformer differential protection settings

The following are extracts from the transformer differential protection settings used in the case, as set up by EPRI expertise.

1. Relay configuration	
Differential relay characteristics	DRC1: Dual Slope
Restraint current calculation metho	Kres*(|I1|+|I2|+... |I6|)
Restraint current multipling factor (	1.0
2. Settings	
Minimum operating current	0.1 [pu]
High operating current setting for u	5.0 [pu]
Slope in region 1 (%)	20.0 [%]
Slope in region 2 (%)	40.0 [%]
Restraining current at slope 1 chan	2.0 [pu]
Restraining current at slope 2 chan	3.0 [pu]

1. Configuration	
Second harmonic blocking	Enable
Fourth harmonic blocking	Enable
Fifth harmonic blocking	Enable
Enable cross blocking	Disable
2. Harmonic Settings	
Minimum differential current to enable harmonic blocking	0.05 [pu]
|Ih2|/|Iop| threshold for second harmonic blocking	30.0 [%]
|Ih4|/|Iop| threshold for fourth harmonic blocking	30.0 [%]
|Ih5|/|Iop| threshold for fifth harmonic blocking	30.0 [%]
3. Advanced Settings	
Advance setting ?	Disable
Minimum blocking duration	0.001 [s]

Figure 73 Initial transformer differential relay settings

Note that the harmonic blocking thresholds were initially set to 30% of the operating current, but side-investigations conducted during this milestone indicated that 15% for the 2nd, fourth and fifth harmonic led to reduced spurious tripping of the differential relay.

4.3.3 Milestone objectives

The objectives of this milestone were as follows:

- An investigation on whether the properties of a GFM BESS black start unit negatively impacts on the operation of critical network protection relays that are likely to operate during system restoration.
- Where improper relay activation, or a failure to operate, occurs due to a property of a GFM BESS black-start unit, identify how best to address without altering primary plant.

4.3.4 Previous research

Much of the previously related research looked at the relays for the protection of the generators comprising the system [11] [12], rather than, as for this Stage 4 work, those for the protection of network assets. While the performance of generator protection relays is indeed crucial to the success of system restart, they are only a portion of problem to be considered. Hence, this work extended the previous analysis to also include the network protection relays most likely to operate or maloperate during system restart: transformer differential protection (due to the inrush phenomenon), and line distance protection (due to the potential limitation of negative sequence component provision from IBRs).

4.3.5 Line energisation and the operation of distance protection relays

Transmission lines were energised in simulation using a GFM BESS and a GT source to determine whether the performance of the distance relay is sensitive to the black-starter source.

In all cases studied, it was observed that the line distance protection relay operated correctly regardless of the black-start source used, including:

- Not tripping upon black starter source energisation.
- Not tripping upon downstream transformer or line energisation.
- Tripping correctly when a genuine fault occurred on the line.

It can be concluded that for the generic models used in this work, there was no sensitivity to the type of black-starting unit used, and correct operation is likely.

A typical line energisation scenario response is shown in Figure 74, whereby the line is energised at t=5.0 s, and a line-to-ground fault is applied at t=6.0 s. Correct behaviour is observed, and the result is otherwise unremarkable.

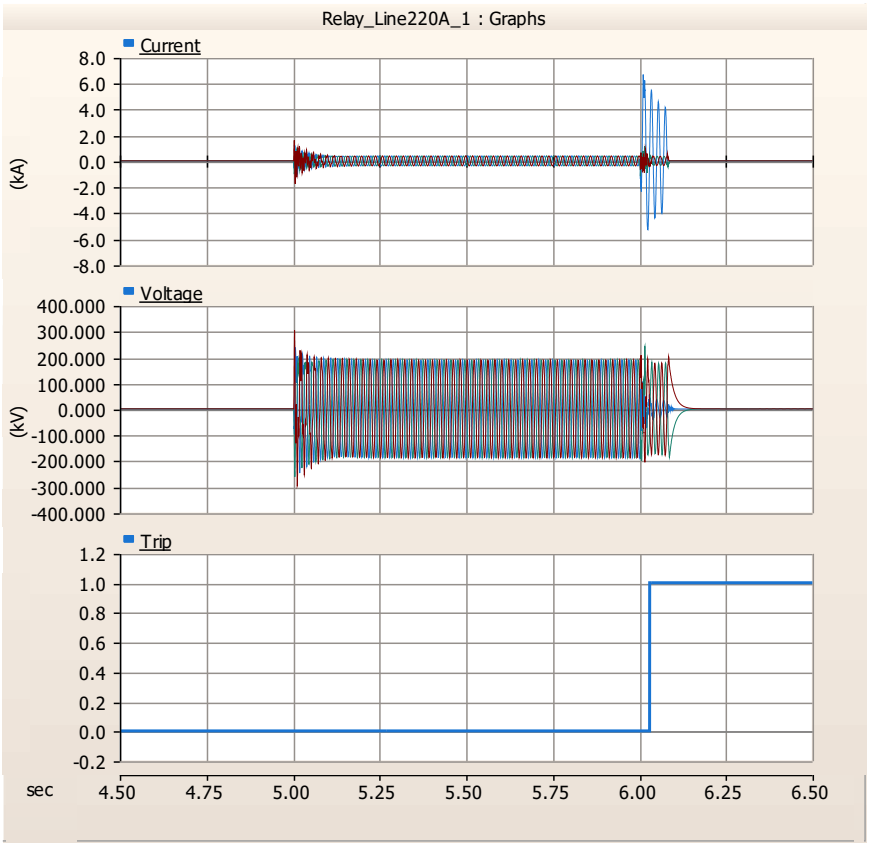

Figure 74 Typical response from a line being energised and an in-zone fault being applied

4.3.6 Transformer differential protection operation and harmonic blocking thresholds

Upon performing line-end transformer energisation studies, it was noted that the transformer differential relay was likely to trip when energised for both synchronous machine and GFM BESS black starters. A typical response appears in Figure 75, showing an attempt to energise a 225 MVA transformer at the end of 110km of 220kV transmission line from a GFM BESS source at t=6.0 s. This is likely to be reflective of a real situation, and an objective of this work was to identify simple changes to better enable a successful network restart.

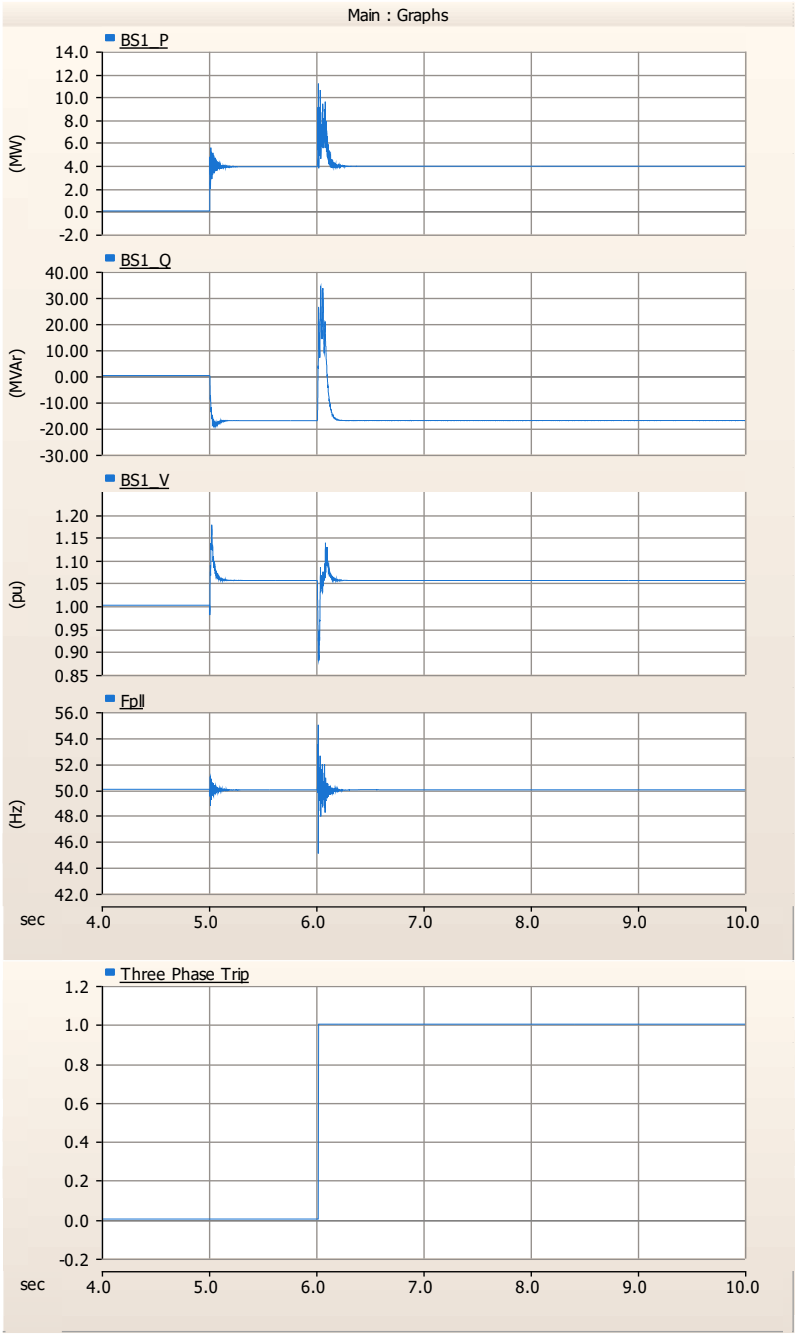

Figure 75 Transformer differential relay tripping upon energisation from a GFM BESS

Hence, a series of sensitivity studies were completed to determine appropriate harmonic restraint settings to allow black-starters to energise network transformers (with flux remanence enabled and) with rated power greater than the source unit, without compromising the protection relay's ability to discriminate among genuine internal faults. These studies considered only reducing, rather than increasing, blocking thresholds, as reducing these thresholds risks compromising the ability to activate for genuine internal faults. Differences between synchronous and IBR sources are studied.

For these scenarios, two disturbances are considered, the first being the transformer energisation, and the second being a transformer internal fault. A successful case would see the transformer differential relay block for the energisation event, but trip for the internal fault. Unless operation is correct for both events, the case is a failure.

The topology of this arrangement is as follows, whereby the transformer to be energised is at the end of 110 km of 220 kV transmission line.

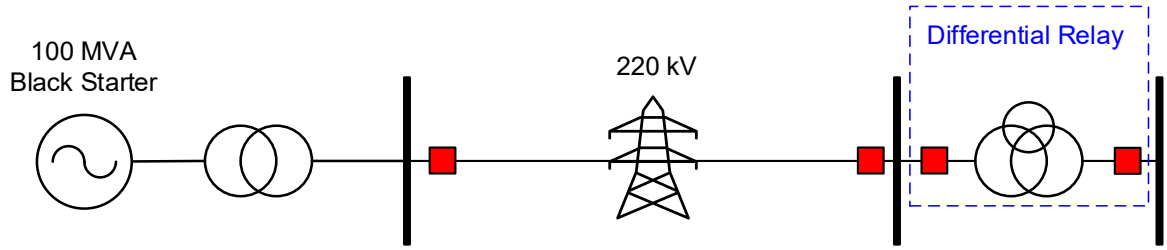

Figure 76 Topology for sensitivity studies

The results of the study are summarised in Table 5. The following findings were made:

- Reducing harmonic blocking thresholds on differential protection relays (relative to system normal settings) can allow successful energisation. The precise setting requirement for the black start context is sensitive to both the transformer size and the type of black-start source, but a reduction in the threshold settings to approximately10-20% of the fundamental harmonic is generally suitable.
- Generally, the GFM BESS black-starting source required less reductions in the thresholds than the synchronous source.

Table 5 Sensitivity study results

Transformer Size (MVA)	Black Start Source	Harmonic Restraint Value*	Energisation Result	Fault result
225	100 MVA GFM BESS (OEM)	30%	Fail	N/A
225	100 MVA GFM BESS (OEM)	25%	Fail	N/A
225	100 MVA GFM BESS (OEM)	20%	Pass	Pass
225	100 MVA GFM BESS (OEM)	5%	Pass	Pass
225	100 MVA OCGT	30%	Fail	N/A
225	100 MVA OCGT	20%	Fail	N/A
225	100 MVA OCGT	15%	Fail	N/A
225	100 MVA OCGT	12.5%	Pass	Pass
225	100 MVA OCGT	10%	Pass	Pass
150	100 MVA GFM BESS (OEM)	30%	Fail	N/A
150	100 MVA GFM BESS (OEM)	25%	Fail	N/A
150	100 MVA GFM BESS (OEM)	20%	Fail	N/A
150	100 MVA GFM BESS (OEM)	15%	Pass	Pass
150	100 MVA OCGT	20%	Fail	N/A
150	100 MVA OCGT	15%	Pass	Pass
150	100 MVA OCGT	10%	Pass	Pass

* For 2nd, 4th, and 5th harmonics. Minimum differential current to enable blocking = 5%.

In Figure 77, comparing the lower-order current harmonic components (up to 7th) contributed from the OCGT (left) and an OEM GFM BESS (right) to those from the remainder of the system, there is a notable difference in the profile produced by the two technology types.

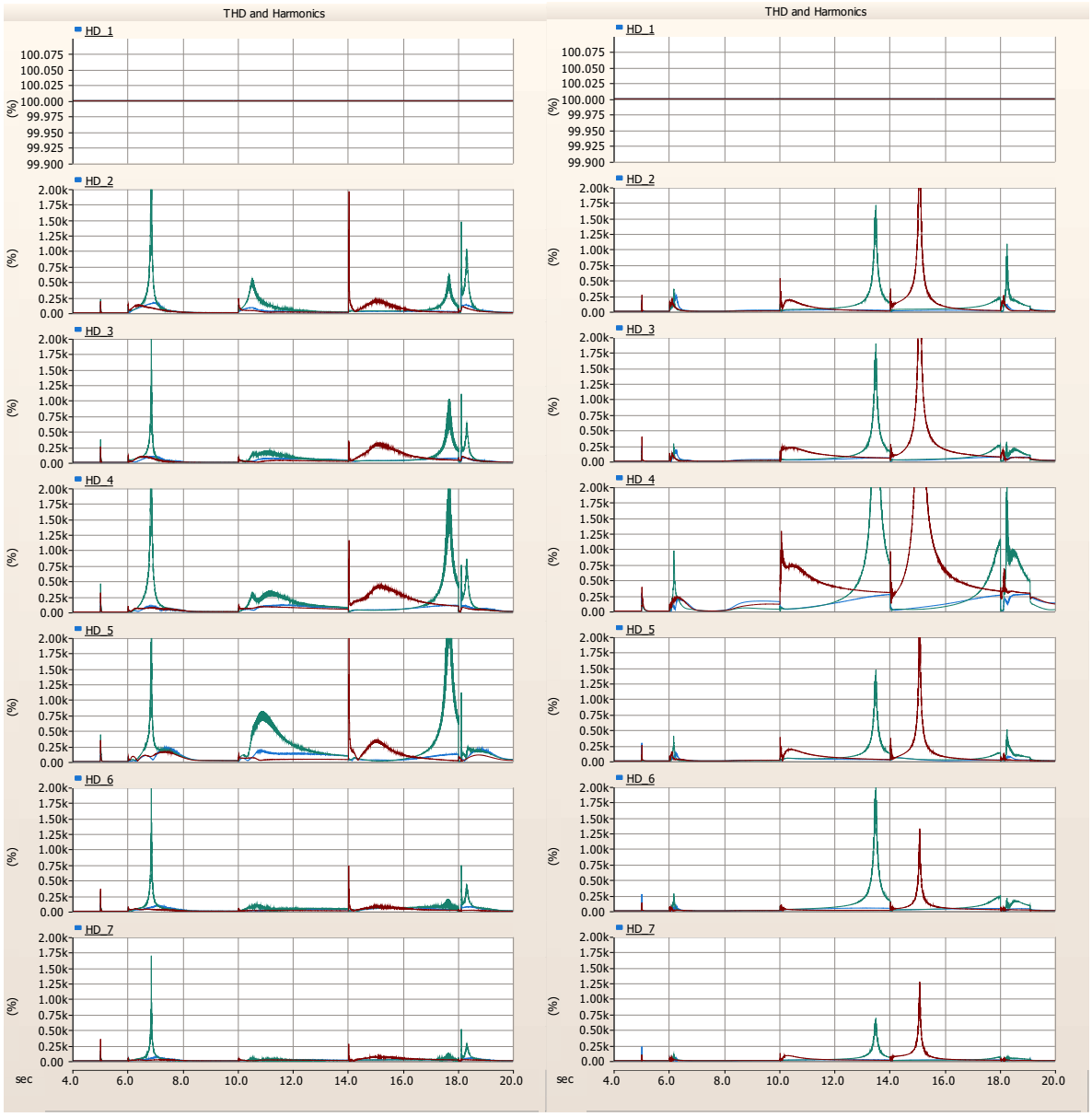

Figure 77 Current harmonic component comparison for transformer energisations. OCGT (left), OEM GFM BESS (right).

This difference in current harmonics behaviour between the two different sources is likely to be a key factor in correct event discrimination by protection relays, given that the differential protection relay harmonic restraint mechanism operates directly on values of the 2nd, 4th and 5th current harmonic orders.

4.3.7 Multiple transformer energisations

Based on the above sensitivity studies, a 15% harmonic blocking threshold was used as a starting point for these multiple energisation studies.

The setup is as shown in Figure 78. Transformers are sequentially energised (TRX1 → TRX2 → TRX3)

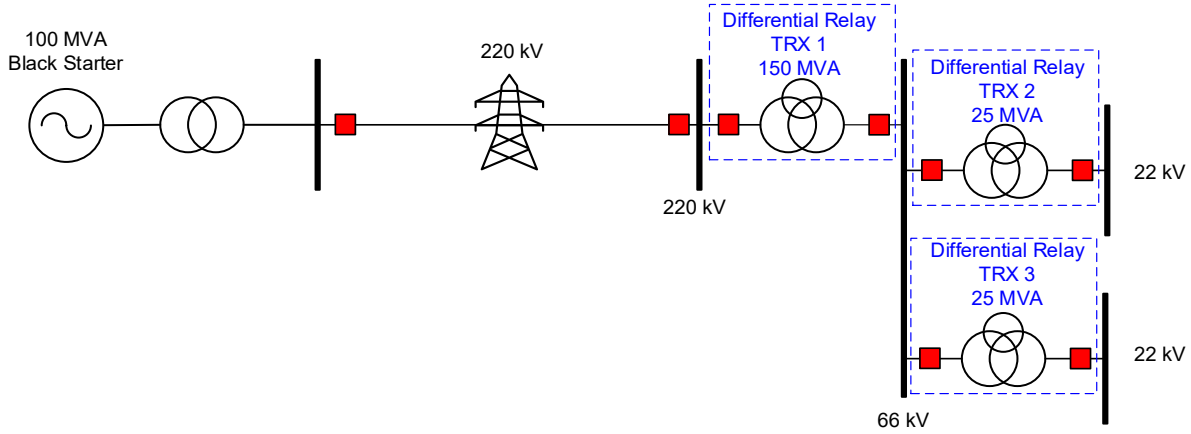

Figure 78 Multiple transformer energisation arrangement

The OCGT black starting source successfully energised all three transformers without issue. However, with a GFM BESS black starter, energisation of TRX2 resulted in tripping the differential protection for TRX1 approximately 1 second after the breaker was closed. As can be seen in Figure 79, after the energisation of TRX2, its inrush current flowed through TRX1 for some time, and was distorted and unbalanced enough to trigger the protection for TRX1.

We were unable to prevent protection operation for this event, despite reducing the protection operation blocking threshold for harmonics to very low values (<5%) and the blocking threshold for differential current to 1%.

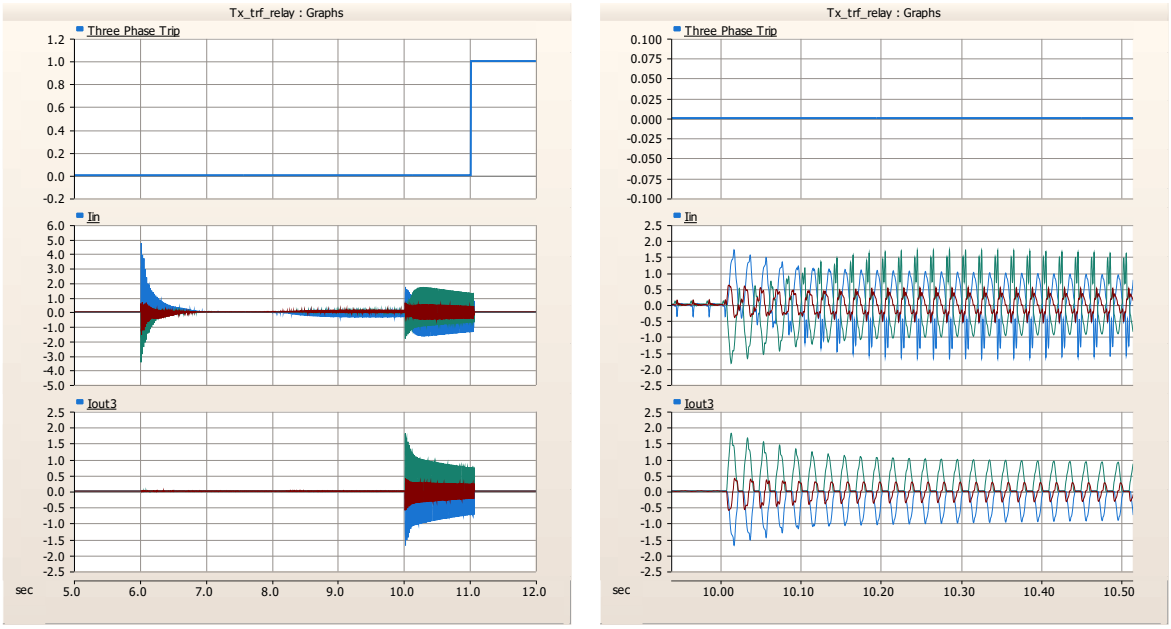

Figure 79 TRX1 currents leading to differential tripping (left), zoomed in (right)

Investigating the difference in current sequence components provided by the black starter reveals the differences shown in Figure 80, where the GFM-supplied current results in transformer tripping, and the OCGT-supplied current does not.

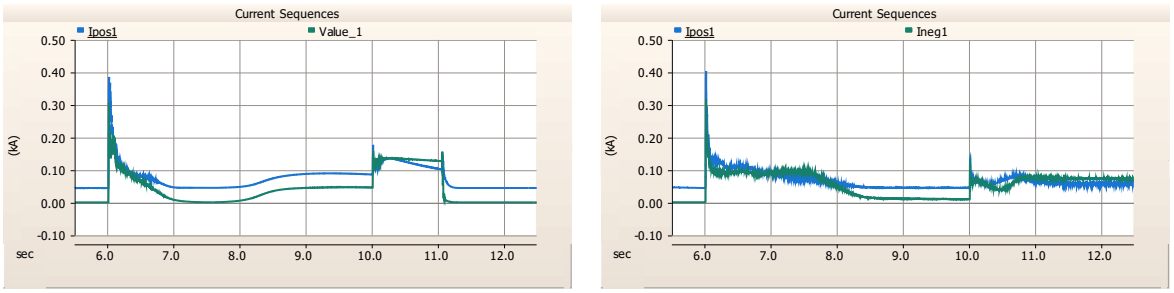

Figure 80 Difference in current positive and negative components supplied from a GFM BESS (left) and an OCGT (right)

The components of provided current are quite different between the two sources. For the OCGT there is a sustained delivery of negative sequence current following the first transformer energisation, whereas the negative sequence current provided by the GFM BESS initially reduces more quickly but is then followed by a ‘reprise’ of increased magnitude two seconds later. This suggests investigating whether this (negative sequence) current ‘reprise’ from the GFM BESS scenario is a significant factor in the tripping of the TRX1 relay during subsequent TRX2 energisation. In particular, determine whether subsequent transformer energisation is more successful if the negative sequence current component is allowed to diminish completely before re-energisation is attempted.

To that end, Figure 81 shows the result where subsequent energisations wait for the negative sequence current components to have completely diminished before the next

breaker is closed (Figure 81 and Figure 82). In this scenario, the harmonic blocking thresholds have been restored to 15%. This approach is successful, as the subsequent transformer energisations do not result in operating the differential protection relays of the already energised transformer.

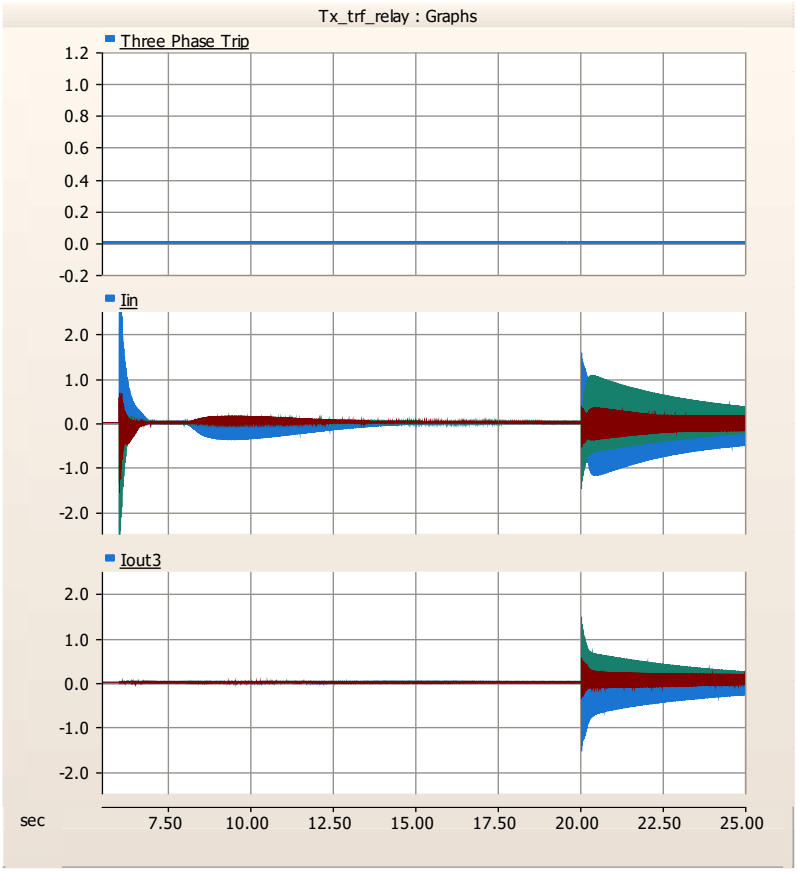

Figure 81 TRX1 differential protection no longer trips on subsequent TRX2 energisation

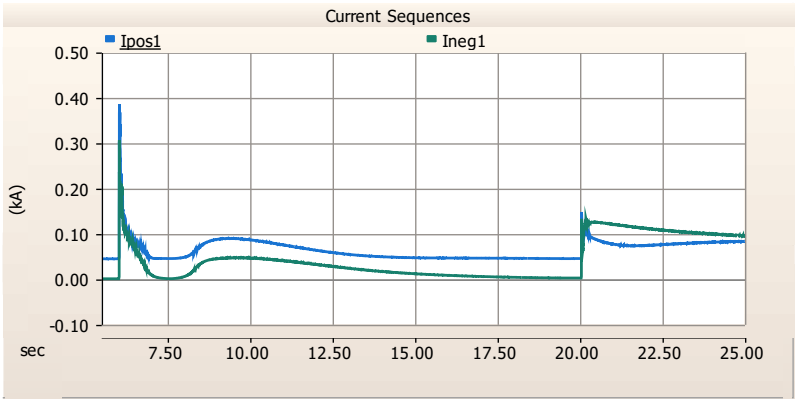

Figure 82 Current sequence components supplied by the GFM BESS

It is clear that the current limits in IBR devices produce a transformer energisation trajectory that is different to that from the OCGT. They are nevertheless not incapable of energising large transformers, although these limitations may necessitate an extended energisation

period, requiring substantially more time to reach steady-state with flux fully established within the transformer core.

Based on this exercise, it is recommended that during restart using an IBR device, current sequence components provided by the black starter should be monitored and negative sequence component returned close to zero before the next network component is energised, in order to minimise risk of upstream protection maloperation.

This recommendation will not necessarily help prevent the subsequent maloperation of differential protection relays of transformers that are further downstream. The settings of these relays may still require specialised tuning for restart.

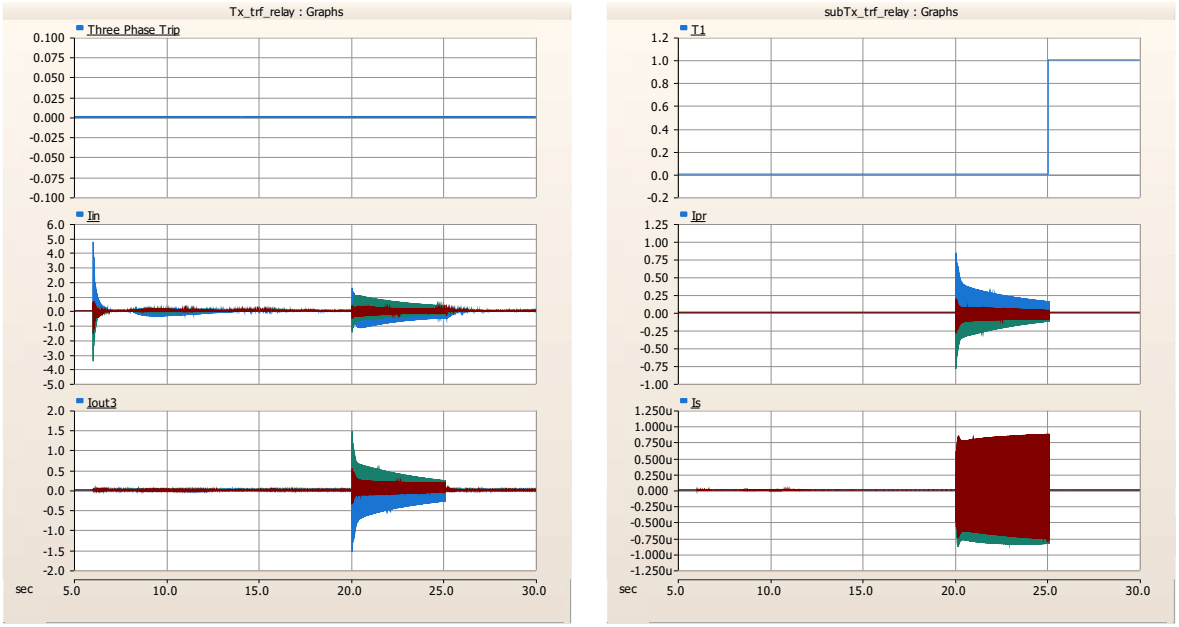

Figure 83 Upstream (left) and downstream (right) transformer current and trip status – IBR source

Current composition comparison

Given that the EPRI GFM models were observed to energise transformers without tripping protection relays, it was decided to compare the sequence components of current provision from the EPRI GFM BESS model, the OEM GFM BESS model, and the OCGT model.

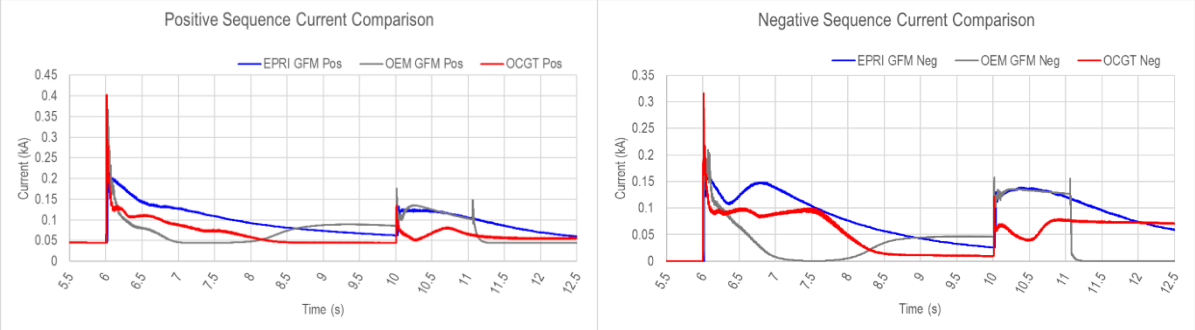

Figure 84 Comparison of current sequence components from different restart sources

As can be seen in Figure 84, the EPRI GFM BESS model seemingly can provide significantly more current during energisation than the OEM GFM BESS, in both the positive and negative sequences. Note that the total current provided by the EPRI GFM BESS model throughout this process is well within its nameplate rating, and the simulation result is likely reflective of a more effective control system algorithm rather than an overoptimistic misrepresentation of its overcurrent capabilities. This is confirmed by Figure 85, which demonstrates that the phase current remained well below its rating of 0.262 kA (100 MVA at 220 kV).

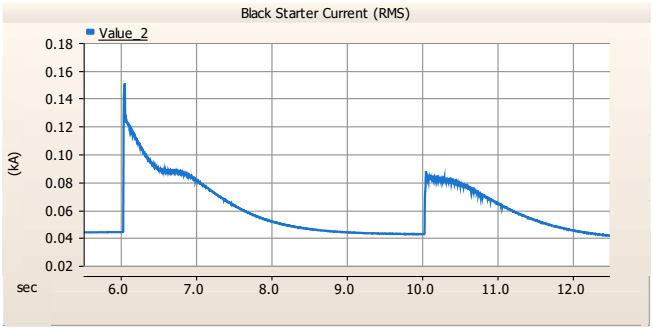

Figure 85 Black starter RMS current during multiple transformer energisations

4.3.8 Multiple line energisations

Similar to the investigations on whether multiple, series or parallel, transformer energisations result in maloperation of protection relays, multiple line energisations were investigated where each line is protected by a differential relay. Sensitivities to the black-start source were evaluated, with both OCGT and an OEM-provided GFM BESS used in the studies.

The setup for this work is shown in Figure 86, where three independent, and EPRI specialist tuned, distance protection relays are included, based on the protection models provided by MHI.

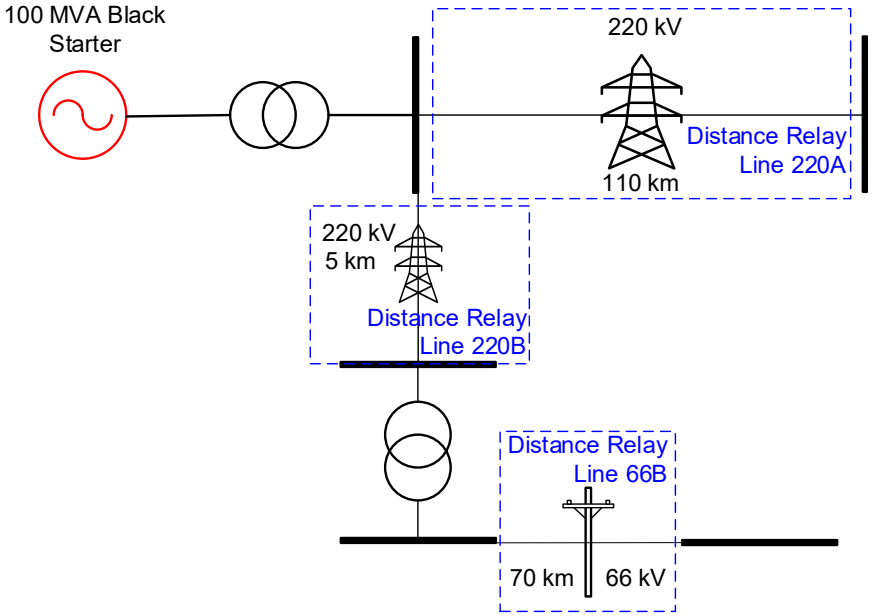

Figure 86 Multiple line energisation with distance protection setup

The sequence of events applied is shown in Figure 87.

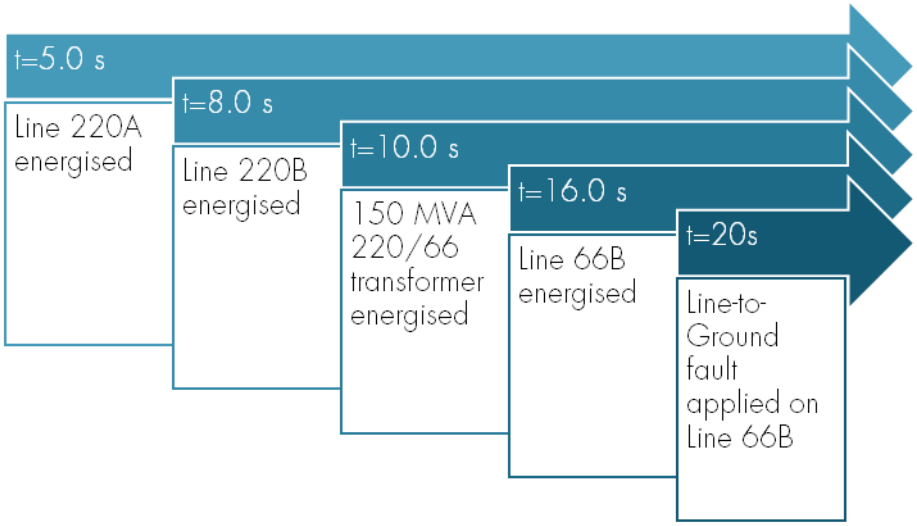

Figure 87 Sequence of events

The performance of the protection relays were then evaluated against the following criteria for both OCGT and GFM BESS black start sources. The protection relays must:

- Block tripping for in-zone line energisation,
- Block on out-of-zone line energisation,
- Correctly detect a fault within its zone and trip, and
- Block trips for faults outside of its zone.

Results from this test are shown in Table 6. Interestingly, the GFM BESS black starter unit allowed better performance than the OCGT in terms of blocking for out-of-zone tripping.

Table 6 Distance relay operation evaluation

Line		OCGT Black Starter	GFM BESS Black Starter
220A	Blocked tripping for in-zone energisation	Pass	Pass
	Blocked tripping for out-of-zone energisation	Pass	Pass
	Trip for in-zone fault	Pass	Pass
	Block trip of out-of-zone fault	Fail	Pass
220B	Blocked tripping for in-zone energisation	Pass	Pass
	Blocked tripping for out-of-zone energisation	Pass	Pass
	Trip for in-zone fault	Pass	Pass
	Block trip of out-of-zone fault	Pass	Pass
66B	Blocked tripping for in-zone energisation	Pass	Pass
	Blocked tripping for out-of-zone energisation	Pass	Pass
	Trip for in-zone fault	Pass	Pass
	Block trip of out-of-zone fault	Pass	Pass

4.3.9 Pre-insertion resistors

As requested by an AR-PST partner, investigations were conducted to determine whether the use of pre-insertion resistors (PIR) can help IBR-based restart devices to successfully energise transformers during system restart, in circumstances where energisation otherwise activated network protection. Priority was given to investigating PIRs rather than point-on-wave circuit breakers, as PIRs are simpler and hence more reliable.

Studies were completed whereby a relatively small GFM BESS (100 MVA) was tasked with hard-energising an 800 MVA transformer at different locations within the network without any supporting services available, both with and without a PIR. The transformer to be energised would include a pessimistic representation of core flux remanence, and its circuit breaker closed at deliberately the worst possible moment in opposition to the remnant flux. Recall that this occurs for a remnant flux of 0.8/-0.8/0.0 in phase order, and the circuit breaker is closed on the negative to positive zero-crossing of the A phase voltage (as was used in other sections of this work).

The setup for this analysis used the same detailed limited-area model as in previous sections, however the target 800 MVA transformer was moved to various physical locations in the network and hard-energised from the 100 MVA GFM BESS black starter, as shown in Figure 88. The harmonic blocking thresholds within the differential transformer were deliberately set to a relatively high value of 30% which results in a higher propensity for tripping.

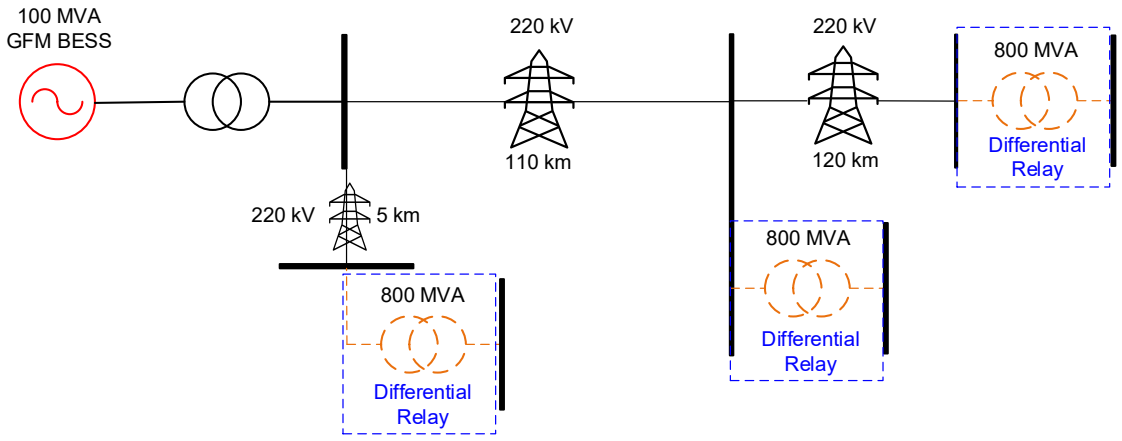

Figure 88 Case setup

The analysis found that, providing the PIR has been sized correctly, it prevented the tripping of the transformer differential relay for all cases studied. Representative samples of the difference the PIR made to inrush current sequence components are shown in Figure 89 and Figure 90.

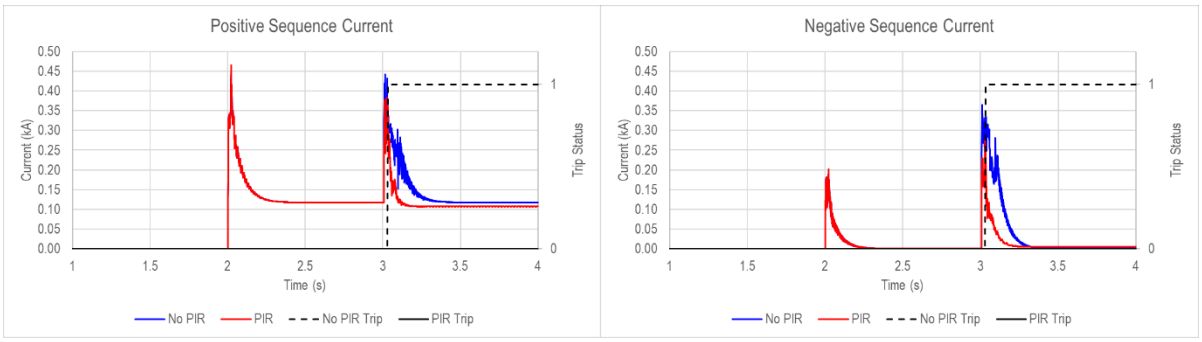

Figure 89 Comparison of current sequence component changes when PIR introduced: 230km from source, 3pu PIR impedance

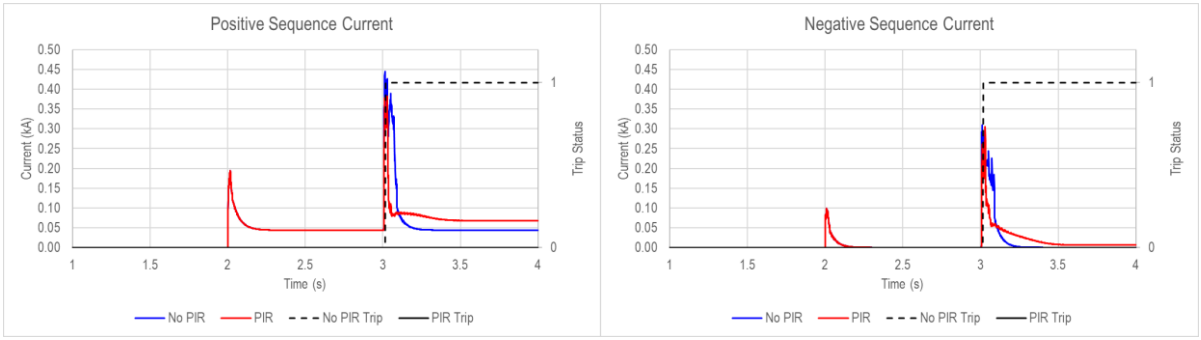

Figure 90 Comparison of current sequence component changes when PIR introduced: 0km from source, 1pu PIR impedance

Furthermore, it was found that there was an approximately linear relationship between the electrical distance of the transformer from the black-starting source, and the size of the pre-insertion resistor required. For the system characteristics and settings studied in this model, the PIR sizing profile shown in Figure 91 was applied to prevent differential relay tripping.

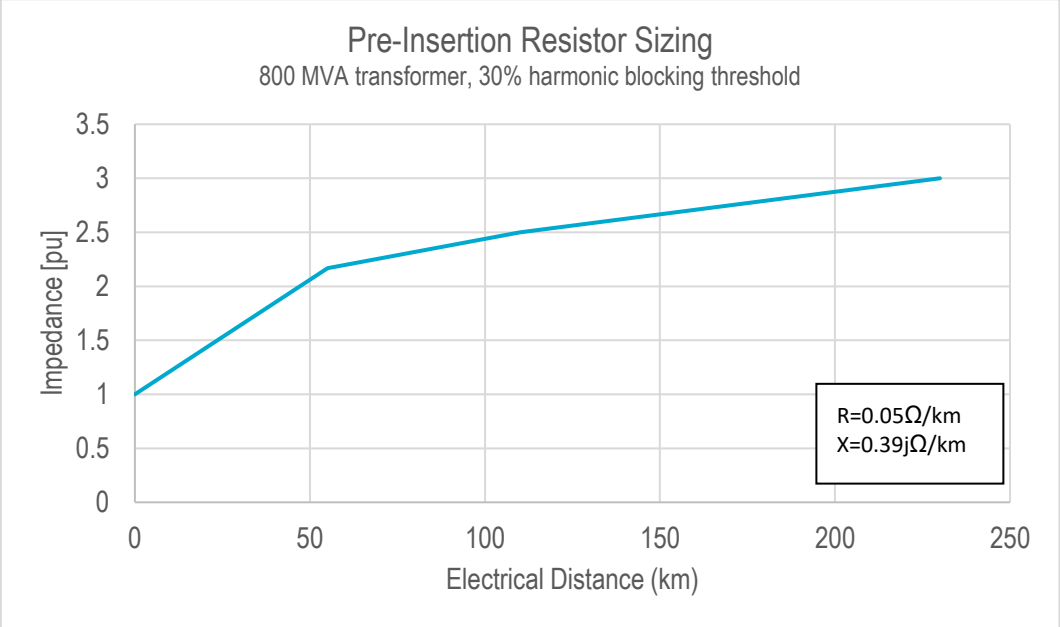

Figure 91 Pre-insertion resistor size versus electrical distance

Given the consistent behaviour of PIR in preventing the maloperation of the transformer differential relay for the scenarios and models used in this work, it is a recommendation that where studies show an inability for an IBR device to hard-energise a large transformer, a PIR is considered as a robust remediation option.

4.4 Milestone 4 – Procurement timeline

Milestone 4 sought to develop a high-level timeline to estimate how far in the future GFM IBR will need to begin playing a role to support the restoration of the NEM following a major supply disruption.

4.4.1 Key findings summary

- The characteristics of the immediate local network connecting to a black starter have a large bearing on its ability to initiate system restart, hence it is extremely difficult to make generalisations of the ability of any one type of black starter against another. To accurately determine the amount of GFM IBR required, detailed studies are unavoidable.
- A generic calculation method was developed to estimate the proportion of GFM IBR capability required to replace a retiring synchronous machine's restart capability, based on its size, connection voltage, physical position within the NEM, and neighbouring generators.
- Trends show that approximately 35-40% of the retiring synchronous machine nameplate capacity should be replaced with GFM IBR to maintain a similar level of network restart capability.

4.4.2 Milestone 4 objective

The objectives of this milestone were originally as follows:

- An analytical screening tool for each NEM region to be restarted, which will produce the amount of GFM IBR to be procured for SRAS purposes year on year.
- EMT studies confirming the validity of such an approach or otherwise identifying deficiencies that prevent such a generalised approach to be implemented, with recommendations for rectification.

However, as this work progressed in this Milestone, it became evident that it would not be possible to make clear, NEM-specific recommendations, because the details of surrounding local network are often the most important determining factor to restart success, and such information is not publicly available.

Following discussion with AR-PST partners, it was instead decided to generalise this analysis, based on benchmarking generic network restoration capability of a synchronous machine versus GFM IBR in PSCAD, which can then support quantitative analysis of GFM IBR required to replace restart capability of retiring synchronous generators.

4.4.3 Methodology

The methodology for this work comprises the following major steps shown in Figure 92, which is further described in the subsequent sections.

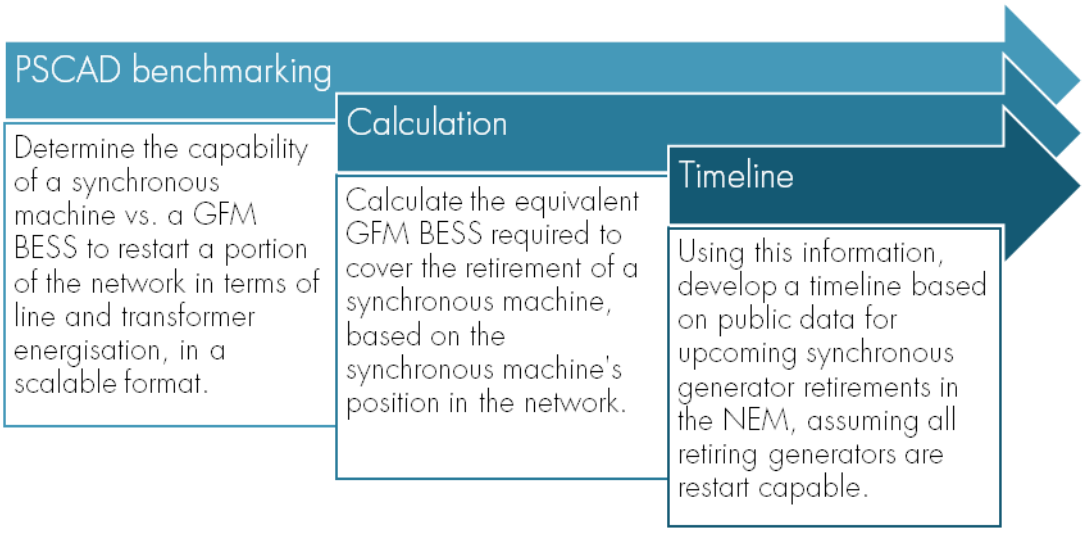

Figure 92 High level process overview

PSCAD Benchmarking

The benchmarking of the two generation types is completed in PSCAD using the same synchronous machine (OCGT) and GFM BESS model used for previous work in this stage. An example is shown in Figure 93. Both black start sources are 100 MVA in size. Each is subjected to an iterative process of energising a transmission line and a transformer at the end of the transmission line[12], as the length of the line and size of the transformer are varied.

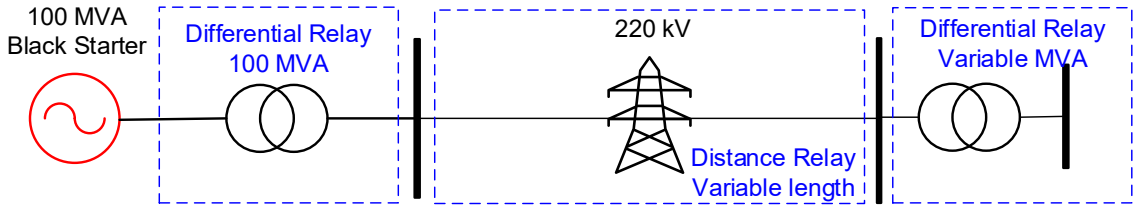

Figure 93 Benchmarking arrangement

If a unit becomes unstable, hits an internal limit (such as a underexcitation limiter for the OCGT), or causes a protection mechanism to trip at any point in the system (generator or network), or if a line-end exceeds 1.15 pu voltage, this will be taken to reflect the capability limit of the generator.

This process is repeated for a variety of combinations of line length and transformer size, resulting in a capability matrix for each generator type, showing transmission line length (or MVAr absorption capacity) vs. transformer size (energisation capability) for each unit type.

[12] This was confirmed with an AR-PST partner who specialises in black start studies to be an effective method to determine unit capability, as the combined energisation of transmission line and transformers is often the most challenging scenario undertaken during early restart.

Equivalent GFM calculations

For each retiring generator considered, its location in the network is identified, and the other dispatchable generator (synchronous machine or BESS) that is next closest in approximate electrical distance is determined through AEMO's public network maps. The aim is to re-energise the network locally to this other dispatchable generator and to energise its unit transformer, in order to begin forming a 'restoration island'; a combination of generators, network and load from which broader network re-energisation efforts can be launched. The requirements the energisation target, which are required by the next analysis step, are represented by the local network transmission line voltage and length, and the capacity of the nearby dispatchable generator[13] (and hence its unit transformer).

Next, using the previously found using the standardised (100 MVA) capability matrix for a reference synchronous machine, the approximate capability of each retiring generator in the NEM is estimated.

For example, consider a retiring 350 MVA synchronous generator that will need to energise a 200 MVA synchronous generator that is located 20 km away on a 220 kV line.

If the reference 100 MVA synchronous generator can simultaneously energise a transformer up to 250 MVA and 7 km of 220 kV transmission line, then a 350 MVA synchronous generator should be able to simultaneously energise an 875 MVA transformer and 25 km of transmission line[14]:

1. $350\ MVA_{generator} / 100\ MVA_{referece\_generator} = 3.5; 3.5 \times 250\ MVA_{transformer} = 875\ MVA_{transformer}$
2. $350\ MVA_{generator} / 100\ MVA_{referece\_generator} = 3.5; 3.5 \times 7\ km_{line} = 25\ km_{line}$

It is clearly a viable option for this 350 MVA synchronous machine to restore the 200 MVA machine some 20 km away. But of course, this machine is retiring, and we need to determine what equivalent amount of GFM IBR would be required to replace this capability.

The capability matrix (section 4.4.4) for the GFM IBR shows that a 350 MVA GFM IBR device could energise up 2800 MVA of transformers and 700 km of 220 kV line. This is far more than what is required to re-energise the nearby generator.

The capacity of GFM IBR required to have the equivalent re-energisation capability of the original 350 MVA synchronous machine can be determined by:

3. $875\ MVA_{SG\_transformer\_capability} / 2800\ MVA_{GFM\_transformer\_capability} = 0.3125$
4. $25\ km_{SG\_line\_capability} / 700\ km_{GFM\_line\_capability} = 0.0357$

[13] This information can be readily found in the NEM Registration list on the AEMO website.

[14] See Appendix D for PSCAD simulations confirming this assumption is valid.

5. The maximum of these two numbers, 0.3125, is the proportion required to satisfy the most demanding component of the two: line restoration and transformer restoration.

Multiply 0.3125 by the original 350 MVA of the synchronous machine to give **109 MVA of GFM IBR, which is an upper bound on that required** to have at least the same capability as the original 350 MVA machine, and to pick up the next closest dispatchable generator[15].

Note that provisions are made in these calculations for alternative voltage ratings for the transmission lines, resulting in different susceptances, which is the underlying factor limiting the transmission line energisation. Table 7 shows the values used in this work for the reactive charging requirements for transmission lines of various voltage ratings, based on common tower geometry, bundling and conductor types used in NEM regions.

Table 7 Approximate line charging amounts for typical line configurations and voltages

Line nominal voltage (kV_{L-L})	MVAr of line charging per 100 km
66	1.6
132	8
220	14
275	31
330	40
500	101

Restart capacity timeline estimation

A timeline for synchronous machine closures was estimated based on data for upcoming generation closures from the AEMO website[16] and this was used to estimate the capacity of GFM IBR sufficient to replace the equivalent lost restart capability. For this work, it was assumed that all the upcoming generator retirements are of plant that are restart capable. This is not the case in reality. The restart capability of plants in the NEM is confidential. Hence, this work is proof of concept rather than calculating definitive procurement requirements. The result of the calculations here are in principle an upper bound on actual GFM IBR procurement requirements.

For each retiring generator, the year of closure and unit size[17] was found from the NEM Registration and Exemption List[18], available on the AEMO website. Each retiring generator

[15] See Appendix D for PSCAD simulations confirming this assumption is valid.

[16] Available here: https://www.aemo.com.au/energy-systems/electricity/national-electricity-market-nem/nem-forecasting-and-planning/forecasting-and-planning-data/generation-information

[17] Note that the list expresses generator sizes only in MW. As MVA figures are required for this work, it was assumed that each synchronous machine was capable of operating at 0.9 pf, e.g., a 720 MW generator is 800 MVA.

[18] Available here: https://www.aemo.com.au/-/media/files/electricity/nem/participant_information/nem-registration-and-exemption-list.xlsx

was then subjected to the calculation methodology previously described, and an equivalent GFM IBR amount determined. This was then plotted against a timeline.

Generation closure and GFM IBR replacement was forecast only until 2034, because closures for periods beyond that date are increasingly uncertain, given the rapid changes in the structure of the NEM expected at this time.

4.4.4 Synchronous generator and GFM IBR capability charts

Note that for the benchmarking investigation, the transmission line voltage was rated at 220 kV, and has a nominal reactive power charging requirement of 14 MVAr per 100 km. The transformer differential protection relays had their harmonic blocking threshold set to 15%, which had been found in Milestone 3 work (network protection relays) to be the maximum permissible without resulting in tripping on energisation.

Through iterative studies in PSCAD, the following tables were developed which summarise the capabilities of the synchronous machine and GFM IBR modelled in this work. Table 8 outlines the performance of the 100 MVA synchronous generator, modelled on an OCGT. The two key aspects to note are that:

- Approximately 30 MVAr of reactive power appears to be the maximum absorption capability of this unit without underexcitation that results in large overvoltages in the network.
- The ability of the OCGT to energise large transformers decreases with the target's distance from the source unit. A maximum transformer size, of 3x nameplate rating of the black start source capacity, was energised only if very close to the terminals of the source unit. The primary failure mechanism was tripping of the differential relay of the transformer being energised.

Table 8 OCGT Line and transformer restart capability

	5 km (1 MVAr)	50 km (7 MVAr)	100 km (14 MVAr)	150 km (21 MVAr)	200 km (28 MVAr)	250 km (35 MVAr)
50 MVA	Pass	Pass	Pass	Pass	Pass	Fail FC
100 MVA	Pass	Pass	Pass	Pass	Fail DR	Fail FC
150 MVA	Pass	Pass	Pass	Fail DR	Fail DR	-
200 MVA	Pass	Pass	Pass	Fail DR	Fail DR	-
250 MVA	Pass	Fail DR	Fail DR	-	-	-
300 MVA	Pass	Fail DR	Fail DR	-	-	-
800 MVA	Fail DR	Fail DR	-	-	-	-

FC = Field Current too low / sustained UEL activation / overvoltage
DR = Transformer differential relay trip

Table 9 outlines the corresponding restart capability of the 100 MVA GFM BESS. Note that this was investigated both for the generic GFM BESS model developed by EPRI, and for an OEM model. The results were the same.

The only limiting factor observed, for transformer energisation up to 8x nameplate rating of the source, was that overvoltages were consistently observed when the line susceptance was greater than approximately 30 MVAr (~250 km for the 220 kV line model used here).

Table 9 GFM BESS Line and transformer restart capability

	5 km (1 MVAr)	50 km (7 MVAr)	100 km (14 MVAr)	150 km (21 MVAr)	200 km (28 MVAr)	250 km (35 MVAr)
50 MVA	Pass	Pass	Pass	Pass	Pass	Fail OV
100 MVA	Pass	Pass	Pass	Pass	Pass	Fail OV
150 MVA	Pass	Pass	Pass	Pass	Pass	Fail OV
200 MVA	Pass	Pass	Pass	Pass	Pass	Fail OV
250 MVA	Pass	Pass	Pass	Pass	Pass	Fail OV
300 MVA	Pass	Pass	Pass	Pass	Pass	Fail OV
500 MVA	Pass	Pass	Pass	Pass	Pass	Fail OV
800 MVA	Pass	Pass	Pass	Pass	Pass	Fail OV
OV = Overvoltage at black-starter end						

A note on the GFM BESS capability

The researchers were surprised that such large transformers (up to 8x GFM nameplate) could be routinely energised in simulation without resulting in tripping of any protection mechanisms, network or generator.

Additional studies were done to investigate whether this was due to a modelling error. However regardless of the GFM BESS model used (whether the EPRI generic, or OEM supplied, GFM BESS model), the ultimate result was identical. The sequence components of the currents in Figure 94 indeed show nothing of concern: No currents exceeding maximum limits, no sustained distortion, and voltage (not shown) consistently recovers to nominal target values. Transformer breaker closing was also confirmed to occur at "the worst possible moment" as previously described in Section 4.3.2.

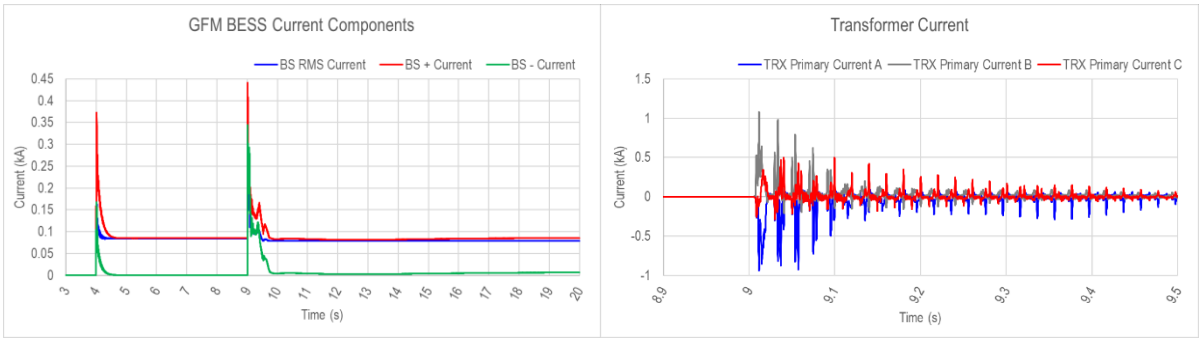

Figure 94 Energisation of an 800 MVA transformer, 200 km from the GFM BESS black-start source

It was therefore concluded that this is indeed genuine capability (up to the model representation accuracy). The current limitation of the device and/or the impedance of the transmission line may act similarly to a pre-insertion resistance for the transformer, limiting the differential relay tripping as described in Section 4.3.9.

4.4.5 Upcoming synchronous generator retirements

The following list comprises synchronous generators that are classified as "scheduled" and therefore have additional capabilities and visibility to AEMO. Non-scheduled generators were ignored for the purpose of this exercise.

Table 10 Upcoming major synchronous generator retirements between 2024 and 2034

Region	Closure Year	Name	Size (MW)[19]
SA	2026	Osborne	1x 120 1x 60
SA	2026	Torrens Island B	4x 200
NSW	2026	Broken Hill GTs	2x 25
NSW	2027	Eraring 1 & 2	2x 720
NSW	2027	Eraring 3 & 4	2x 720
QLD	2028	Callide B	2x 350
SA	2028	Port Lincoln GT	2x 25 1x 23.5
SA	2028	Snuggery	1x 63 3x 21
VIC	2028	Yallourn W	2x 360 2x 380
SA	2030	Dry Creek	3x 52
SA	2030	Mintaro	90
NSW	2032	Eraring GT	42
SA	2032	Hallett GTs	217
QLD	2033	Mt Stuart	2x 144 1x 131
NSW	2033	Bayswater	4x 660
NSW	2033	Vales Point B	2x 660
QLD	2034	Barcaldine	37
QLD	2034	Roma GTs	2x 40

4.4.6 Retirement and GFM procurement timeline

Combining these items together, the following trajectories in Figure 95 and Figure 96 show both synchronous generator retirements and the GFM IBR sufficient to replace their (maximum) black-starting capability (that is, assuming each is black-start capable). A breakdown of the calculation results is shown in Table 11.

Analysing at the proportions of GFM black start capable IBR sufficient to maintain the same capability as the synchronous generation, there is little variation across regions, which ranges from 35% (SA) to 40% (NSW & QLD).

[19] Based on registered capacity of the NEM Registration and Exemption list (not maximum capacity).

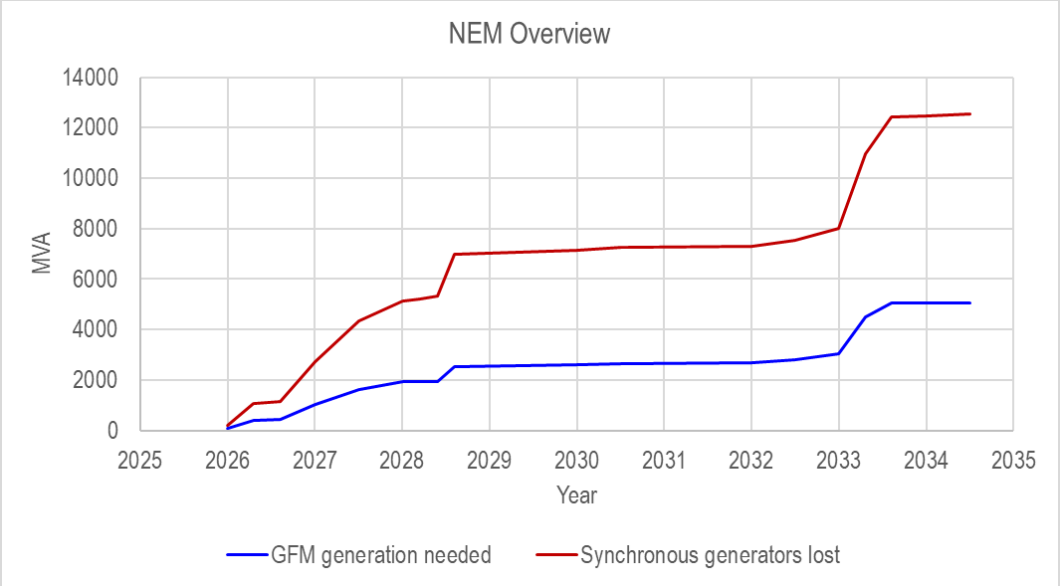

Figure 95 Forecast retirements of large synchronous machines in the NEM and calculated GFM IBR sufficient to facilitate a restart

This can be further broken down into regions, as shown in Figure 96.

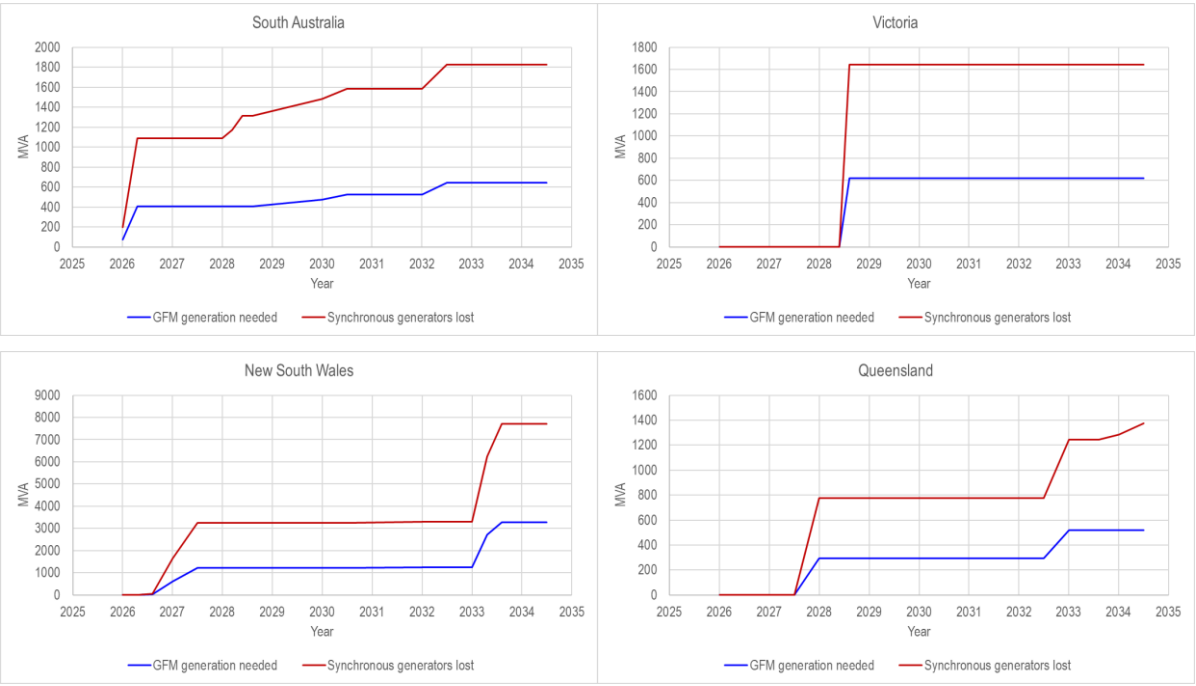

Figure 96 Regional breakdown[20] of forecast retirement in large synchronous machines in the NEM and calculated GFM IBR sufficient to facilitate a restart

[20] Note that there are no synchronous machine closures within Tasmania for the period evaluated

Table 11 Calculation of GFM capacity to replace existing synchronous machines

Region	Closure Year	Name	Size (MW)	Connection Voltage (kV)	Nearest generator	Distance to nearest generator (km)	Nearest generator unit size (MW)	Transformer single SG could energise at that distance (MVA)	Equivalent GFM IBR to match SG capability (MVA)	Total proposed replacement GFM capacity (MVA)	Notes
SA	2026	Osborne	1x 120 1x 60	66	Quarantine	5	128	400	50	75	-
SA	2026	Torrens Island B	4x 200	275	Quarantine	4	128	667	83	332	-
NSW	2026	Broken Hill GTs	2x 25	220	Broken Hill BESS	1	50	83	10	20	Once energised, cannot go further
NSW	2027	Eraring 1 & 2	2x 720	330	Colongra	20	181	2400	300	600	-
NSW	2027	Eraring 3 & 4	2x 720	330	Colongra	20	181	2400	300	600	-
QLD	2028	Callide B	2x 350	275	Callide C	1	420	1167	146	292	-
SA	2028	Port Lincoln GT	2x 25 1x 23.5	132	-	300+	-	-	-	-	Too isolated to be considered
SA	2028	Snuggery	1x 63 3x 21	66	Mortlake	220	283	-	-	-	Not viable, three voltage levels including 100km+ 500 kV
VIC	2028	Yallourn W	2x 360 2x 380	220	Jeeralang	13	76	1200	150	617	-
SA	2030	Dry Creek	3x 52	66	Quarantine	15	128	173	22	66	-
SA	2030	Mintaro	90	132	Quarantine	140	128	200	50	50	-
NSW	2032	Eraring GT	42	330	Colongra	20	181	47	25	25	Unable to pick up unit
SA	2032	Hallett GTs	217	275	Hornsdale BESS	36	150	482	121	121	-
QLD	2033	Mt Stuart	2x 144 1x 131	275	Townsville GT	30	160	320	78	227	-
NSW	2033	Bayswater	4x 660	330	Colongra	140	181	1467	369	1476	-
NSW	2033	Vales Point B	2x 660	330	Colongra	6	181	2200	275	550	-
QLD	2034	Barcaldine	37	110	-	500+	-	-	-	-	Too isolated to be considered
QLD	2034	Roma GTs	2x 40	275	Condamine	150	-	-	-	-	Too isolated to be considered

Assumptions for generating Table 11

- The aim is to meet the same amount of black start and helper potential as there is today.
  - The listed generators are not necessarily all black-start capable units, and status of ones which *are* black start units is confidential. This analysis is being applied to all units intentionally to obfuscate the identity of actual black start units, and therefore in principle represents an overestimate of requirements for replacement black start capacity.
- Only scheduled generation plant is permitted to be a target for the next closest power station to energise.
- Where the next closest power station has multiple sized units, the largest unit is the energisation target.
  - The control room operates to the largest island principle: Focus on establishing the largest island possible.
- Generation capacity is only Registered capacity, not maximum capacity.

5 Insights

This section summarises the following insights, which were developed through the work conducted in this Stage.

5.1 DER findings

The investigation of the behaviour of DER during black start found the following.

- The black-start source influences the likelihood of DER protection operating, during restart when transformers are hard-energised in the system. It was seen that:
  - GFM BESS restart technology will result in shallower voltage dips than for synchronous, but recovery to nominal voltage envelopes can be slower, taking seconds to tens of seconds, leading to DER trips on undervoltage.
  - Synchronous restart technology will result in slightly deeper voltage dips, but recovery to nominal voltage envelopes occurs more quickly, within a few seconds, reducing DER trips.
- Extended voltage dips after transformer energisations were observed to be the primary cause for DER to trip offline, for the scenarios considered. Depending on the restart technology, this may be either or both a challenge, and an opportunity, during the restart process.
- Variability in generation output of DER energy sources across the length of a feeder showed no adverse impact on the restarting system, as both synchronous and GFM BESS technology were easily able to compensate for what were ultimately slow changes in system voltage and frequency, provided the black start source units have a frequency correction controller active (N.B. isochronous mode for the synchronous generator).
- For the distribution and DER model studied, DER response to a phase angle jump disturbance does not appear to be materially affected by the restart source. Both GFM BESS and synchronous sources supported DER ride-through for major phase angle changes.
- DER, with penetration levels at and beyond 80% of the nameplate rating of the GFM BESS black start source, experienced DER PLL tracking instabilities even in absence of any disturbance. However, such behaviour was not observed with the synchronous machine black start source.

5.2 Operational changes findings

The investigation of options for operational changes to enhance the likelihood of black start success found the following.

- The most common cause of instabilities seen in the studies was an ill-conditioned PPCs on GFL plant, in that the PPCs have controller gains unsuitable for a very weak system. Multi-tiered PPCs appeared to be particularly prone to instability, indicating that controller time delays are also a factor.
- Major disturbances, or transformer energisations, near AC or DC-coupled hybrid plant with high internal power transfer result in very large MW injections or absorptions across units within the plant, destabilising and collapsing the system.

- Some GFL equipment may have relatively tight cut-in voltage and frequency requirements that must be satisfied before the device connects to the system. Readings (or measurement estimates) of such quantities may be affected by a "noisy" system, or by protracted low voltages following extended or incomplete transformer energisation, preventing the devices from connecting to the system.
- Transformer energisations near GFL plant that is already online can destabilise it.
- Wider frequency droop settings (larger tolerances in frequency deviation for a given quantity of compensatory balancing power provided) in the GFM plant will result in it being off nominal frequency more often, so that GFL devices may not even attempt to connect. Once the GFL plant is re-connected however, their frequency control capability is normal.
- Tighter frequency droop settings in GFM devices results in similar behaviour to high controller gains in GFL devices. Droop settings that are too tight will likely result in instability during restart. A droop setting of 3% was found to be acceptable for the studies conducted.
- GFM technology that implements a frequency-power droop mode will have an inherent frequency droop profile by definition. It follows that a true "isochronous mode", maintaining a constant frequency at precisely 50 Hz, is not simultaneously possible.
- With PPC frequency controllers enabled, faults may result in a shift in the operating points of all generators, leading to possible system instability or collapse.
- Where individual inverters within a park are energised by remain disconnected due to an inverter control system matter (such as frequency cut-in bands not being met), their corresponding master PPC may wind up their setpoint commands to maximum. When the inverters eventually reconnect, it may result in a large step-change.
- Re-energising GFL devices may suddenly inject active power at a rate that destabilises the stability of the island, hence their controller setpoints should be set to zero at the moment of energisation.
- When large transformers are sequentially energised nearby to one another, as would occur during a REZ restart scenario, transformer re-energisation phenomena may result in already energised and stabilised transformers becoming unbalanced in flux, and draw highly unbalanced, distorted currents.
- VSM type GFM devices may develop slow (<5Hz), poorly damped, unstable modes across all controlled quantities, particularly where there are multiple VSM devices separated by considerable network impedance magnitudes "early" in a system rebuild process.
- Disturbances that induce large phase-angle shifts (e.g., fault and loss of load, in an intraconnecting line or a section of the network) may result in some GFL IBR losing stability.

5.3 Protection operation findings

The investigation of protection behaviour during black start processes found the following.

- The behaviour of distance protection relays during restart was generally unremarkable, with even less maloperation noted for GFM IBR sources than for an OCGT. Of network protection, transformer differential protection maloperation remains the most challenging to rectify, regardless of black starter type.

- The harmonic blocking thresholds (Ih_x/Iop) of transformer differential protection relays may need to be reduced to allow successful energisation of transformers from all black start sources. In this work, setting such thresholds to 10-20% saw successful energisation from OEM-specific IBR sources, without compromising fault detection and correct differential protection relay operation.
- The generic models outperformed OEM models in allowing transformer energisation without tripping differential protection. Further investigation is required into whether the generic models employ better control algorithms for energy delivery, and/or whether the OEM models more accurately represent limitations in plant capability.
- Multiple energisations of series transformer may result in differential relay tripping. However, such maloperations can be minimised (N.B. not entirely prevented) if sufficient time (minutes) between energisations is allowed for the decay of current distortion, in particular, for negative sequence current drawn by the black start target to reduce to pre-disturbance values (or zero).
- Multiple energisations of series transformer may cause unnecessary tripping of differential protection relays, with either GFM BESS or OCGT restart technologies. There was no simple remedy found other than changes to protection relay setting.
- There is a notable 4th harmonic "reprise" several seconds past energisation that is evident on GFM BESS transformer energisations but not present with OCGT-based black starters. Further investigations are required to assess its significance.
- The use of pre-insertion resistors appears to be a robust and extremely effective option to minimise voltage dips, and to avoid tripping of transformer differential protection, during transformer energisation. However, it does require the (advance) installation of primary plant.

5.4 Procurement timeline findings

- The characteristics of the immediately local network connecting to a black start source have a large bearing on system restart, hence it is difficult to reason generally about the black start capability of any given generation source. To accurately determine the amount of GFM IBR required in the NEM, detailed studies are unavoidable.
- Nevertheless, high-level analysis found that, on average, GFM IBR with capacity of approximately 35-40% of the nameplate of a retiring synchronous machine is typically sufficient to provide equivalent restoration capability.
- The current limitations of IBR devices may be advantageous for avoiding the tripping of transformer differential protection relays. Future work should investigate whether implementing a virtual impedance may further extend the black start energisation capability of IBR beyond that of synchronous machines, under the contemporary paradigm for protection system design and relay tuning.

6 Future Work Recommendations

Based on the work conducted in this and previous rounds, the following topics are recommended for further investigation.

- Studies into possible methods and requirements for Renewable Energy Zones to act as a system restart source, restarting both plant within the zone and a portion of the nearby network beyond its point of connection.
  - This includes the particularly challenging energisation of large (>1 GVA), network-owned, transformers from inverter-based resources.
- Evaluate the capability of an expanded set of technologies to assist in a system restart, such as pumped hydro devices and modern HVDC links. Furthermore, evaluate their other possible interactions with GFM IBR restart sources.
- Consider how future network topology changes, which are expected over the next 10 years, may aid or hinder the restart process (e.g., increased meshing of the network compared with the connection of new generation centres using higher-voltage, and series-compensated, circuits).
- Extend DER studies to consider other consumer energy resources (CER), such as residential BESS, EV charging, and heat-pumps. Explore whether materially different DER performance is expected for this expanded set of equipment, and whether preliminary conclusions reported here still hold.
  - Investigate changes to design principles or technical standards that could enable CER to participate more effectively in system restart.
- Investigate and establish a GFM-BESS restart test plan for full scale generation equipment, to develop confidence in its capability to restart a portion of the system.
  - Initially through simulation using Hardware-In-Loop (HIL) / real-time simulation facilities.
  - Ultimately, through testing of a real, full scale-scale, in-NEM, facility deemed appropriate (noting that such in-field testing is operationally challenging, requiring coordination across many parties, and so would likely be a multi-year exercise).
- Test real network protection relays within a hardware-in-loop setup, to confirm that the conclusions from this Stage 4 investigation for simulated protection relays also apply to common, manufacturer-specific, devices used in the NEM.
- Further investigate the implementation of a virtual pre-insertion resistor during transformer energisation by modulating the virtual fault impedance of an IBR black start source.
- Where hardware-in-loop studies are conducted, compare the results between offline EMT studies and HIL studies to confirm the validity of the simulation tools.
- Investigate options to modify network support equipment, such as SVCs, STATCOMs, and series compensated devices, to better support power system operation during 100% IBR restart. Investigate whether equipment with limited capability (such as SVCs) will remain appropriate for network voltage support in the medium- to long-term.
- Investigate the possibility of multi-plant hybrid black starters, whereby a GFM BESS might be supplemented by combining with a geographically distant variable energy source GFL IBR (wind,

solar, etc.) to form a restart service, thereby eliminating the large energy storage reserve it would otherwise required.

- Investigate restart, by 100% IBR in regions of high GFL IBR penetration, of large induction motors (such as those used in thermal plant or industrial processes), including stability analysis of variable speed drive energisation and operation.
- Further investigate the stability of DER interactions with distribution and sub-transmission connected embedded generators, and whether GFM embedded generation can mitigate any instabilities observed.
- Evaluate limitations of generic models compared to OEM models, especially regarding fault/inrush current, and harmonic and sequence components of current. Identify control algorithms (where discernible) that are most likely to support stable operation of a restarting system without protection maloperation.

7 References

[1] CIGRE, “Power system restoration accounting for a rapidly changing power system and generation mix,” CIGRE, 2023. [Online]. Available: https://www.e-cigre.org/publications/detail/911-power-system-restoration-accounting-for-a-rapidly-changing-power-system-and-generation-mix.html. [Accessed 2025].

[2] AEMC, “Issues Paper - Review of the System Restart Standard,” 2024. [Online]. Available: https://www.aemc.gov.au/sites/default/files/2024-12/Issues%20Paper%20-%20Review%20of%20the%20System%20Restart%20Standard.pdf . [Accessed 2025].

[3] AEMC, “System Restart Standard,” AEMC, 2021. [Online]. Available: https://www.aemc.gov.au/sites/default/files/2021-01/SRS%20Review%20-%20System%20Restart%20Standard%20-%20FOR%20PUBLICATION_0.pdf. [Accessed 2025].

[4] AEMC, “Reliability Panel,” AEMC, 2024. [Online]. Available: https://www.aemc.gov.au/about-us/reliability-panel . [Accessed 2025].

[5] CIGRE, “TB039 Guidelines for representation of network elements when calculating transients,” CIGRE, 1990.

[6] Hitachi, “High Voltage Surge Arresters Buyer's Guide,” Hitachi, 2024. [Online]. Available: https://publisher.hitachienergy.com/preview?DocumentID=2GHE167330&LanguageCode=en&DocumentPartId=&Action=launch&DocumentRevisionId=A. [Accessed 2025].

[7] ArresterWorks, “Arrester Reference Voltage,” arresterworks.com, 2001. [Online]. Available: http://www.arresterworks.com/arresterfacts/pdf_files/ArresterFacts_027_Arrester_Reference_Voltage.pdf. [Accessed 2025].

[8] PSCAD, “Grid Forming Inverter Models,” PSCAD, 2023. [Online]. Available: https://www.pscad.com/knowledge-base/article/894. [Accessed 2025].

[9] EPRI, “Applicability of Transmission and Distribution Co-Simulation for Accurate Capture of Load and DER Dynamic Behavior: 2021 Update,” Electric Power Research Institute, 2021. [Online]. Available: https://www.epri.com/research/products/000000003002021940. [Accessed 2025].

[10] EPRI, “Model User Guide for Generic Renewable Energy System Models,” Electric Power Research Institute, 2023. [Online]. Available: https://restservice.epri.com/publicdownload/000000003002027129/0/Product . [Accessed 2025].

[11] CSIRO, “G-PST Topic 5: The Role of Inverter-Based Resources During System Restoration (Stage 3),” Aurecon, 2024. [Online]. Available: https://www.csiro.au/-/media/EF/Files/GPST-Roadmap/Stage3-Final/Topic-5_The-role-of-inverter-based-resources.pdf. [Accessed 2025].

[12] CSIRO, “G-PST Topic 5: The Role of Inverter-Based Resources During System Restoration (Stage 2),” Aurecon, 2023. [Online]. Available: https://www.csiro.au/-/media/EF/Files/GPST-Roadmap/Final-Reports/Topic-5-GPST-Stage-2.pdf. [Accessed 2025].

[13] AEMC, “Efficient management of system strength on the power system,” AEMC, 2021. [Online]. Available: https://www.aemc.gov.au/sites/default/files/2021-10/ERC0300%20-%20Information%20sheet%20for%20final%20determination%20%281%29.pdf. [Accessed 2025].

[14] AEMO, “System Strength Impact Assessment Guidelines,” AEMO, 2024. [Online]. Available: https://aemo.com.au/-/media/files/stakeholder_consultation/consultations/nem-

consultations/2024/ssiag/system-strength-impact-assessment-guidelines-v22.pdf?la=en. [Accessed 2025].

[15] Y. Li, Y. Gu and T. C. Green, “Revisiting Grid-Forming and Grid-Following Inverters: A Duality Theory,” *IEEE Transactions on Power Systems,* vol. 37, no. 6, pp. 4541-4554, 2022.

[16] M. Cheng, D. Zhou and F. Blaabjerg, “Multivariable Grid-Forming Converters with Direct States Control,” Aalborg University, Aalborg, Denmark, 2022.

[17] H. Zhang, J. Ma and X. Li, “Dynamic Current-Limitation Strategy of Grid-Forming Inverters Based on SR Latches,” *Electronics,* 2024.

Appendix A List of models developed or integrated

Table 12 List of models developed or integrated

Item	Completed
Circuit breaker model	• Parameterised a PSCAD library model breaker to be suitable for use for black-start studies, notably correcting default impedances to prevent current leakage pre-establishing fluxes
Feeder models (12.47 kV)	• Provided by EPRI as part of their DER/CMPLD model
Gas-turbine model	• Developed a machine model based on anonymised data • Developed an AVR model based on default PSCAD parameters and anonymised project data • Parameterized an E-TRAN library GASTWD turbine model based on anonymised project data • OEL and UEL models available through Topic 6 work
GFL BESS (OEM 1)	• Sourced from OEM 1 through an NDA • Confirmed ability to come online following extended period of zero terminal voltage • Converted to a PNI-compatible model through use of transformer impedance borrowing • Migrated crucial measurements to network page through use of PNI signal transports • Replaced step-up transformer with saturable one, included flux remanence for realistic plant energisation scenarios • Added a MV-enable breaker that only energises the plant after the MV voltage has settled following transformer energisation
GFL Hybrid PV & BESS (OEM 2)	• Sourced from OEM 2 through an NDA • Tuned configuration files to operate with weaker system (not too weak), altered voltage and appropriate MVA size for the network being developed • Confirmed ability to come online following extended period of zero terminal voltage • Converted to a PNI-compatible model through use of transformer impedance borrowing • Migrated crucial measurements to network page through use of PNI signal transports • Replaced step-up transformer with saturable one, included flux remanence for realistic plant energisation scenarios • Added a MV-enable breaker that only energises the plant after the MV voltage has settled following transformer energisation
GFL Hybrid PV & BESS (OEM 1)	• Sourced from OEM 1 through an NDA • Confirmed ability to come online following extended period of zero terminal voltage • Converted to a PNI-compatible model through use of transformer impedance borrowing • Migrated crucial measurements to network page through use of PNI signal transports • Replaced step-up transformer with saturable one, included flux remanence for realistic plant energisation scenarios • Added a MV-enable breaker that only energises the plant after the MV voltage has settled following transformer energisation
GFL PV (OEM 2)	• Sourced from OEM 2 through an NDA • Tuned configuration files to operate with weaker system (not too weak), altered voltage and appropriate MVA size for the network being developed • Confirmed ability to come online following extended period of zero terminal voltage • Converted to a PNI-compatible model through use of transformer impedance borrowing • Migrated crucial measurements to network page through use of PNI signal transports • Replaced step-up transformer with saturable one, included flux remanence for realistic plant energisation scenarios • Added a MV-enable breaker that only energises the plant after the MV voltage has settled following transformer energisation
GFL PV (OEM 1)	• Sourced from OEM 1 through an NDA • Confirmed ability to come online following extended period of zero terminal voltage • Converted to a PNI-compatible model through use of transformer impedance borrowing • Migrated crucial measurements to network page through use of PNI signal transports • Replaced step-up transformer with saturable one, included flux remanence for realistic plant energisation scenarios • Added a MV-enable breaker that only energises the plant after the MV voltage has settled following transformer energisation
GFM BESS (OEM 1)	• Sourced from OEM 1 through an NDA • Converted to a PNI-compatible model through use of transformer impedance borrowing • Tuned it for an islanded scenario • Resolved its initialization issue (needs 3 seconds of source before switching out to islanded mode)
Harmonic visualization tools	• Developed a harmonics visualization tool capable of representing voltage harmonic content at any given bus

Item	Completed
	• Focuses on lower-order harmonics likely to be important to understand when transformer energisation and protection relay operation takes place
Protection relay models	• All synchronous generator and crucial network protection relay models (transformer differential, impedance-based) models sourced from MHI • Releasable model set, but as yet unreleased
Sequence controller	• Developed a methodology for maintaining clarity in creating a restart sequence
Sub-transmission line models (66kV)	• Developed 66kV line model, scalable on kilometres. • Based on publicly available line data (NEXANS catalogue) and remnant knowledge of the conductor type typically used in Victoria • Pole spacing data based on remnant knowledge and direct observation of nearby poles.
Surge arresters	• Developed based on publicly available information from the ABB PEXLIM series (common across Australia) • Developed for 330, 220, and 66kV use • Tested and some minor variations made to the 220kV series due to non-congruent data points in the ABB datasheet
Transformer models (220/66kV)	• Developed based on remnant knowledge and typical parameters for network transformers (vector groups, impedances and sizes typical of those in use within Victoria) • Leveraged existing PSCAD models as the base (notably comprising three single-phase devices) • Included effects of saturation and flux remanence for those which will be energized as part of the restoration plan • Analysis performed to determine whether there is a material difference between inrush performance of an autotransformer and a three-winding transformer configuration. Determined insufficient difference to warrant the development of autotransformer models
Transformer models (66/22kV)	• Developed based on remnant knowledge and typical parameters for network transformers (vector groups, impedances and sizes typical of those in use within Victoria) • Leveraged existing PSCAD models as the base • Included effects of saturation and flux remanence for those which will be energized as part of the restoration plan
Transformer models (step-up)	• Developed based on anonymized and altered plant data • Many provided as part of OEM models • Included effects of saturation and flux remanence for those which will be energized as part of the restoration plan
Transmission line models (220kV)	• Developed dual-circuit 220kV line model, scalable on kilometers. • Based on publicly available line data (NEXANS catalogue) and remnant knowledge of the conductor type typically used in Victoria • Tower data based on remnant knowledge and direct observation of nearby towers.

Appendix B Example DER parameters

Table 13 Example DER parameters

Substation Transformer and Overall Distribution System			
Peak active power load of distribution system	**30**	**MW**	
Design power factor of distribution system	**0.98**		
Ratio of transformer ONAF rating to peak load	**1.3**		
Ratio of transformer ONAF/ONAN rating	**1.33**		
Self-cooled rating (ONAN) of transformer	**29.92174313**	**MVA**	
Transformer impedance on ONAN base	**0.07**		
Transformer X/R ratio	**30**		
Transformer reactance	**0.069961143**	**p.u.**	
Transformer resistance	**0.002332038**	**p.u.**	
Nominal distribution primary voltage (line-to-line)	**12.47**	**kV**	
Transformer resistance	**0.012119415**	**ohms**	(distribution side)
Transformer reactance	**0.363582453**	**ohms**	(distribution side)
Reference 3-phase Backbone Feeder			
First section conductor	**336**	**kcmil**	for reference, numeric value is not used in calculations
Feeder ampacity	**500**	**A**	
Assumed pf for ampacity calculation	**0.9**		
Loading of feeder at system peak	**0.8**		relative to thermal capacity
Feeder active power loading at peak	**7.775522485**	**MW**	
Capacity scaling factor	**3.858261622**		divide model impedances by this factor to scale representative feeder to equivalent of total distribution system
Feeder X0/X1 ratio	**2.8**		use for both sections
Feeder R0/X1 ratio	**0.9**		use for both sections
Feeder positive sequence surge impedance	**450**	**W**	to determine shunt capacitance; use for both sections
Feeder zero sequence surge impedance	**900**	**W**	to determine shunt capacitance; use for both sections
1st section + sequence resistance per 1000'	**0.0625**	**W/kft**	
1st section + sequence reactance per 1000'	**0.116**	**W/kft**	
1st section 0 sequence resistance per 1000'	**0.1044**	**W/kft**	
1st section 0 sequence reactance per 1000'	**0.3248**	**W/kft**	
Total length of first section	**2**	**miles**	
Total length of second section	**3**	**miles**	
Location of 1st section equiv load	**0.5**		percentage of distance along the first section
Location of second section equiv load	**0.5**		percentage of distance along the second section (from the interface with the first section)
Second section conductor	**2/0**	**AWG**	for reference, numeric value is not used in calculations
Second section ampacity	**276**	**A**	for reference, numeric value is not used in calculations
2nd section + sequence resistance per 1000'	**0.176**	**W/kft**	
2nd section + sequence reactance per 1000'	**0.152**	**W/kft**	
2nd section 0 sequence resistance per 1000'	**0.1368**	**W/kft**	
2nd section 0 sequence reactance per 1000'	**0.4256**	**W/kft**	
Scaled 3-phase Backbone Feeder Model			
pos. seq. resistance Bus 1 - Bus 2	**0.085530747**	**W**	
pos. seq. inductance Bus 1 - Bus 2	**0.421074448**	**mH**	
pos. seq. shunt capacitance Bus 1 - Bus 2	**0.00207938**	**mF**	
zero seq. resistance Bus 1 - Bus 2	**0.14287056**	**W**	
zero seq. inductance Bus 1 - Bus 2	**1.179008456**	**mH**	
zero seq. shunt capacitance Bus 1 - Bus 2	**0.001455566**	**mF**	
pos. seq. resistance Bus 2 - Bus 3	**0.40404725**	**W**	

pos. seq. inductance Bus 2 - Bus 3	**1.038166313**	**mH**	
pos. seq. shunt capacitance Bus 2 - Bus 3	**0.005126747**	**mF**	
zero seq. resistance Bus 2 - Bus 3	**0.945080546**	**W**	
zero seq. inductance Bus 2 - Bus 3	**2.906865675**	**mH**	
zero seq. shunt capacitance Bus 2 - Bus 3	**0.003588723**	**mF**	
Load Allocation			
Percentage of load in Zone 1	**0.55**		
Zone 1 total load	**4.276537367**	**MW**	
Percent commercial/light industrial in Zone 1	**0.35**		percentage of Zone 1's total load that is commercial/industrial, served three-phase
Load 1.2 active power	**1.496788078**	**MW**	
Percent residential in Zone 1	**0.65**		
% of Zone 1 residential load on/near main feeder	**0.2**		
Load 1.1 active power	**0.555949858**	**MW**	
% of Zone 1 residential load on longer laterals	**0.8**		
Allocation of Zone 1 lateral load to Phase A	**0.28**		
Allocation of Zone 1 lateral load to Phase B	**0.4**		
Allocation of Zone 1 lateral load to Phase C	**0.32**		adjusted to make a sum of 100% for the phases
Load 1.3a active power	**0.622663841**	**MW**	
Load 1.3b active power	**0.889519772**	**MW**	
Load 1.3c active power	**0.711615818**	**MW**	
Percentage of load in Zone 2	**0.45**		
Zone 2 total load	**3.498985118**	**MW**	
Percent commercial/light industrial in Zone 2	**0.2**		percentage of Zone 2's total load that is commercial/industrial, served three-phase
Load 2.2 active power	**0.699797024**	**MW**	
Percent residential in Zone 2	**0.8**		
% of Zone 2 residential load on/near main feeder	**0.15**		
Load 2.1 active power	**0.419878214**	**MW**	
% of Zone 2 residential load on longer laterals	**0.85**		
Allocation of Zone 2 lateral load to Phase A	**0.5**		
Allocation of Zone 2 lateral load to Phase B	**0.2**		
Allocation of Zone 2 lateral load to Phase C	**0.3**		
Load 2.3a active power	**1.18965494**	**MW**	
Load 2.3b active power	**0.475861976**	**MW**	
Load 2.3c active power	**0.713792964**	**MW**	
Universal DER Parameters			
Percentage of residential customers with DER	**0.95**		Measured in terms of the customer demand, rather than the number of customers
Average DER capacity relative to coincident demand	**0.95**		I.e., the ratio of DER nameplate capacity relative to the coincident demand of that customer
DER output at time of system peak, relative to nameplate	**0.4**		System demand tends to be late in afternoon when PV is reduced; also consider average of cloud shading
U-DER interconnection transformer % resistance	**0.006**		
U-DER interconnection transformer % reactance	**0.05**		
Universal Load Parameters			
Commercial non-motor load power factor	**0.99**		
Commercial (3-ph) motor power factor	**0.9**		
Commercial % motor load	**0.2**		
Residential non-motor load power factor	**0.99**		
Residential (1-ph) motor power factor	**0.9**		
Residential % motor load	**0.15**		
Three-phase (commercial) transformer %R	**0.007**		
Three-phase (commercial) transformer %X	**0.04**		

Reference Residential Distribution Transformer			
Rating of transformer	**25**	**kVA**	single-phase transformer
Connection	**L-G:L-G**		
Number of residential services per transformer	**4**		
Single-phase (residential) transformer %R	**0.01**		
Single-phase (residential) transformer %X	**0.018**		
Primary voltage	**7199.557857**		single-phase transformer
Secondary voltage	**415**	**V**	
Reference Service Cable			
Cable size	**#1/0**		for reference, numeric value is not used in calculations
Cable length	**100**	**feet**	
Service cable conductor resistance per 1000'	**0.675**	**W/kft**	one-way resistance, need to double for 240 V load
Service cable reactance per 1000'	**0.128**	**W/kft**	one-way reactance, need to double for 240 V load
Reference Motor Branch Circuit Cable			
Reference motor demand	**4**	**kVA**	
Reference motor power	**3.6**	**kW**	
Branch circuit conductor	**#10 Cu**		for reference, numeric value is not used in calculations
Conductor resistance	**0.999**	**W/kft**	ignore reactance, it is very small relative to resistance, thus cable tables don't provide this datum
Branch circuit length	**40**	**ft**	
LOAD 1.1			
Primary lateral conductor	**#6**	**AWG**	for reference, numeric value is not used in calculations
Number of homes served per phase	**15**		
Coincident demand per home	**2**	**kW**	
Coincident 3-ph loading of laterals at system peak	**90**	**kW**	
Load 1.1 scaling factor	**6.177220641**		divide model impedances by this factor to scale representative lateral to equivalent for total distribution system
Location of equivalent load along lateral	**0.5**		distance from feeder tap to equivalent load relative to total lateral length
Length of lateral	**500**	**feet**	
Lateral conductor resistance per 1000'	**0.675**	**W/kft**	one-way resistance; double for primary + neutral loop
Lateral conductor reactance to 1' spacing per 1000'	**0.128**	**W/kft**	one-way "internal" reactance, need to add "external" reactance due to spacing, and double
Model Z1 resistance	**0.014160839**	**W**	
Model Z1 inductance	**0.009348741**	**mH**	
Number of distribution transformer per phase on lateral	**3.75**		
Distribution transformer resistance (referred to primary)	**0.231982695**	**W**	
Distribution transformer resistance (referred to primary)	**1.107609683**	**mH**	
Model Z2 resistance	**0.007552448**	**W**	
Model Z2 inductance	**0.003798854**	**mH**	
Model Z3 resistance	**0.000397497**	**W**	
Model Z3 inductance	**0.00019994**	**mH**	
Non-DER customer motor load	**16.0875**	**kVA**	
Non-DER customer motor load ref. scaling factor	**4.021875**		
Model Z4 resistance	**0.000833762**	**W**	
Non-DER customer motor load	**305.6625**	**kVA**	
Non-DER customer motor load ref. scaling factor	**76.415625**		

Model Z5 resistance	**4.38822E-05**	**W**	
Load L1	**91.1625**	**kW**	
	12.98995271	**kVAR**	
Load L2	**1732.0875**	**kW**	
	246.8091016	**kVAR**	
Motor M1	**16.0875**	**kW**	
	7.791531862	**kVAR**	
Motor M2	**305.6625**	**kW**	
	148.0391054	**kVAR**	
R-DER rating	**1645.483125**	**kW**	
R-DER output	**658.19325**	**kW**	
Reference Commercial Load			
Load demand at system peak	**600**	**kW**	
Service nominal voltage	**415**	**V**	
Transformer rating	**750**	**kVA**	
Reference motor rating	**25**	**kW**	
Motor branch circuit current	**38.64459633**	**A**	
Motor branch circuit conductor	**#4 Cu**	**AWG**	for reference, numeric value is not used in calculations
Motor branch circuit length	**200**	**feet**	
Motor branch circuit resistance	**0.249**	**W/kft**	
LOAD 1.2			
Load 1.2 total active power	**1.496788078**	**MW**	copied from above for convenience
Load 1.2 scaling factor	**2.494646797**		divide model impedances by this factor to scale representative lateral to equivalent for total distribution system
Distribution transformer resistance (referred to primary)	**0.150788752**	**W**	
Distribution transformer resistance (referred to primary)	**2.28554379**	**mH**	
Motor M1 active power	**1155**	**kW**	
Motor M1 reactive power	**559.3920311**	**kVAR**	
Motor scaling factor	**46.2**		
Model Z1 resistance	**0.00027938**	**W**	
Load L1 active power	**4620**	**kW**	
	2237.568124	**kVAR**	
Lateral 1a and Load 1.3a			
Primary lateral conductor	**#2**	**AWG**	for reference, numeric value is not used in calculations
Number of homes served per phase	**50**		
Coincident demand per home	**2**	**kW**	
Coincident 1-ph loading of lateral at system peak	**100**	**kW**	
Load 1a scaling factor	**6.226638406**		divide model impedances by this factor to scale representative lateral to equivalent for total distribution system
Location of equivalent load along lateral	**0.4**		distance from feeder tap to equivalent load relative to total lateral length
Length of lateral	**1800**	**feet**	
Lateral conductor resistance per 1000'	**0.267**	**W/kft**	one-way resistance; double for primary + neutral loop
Lateral conductor reactance to 1' spacing per 1000'	**0.109**	**W/kft**	one-way "internal" reactance, need to add "external" reactance due to spacing, and double

Primary lateral resistance	**0.016003996**	**W**	
Primary lateral inductance	**0.023689838**	**mH**	
Number of distribution transformer per phase on lateral	**12.5**		
Distribution transformer resistance (referred to primary)	**0.069042469**	**W**	
Distribution transformer resistance (referred to primary)	**0.329645739**	**mH**	
Model Z1 resistance	**0.002247752**	**W**	
Model Z1 inductance	**0.001130611**	**mH**	
Model Z2 resistance	**0.000118303**	**W**	
Model Z2 inductance	**5.95059E-05**	**mH**	
Non-DER customer motor load	**18.018**	**kVA**	
Non-DER customer motor load ref. scaling factor	**4.5045**		
Model Z3 resistance	**0.000738522**	**W**	
Non-DER customer motor load	**342.342**	**kVA**	
Non-DER customer motor load ref. scaling factor	**85.5855**		
Model Z4 resistance	**3.88696E-05**	**W**	
Load L1	**102.102**	**kW**	
	14.54874704	**kVAR**	
Load L2	**1939.938**	**kW**	
	276.4261938	**kVAR**	
Motor M1	**18.018**	**kW**	
	8.726515685	**kVAR**	
Motor M2	**342.342**	**kW**	
	165.803798	**kVAR**	
R-DER rating	**1842.9411**	**kW**	
R-DER output	**737.17644**	**kW**	
Lateral 1b and Load 1.3b			
Primary lateral conductor	**#2**	**AWG**	for reference, numeric value is not used in calculations
Number of homes served per phase	**50**		
Coincident demand per home	**2**	**kW**	
Coincident 1-ph loading of lateral at system peak	**100**	**kW**	
Load 1b scaling factor	**8.895197723**		divide model impedances by this factor to scale representative lateral to equivalent for total distribution system
Location of equivalent load along lateral	**0.4**		distance from feeder tap to equivalent load relative to total lateral length
Length of lateral	**2400**	**feet**	
Lateral conductor resistance per 1000'	**0.267**	**W/kft**	one-way resistance; double for primary + neutral loop
Lateral conductor reactance to 1' spacing per 1000'	**0.109**	**W/kft**	one-way "internal" reactance, need to add "external" reactance due to spacing, and double
Primary lateral resistance	**0.014937063**	**W**	
Primary lateral inductance	**0.022110515**	**mH**	
Number of distribution transformer per phase on lateral	**12.5**		
Distribution transformer resistance (referred to primary)	**0.048329728**	**W**	
Distribution transformer resistance (referred to primary)	**0.230752017**	**mH**	
Model Z1 resistance	**0.001573427**	**W**	

Model Z1 inductance	**0.000791428**	**mH**	
Model Z2 resistance	**8.28119E-05**	**W**	
Model Z2 inductance	**4.16541E-05**	**mH**	
Non-DER customer motor load	**25.74**	**kVA**	
Non-DER customer motor load ref. scaling factor	**6.435**		
Model Z3 resistance	**0.000361876**	**W**	
Non-DER customer motor load	**489.06**	**kVA**	
Non-DER customer motor load ref. scaling factor	**122.265**		
Model Z4 resistance	**1.90461E-05**	**W**	
Load L1	**145.86**	**kW**	
	20.78392434	**kVAR**	
Load L2	**2771.34**	**kW**	
	394.8945625	**kVAR**	
Motor M1	**25.74**	**kW**	
	12.46645098	**kVAR**	
Motor M2	**489.06**	**kW**	
	236.8625686	**kVAR**	
R-DER rating	**2632.773**	**kW**	
R-DER output	**1053.1092**	**kW**	
Lateral 1c and Load 1.3c			
Primary lateral conductor	**#2**	**AWG**	for reference, numeric value is not used in calculations
Number of homes served per phase	**50**		
Coincident demand per home	**2**	**kW**	
Coincident 1-ph loading of lateral at system peak	**100**	**kW**	
Load 1c scaling factor	**7.116158179**		divide model impedances by this factor to scale representative lateral to equivalent for total distribution system
Location of equivalent load along lateral	**0.4**		distance from feeder tap to equivalent load relative to total lateral length
Length of lateral	**1500**	**feet**	
Lateral conductor resistance per 1000'	**0.267**	**W/kft**	one-way resistance; double for primary + neutral loop
Lateral conductor reactance to 1' spacing per 1000'	**0.109**	**W/kft**	one-way "internal" reactance, need to add "external" reactance due to spacing, and double
Primary lateral resistance	**0.01166958**	**W**	
Primary lateral inductance	**0.01727384**	**mH**	
Number of distribution transformer per phase on lateral	**12.5**		
Distribution transformer resistance (referred to primary)	**0.06041216**	**W**	
Distribution transformer resistance (referred to primary)	**0.288440022**	**mH**	
Model Z1 resistance	**0.001966783**	**W**	
Model Z1 inductance	**0.000989285**	**mH**	
Model Z2 resistance	**0.000103515**	**W**	
Model Z2 inductance	**5.20676E-05**	**mH**	
Non-DER customer motor load	**20.592**	**kVA**	
Non-DER customer motor load ref. scaling factor	**5.148**		

Model Z3 resistance	**0.000565431**	**W**	
Non-DER customer motor load	**391.248**	**kVA**	
Non-DER customer motor load ref. scaling factor	**97.812**		
Model Z4 resistance	**2.97595E-05**	**W**	
Load L1	**116.688**	**kW**	
	16.62713947	**kVAR**	
Load L2	**2217.072**	**kW**	
	315.91565	**kVAR**	
Motor M1	**20.592**	**kW**	
	9.973160783	**kVAR**	
Motor M2	**391.248**	**kW**	
	189.4900549	**kVAR**	
R-DER rating	**2106.2184**	**kW**	
R-DER output	**842.48736**	**kW**	

LOAD 2.1

Primary lateral conductor	**#6**	**AWG**	for reference, numeric value is not used in calculations
Number of homes served per phase	**15**		
Coincident demand per home	**2**	**kW**	
Coincident 3-ph loading of laterals at system peak	**90**	**kW**	
Load 2.1 scaling factor	**4.665313491**		divide model impedances by this factor to scale representative lateral to equivalent for total distribution system
Location of equivalent load along lateral	**0.5**		distance from feeder tap to equivalent load relative to total lateral length
Length of lateral	**1000**	**feet**	
Lateral conductor resistance per 1000'	**0.675**	**W/kft**	one-way resistance; double for primary + neutral loop
Lateral conductor reactance to 1' spacing per 1000'	**0.128**	**W/kft**	one-way "internal" reactance, need to add "external" reactance due to spacing, and double
Model Z1 resistance	**0.0375**	**W**	
Model Z1 inductance	**0.024756852**	**mH**	
Number of distribution transformer per phase on lateral	**3.75**		
Distribution transformer resistance (referred to primary)	**0.307162272**	**W**	
Distribution transformer resistance (referred to primary)	**1.466557265**	**mH**	
Model Z2 resistance	**0.01**	**W**	
Model Z2 inductance	**0.005029964**	**mH**	
Model Z3 resistance	**0.000526316**	**W**	
Model Z3 inductance	**0.000264735**	**mH**	
Non-DER customer motor load	**12.15**	**kVA**	
Non-DER customer motor load ref. scaling factor	**3.0375**		
Model Z4 resistance	**0.001461728**	**W**	
Non-DER customer motor load	**230.85**	**kVA**	
Non-DER customer motor load ref. scaling factor	**57.7125**		
Model Z5 resistance	**7.69331E-05**	**W**	
Load L1	**68.85**	**kW**	
	9.810593659	**kVAR**	

Load L2	**1308.15**	**kW**	
	186.4012795	**kVAR**	
Motor M1	**12.15**	**kW**	
	5.884513574	**kVAR**	
Motor M2	**230.85**	**kW**	
	111.8057579	**kVAR**	
R-DER rating	**1242.7425**	**kW**	
R-DER output	**497.097**	**kW**	
LOAD 2.2			
Load 2.2 total active power	**0.699797024**	**MW**	copied from above for convenience
Load 2.2 scaling factor	**1.166328373**		divide model impedances by this factor to scale representative lateral to equivalent for total distribution system
Distribution transformer resistance (referred to primary)	**0.322520385**	**W**	
Distribution transformer resistance (referred to primary)	**4.888524217**	**mH**	
Motor M1 active power	**540**	**kW**	
Motor M1 reactive power	**261.5339366**	**kVAR**	
Motor scaling factor	**21.6**		
Model Z1 resistance	**0.000597563**	**W**	
Load L1 active power	**2160**	**kW**	
	1046.135746	**kVAR**	
Lateral 2a and Load 2.3a			
Primary lateral conductor	**#2/0**	**AWG**	for reference, numeric value is not used in calculations
Number of homes served per phase	**50**		
Coincident demand per home	**2**	**kW**	
Coincident 1-ph loading of lateral at system peak	**100**	**kW**	
Load 2a scaling factor	**11.8965494**		divide model impedances by this factor to scale representative lateral to equivalent for total distribution system
Location of equivalent load along lateral	**0.4**		distance from feeder tap to equivalent load relative to total lateral length
Length of lateral	**15000**	**feet**	
Lateral conductor resistance per 1000'	**0.134**	**W/kft**	one-way resistance; double for primary + neutral loop
Lateral conductor reactance to 1' spacing per 1000'	**0.122**	**W/kft**	one-way "internal" reactance, need to add "external" reactance due to spacing, and double
Primary lateral resistance	**0.03503268**	**W**	
Primary lateral inductance	**0.112342019**	**mH**	
Number of distribution transformer per phase on lateral	**12.5**		
Distribution transformer resistance (referred to primary)	**0.036136738**	**W**	
Distribution transformer resistance (referred to primary)	**0.172536149**	**mH**	
Model Z1 resistance	**0.001176471**	**W**	
Model Z1 inductance	**0.00059176**	**mH**	
Model Z2 resistance	**6.19195E-05**	**W**	
Model Z2 inductance	**3.11453E-05**	**mH**	
Non-DER customer motor load	**34.425**	**kVA**	

Non-DER customer motor load ref. scaling factor	**8.60625**		
Model Z3 resistance	**0.000202315**	**W**	
Non-DER customer motor load	**654.075**	**kVA**	
Non-DER customer motor load ref. scaling factor	**163.51875**		
Model Z4 resistance	**1.06482E-05**	**W**	
Load L1	**195.075**	**kW**	
	27.79668203	**kVAR**	
Load L2	**3706.425**	**kW**	
	528.1369586	**kVAR**	
Motor M1	**34.425**	**kW**	
	16.67278846	**kVAR**	
Motor M2	**654.075**	**kW**	
	316.7829807	**kVAR**	
R-DER rating	**3521.10375**	**kW**	
R-DER output	**1408.4415**	**kW**	
Lateral 2b and Load 2.3b			
Primary lateral conductor	**#1/0**	**AWG**	for reference, numeric value is not used in calculations
Number of homes served per phase	**50**		
Coincident demand per home	**2**	**kW**	
Coincident 1-ph loading of lateral at system peak	**100**	**kW**	
Load 2b scaling factor	**4.758619761**		divide model impedances by this factor to scale representative lateral to equivalent for total distribution system
Location of equivalent load along lateral	**0.4**		distance from feeder tap to equivalent load relative to total lateral length
Length of lateral	**2200**	**feet**	
Lateral conductor resistance per 1000'	**0.168**	**W/kft**	one-way resistance; double for primary + neutral loop
Lateral conductor reactance to 1' spacing per 1000'	**0.124**	**W/kft**	one-way "internal" reactance, need to add "external" reactance due to spacing, and double
Primary lateral resistance	**0.016104575**	**W**	
Primary lateral inductance	**0.041700618**	**mH**	
Number of distribution transformer per phase on lateral	**12.5**		
Distribution transformer resistance (referred to primary)	**0.090341845**	**W**	
Distribution transformer resistance (referred to primary)	**0.431340372**	**mH**	
Model Z1 resistance	**0.002941176**	**W**	
Model Z1 inductance	**0.001479401**	**mH**	
Model Z2 resistance	**0.000154799**	**W**	
Model Z2 inductance	**7.78632E-05**	**mH**	
Non-DER customer motor load	**13.77**	**kVA**	
Non-DER customer motor load ref. scaling factor	**3.4425**		
Model Z3 resistance	**0.001264471**	**W**	
Non-DER customer motor load	**261.63**	**kVA**	
Non-DER customer motor load ref. scaling factor	**65.4075**		
Model Z4 resistance	**6.65511E-05**	**W**	
Load L1	**78.03**	**kW**	

	11.11867281	**kVAR**	
Load L2	**1482.57**	**kW**	
	211.2547834	**kVAR**	
Motor M1	**13.77**	**kW**	
	6.669115384	**kVAR**	
Motor M2	**261.63**	**kW**	
	126.7131923	**kVAR**	
R-DER rating	**1408.4415**	**kW**	
R-DER output	**563.3766**	**kW**	
Lateral 2c and Load 2.3c			
Primary lateral conductor	**#2/0**	**AWG**	for reference, numeric value is not used in calculations
Number of homes served per phase	**50**		
Coincident demand per home	**2**	**kW**	
Coincident 1-ph loading of lateral at system peak	**100**	**kW**	
Load 2c scaling factor	**7.137929642**		divide model impedances by this factor to scale representative lateral to equivalent for total distribution system
Location of equivalent load along lateral	**0.4**		distance from feeder tap to equivalent load relative to total lateral length
Length of lateral	**10000**	**feet**	
Lateral conductor resistance per 1000'	**0.134**	**W/kft**	one-way resistance; double for primary + neutral loop
Lateral conductor reactance to 1' spacing per 1000'	**0.122**	**W/kft**	one-way "internal" reactance, need to add "external" reactance due to spacing, and double
Primary lateral resistance	**0.0389252**	**W**	
Primary lateral inductance	**0.124824466**	**mH**	
Number of distribution transformer per phase on lateral	**12.5**		
Distribution transformer resistance (referred to primary)	**0.060227896**	**W**	
Distribution transformer resistance (referred to primary)	**0.287560248**	**mH**	
Model Z1 resistance	**0.001960784**	**W**	
Model Z1 inductance	**0.000986267**	**mH**	
Model Z2 resistance	**0.000103199**	**W**	
Model Z2 inductance	**5.19088E-05**	**mH**	
Non-DER customer motor load	**20.655**	**kVA**	
Non-DER customer motor load ref. scaling factor	**5.16375**		
Model Z3 resistance	**0.000561987**	**W**	
Non-DER customer motor load	**392.445**	**kVA**	
Non-DER customer motor load ref. scaling factor	**98.11125**		
Model Z4 resistance	**2.95783E-05**	**W**	
Load L1	**117.045**	**kW**	
	16.67800922	**kVAR**	
Load L2	**2223.855**	**kW**	
	316.8821752	**kVAR**	
Motor M1	**20.655**	**kW**	
	10.00367308	**kVAR**	

Motor M2	**392.445**	**kW**	
	190.0697884	**kVAR**	
R-DER rating	**2112.66225**	**kW**	
R-DER output	**845.0649**	**kW**	
Zone 1 U-DER			
DER active power rating, per feeder	**5**	**MW**	
scaled DER output	**18.32674271**	**MW**	
Scaled Zone 1 U-DER rating	**19.29130811**	**MW**	
Ratio of xfmr kVA to kW rating	**1.1**		
Transformer VA rating	**21.22043892**	**MVA**	
Transformer resistance (referred to MV side)	**0.0439673**	**W**	
Transformer inductance (referred to MV side)	**0.971867812**	**mH**	
Zone 2 U-DER			
DER active power rating, per feeder	**5**	**MW**	
scaled DER output	**18.32674271**	**MW**	
Scaled Zone 2 U-DER rating	**19.29130811**	**MW**	
Ratio of xfmr kVA to kW rating	**1.1**		
Transformer VA rating	**21.22043892**	**MVA**	
Transformer resistance (referred to MV side)	**0.0439673**	**W**	
Transformer inductance (referred to MV side)	**0.971867812**	**mH**	
Capacitor Cap 2			
Zone 1 gross active power (scaled)	**16500**	**kW**	
Zone 1 DER output (scaled)	**21617.70896**	**kW**	
Zone 1 net active power (scaled)	**-5117.708957**	**kW**	
Zone 1 reactive power (scaled)	**4875.108613**	**kVAR**	
Target pf	**1**		
Required kVAR	**4875.108613**	**kVAR**	
Capacitance per phase	**83.15914944**	**mF**	
Capacitor Cap 3			
Zone 2 gross active power (scaled)	**13500**	**kW**	
Zone 2 DER output (scaled)	**21640.72271**	**kW**	
Zone 2 net active power (scaled)	**-8140.722707**	**kW**	
Zone 2 reactive power (scaled)	**3400.350647**	**kVAR**	
Target pf	**1**		
Required kVAR	**3400.350647**	**kVAR**	
Capacitance per phase	**58.00286518**	**mF**	
total DER operating penetration	**1.441947722**		note; this is at peak load
total DER capacity penetration	**0.576779089**		note; this is at peak load, penetration at minimum daytime load can easily by twice as high
total Single phase motor load	**3228.75**	**kW**	
total Three phase motor load	**1695**	**kW**	
total static load	**25076.25**	**kW**	

Appendix C Destabilising GFM results

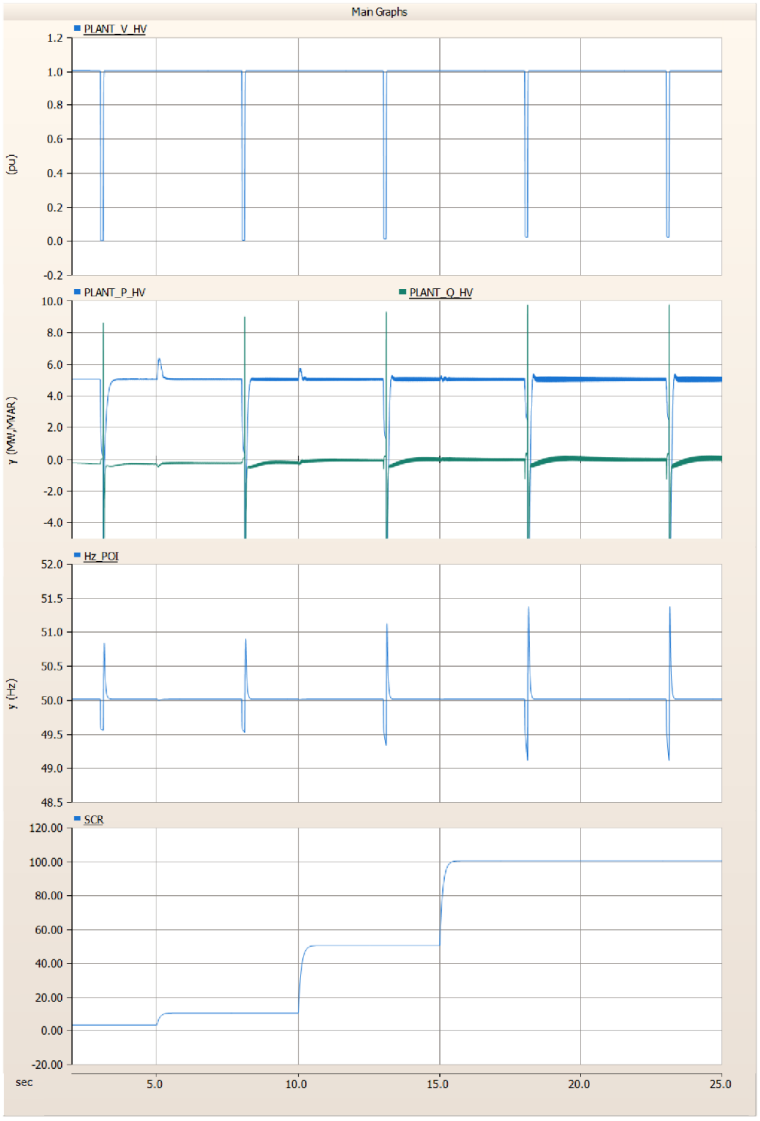

Figure 97 OEM 2 droop GFM. 3% frequency droop mode. PPC enabled. SCR stepped from 3 to 100. X/R = 10.

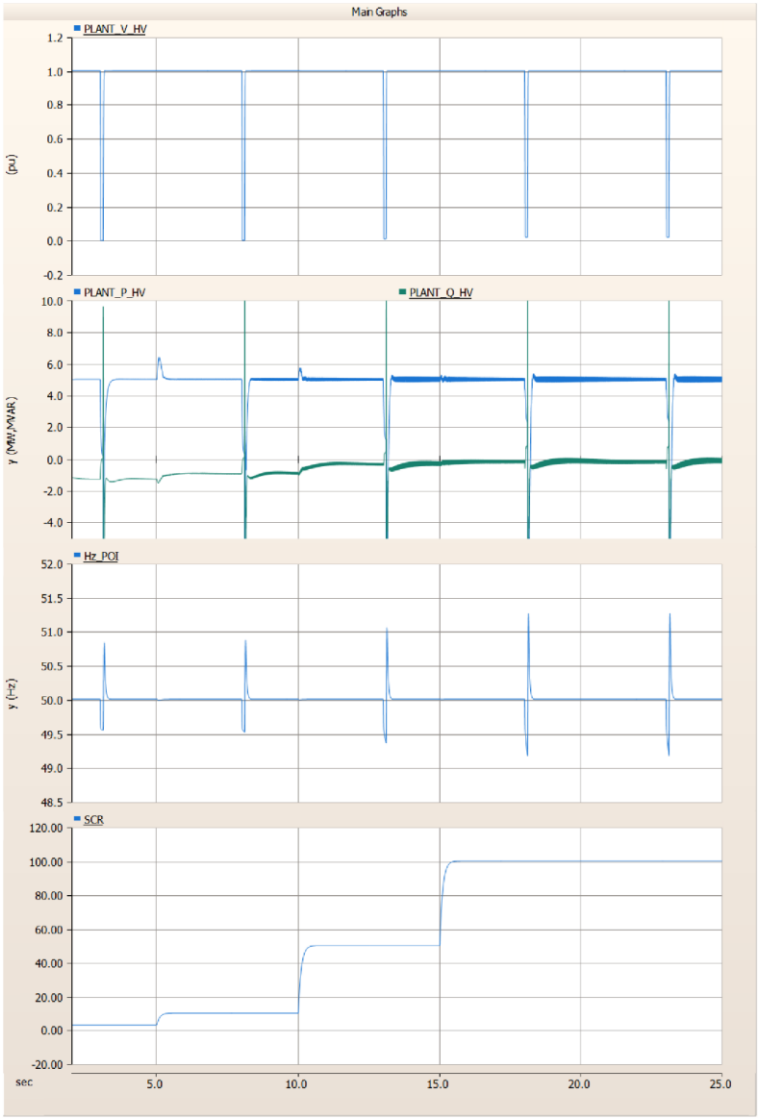

Figure 98 OEM 2 droop GFM. 3% frequency droop mode. PPC enabled. SCR stepped from 3 to 100. X/R = 3.

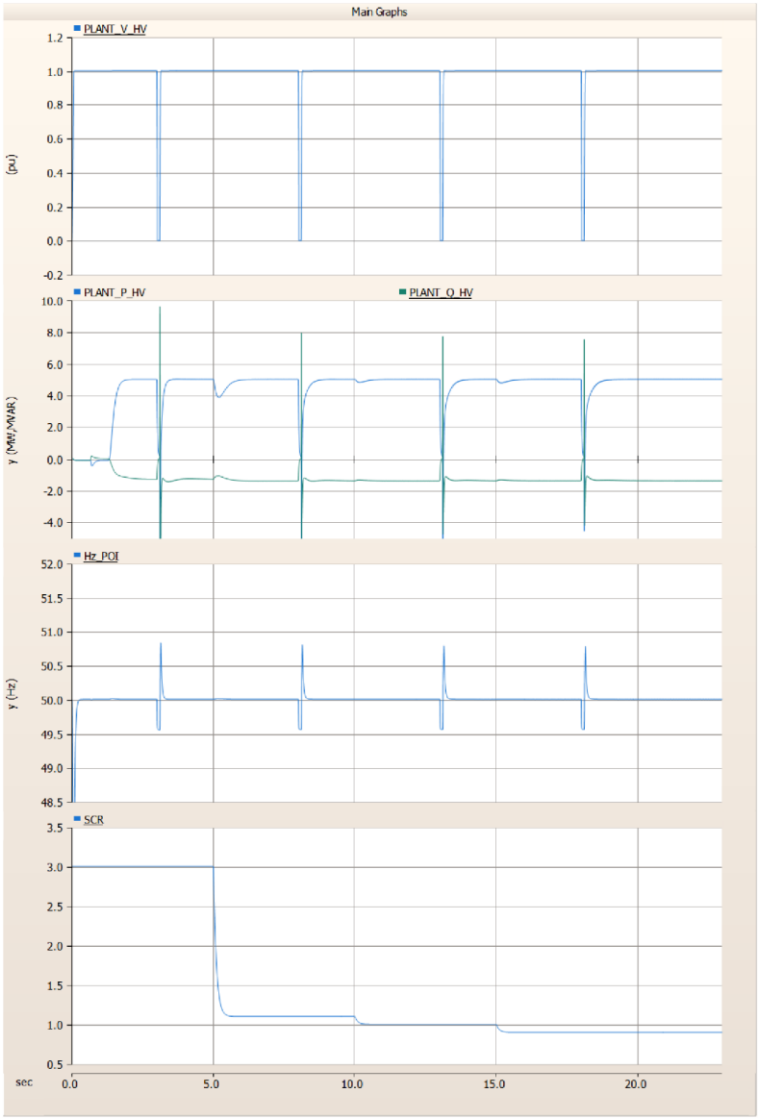

Figure 99 OEM 2 droop GFM. 3% frequency droop mode. PPC enabled. SCR stepped from 3 to 0.9. X/R = 3.

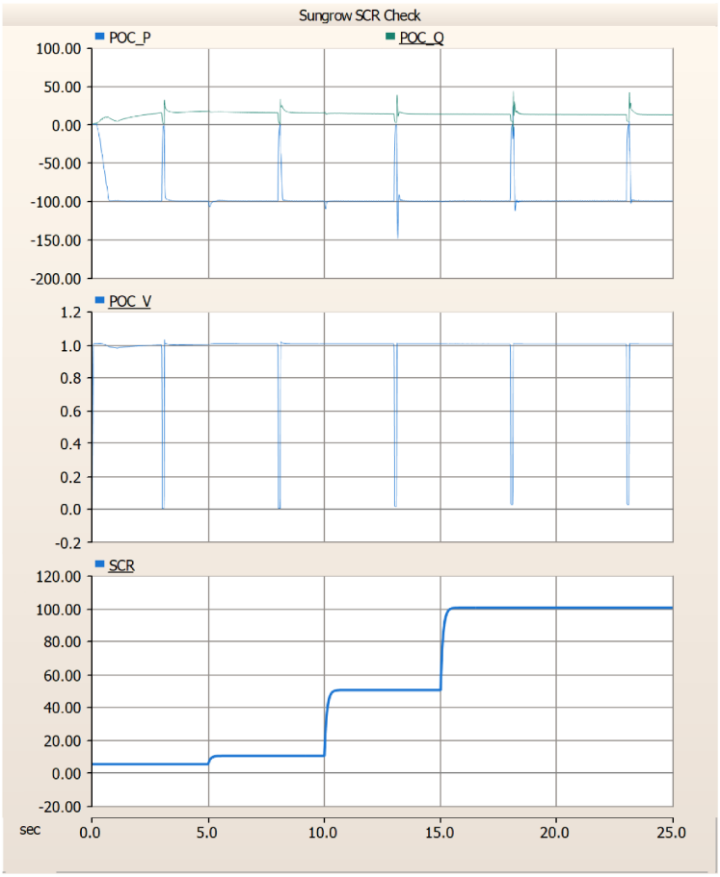

Figure 100 SMIB arrangement, 100 MW import with PPC enabled. SCR stepped from 5 to 100. X/R = 10.

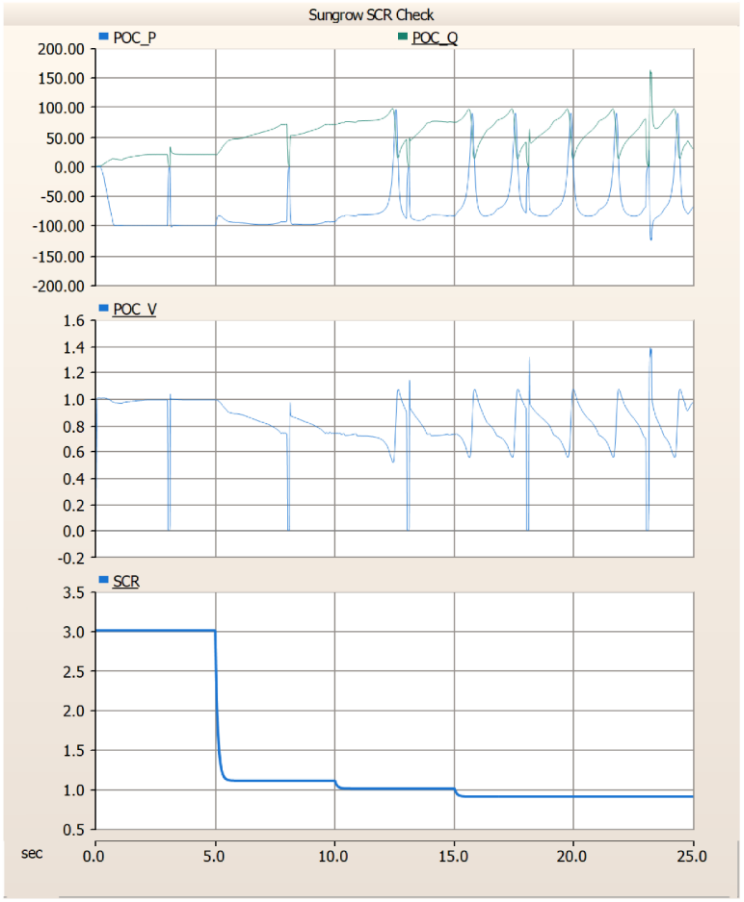

Figure 101 SMIB arrangement, 100 MW import with PPC enabled. SCR stepped from 3 to 0.9. X/R = 10.

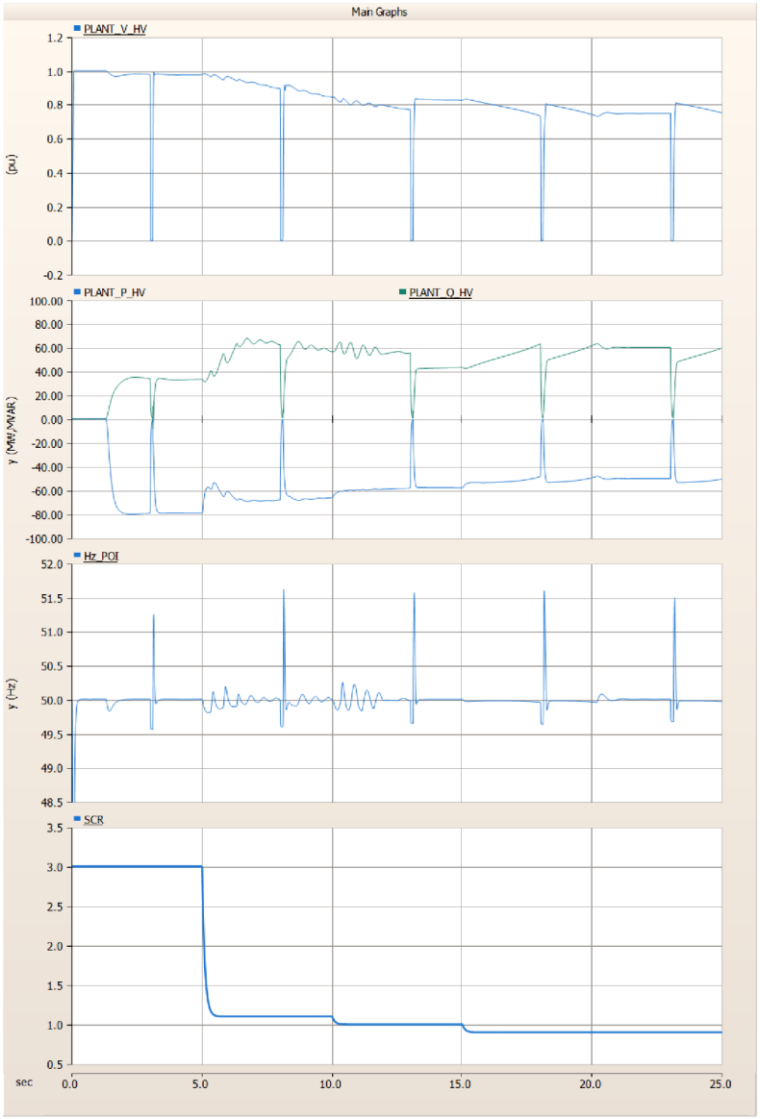

Figure 102 SMIB arrangement, 80 MW import with PPC enabled. SCR stepped from 3 to 0.9. X/R = 3.

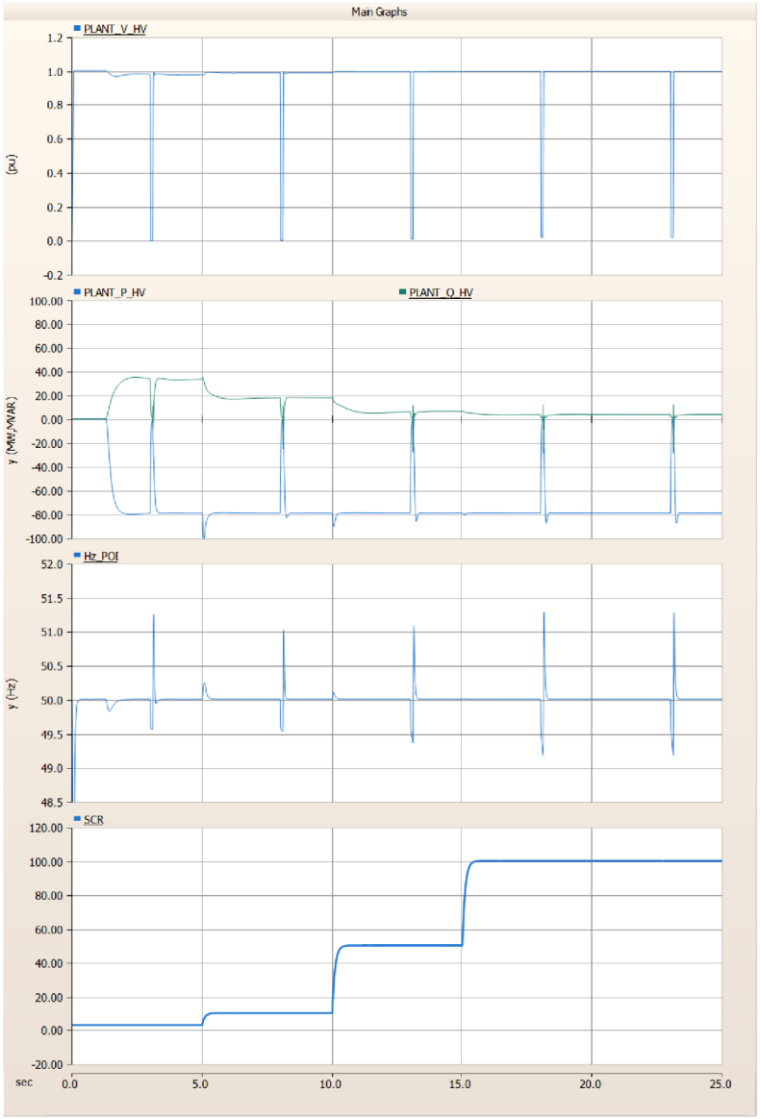

Figure 103 SMIB arrangement, 80 MW import with PPC enabled. SCR stepped from 5 to 100. X/R = 3.

C.1 GFM Withstand SCR tests – Droop mode – Multi-device

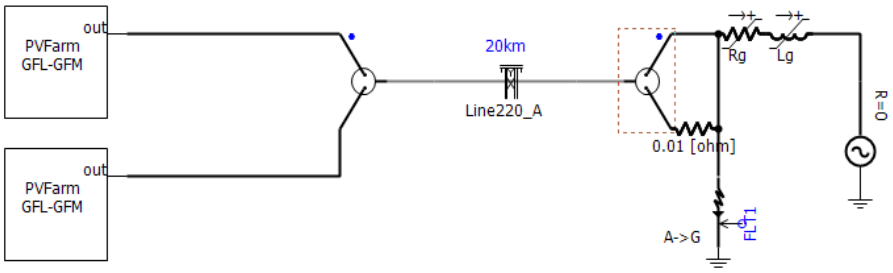

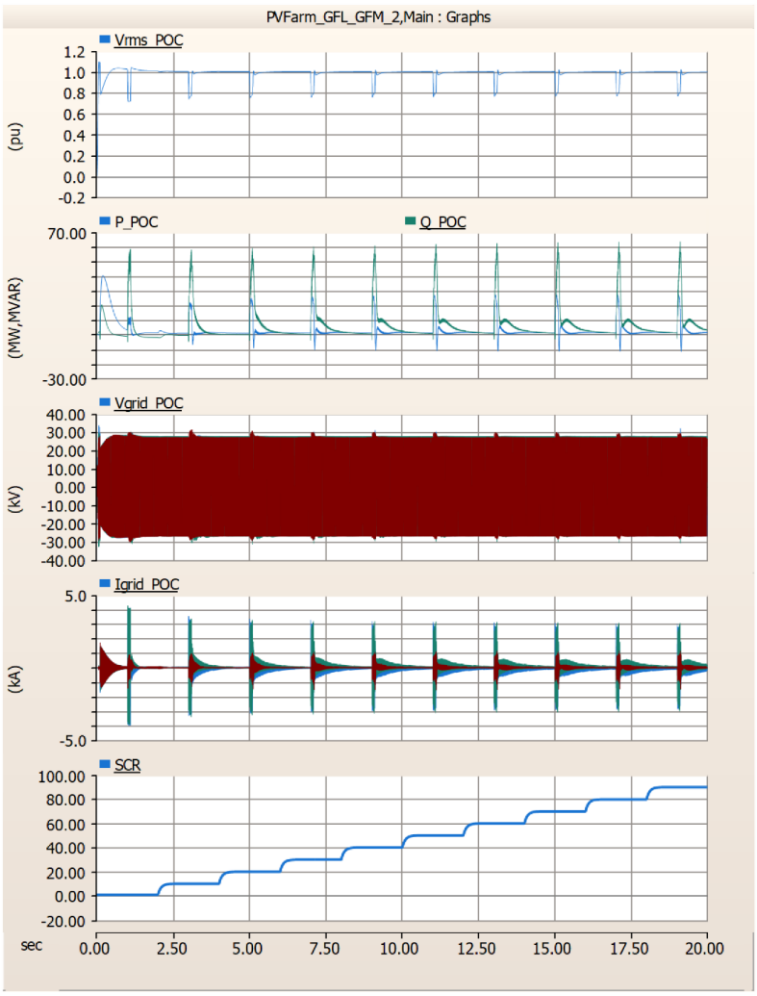

C.2 GFM SCR Withstand test – OEM model

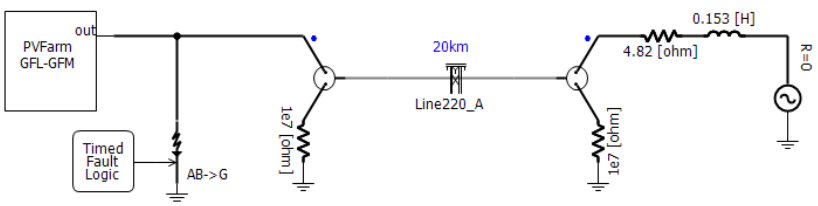

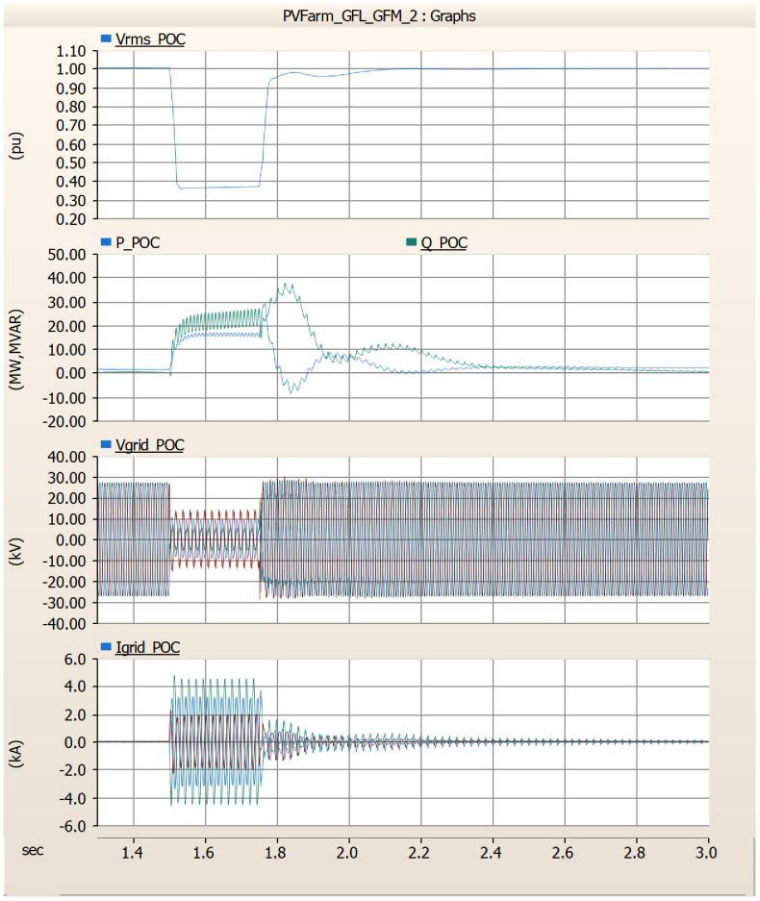

Figure 104 VSM GFM vs. voltage source (SCR=10, X/R=10)

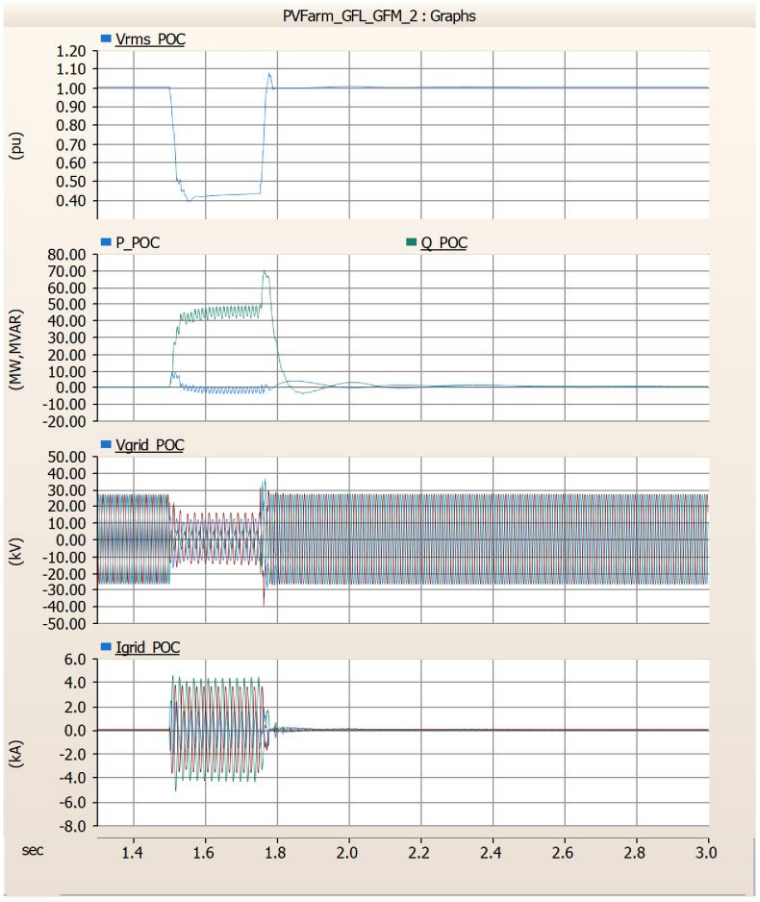

Figure 105 VSM GFM vs. VSM GFM (100 MVA:1000 MVA, inertia 1s:1s)

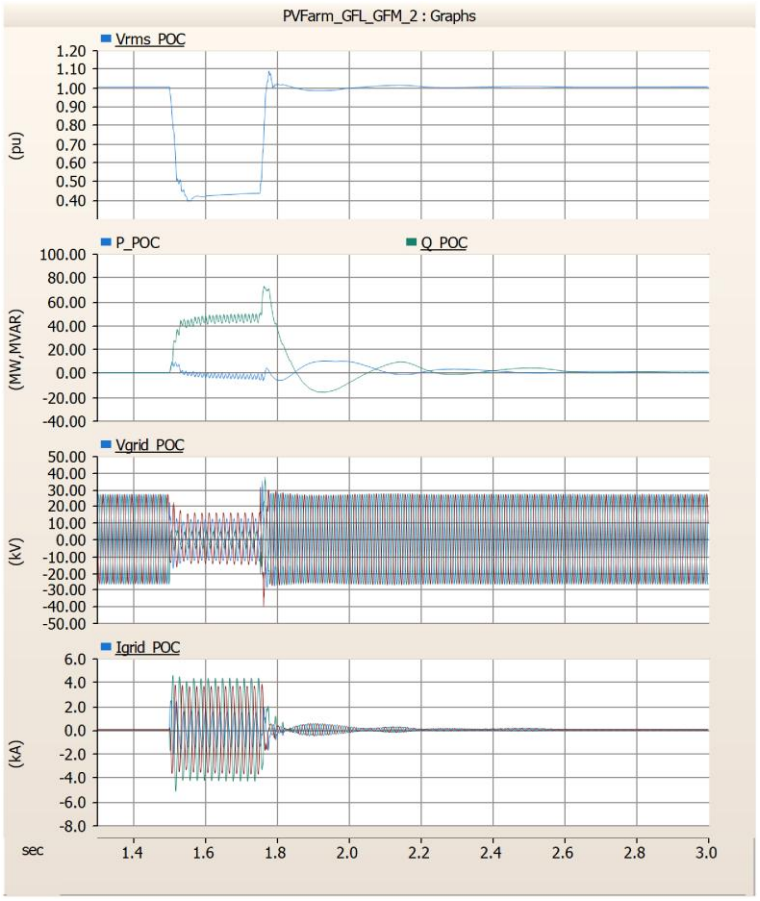

Figure 106 VSM GFM vs. VSM GFM (100 MVA:1000 MVA, inertia 1s:7s)

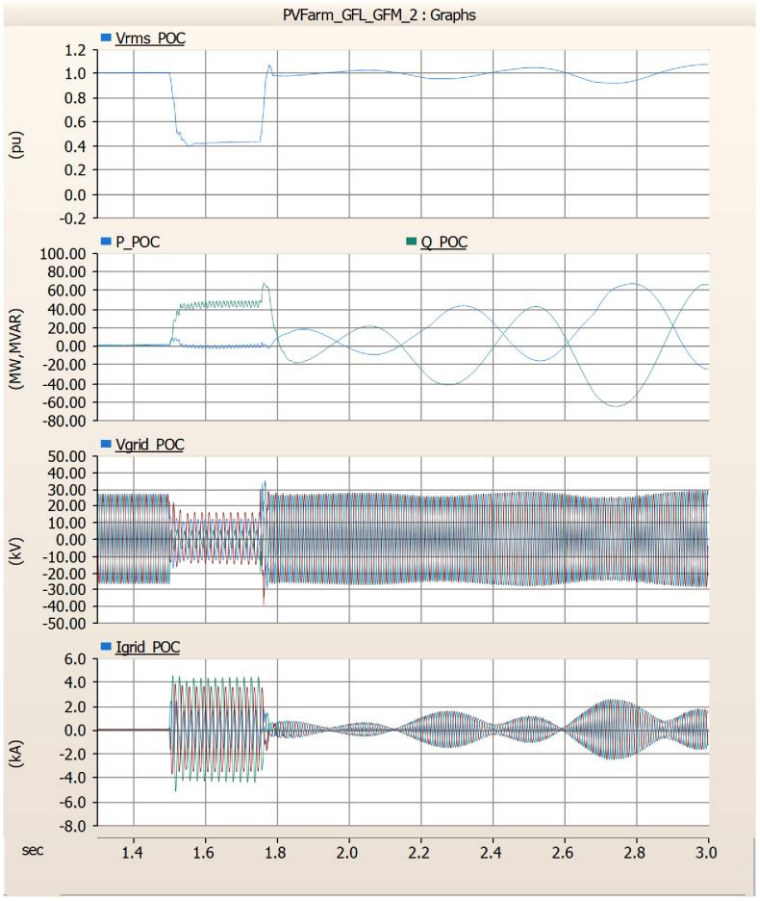

Figure 107 VSM GFM vs VSM GFM (100 MVA:1000 MVA, inertia 7s:1s)

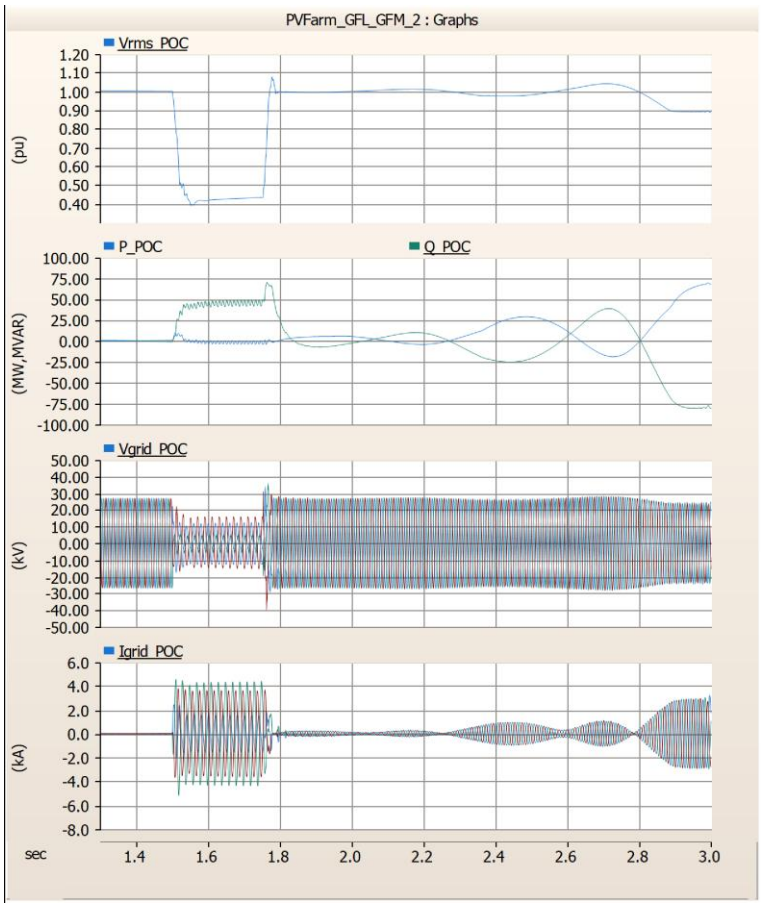

Figure 108 VSM GFM vs VSM GFM (100 MVA:1000 MVA, inertia 7s:7s)

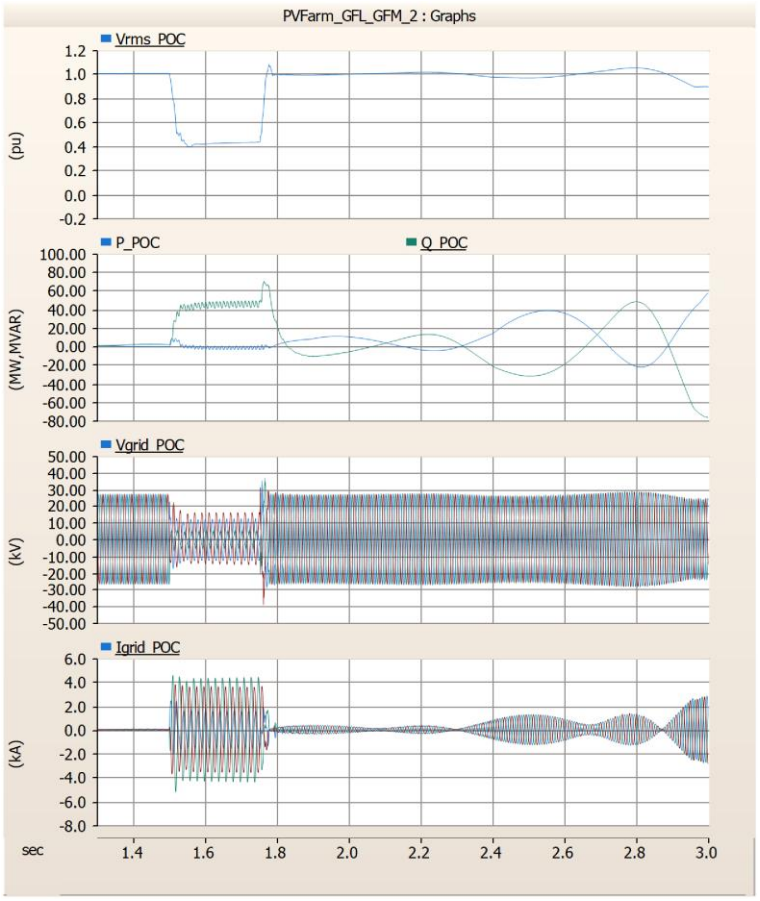

Figure 109 VSM GFM vs VSM GFM (100 MVA:1000 MVA, inertia 7s:15s)

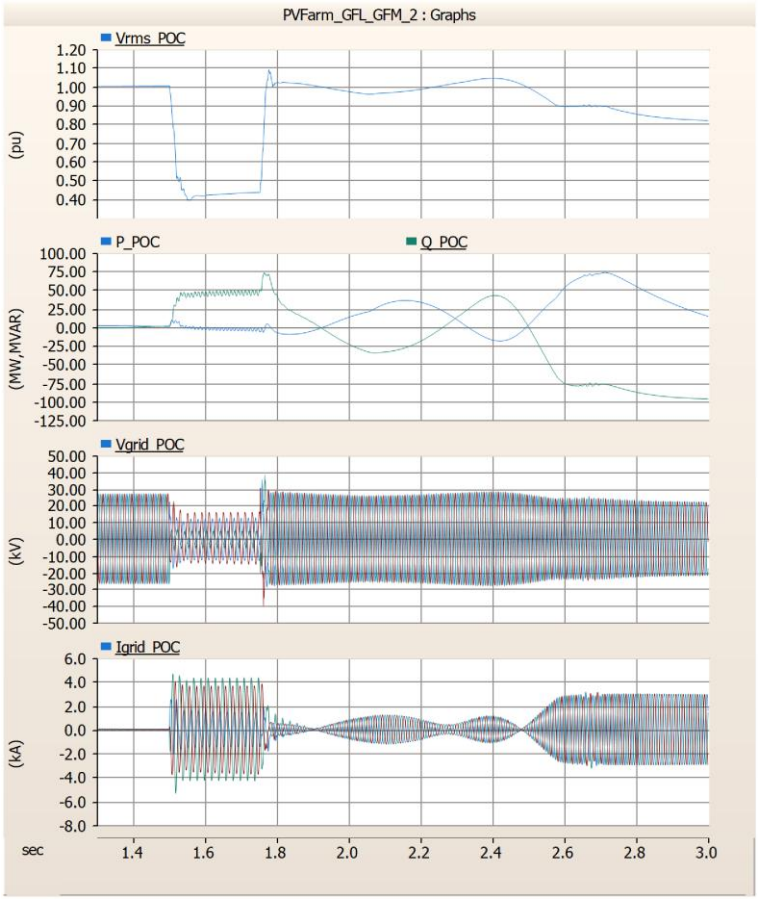

Figure 110 VSM GFM vs VSM GFM (100 MVA:1000 MVA, inertia 7s:99s)

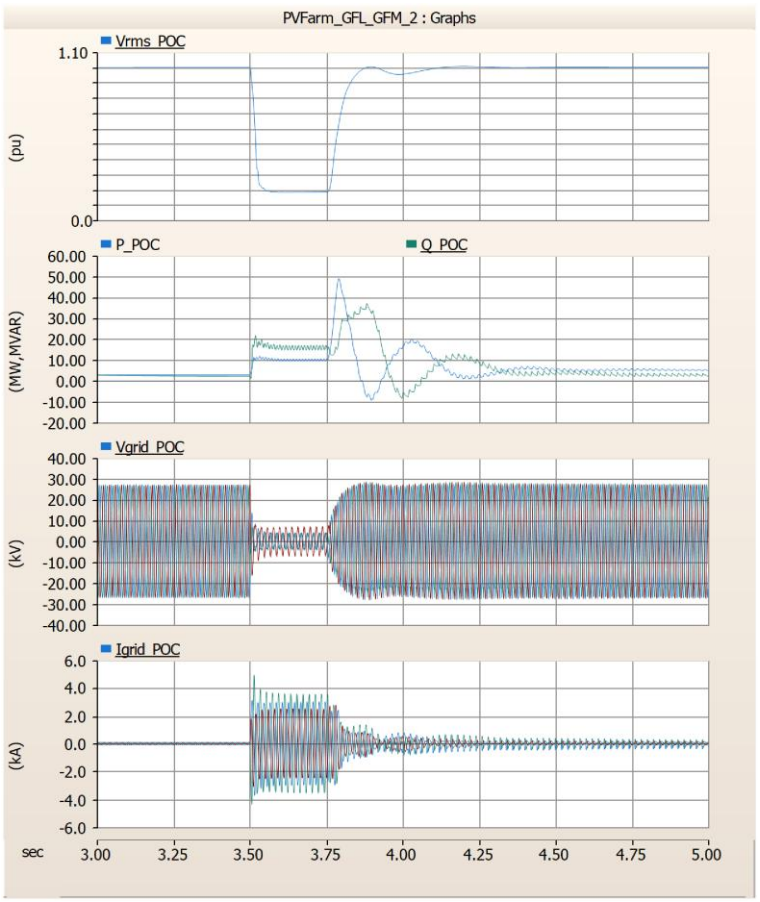

Figure 111 VSM GFM vs SyncCon (100 MVA:1000 MVA, inertia 1s:7s)

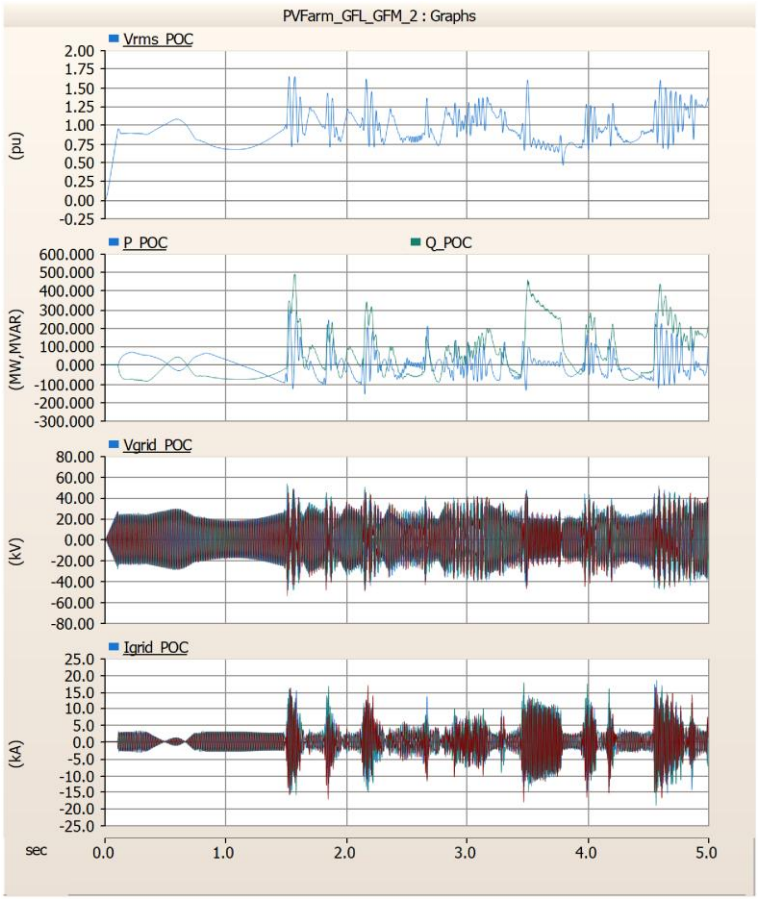

Figure 112 VSM GFM vs SyncCon (100 MVA:1000 MVA, inertia 7s:7s)

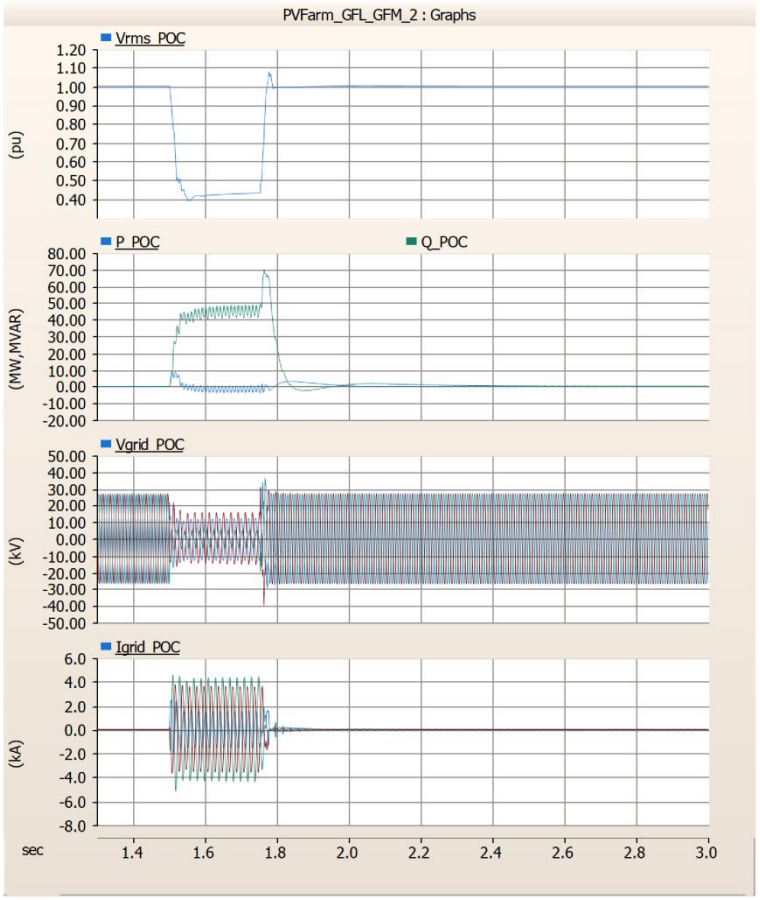

Figure 113 Droop GFM vs Droop GFM (100 MVA:1000 MVA)

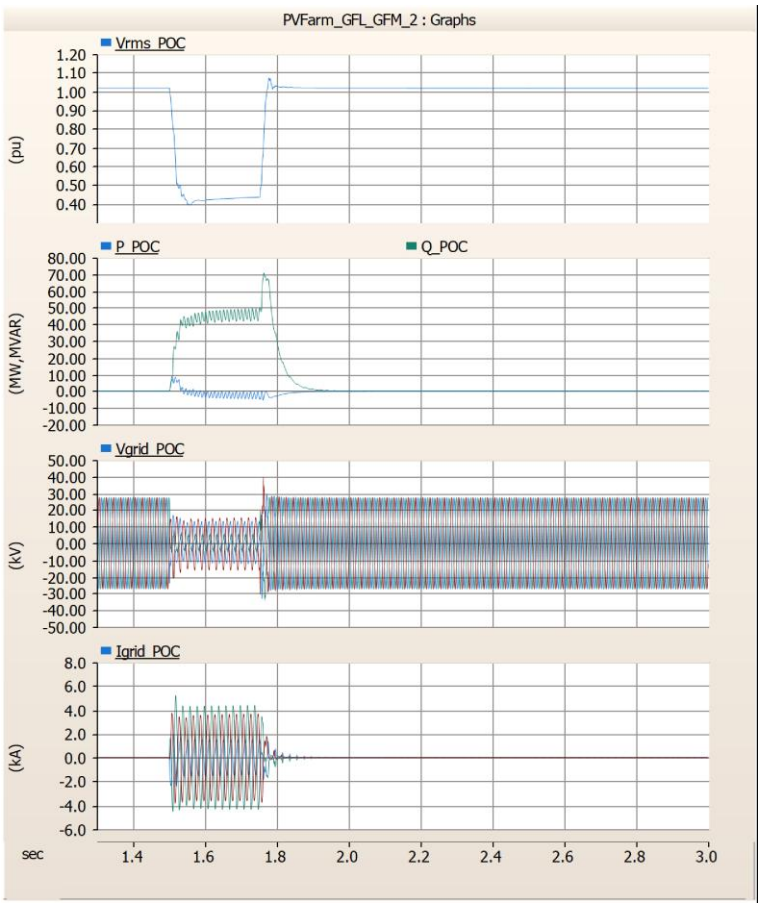

Figure 114 dVOC GFM vs dVOC GFM (100 MVA:1000 MVA)

C.3 GFM withstand SCR tests – VSM mode

SMIB. VSM mode with inertia constant set to 1.0 and damping constant set to 1.0. Variation of grid strength (SCR) from 1.0 to 9.0, X/R held at 10.

Stable. Some increase in hash in the Id/Iq references, but always returned to stable point.

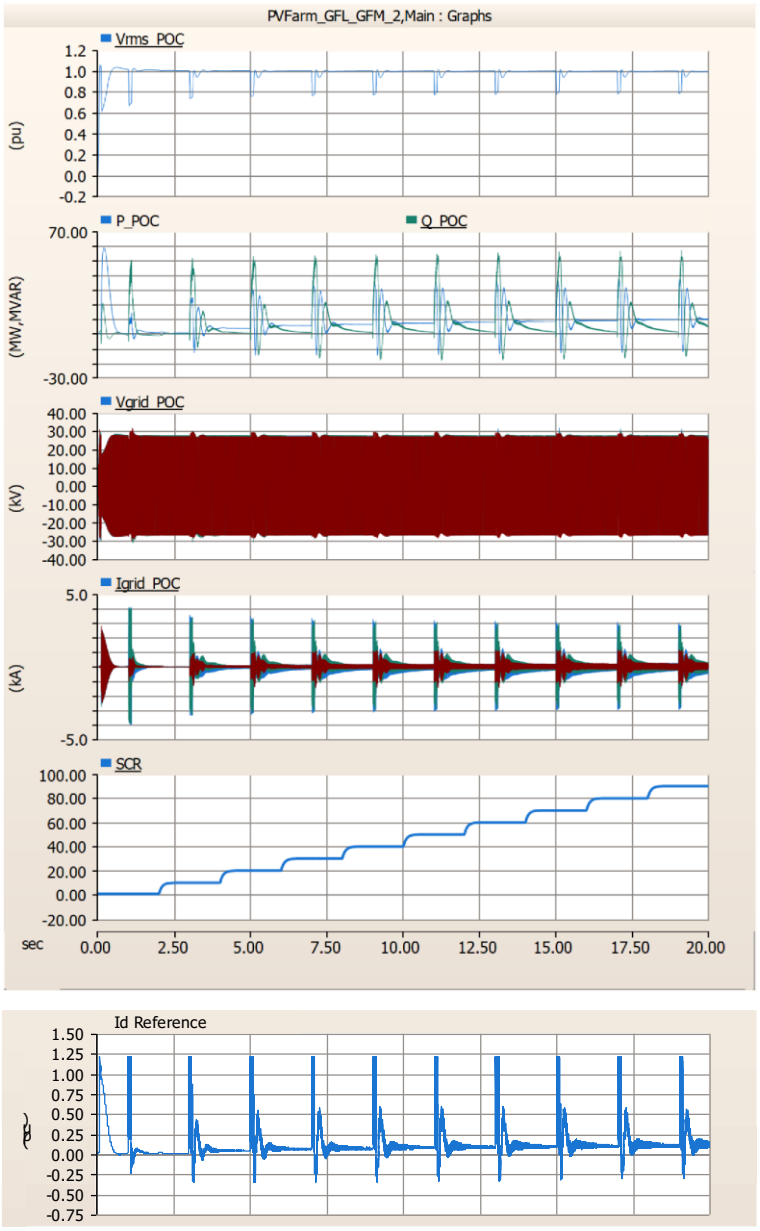

Appendix D Scaling assumption example

The following results show that the unit scaling assumption used in the Milestone 4 work holds for larger sizes of generators and transformers. Transformer energisation was timed to occur on the negative to positive crossing of the phase A voltage, with a flux remanence of 0.8/-0.8/0.0.

D.1 OCGT energisation

A 350 MVA synchronous generator energises an 875 MVA transformer at the end of 25 km transmission line.

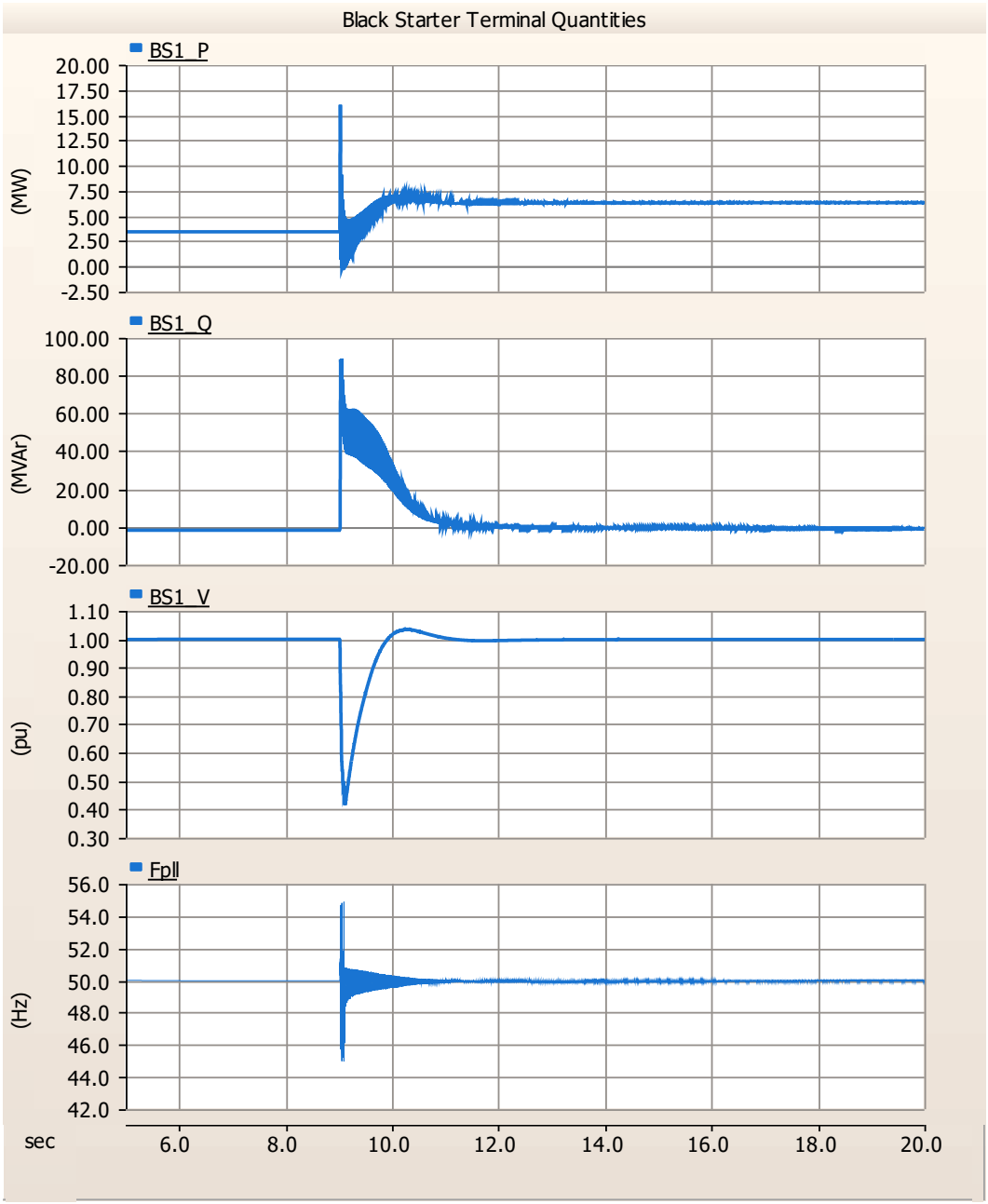

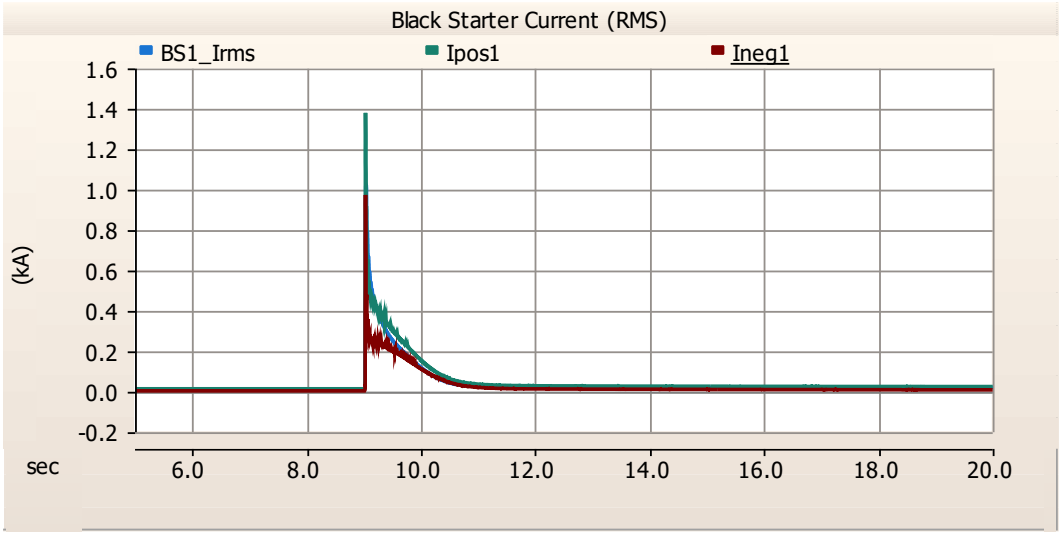

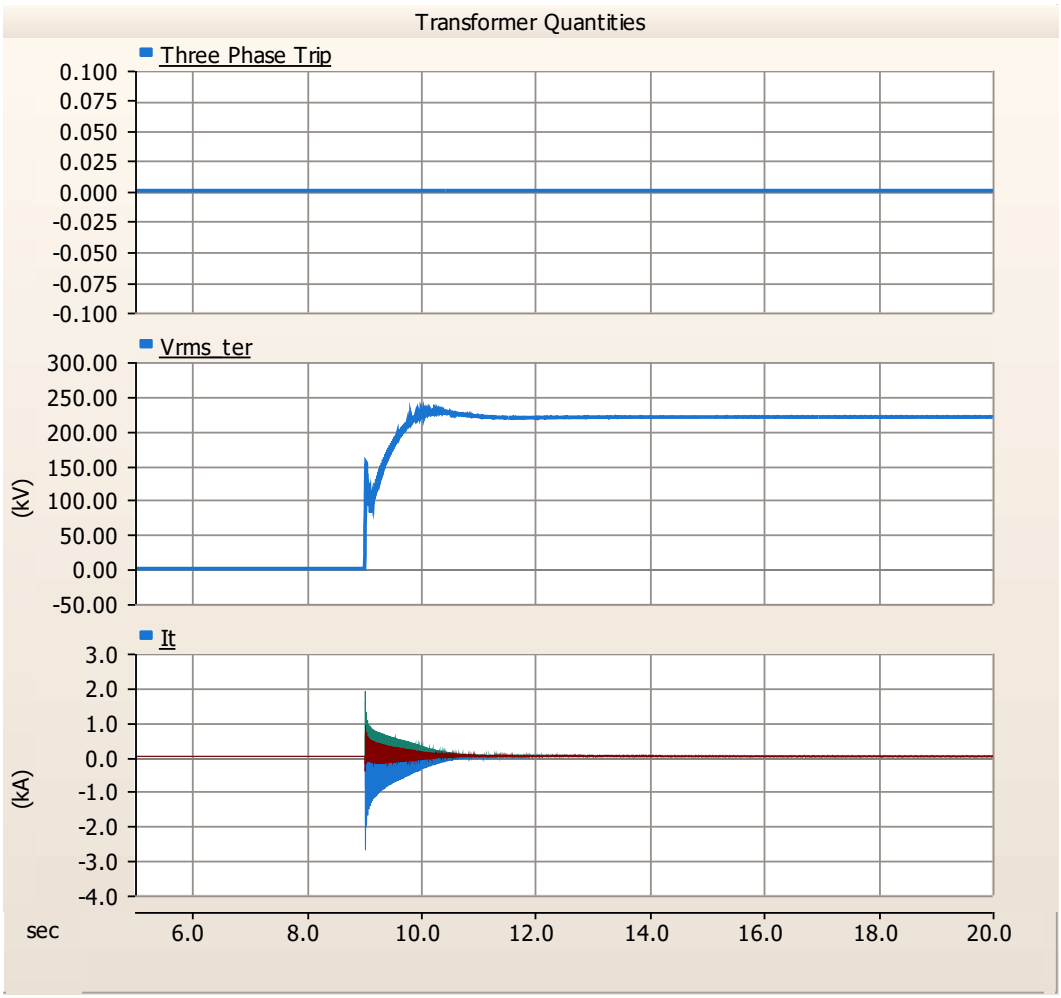

Note that no transformer differential relay trip was observed.

D.2 GFM BESS energisation

A 100 MVA GFM BESS generator energises an 875 MVA transformer at the end of 25 km transmission line.

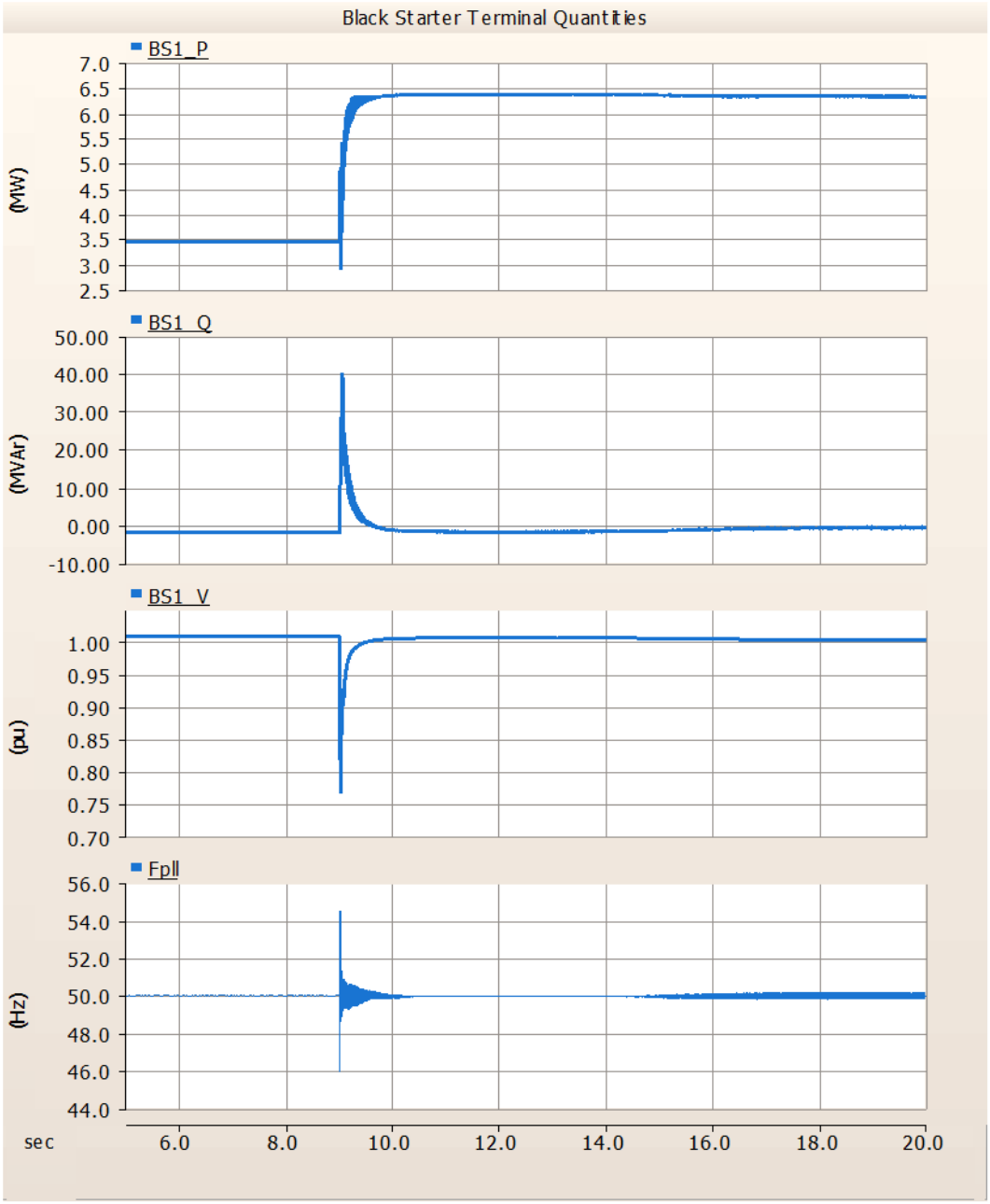

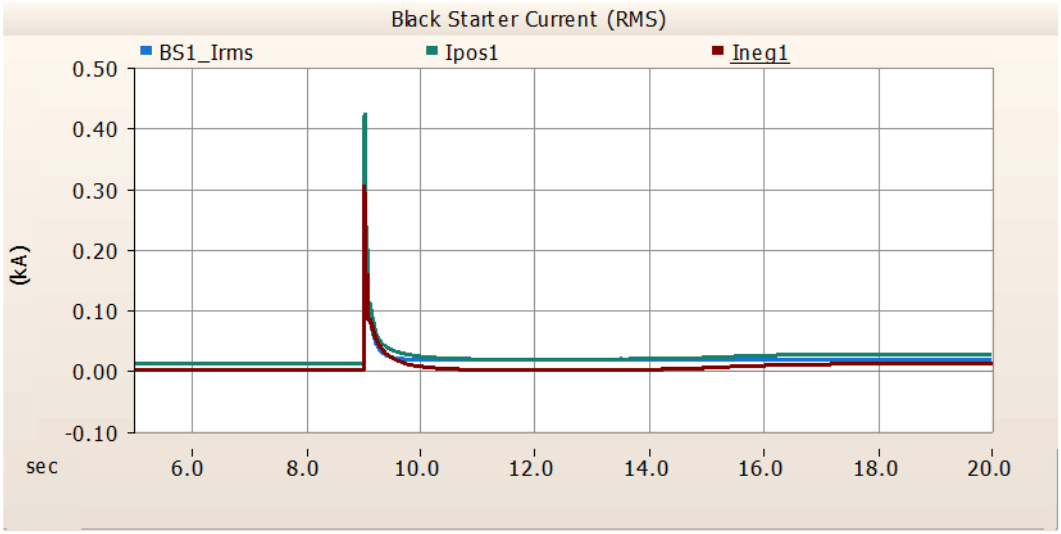

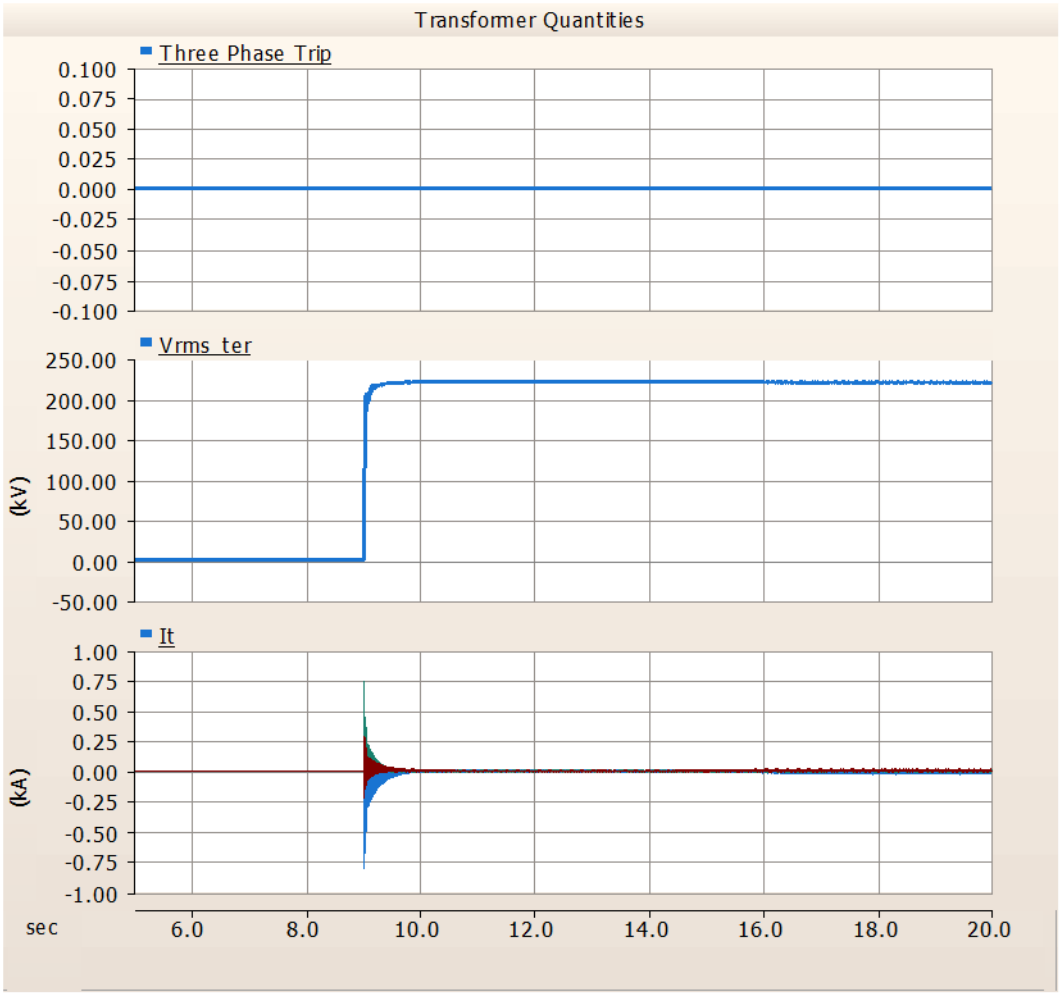

Note that no transformer differential relay trip was observed.

Shortened forms

Acronym	Meaning
ACSR	Aluminium Clad, Steel Reinforced
AEMC	Australian Energy Market Commission
AEMO	Australian Energy Market Operator
AR-PST	Australian Research in Power System Transition
BESS	Battery Energy Storage System
C	Capacitor
CB	Circuit Breaker
CSIRO	Commonwealth Science and Industrial Research Organisation
DC	Direct Current
DER	Distributed Energy Resources
EMT	Electromagnetic Transient
EPRI	Electric Power Research Institute
FFT	Fast Fourier Transform
FRT	Fault Ride-through
G-PST	Global Power Systems Transition
GFL	Grid following
GFM	Grid forming
GT	Gas Turbine
HVRT	High-voltage ride-through
IBR	Inverter based loads
kA	kiloamp
kV	kilovolt
kW	kiloWatt
L	Inductor
LV	Low Voltage
LVRT	Low-voltage ride-through
MHI	Manitoba Hydro International
MMIB	Multiple Machine, Infinite Bus
MPPT	Maximum Power-Point Tracking
MV	Medium Voltage
MVA	Mega volt-amp
MVAr	Mega volt-amp reactive
MW	Megawatt
NDA	Non-Disclosure Agreement
NEM	National Electricity Market
OCGT	Open-cycle Gas Turbine
OEM	Original Equipment Manufacturer
P	Active Power
pf	Power Factor
PLL	Phase-locked loop
PoC	Point of Connection
PPC	Plant Park Control / Park Power Controller

Acronym	Meaning
PSCAD	Power Systems Computer Aided Design
pu	Per-unit
PV	Photovoltaic
Q	Reactive Power
REZ	Renewable Energy Zone
RoCoF	Rate of Change of Frequency
SCR	Short Circuit Ratio
SMIB	Single Machine, Infinite Bus
SRAS	System Restart Ancillary Services
SRS	System Restart Standard
TRX	Transformer
VSM	Virtual Synchronous Machine
WECC	Western Electricity Coordination Council

As Australia's national science agency and innovation catalyst, CSIRO is solving the greatest challenges through innovative science and technology.

CSIRO. Unlocking a better future for everyone.

Contact us

1300 363 400
+61 3 9545 2176
csiro.au/contact
csiro.au